

NUREG/CR-0342  
ORNL/NUREG-51

## ORTCAL—A Code for THTF Heater Rod Thermocouple Calibration

L. J. Ott  
R. A. Hedrick

Prepared for the U.S. Nuclear Regulatory Commission  
Office of Nuclear Regulatory Research  
Under Interagency Agreements DOE 40-551-75 and 40-552-75

120555004121 1 R2  
US NRC  
RES SUPPORT BRANCH  
BRANCH CHIEF  
1130SS  
WASHINGTON DC 20555

**OAK RIDGE NATIONAL LABORATORY**  
OPERATED BY UNION CARBIDE CORPORATION · FOR THE DEPARTMENT OF ENERGY

79-111-2274

Printed in the United States of America. Available from  
National Technical Information Service  
U.S. Department of Commerce  
5285 Port Royal Road, Springfield, Virginia 22161

This report was prepared as an account of work sponsored by the United States Government. Neither the United States nor any of its employees, nor any of its contractors, subcontractors, or their employees, makes any warranty, express or implied, or assumes any legal liability or responsibility for the accuracy, completeness or usefulness of any information, apparatus, product or process disclosed, or represents that its use would not infringe privately owned rights.

NUREG/CR-0342  
ORNL/NUREG-51  
Dist. Category R2

Contract No. W-7405-eng-26

Engineering Technology Division

ORTCAL — A CODE FOR THTF HEATER ROD  
THERMOCOUPLE CALIBRATION

L. J. Ott    R. A. Hedrick

Manuscript Completed — January 15, 1979  
Date Published — February 1979

Prepared for the  
U.S. Nuclear Regulatory Commission  
Office of Nuclear Regulatory Research  
Under Interagency Agreements DOE 40-551-75 and 40-552-75  
NRC FIN No. B0125

Prepared by the  
OAK RIDGE NATIONAL LABORATORY  
Oak Ridge, Tennessee 37830  
operated by  
UNION CARBIDE CORPORATION  
for the  
DEPARTMENT OF ENERGY

## Contents

	<u>Page</u>
LIST OF TABLES .....	v
LIST OF FIGURES .....	vii
ABSTRACT .....	1
1. INTRODUCTION .....	1
1.1 Background .....	1
1.2 Test Facilities .....	2
1.3 Heater Rod Description .....	3
1.4 Heater Rod Bundle .....	9
1.4.1 Radial dimensions .....	19
1.4.2 Physical properties of components .....	19
1.4.3 Calibration objectives .....	21
2. ROD CLASSIFICATION PROCEDURE .....	23
2.1 Preliminary Notes .....	23
2.1.1 Thermocouples .....	23
2.1.2 Power peaking factors .....	24
2.1.3 Experiments .....	27
2.2 ORTCAL - Part I .....	31
2.2.1 Production and description of the "statistics" tape read by ORTCAL - Part I .....	31
2.2.2 Code logic and methods used .....	31
2.3 ORTCAL - Part II .....	45
2.4 ORTCAL - Part III .....	57
2.5 ORTCAL - Part IV .....	65
3. CONSEQUENCES OF NONCALIBRATION OF FUEL PIN SIMULATORS .....	73
4. CONCLUSIONS .....	107
REFERENCES .....	109
APPENDIX A. PHYSICAL PROPERTIES DATA .....	113
APPENDIX B. ....	129
APPENDIX C. EXAMPLES OF ORTCAL - PART I OUTPUT .....	135
APPENDIX D. EXAMPLES OF ORTCAL - PART II OUTPUT .....	147
APPENDIX E. EXAMPLE OF ORTCAL - PART III OUTPUT .....	165
APPENDIX F. EXAMPLE OF ORTCAL - PART IV OUTPUT .....	183
APPENDIX G. DEVELOPMENT OF THE MODIFIED RUSSELL EQUATION .....	205

## LIST OF TABLES

<u>Number</u>	<u>Identification</u>	<u>Page</u>
1.1	Nominal power profile for the THTF indirect heater with average power of 12 kW/ft	8
1.2	Nominal location of thermocouples in THTF bundle 1 relative to power zone steps and grid spacers	15
1.3	Radial dimensions of THTF heater	20
2.1	Information contained on an ORTCAL thermocouple history tape	33
2.2	Calibration results for position TE-318BG in THTF bundle 1	55
2.3	Calibration results for position TE-301DJ in THTF bundle 1	63
2.4	Bundle 1 estimated MgO core porosities	66
2.5	The ORTCAL - Part IV contribution to the CDT file for position TE-318BG in THTF bundle 1	70
3.1	Comparison of case 1 and case 2 surface conditions for level E at 0 and 2 sec	84
3.2	Local fluid pressure required to achieve surface temperatures for case 2 during nucleate boiling	86
A.1	Physical property data for Inconel 600	115
A.2	Physical property data for Cupronickel	118
A.3	Physical property data for 316 stainless steel	121
A.4	Physical property data for magnesium oxide	124
A.5	Physical property data for boron nitride	126
C.1	THTF thermocouple calibration runs	137
C.2	Example of ORTCAL - Part I output for thermocouple TE-318BG	138
C.3	Example of ORTCAL - Part I output for thermocouple TE-301DJ	142
D.1	Example of ORTCAL - Part II output for thermocouple TE-318BG	149
D.2	Example of ORTCAL - Part II output for thermocouple TE-301DJ	154
D.3	Example of ORTCAL - Part II output for thermocouple TE-322BF	159
F.1	ORTCAL - Part IV level regression for G level (at thermocouple position TE-318BG)	185
F.2	ORTCAL - Part IV individual regression for TE-318BG	190

<u>Number</u>	<u>Identification</u>	<u>Page</u>
F.3	Summary of ORTCAL -- Part IV regression for TE position 318BG	195
F.4	Summary of ORTCAL -- Part IV regressions for THTF bundle 1 through run 24.1	196

## LIST OF FIGURES

<u>Number</u>	<u>Title</u>	<u>Page</u>
1.1	Thermal-Hydraulic Test Facility	3
1.2	Indirect heater rod assembly (1 in. = 2.54 cm)	4
1.3	Heater rod cross section (1 in. = 2.54 cm)	5
1.4	Power profile of prototype heater (1 ft = 30.48 cm)	6
1.5	Integrated power profile of stepped, chopped-cosine heater rod compared to the integrated power profile of a smooth chopped-cosine curve (1 ft = 30.48 cm)	7
1.6	Typical thermocouple junction configuration	9
1.7	Cross section of BDHT heater 150-5	10
1.8	Cross section of sheath thermocouples in BDHT heater 150-5	11
1.9	Segment of heater showing mean dimensions in the thermocouple area (1 in. = 2.54 cm)	12
1.10	Low-pressure-drop spacer grid assembly (1 in. = 2.54 cm)	13
1.11	Test section using indirect heater rod in 49-rod bundle (1 ft = 0.3048 m)	14
1.12	Distribution of thermocouples in THTF test bundle 1 (May 24, 1976)	16
1.13	Location of thermocouples in THTF bundle 1 (1 in. = 2.54 cm)	17
1.14	THTF test bundle 1 rods monitored by metrascope (shown by cross hatching)	18
2.1	Fill test configuration	25
2.2	Fuel pin simulator zone designations with thermocouple levels (bundle 1) and enlarged active component assembly	26
2.3	Surface heat flux perturbation due to thermocouple presence and 0.015-in. heater eccentricity	29
2.4	Updated ORTCAL thermocouple history tape	32

<u>Number</u>	<u>Title</u>	<u>Page</u>
2.5	Schematic of fuel pin simulator with inset showing thermocouple and groove superimposed on solid inner stainless steel sheath	35
2.6	Notation relative to the derivation of the heat transfer model at the interface of the inner and outer stainless steel sheaths	36
2.7	Notation relative to the derivation of the heat transfer model at the heater surface	37
2.8	Gap aging history at thermocouple position TE-318BG	42
2.9	Gap aging history at thermocouple position TE-301DJ (constant surface temperature)	43
2.10	Gap aging history at thermocouple position TE-301DJ (constant power-generation rate)	44
2.11	Schematic of fuel pin simulator with sheath and middle thermocouples in insets with typical pin radial temperature profile at steady state	46
2.12	Boron nitride thermal conductivity at 318BG (comparison of regression results with literature data)	49
2.13	Boron nitride thermal conductivity at 301DJ (comparison of regression results with literature data)	50
2.14	Radial $\Delta T$ as a function of rod power (thermocouple position 318BG)	52
2.15	Radial $\Delta T$ as a function of rod power (thermocouple position 301DJ)	53
2.16	Radial $\Delta T$ as a function of rod power (thermocouple position 322BF)	54
2.17	Lines of information flow for ORTCAL - Part II	56
2.18	Lines of information flow required for complete $k_{BN}$ classification at all bundle thermocouple positions	58
2.19	Boron nitride thermal conductivity for bundle 1 (comparison of regression results with literature data)	59
2.20	MgO thermal conductivity as a function of temperature and porosity (literature data, Ref. 6)	60



<u>Number</u>	<u>Title</u>	<u>Page</u>
2.21	MgO thermal conductivity as a function of temperature and porosity (comparison of regression results at 318BG and 301DJ with literature data, Ref. 6)	62
2.22	Lines of information flow for ORTCAL - Part III	64
2.23	Estimated MgO core porosity for THTF bundle 1	66
2.24	Notation relative to the mathematical model of the thermomechanical behavior of the gap between the inner and outer stainless steel sheaths	68
2.25	Lines of information flow for ORTCAL - Part IV	69
3.1	ORINC rod surface temperatures, level E, THTF test 105, case 1	74
3.2	ORINC rod surface temperatures, level G, THTF test 105, case 1	75
3.3	ORINC rod surface heat fluxes, level E, THTF test 105, case 1	76
3.4	ORINC rod surface heat fluxes, level G, THTF test 105, case 1	77
3.5	ORINC rod surface temperatures, level E, THTF test 105, case 2	78
3.6	ORINC rod surface temperatures, level G, THTF test 105, case 2	79
3.7	ORINC rod surface heat fluxes, level E, THTF test 105, case 2	80
3.8	ORINC rod surface heat fluxes, level G, THTF test 105, case 2	81
3.9	Element notation at the inner stainless steel sheath to the outer stainless steel sheath interface	82
3.10	Element notation at the heater surface	83
3.11	Distribution of pressure superimposed on cross section of bundle 1 core	86
3.12	ORINC rod surface heat flux, TE-318BG, THTF test 105, 0-18 sec	88

<u>Number</u>	<u>Title</u>	<u>Page</u>
3.13	ORINC rod surface temperature, TE-318BG, THTF test 105, 0-18 sec	89
3.14	Rod centerline temperature, TE-318BG, THTF test 105, 0-18 sec	90
3.15	ORINC rod surface heat flux, TE-318BG, THTF test 105, 0-0.5 sec	92
3.16	ORINC rod surface heat flux, TE-318BG, THTF test 105, 0.5-2 sec	93
3.17	ORINC rod surface heat flux, TE-318BG, THTF test 105, 2.0-8 sec	94
3.18	ORINC rod surface heat flux, TE-318BG, THTF test 105, 5.0-18 sec	95
3.19	ORINC rod surface temperature, TE-318BG, THTF test 105, 0-0.5 sec	96
3.20	ORINC rod surface temperature, TE-318BG, THTF test 105, 0.5-2 sec	97
3.21	ORINC rod surface temperature, TE-318BG, THTF test 105, 2.0-8 sec	98
3.22	ORINC rod surface temperature, TE-318BG, THTF test 105, 5.0-18 sec	99
3.23	Comparison of surface heat fluxes, cases 1 and 3	100
3.24	Calculated pin internal thermal response, 0-0.75 sec	101
3.25	Calculated pin internal thermal response, 1.0-1.75 sec	102
3.26	Calculated pin internal thermal response, 2.0-2.75 sec	103
3.27	Calculated pin internal thermal response, 3.0-3.75 sec	104
3.28	Calculated pin internal thermal response, 4.0-4.75 sec	105
A.1	Thermal conductivity of Inconel 600	116
A.2	Specific heat of Inconel 600	117
A.3	Thermal conductivity of Cupronickel	119
A.4	Specific Heat of Cupronickel	120

<u>Number</u>	<u>Title</u>	<u>Page</u>
A.5	Thermal conductivity of 316 stainless steel	122
A.6	Specific heat of 316 stainless steel	123
A.7	Specific heat of magnesium oxide	125
A.8	Specific heat of boron nitride	127
G.1	MgO thermal conductivity as a function of temperature and porosity (literature data)	209
G.2	$k_{MgO}$ vs temperature for 5% porous MgO [literature data and regression fit of Eq. (G.8)]	211
G.3	$k_{MgO}$ vs temperature for 22% porous MgO [literature data and regression fit of Eq. (G.8)]	212
G.4	$k_{MgO}$ vs temperature for 5% porous MgO [literature data and regression fit of Eq. (G.12)]	214
G.5	$k_{MgO}$ vs temperature for 22% porous MgO [literature data and regression fit of Eq. (G.12)]	215
G.6	MgO thermal conductivity as a function of temperature and porosity [modified Russell equation - Eq. (G.12)]	216

ORTCAL - A CODE FOR THTF HEATER ROD  
THERMOCOUPLE CALIBRATION

L. J. Ott     R. A. Hedrick

ABSTRACT

This report develops and presents an experimental thermocouple calibration procedure and a four-part calibration program, ORTCAL (ORNL Thermocouple Calibration), which supplies heater rod performance information to the inverse heat conduction code ORINC. Case studies are presented to illustrate the effect of noncalibration of fuel pin simulators on the inverse calculations.

1. INTRODUCTION

1.1 Background<sup>1</sup>

The ORNL Pressurized-Water Reactor Blowdown Heat Transfer (PWR-BDHT) Program is an experimental separate-effects study of the relations among the principal variables that can alter the rate of blowdown, the presence of flow reversal and rereversal, time delay to critical heat flux (CHF), the rate at which dryout progresses, and similar time- and space-related functions that are important to loss-of-coolant accident (LOCA) analysis.

Overall program objectives are (1) to concurrently determine, for a wide range of parameters, pre-CHF heat fluxes,  $\Delta T$  (surface driving potential), heat transfer coefficients, and local fluid properties; time to CHF; and post-CHF heat fluxes,  $\Delta T$ , heat transfer coefficients, and local fluid properties; and (2) to test the ability of existing codes such as RELAP to predict the behavior of the single- and multirod loops under blowdown conditions.

The parameters to be studied include (1) single- and double-ended coolant line breaks of varying area ratio; (2) depressurization rates; (3) different combinations of system power and pressure to obtain different values of departure from nuclear boiling ratio (DNBR); (4) a range of power cutoff delays; and (5) a range of power decay rates.

Secondary objectives are (1) to obtain CHF data under steady-state conditions over a range of coolant pressures, inlet and exit subcooling, and inlet flow rate appropriate to PWR interests; (2) to evaluate the thermal-hydraulic behavior of the test loops during simulated operational upsets that include variations in local power, system pressure, or coolant flow using a typical anticipated transient without scram (ATWS<sup>2</sup>) as a guide; and (3) to determine the effect of different spacer grids and power distribution profiles on both transient and steady-state CHF.

## 1.2 Test Facilities<sup>1</sup>

Primary test results are obtained from the Thermal-Hydraulic Test Facility (THTF), a large nonnuclear experimental loop with a test section that contains a  $7 \times 7$  array of 365.76-cm (12-ft) stepped, chopped-cosine heater rods with outside diameters of 1.0719 cm (0.422 in.).

A schematic of the THTF is shown in Fig. 1.1. Fluid discharged from the pump flows through two control valves, where excess pump head is dissipated and flow adjusted to the desired level by diverting a portion through the bypass line. Heat generated in the fluid by the pump is removed in the small Graham "Heliflow" heat exchanger in the bypass line. The primary flow then passes through inlet instrumented spool pieces 1 and 2, where flow conditions are monitored by a combination of a drag disk, gamma densitometer, turbine meter, and temperature and pressure sensors in each spool piece. Flow enters the test section at the top of the rectangular shroud box, flows down its length, and enters the bottom of the rod bundle. The fluid exits the bundle through outlet spool pieces 1 and 2, which are identical to those on the inlet. The energy added by the test section heater rods is removed by Graham "Heliflow" heat exchangers A, B, and C. Finally, the fluid returns to the pump suction past the line from the pressurizer, which provides the primary pressure control for the loop and at the same time serves as a surge tank.

Supporting experiments are carried out in the Forced Convection Test Facility (FCTF). The primary purpose of the FCTF is to qualify prototype heaters for use in the THTF and to obtain blowdown heat transfer and steady-state CHF results for single rods in an annular geometry. In its

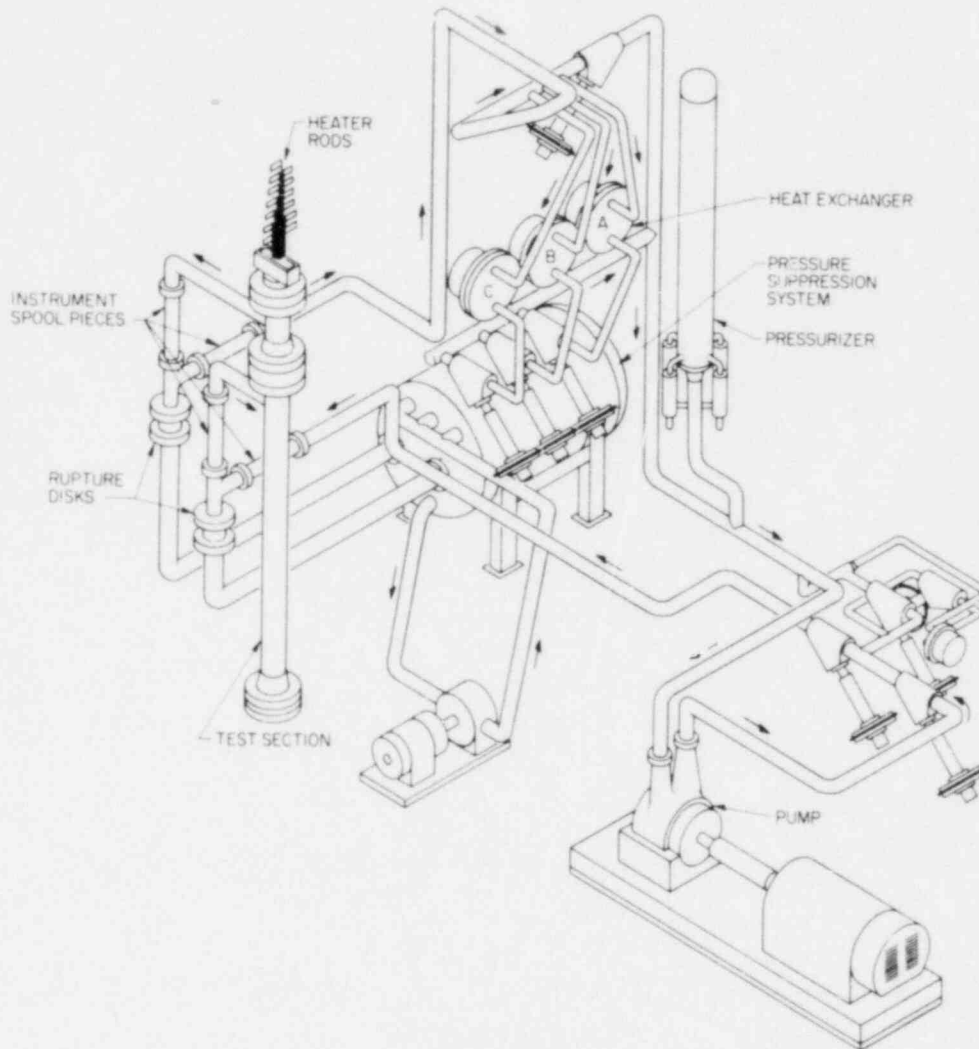


Fig. 1.1. Thermal-Hydraulic Test Facility.

present configuration, the FCTF is capable of conducting only single-ended break tests.

### 1.3 Heater Rod Description<sup>1</sup>

The indirect electric heater rods used in THTF bundle 1 are 1.0719 cm in diameter (0.422 in.) with a stepped, chopped-cosine power profile length of 365.76 cm (12 ft) (see Fig. 1.2). The overall rod length is 548.64 to 640.08 cm (18 to 21 ft), depending on its location in the bundle. The rod

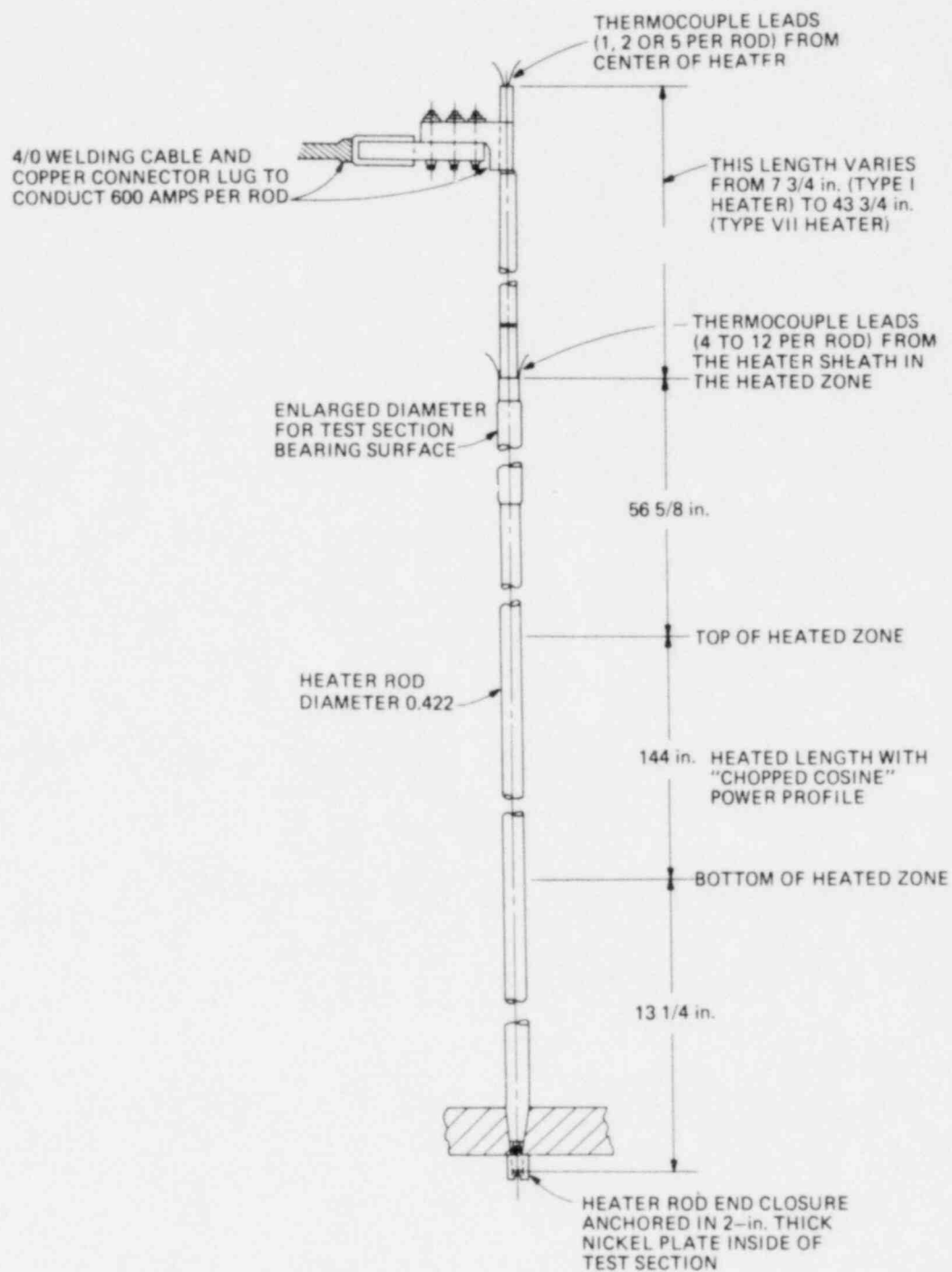


Fig. 1.2. Indirect heater rod assembly (1 in. = 2.54 cm).

is double-ended, with the sheath and ground-lead extension welded together at the lower end and the power lead insulated from the sheath at the upper end.

The heater rods have a dual-sheath design (see rod cross section in Fig. 1.3). The outer sheath is 0.0254-cm-thick (0.010-in.) stainless steel; the inner sheath is 0.0762-cm-thick (0.030-in.) stainless steel and is grooved to accept the 0.0508-cm (0.020-in.) Chromel vs Alumel thermocouples. The next inner layer is boron nitride (BN), which electrically insulates the heating element from the stainless steel sheaths. The heater element consists of a series of oversleeves swaged over a central base tube to provide the heat-generation zones. The central "hot zone," which consists of only the base Inconel 600 heater tube, has the highest electrical resistance and the maximum heat-generation rate. Successive oversleeves of Inconel 600 or Cupronickel are swaged over the heater element with each succeeding oversleeve extending to the end. As oversleeves are added between the central zone and the ends, the resistance and heat-generation rates of that particular zone decrease so that

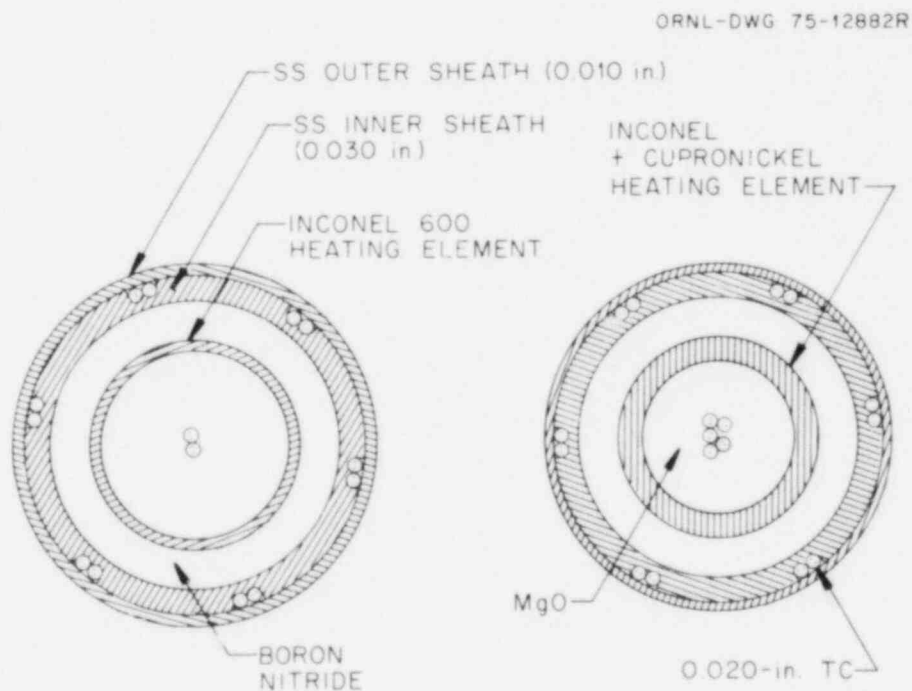


Fig. 1.3. Heater rod cross section (1 in. = 2.54 cm).



the step changes approximate the desired chopped-cosine power profile shown in Fig. 1.4. The lengths of the steps for different power levels were chosen to match the integrated chopped-cosine power profile (Fig. 1.5). Nominal heated zone lengths, power ratios, and local powers for

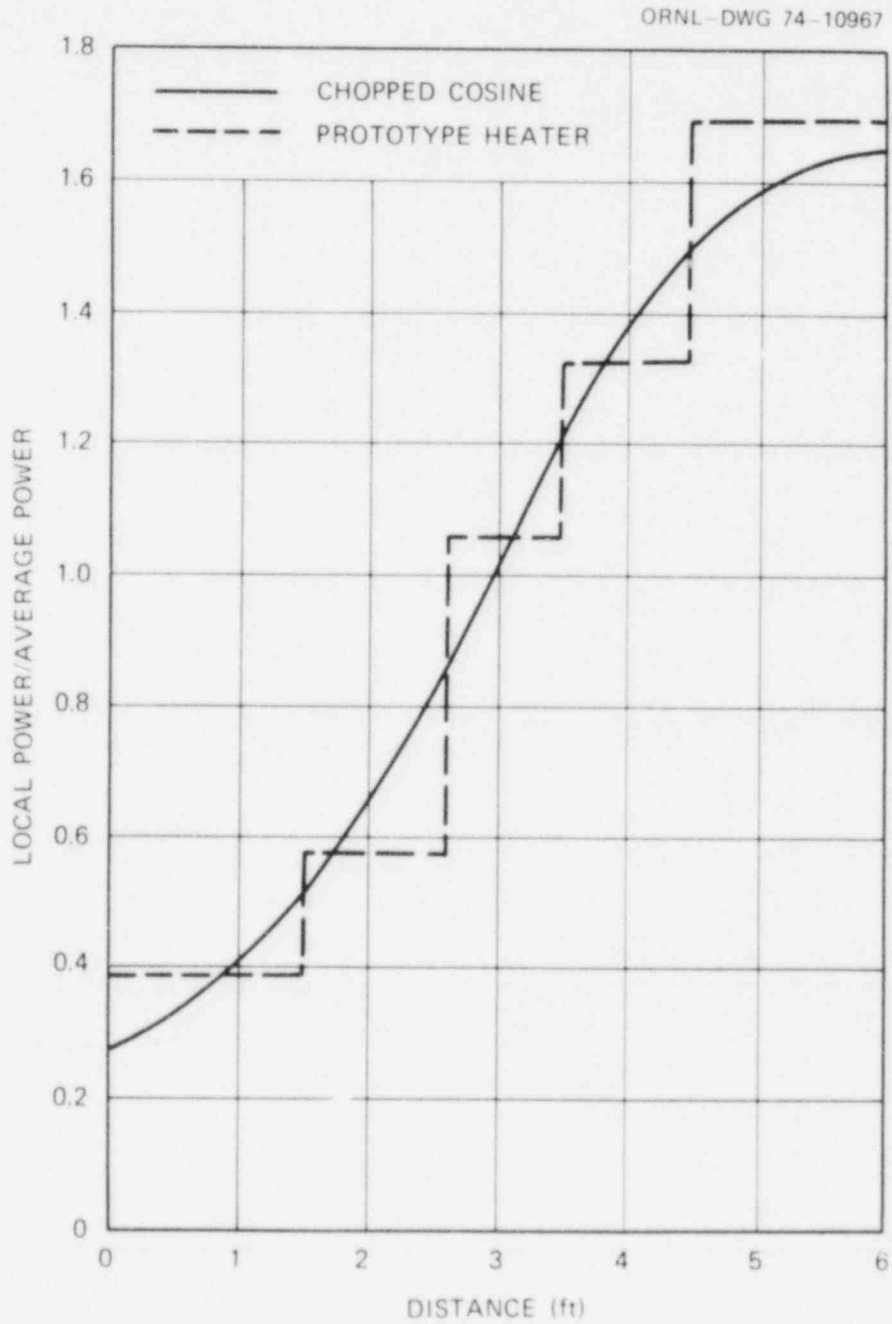


Fig. 1.4. Power profile of prototype heater (1 ft = 30.48 cm).

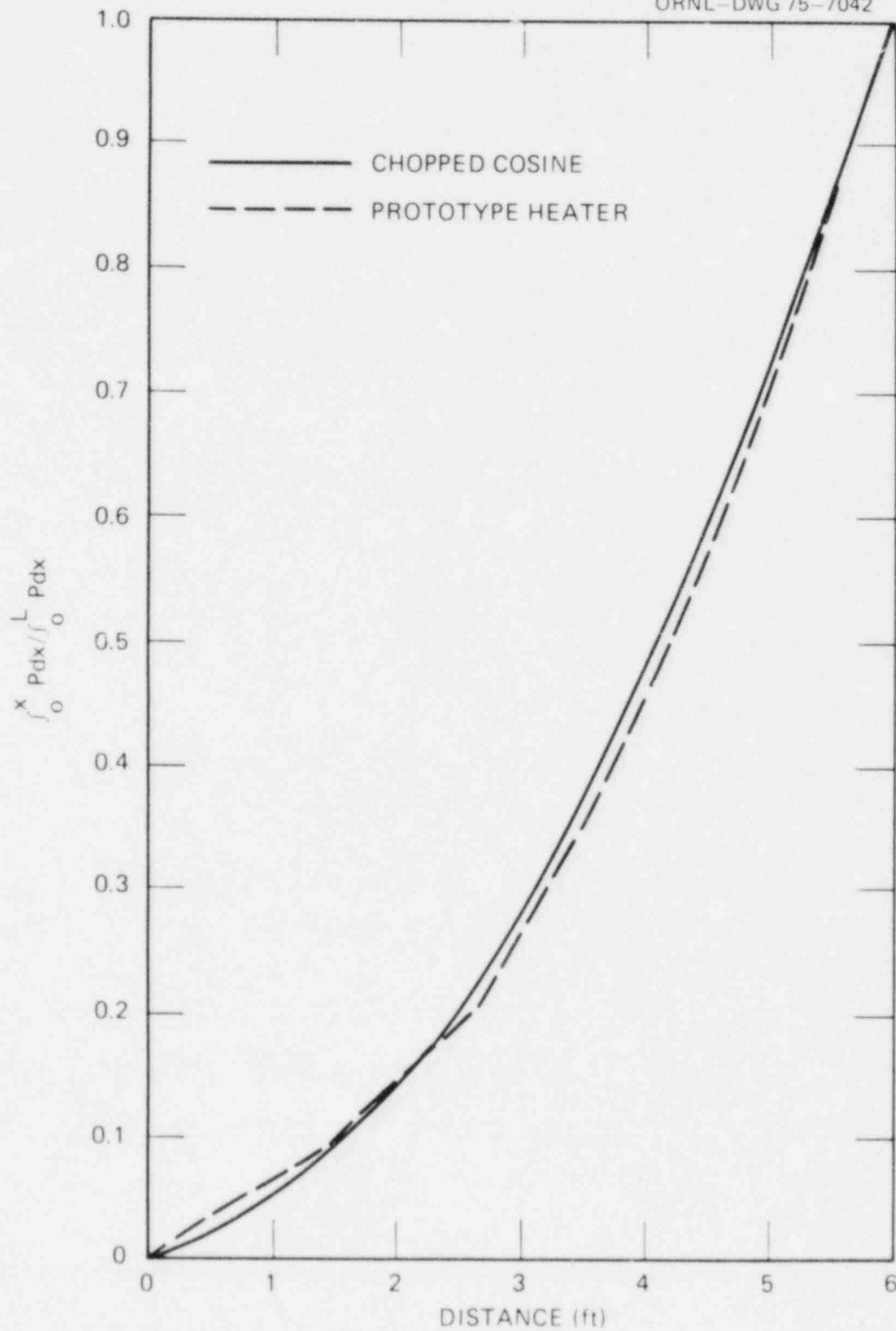


Fig. 1.5. Integrated power profile of stepped, chopped-cosine heater rod compared to the integrated power profile of a smooth chopped-cosine curve (1 ft = 30.48 cm).

THTF heaters are given in Table 1.1. The core of the heater element is filled with magnesium oxide (MgO), which serves as both a filler and an insulator between the heating element and the central rod thermocouple sheaths.

Table 1.1. Nominal power profile for the THTF indirect heater with average power of 12 kW/ft<sup>2</sup>

Length of heated zone from beginning (in.)	Local/average power ratio	Local power rate (kW/ft)
0-18	0.422	5.06
18-31.5	0.597	7.16
31.5-42	1.065	12.78
42-54	1.285	15.42
54-90	1.67	20.0
90-102	1.285	15.42
102-112.5	1.065	12.78
112.5-126	0.597	7.16
126-144	0.422	5.06

<sup>a</sup>1 in. = 2.54 cm; 1 kW/ft = 3.28084 kW/m.

The sheath thermocouples are located in axial grooves (two per groove) machined in the inner sheath. After the tips of the thermocouple sheath are spot-welded at the proper location, a stainless steel filler rod is added to the remainder of the groove (Fig. 1.6). The heater is then slipped into the 0.0254-cm-thick outer sheath and the whole assembly swaged to a 1.0719-cm OD.

BDHT heater 150-5 (originally S/N-5) was cross sectioned and micro-photographed<sup>3</sup> by the Y-12 Development Division Metallurgical Department. A typical cross-sectional view (Fig. 1.7) shows the peripheral location of sheath thermocouples and heater components. An enlarged view of the inner sheath groove area (Fig. 1.8) reveals that the groove has been milled to a depth of 0.0394 cm (0.0155 in.), which is less than the original 0.0508-cm OD of the thermocouple. As a result, during swaging operations the thermocouple is crushed to a somewhat elliptical shape and the

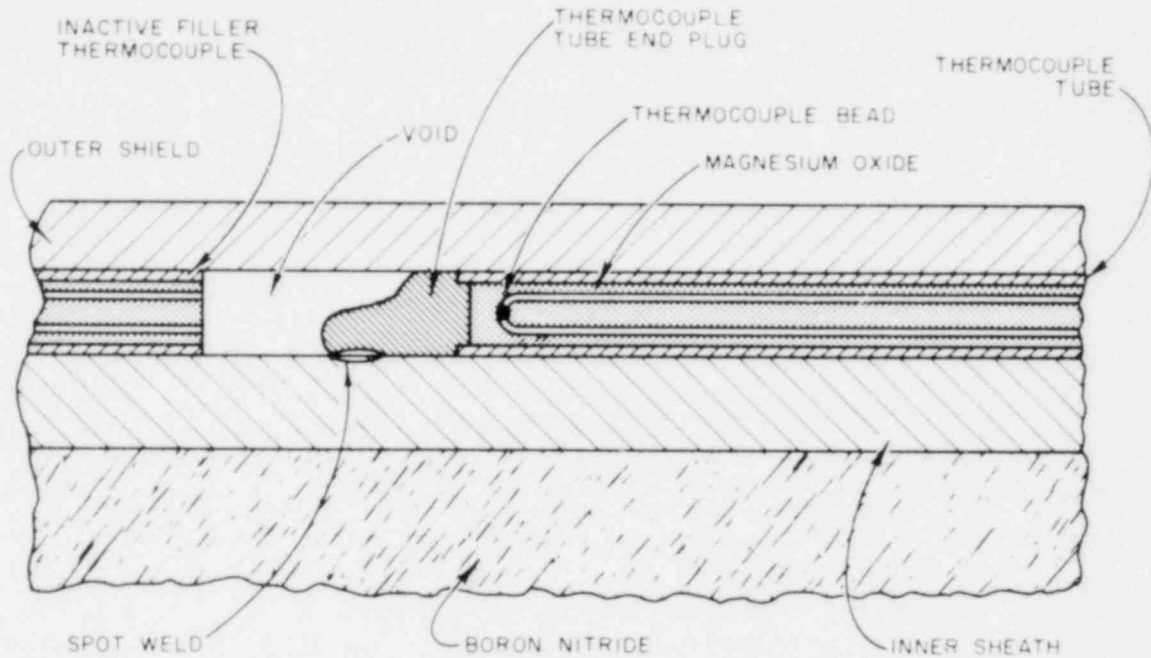


Fig. 1.6. Typical thermocouple junction configuration.

edge of the milled groove is pulled away from the outer sheath (Fig. 1.8). A review of all photographs of cross sections at thermocouple bead junctions in heater 150-5 results in the composite drawing shown in Fig. 1.9.

The heater rod is reduced to its final diameter by swaging, often creating an imperfect fit between the inner and outer sheaths at the thermocouple locations and resulting in a gap between the thermocouple junction and the outer sheath (Figs. 1.7 and 1.8). The thermocouple is welded to the inner sheath; thus, the gap between the junction and outer sheath grows with increasing fluid temperature and closes with increasing heater power. With successive blowdown transients, the residual gap increases, apparently due to plastic deformation of the outer sheath.

#### 1.4 Heater Rod Bundle<sup>1</sup>

Bundle 1 consists of 49 rods in a  $7 \times 7$  array spaced on 1.43-cm (0.563-in.) centers which are contained in a 10.16-cm-square (4-in.) shroud box. Low-pressure-drop grid spacers (Fig. 1.10) are provided at

ORNL PHOTO 3284-77

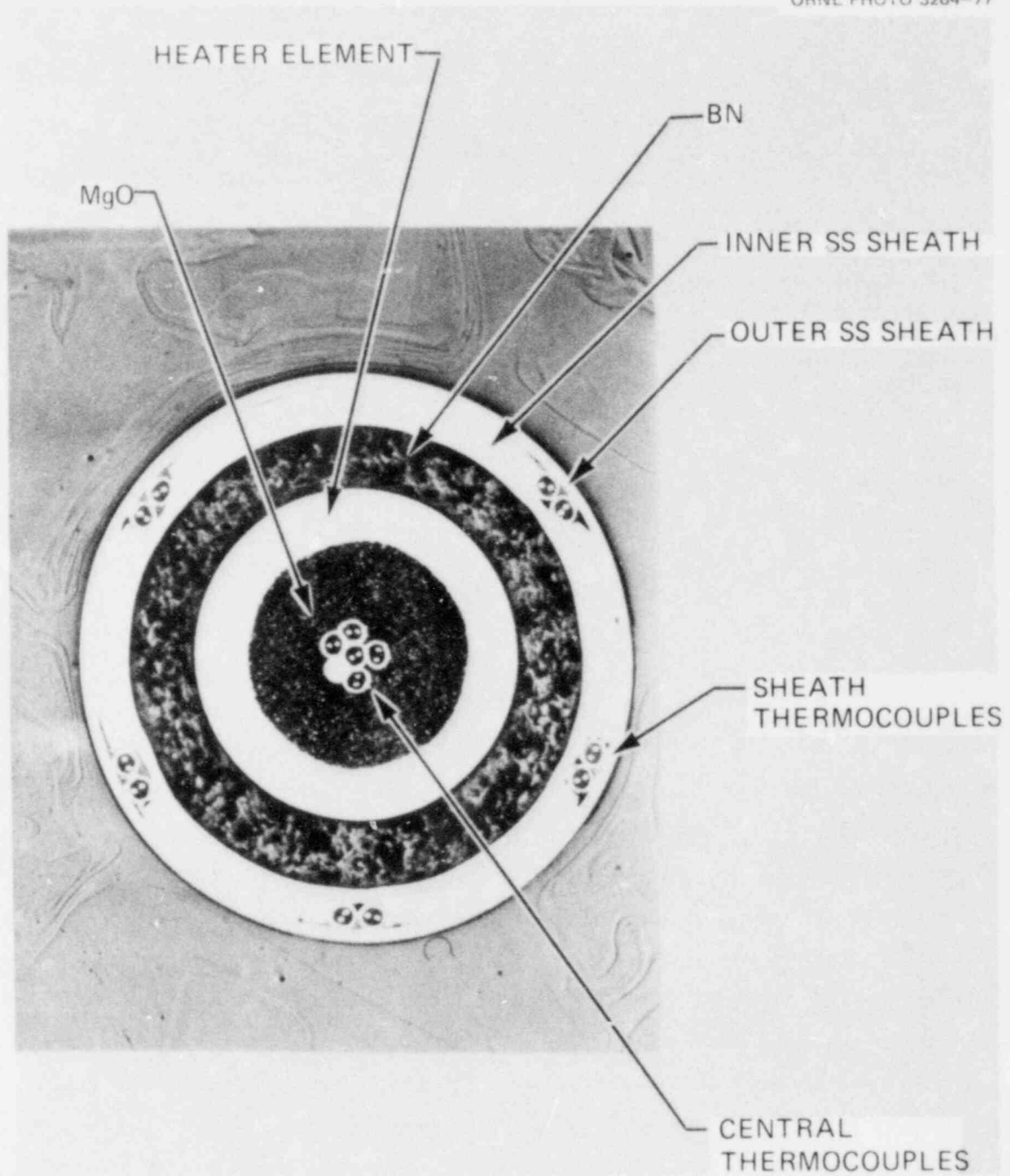


Fig. 1.7. Cross section of BDHT heater 150-5.

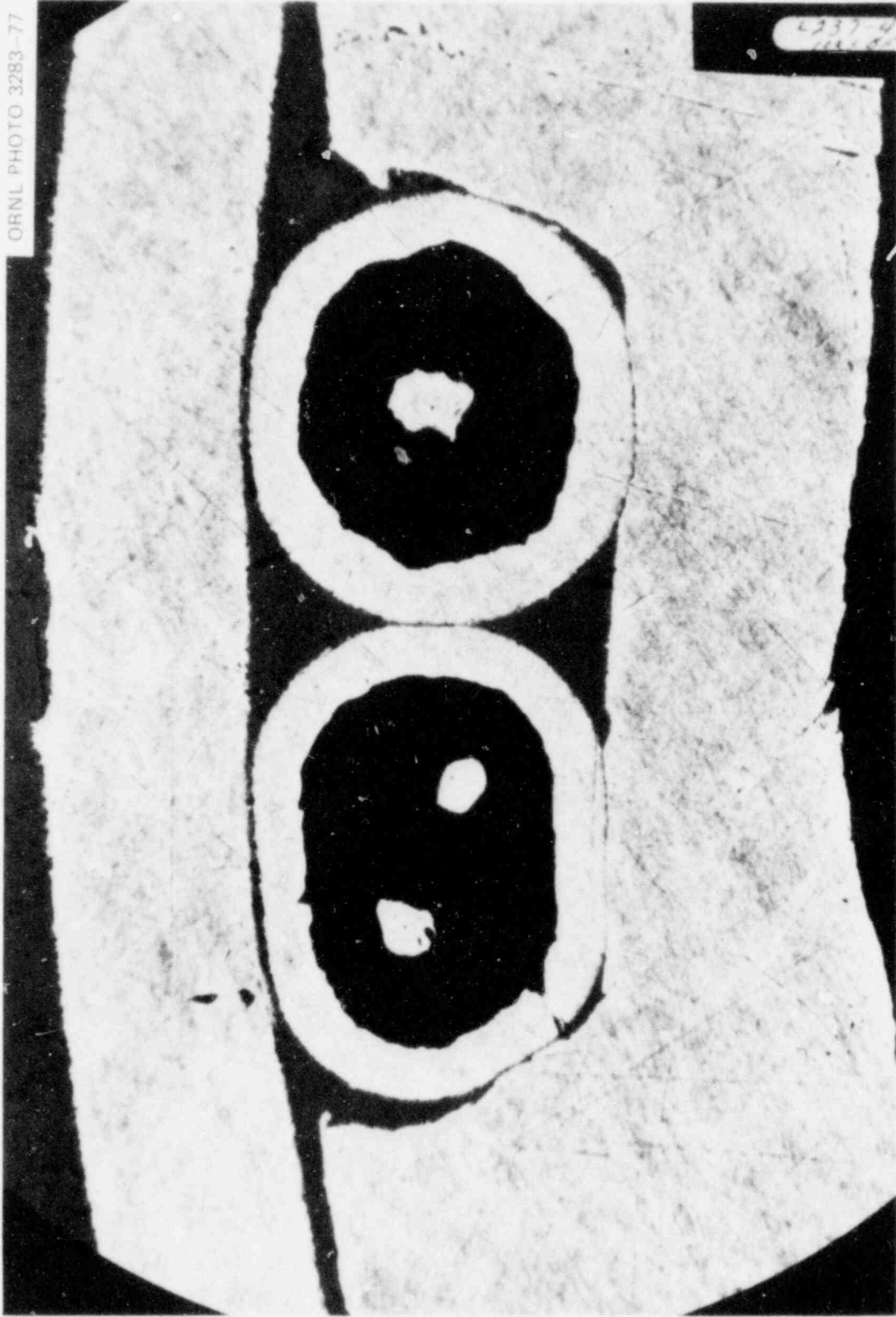


Fig. 1.8. Cross section of sheath thermocouples in BDHT heater 150-5.

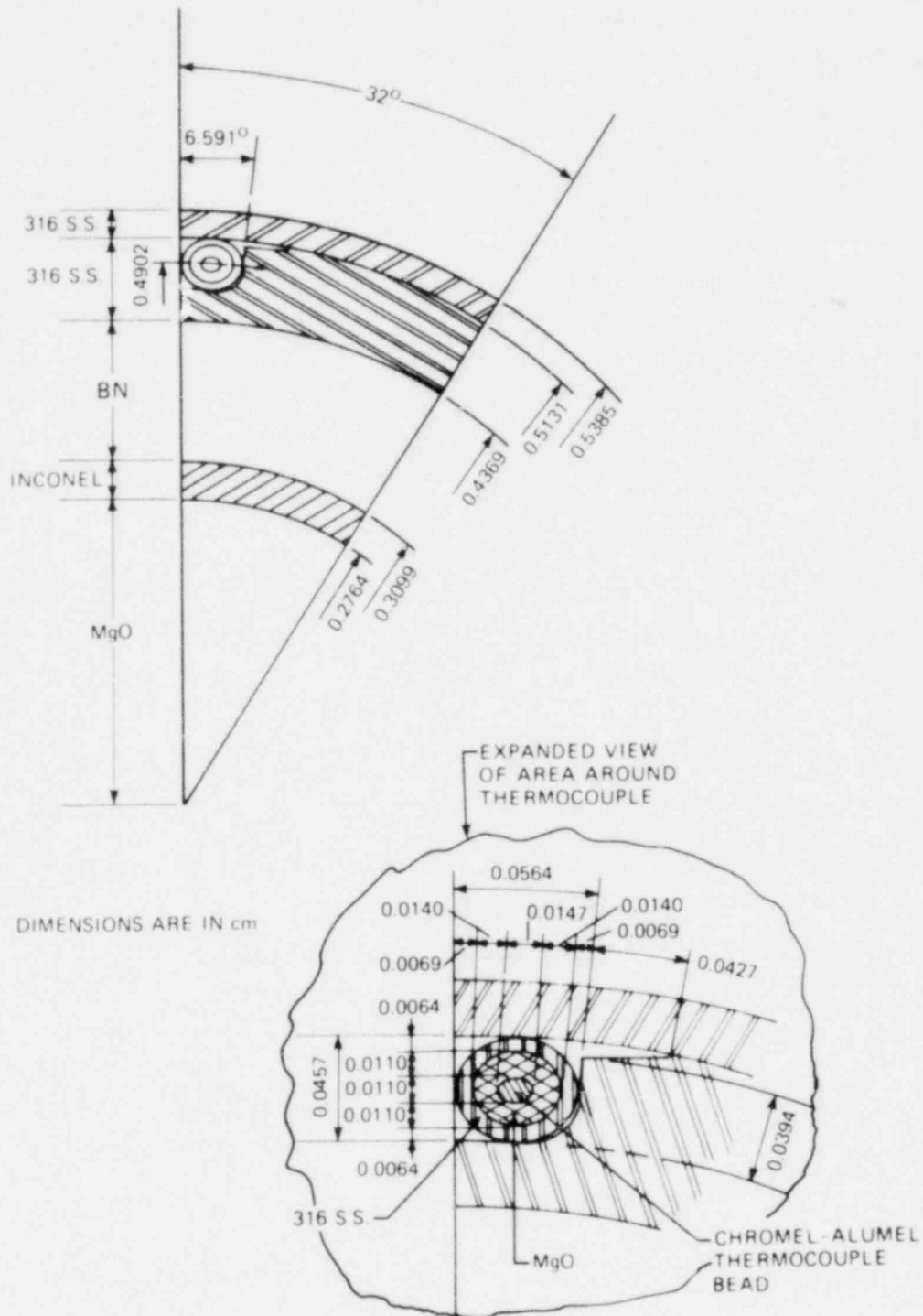


Fig. 1.9. Segment of heater showing mean dimensions in the thermocouple area (1 in. = 2.54 cm).

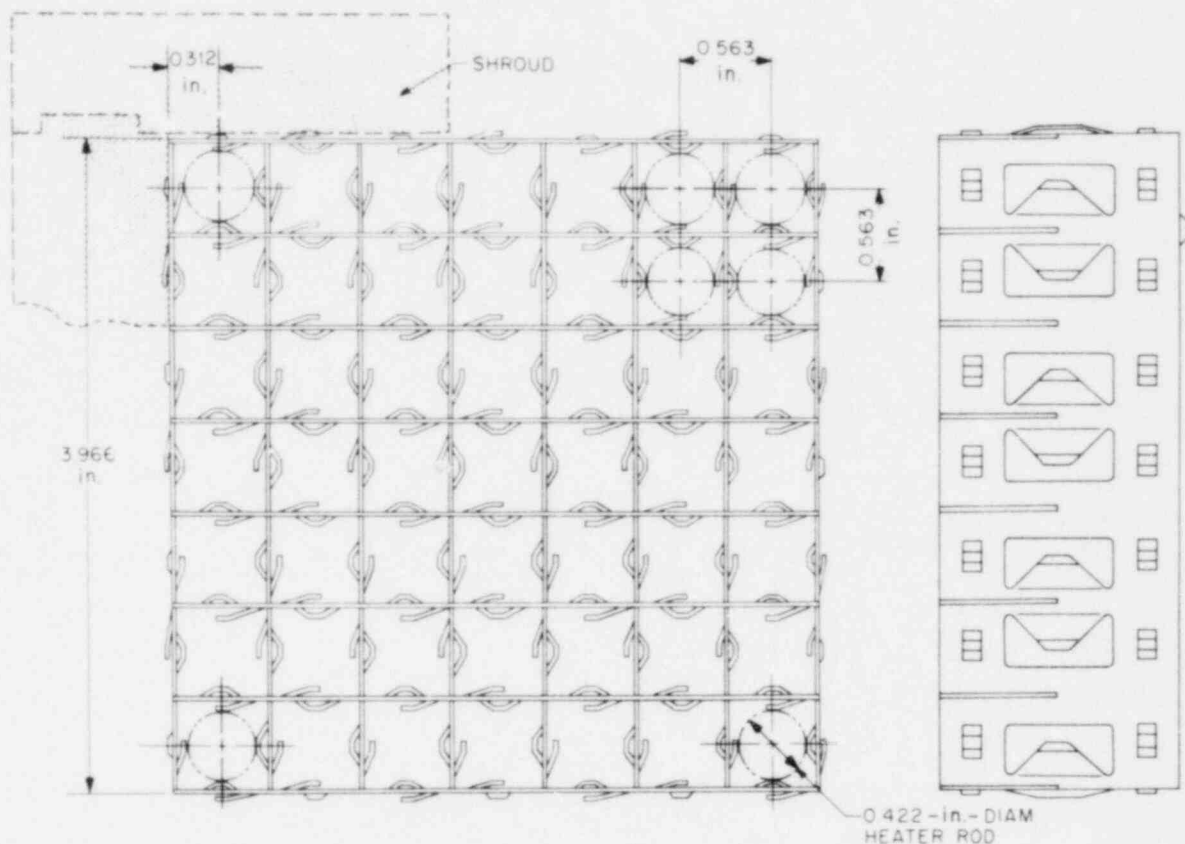


Fig. 1.10. Low-pressure-drop spacer grid assembly (1 in. = 2.54 cm).

approximately 30.48-cm (12-in.) intervals along the box which supports the spacer grids and forms the bundle flow channel. A cross-sectional view of the test section with the shroud box and bundle assembly in place is shown in Fig. 1.11.

The nominal locations of thermocouples, together with locations of power steps and spacer grids, are summarized in Table 1.2. After THTF bundle 1 was assembled, all thermocouples were tested for open circuits; 337 of 348 sheath thermocouples and 75 of 106 center thermocouples were in good condition. The distribution of these thermocouples in bundle 1 is presented in Fig. 1.12; a schematic illustration showing the locations of thermocouples at different levels is given in Fig. 1.13.

Of the available "good" sheath thermocouples, 50 are monitored by a multichannel temperature monitor (metrascope) with the thermal responses visually displayed. The cross-hatched rods in Fig. 1.14 are monitored



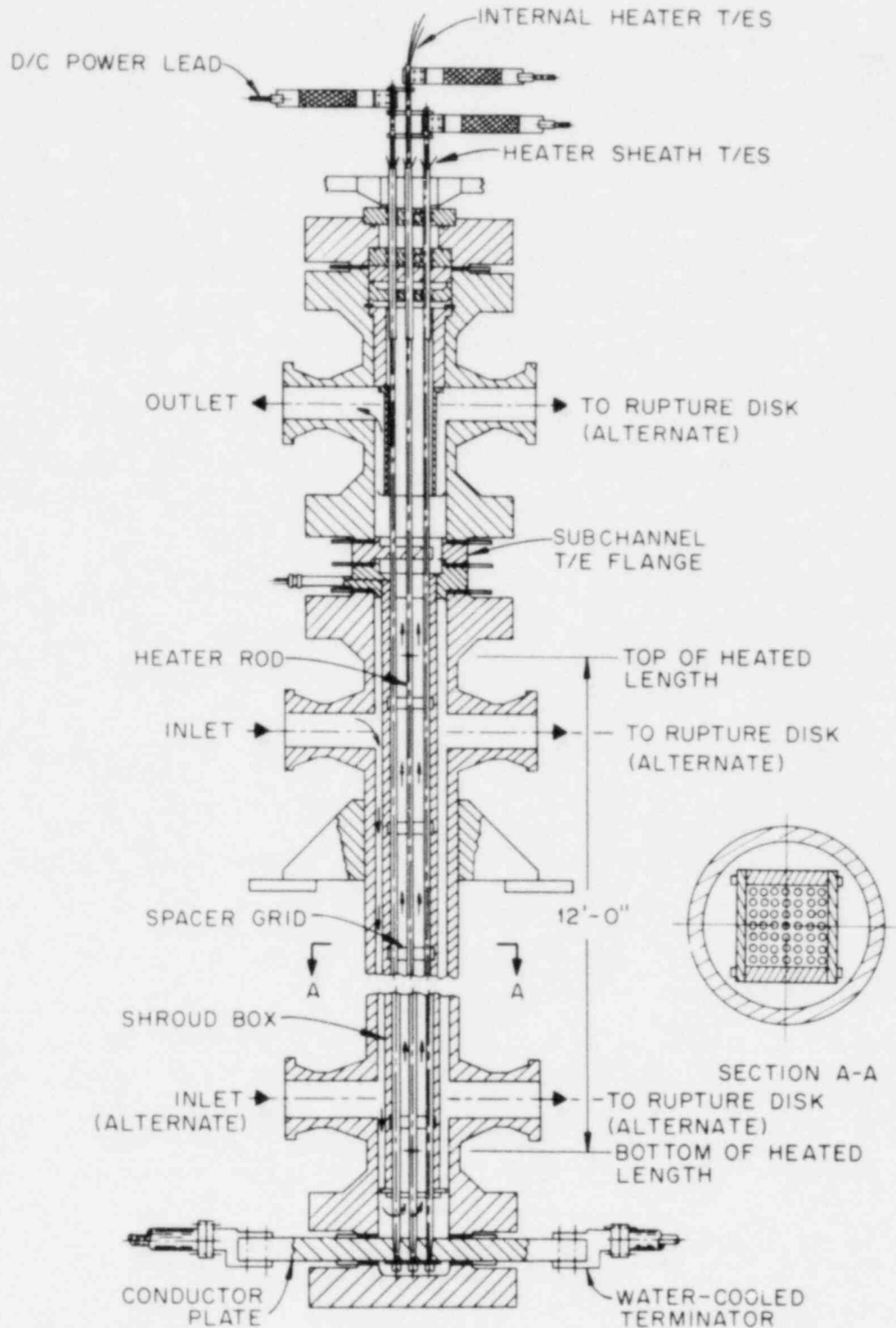


Fig. 1.11. Test section using indirect heater rod in 49-rod bundle (1 ft = 0.3048 m).

Table 1.2. Nominal location of thermocouples in THTF bundle 1 relative to power zone steps and grid spacers (1 in. = 2.54 cm)

Distance (in.) from lower end of heated zone <sup>a</sup>	Grid spacer location	Nominal power		Thermocouple level
		kW/m	kW/ft	
-3/4 to +3/4	X			
1				A
11 1/2 to 12 5/8	X	14.12	4.30	
13 1/8				B
18				
19		19.95	6.08	
23 to 24 1/2	X			
31 1/2				
34 7/8 to 36 3/8	X			
36 7/8		35.56	10.84	
42				
43				E
45 1/2 to 47	X	42.91	13.08	
54				
55				F
58 5/8 to 60 1/8	X			
70 1/2 to 72	X			
77		55.77	17.0	
82 3/8 to 83 7/8	X			
89				H
90				
93				I
93 1/2 to 95	X	42.91	13.08	
101				J
102				
105 5/8				K
106 1/8 to 107 5/8	X	35.56	10.84	
111 1/2				L
112 1/2				
118 to 119 1/2	X			
125		19.95	6.08	
126				
129 7/8 to 131 3/8	X			
141 1/4		14.12	4.30	
141 3/4 to 143 1/4	X			
144				
145 1/4		1.21	0.37	O

<sup>a</sup>Distances in most cases are nominal and  $\pm 1/4$  in.

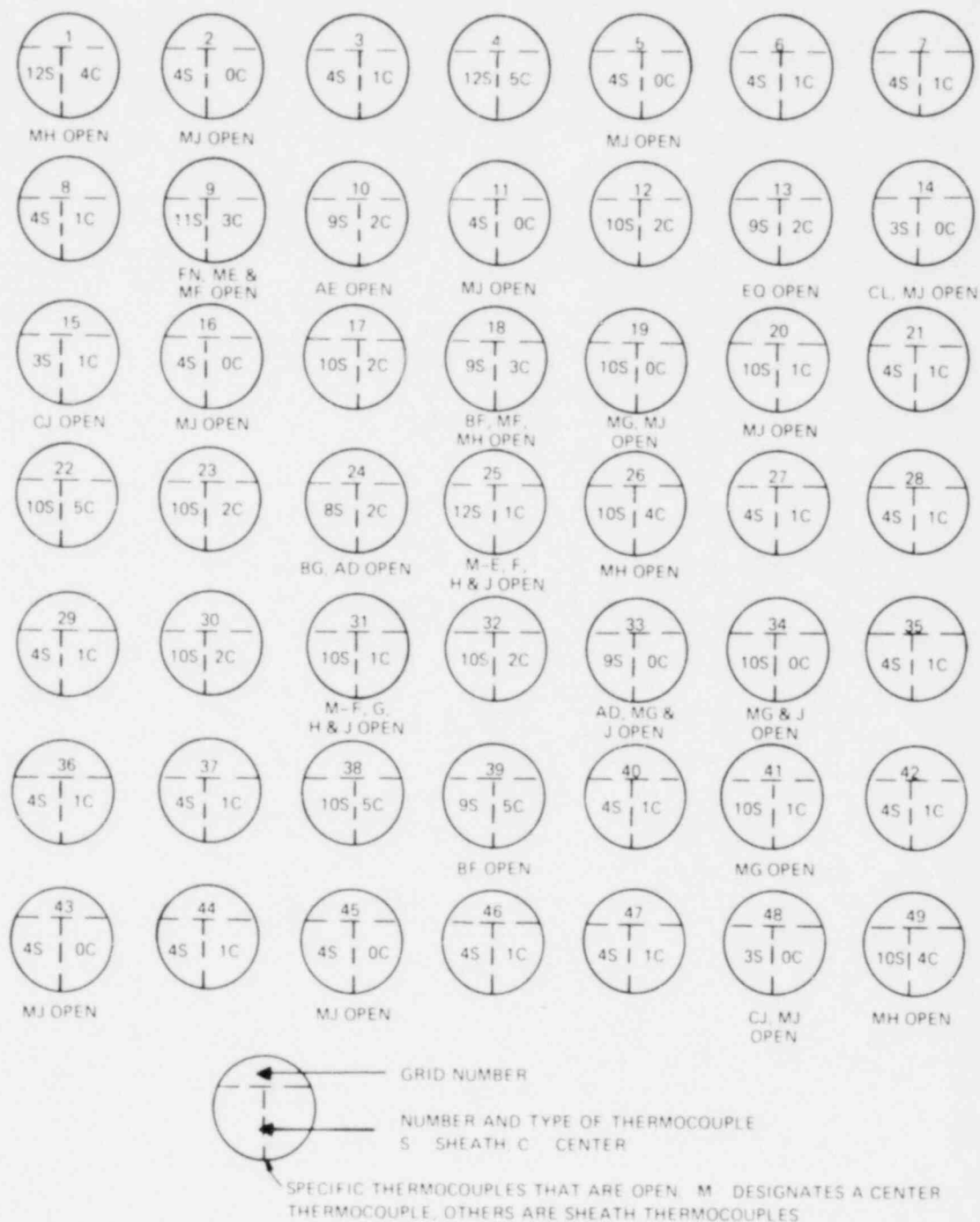


Fig. 1.12. Distribution of thermocouples in THTF test bundle 1 (May 24, 1976).

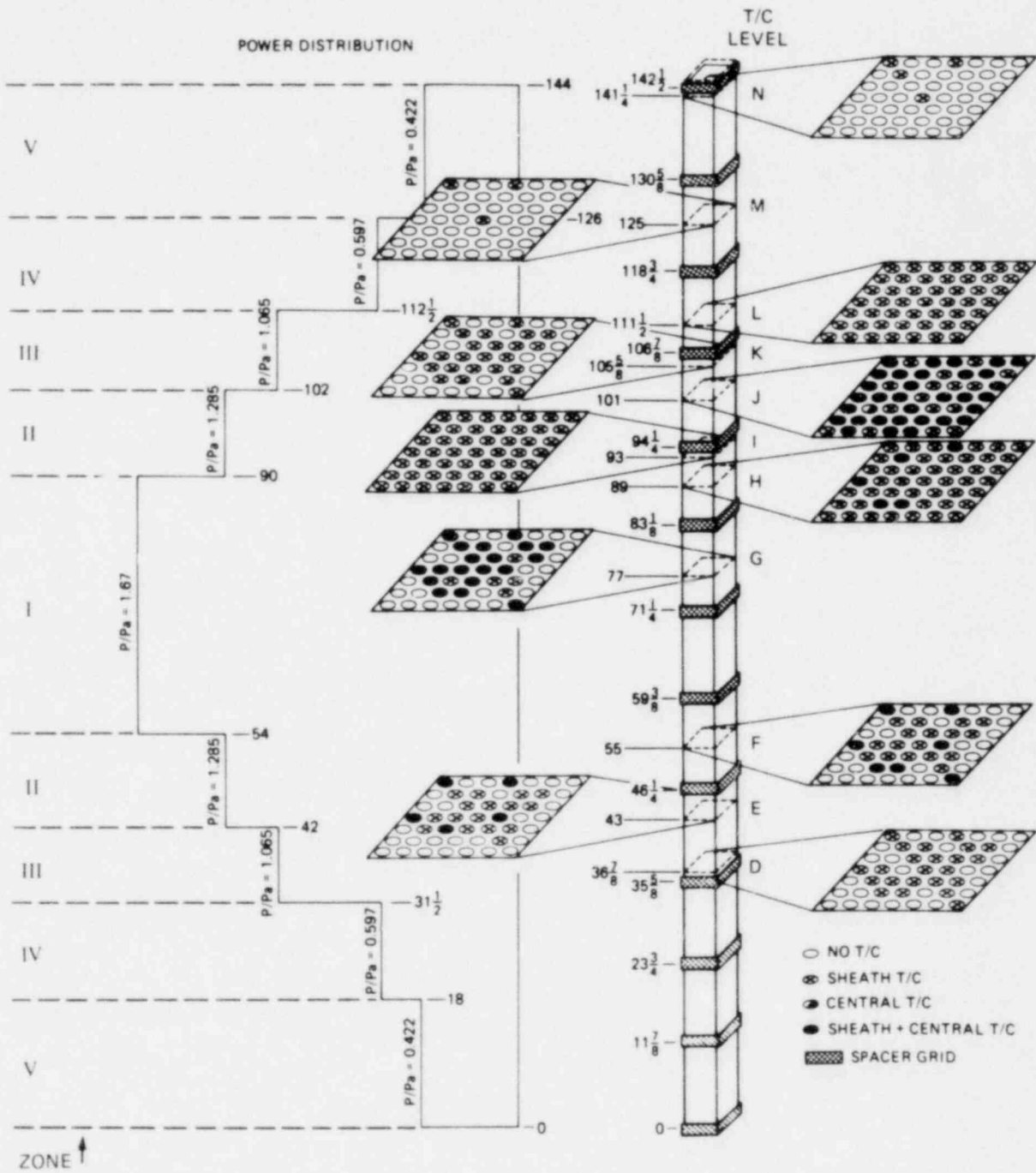


Fig. 1.13. Location of thermocouples in THTF bundle 1 (1 in. = 2.54 cm).

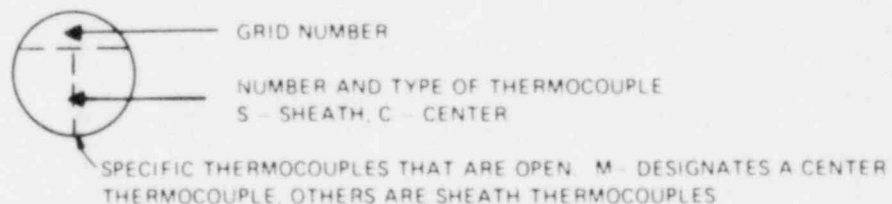
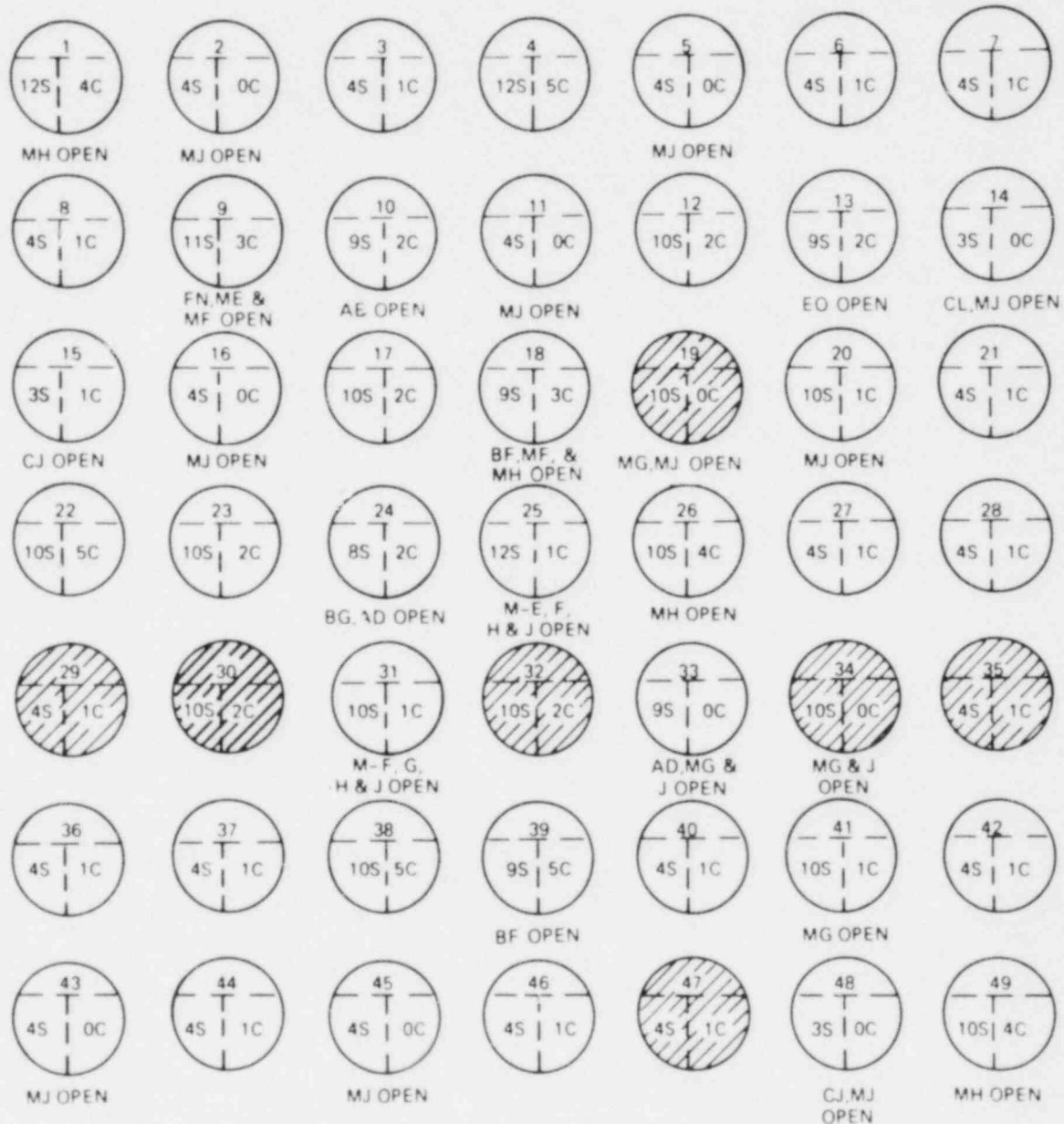


Fig. 1.14. THTF test bundle 1 rods monitored by metrascope (shown by cross hatching).

by the metrascope. Also, there are 19 thermocouples on level 0 for which the inverse model in ORINC<sup>4</sup> is not applicable. Therefore of the thermocouples scanned by the computer-controlled data acquisition system (CCDAS), inverse calculations can be made for 266 possible positions in bundle 1.

#### 1.4.1 Radial dimensions<sup>4</sup>

For the inverse model and calculations and the calibration codes, the internal radial dimensions of the heater rod must be as accurate as possible. However, because of the rod manufacturing procedure, these dimensions are not readily available (i.e., as specifications or in any published form). The following description of the manufacturing procedure clarifies the reasons for this problem. The internal thermocouple cluster and a piano wire stiffener are inserted into the Inconel tube, and MgO cores are inserted over the thermocouple cluster. This assembly is then swaged to a given outer diameter, thus crushing and compacting the MgO. Successive sleeves of Inconel or Cupronickel are swaged over the base tube to a uniform outside diameter (further compacting the core and elongating the assembly). The finished heater assembly is placed inside the inner stainless steel sheath, and BN powder is poured into the annular region and compacted. After another swaging operation, the grooves are milled in the surface. The sheath thermocouples are subsequently tack-welded in the grooves and filler rods are added; this assembly is inserted in the outer sheath for the final swaging operation. Each swaging operation compacts (and elongates) the ceramic insulators and thins (and elongates) the metallic annular regions of the assembly.

The Y-12 Development Division Metallurgical Department measured the internal dimensions<sup>5</sup> of the cross sections of BDHT heater 150-5. The radial dimensions used by ORINC and the calibration codes for THTF bundle 1 are given in Table 1.3 (see Fig. 1.13 for zone designations).

#### 1.4.2 Physical properties of components<sup>4</sup>

The inverse model and calibration codes require the following physical properties for each component in the heater rod: density  $\rho$ , thermal conductivity  $k$ , and specific heat  $C_p$ .

Table 1.3. Radial dimensions of THF heater (1 in. = 2.54 cm)

Zone (refer to Fig. 1.13)	MgO outer diam [cm (in.)]	Base Inconel thickness [cm (in.)]	1st Inconel oversleeve thickness [cm (in.)]	2nd Inconel oversleeve thickness [cm (in.)]	1st Cu-Ni oversleeve thickness [cm (in.)]	2nd Cu-Ni oversleeve thickness [cm (in.)]	BN thickness [cm (in.)]	Inner SS sheath thickness [cm (in.)]	Outer SS sheath thickness [cm (in.)]
I	0.5527 (0.2176)	0.0335 (0.0132)					0.1270 (0.0500)	0.0762 (0.0300)	0.0254 (0.0100)
II	0.5319 (0.2094)	0.0340 (0.0134)	0.0099 (0.0039)				0.1270 (0.0500)	0.0762 (0.0300)	0.0254 (0.0100)
III	0.5126 (0.2018)	0.0348 (0.0137)	0.0099 (0.0039)	0.0089 (0.0035)			0.1270 (0.0500)	0.0762 (0.0300)	0.0254 (0.0100)
IV	0.4831 (0.1902)	0.0356 (0.0140)	0.0099 (0.0039)	0.0089 (0.0035)	0.0140 (0.0055)		0.1270 (0.0500)	0.0762 (0.0300)	0.0254 (0.0100)
V	0.6552 (0.2579)	0.0356 (0.0140)	0.0099 (0.0039)	0.0089 (0.0035)	0.0140 (0.0055)	0.0140 (0.0055)	0.1270 (0.0500)	0.0762 (0.0300)	0.0254 (0.0100)
Zone	MgO outer radius [cm (in.)]	Inconel outer radius [cm (in.)]	Cu-Ni outer radius [cm (in.)]	BN outer radius [cm (in.)]	Inner sheath outer radius [cm (in.)]	Outer sheath outer radius [cm (in.)]			
I	0.2764 (0.1088)	0.3099 (0.1220)		0.4369 (0.1720)	0.5131 (0.2020)	0.5385 (0.2120)			
II	0.2659 (0.1047)	0.3099 (0.1220)		0.4369 (0.1720)	0.5131 (0.2020)	0.5385 (0.2120)			
III	0.2563 (0.1009)	0.3099 (0.1220)		0.4369 (0.1720)	0.5131 (0.2020)	0.5385 (0.2120)			
IV	0.2416 (0.0951)	0.2959 (0.1165)	0.3099 (0.1220)	0.4369 (0.1720)	0.5131 (0.2020)	0.5385 (0.2120)			
V	0.2276 (0.0896)	0.2819 (0.1110)	0.3099 (0.1220)	0.4369 (0.1720)	0.5131 (0.2020)	0.5385 (0.2120)			

An extensive literature search<sup>6-17</sup> was conducted to collect the available physical property information for MgO, Inconel-600, Cupronickel, BN, and 316 stainless steel. Except for the thermal conductivities of MgO and BN, the optimum polynomial fit in terms of temperature was determined for the heat capacity and thermal conductivity of each component. These least-squares fits and graphical displays of the fits are presented in Appendix A.

The difficulty in presenting a single curve for the thermal conductivity of MgO is that it is an extreme function of the packed density (porosity) of the ceramic.<sup>6</sup> As stated in Section 1.4.1, the compaction of the MgO core varies according to the axial position in the rod and thus the effective MgO thermal conductivity must be determined in situ.

There are several obstacles to determining BN thermal conductivity: (1) thermal conductivity is a function of the packed density;<sup>9</sup> (2) most of the available data have been collected at temperatures in excess of 1089 K (1500°F), which is outside the range of our application;<sup>6</sup> and (3) the thermal conductivity is dependent on the direction of the molding (or applied) pressure (i.e., the ratio of the conductivity measured perpendicular to the molding pressure to that measured parallel to the molding pressure can be as much as 2).<sup>11</sup> Therefore, the effective BN thermal conductivity must also be determined in situ.

#### 1.4.3 Calibration objectives

Because of rod-to-rod variance in manufacturing, the mechanical and thermal transients involved during a blowdown of the THTF, and changes in bundle response due to "aging," an extensive thermocouple calibration procedure was needed to supply heater rod performance information to the inverse heat conduction model.

The primary purpose of this report is to develop and present an experimental thermocouple calibration procedure and a four-part calibration program, ORTCAL (ORNL Thermocouple Calibration).

Part I of ORTCAL calculates basic gap information such as width and temperature drop and provides the "aging" history of each location. Part II uses temperatures indicated by the sheath and middle thermocouples to produce the effective thermal conductivity of the BN insulator.



Part III produces the effective thermal diffusivity of the MgO insulator, and Part IV uses regression analysis on the output from Part I to determine the expansion coefficients and proper bias points for the stainless steel annuli forming the gap. The mechanical model<sup>4</sup> chosen to utilize this information is one dimensional, which is consistent with the thermal model used in the inverse calculation.

The combined output from ORTCAL is a coefficient data tape which contains the regression and bias information for each thermocouple position in the THIF bundle. This information is then used by ORINC to simulate the thermomechanical response of the heater rod.

## 2. ROD CLASSIFICATION PROCEDURE

### 2.1 Preliminary Notes

#### 2.1.1 Thermocouples

Before describing the experimental and analytical techniques required to determine the sheath gap behavior and the effective thermal conductivities of the insulators, it must be noted that these determinations are in addition to the normal measures taken by the Instrumentation and Controls Division personnel in the calibration of the loop (THTF or FCTF) instrumentation. In essence, these procedures assume that the thermocouples are calibrated, the junction reference boxes are at the correct temperatures, and the temperature indicated by the thermocouple is that of the thermocouple bead.

Considering the mass of thermocouple leads (454) exiting the top of THTF bundle 1, it is not inconceivable that some would be tagged incorrectly (i.e., the thermocouple tagged TE-349BG could be leaving rod 25 rather than rod 49). To verify the location of both sheath and center thermocouples, power was applied to one rod at a time for all 49 rods in the THTF.<sup>18,19</sup>

Given the fact that the rod locations of the thermocouples are known, the actual axial locations of the thermocouples in the rods must be determined in situ. The thermocouple locations given in Table 1.2 are nominal; even though the acceptable tolerances of  $\pm 0.635$  cm (1/4 in.) are tight, it is possible to miss the desired positioning during the manufacturing process. Not only are the powered zone lengths (Table 1.2 or Fig. 1.13) different for each heater, the swaging operations must be allowed for; that is, the manufacturer must allow for the extrusion of the thermocouples and the constituents of the fuel pin simulator during the swaging operations. For example, the initial placement of TE-322ME might be 100 cm above the ground lead and thus end up at 109.8 cm (43 in.) above it after the final swaging operation. It is also possible to create "false" junctions in the thermocouples (especially during the swaging operations); that is, the thermal elements could touch (thus forming a junction) above the thermocouple bead and therefore respond differently

from the remaining thermocouples on that level. In light of these possibilities and the desire to locate level E, F, H, J, and M thermocouples within 2.54 cm of the powered zone breaks (Fig. 1.13 or Table 1.2), the analyst must know the axial position of the effective thermocouple junction. The pin radial dimensions change with axial position; but, more importantly, the axial power peaking factor is a function of the axial position. Therefore, in addition to x rays of the fuel pin simulators, hot and cold water fill tests (using the configuration shown in Fig. 2.1) are conducted with the bundle in place to determine the axial positions of the bundle thermocouples. In short, the fill tests are conducted at atmospheric pressure (the test section is vented at a spare upper plenum outlet), flow to the test section from the standpipe is adjusted to fill the assembly in approximately 10 min, and the test section level and thermocouples are monitored by the CCDAS for approximately 12 min (about the capacity of one tape).<sup>20</sup>

#### 2.1.2 Power peaking factors

The local axial power peaking factor is defined by

$$PFA_i = P_i / P_a , \quad (2.1)$$

where  $P_i$  is the local linear power generation rate and  $P_a$  is the average linear power generation rate. This approach to the calculation of  $P_i$  is taken because the determination of  $P_a$  by Eq. (2.2) is simple and straightforward:

$$P_a = I_s (V_G / L_{\text{active}}) , \quad (2.2)$$

where  $I_s$  is the shunt amperage,  $V_G$  is the generator voltage, and  $L_{\text{active}}$  is the active heated length of the fuel pin simulator. However, values for  $PFA_i$  and  $L_{\text{active}}$  from Tables 1.1 and 1.2 and Fig. 1.13 cannot be used since they are design values and are nominal. The  $PFA_i$  must be determined individually for each zone of each fuel pin simulator since the electrical resistance  $R_i$  and length  $L_i$  of each zone varies from rod to rod. For instance, the peaking factor in the high-power zone (I in Fig. 1.13 or 2.2) varies from 1.648 to 1.709 in bundle 1 with a mean of

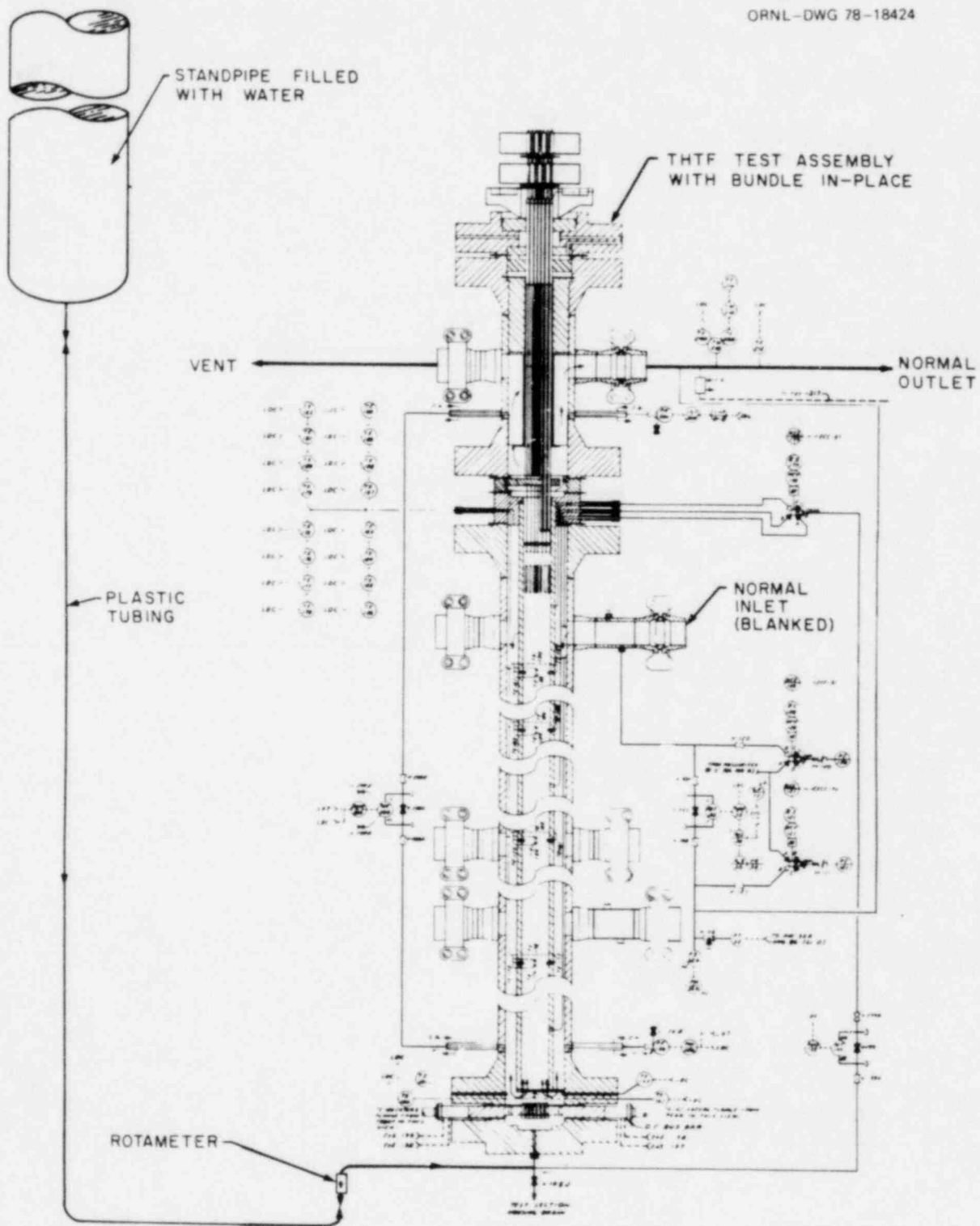


Fig. 2.1. Fill test configuration.

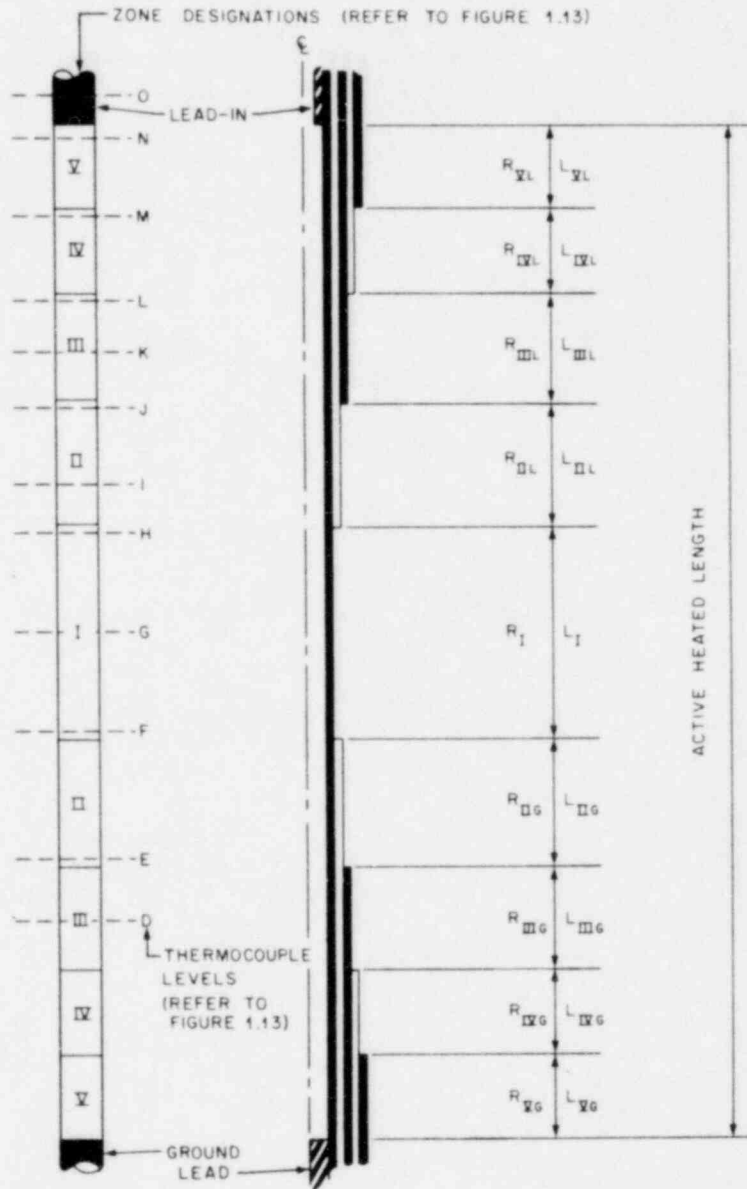


Fig. 2.2. Fuel pin simulator zone designations with thermocouple levels (bundle 1) and enlarged active component assembly.

1.679 and a standard deviation of 0.012. This is not as formidable a task as it would appear, since the data required to make the calculations ( $R_i$ ,  $L_i$  pairs - see Fig. 2.2) were taken on the BDHT inspection reports for each swaged active-component assembly (ACA). Referring to Fig. 2.2, the overall resistance ( $R_0$ ) for the ACA can be determined by

$$R_0 = \sum_{i=VG,VL} L_i R_i . \quad (2.3)$$

Also, the total active heated length is given by

$$L_{\text{active}} = \sum_{i=VG,VL} L_i , \quad (2.4)$$

and the average resistance per foot of active heated length is given by

$$\bar{R} = R_0 / L_{\text{active}} . \quad (2.5)$$

Therefore, the local axial power peaking factor for each power step of the heater is calculated by

$$PFA_i = R_i / \bar{R} , \quad (2.6)$$

for  $i = VG, VL$ .

### 2.1.3 Experiments

Two types of techniques can be used to generate the data required to classify the heater rods. Data from steady-state experiments at different boundary conditions (i.e., varying power generation rate and rod surface temperature) can be reduced to yield the desired gap information and the effective thermal conductivity of the BN insulator. Power drop tests ("controlled" transients) can be performed to determine the effective thermal diffusivity of the MgO core. It is assumed that centerline thermocouples exist in tandem with sheath thermocouples - that is, the rod centerline temperature *must* be monitored at the same axial position as that of the sheath thermocouple if the heater is to be fully classified. Without the centerline thermocouple, *only* the gap information can

be extracted from calibration tests. The consequence of not knowing the in-situ thermal conductivity of BN and the thermal diffusivity of MgO and thus having to use literature relationships for these functions will be discussed in Chapter 3.

The heat sink temperature range over which the experimental calibration runs should be made is largely dependent on the facility. As an upper limit (this is a function of the core flow rate, core inlet temperature, and pressure) the entire rod (at least during initial calibration runs) should be maintained in the forced convection heat transfer regime. This conclusion is based on surface heat flux perturbation studies<sup>21</sup> for the BDHT heaters using HEATING5 (Ref. 22), primarily a two-dimensional (R- $\theta$ ) study of the flux perturbation caused by thermocouples between the sheaths and the 0.038-cm (0.015-in.) heater eccentricity<sup>23</sup> (maximum allowable eccentricity in the manufacturing specifications for bundle 1 BDHT heaters). Figure 2.3, which contains the results of that study along with a schematic of the cross section of the pin modeled, shows a surface flux skew of  $\sim 28\%$ . If the rod were in forced convection, the variation in the surface temperature would be  $\sim 11.7$  K ( $21^\circ\text{F}$ ); however, if the rod were in nucleate boiling, the variation would be only  $\sim 1.2$  K ( $2.2^\circ\text{F}$ ). Given the standard deviation of the temperature measurement of 2.4 K ( $4.3^\circ\text{F}$ ), *it is not possible* to determine whether the heating element is eccentric in relation to the sheaths if the rod is in the nucleate boiling regime. Therefore, for initial calibration runs, the entire rod should be maintained in the forced convection heat transfer regime.

The lower limit of the heat sink temperature range also depends on the facility. The FCTF is more or less limited by the capability of the loop heat exchanger to remove the core and pump energy input into the primary fluid. Initial calibration runs in the FCTF start with a core primary inlet temperature of 422 K ( $300^\circ\text{F}$ ), which is maintained by the loop exchanger up to a core power input of  $\sim 100$  kW. Above this power level, controlling the primary core inlet temperature at 422 K by manipulating the secondary flow to the exchanger becomes exceedingly difficult, and the temperature is allowed to climb.

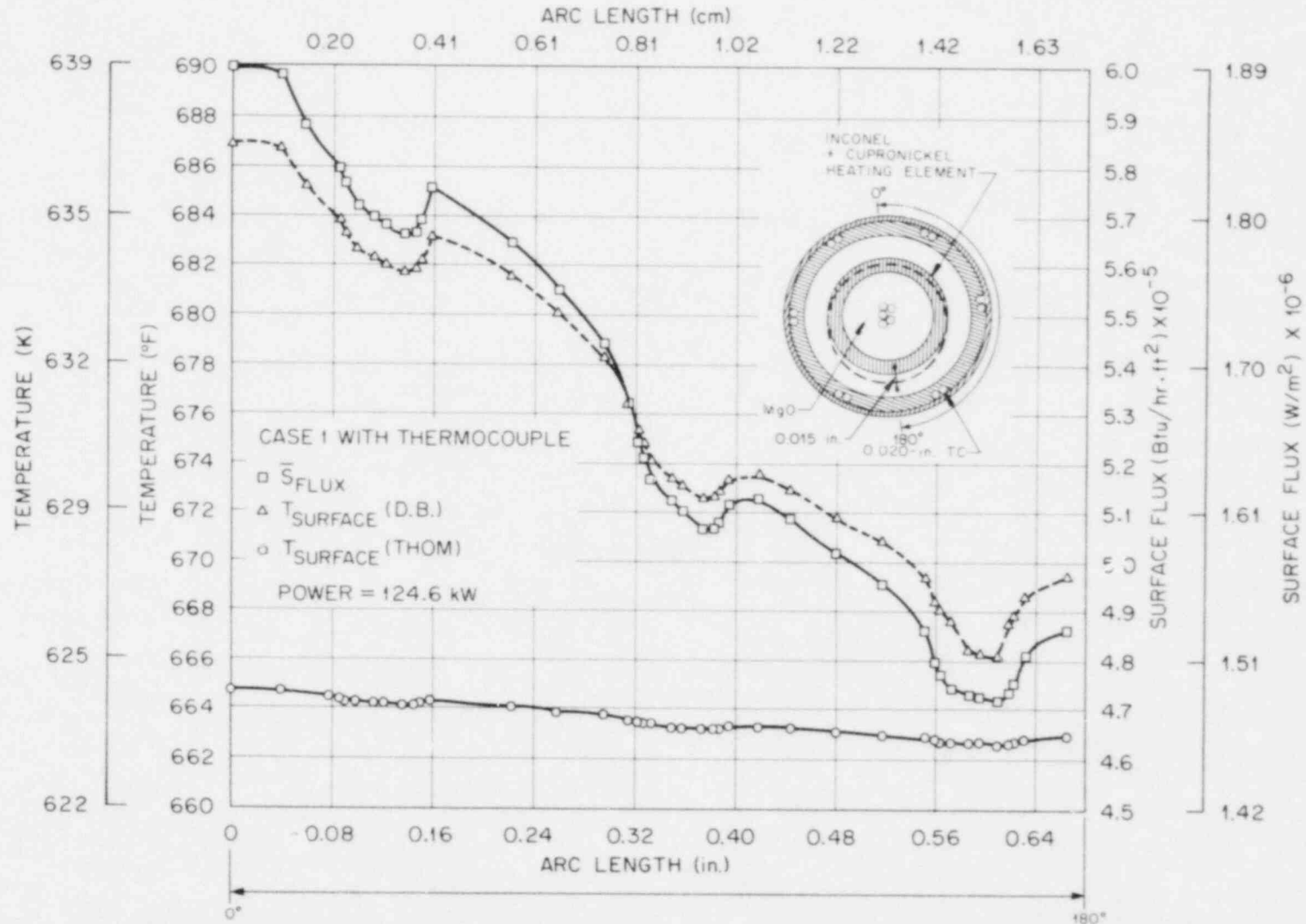


Fig. 2.3. Surface heat flux perturbation due to thermocouple presence and 0.015-in. heater eccentricity.



In the THTF, the lower limit of the heat sink temperature for calibration runs is set by the type (i.e., direct current) of power used by the core. In early 1976, during the first applications of power to bundle 1, temperatures indicated by the core Chromel/Alumel thermocouples were in error by about  $\pm 150\%$  at 373 K. Studies<sup>24,25</sup> showed that these large errors could be attributed to an interaction of the temperature gradient and the magnetic field imposed on the thermocouples - the Ettingshausen-Nernst effect - which produces an electromotive force (emf) in a conductor, such as a thermocouple, placed in a magnetic field and a temperature gradient which are both transverse to the length of the conductor. These thermometry errors in the THTF core disappeared above  $\sim 423$  to 439 K (300-330°F), the Curie temperature of Alumel at which a material transforms from the ferromagnetic to the paramagnetic state; however, these thermometry errors do not occur when ac power (as in the FCTF) is used rather than dc power. With ac power, both the magnitude and direction of the magnetic field oscillate; therefore, the Ettingshausen-Nernst emf appears as an oscillating emf on the thermocouple output and is removed by the filters of the data acquisition system. In the THTF facility, the initial calibration points start at a core inlet temperature of  $\sim 478$  K (400°F), which is 39 to 55 K above the Curie temperature of Alumel.

As a final note, only calibration scans above the 30 kW/rod power level are used for the regression runs. In essence, at 10 kW/rod, the approximate temperature difference between the temperature indicated by the sheath thermocouple and that of the middle thermocouple is 13.9 K (25°F) for zones I and II in Fig. 2.2. This is of the same magnitude as the combined three standard deviations of the two temperature measurements, 14.3 K (25.7°F). Therefore, the 30-kW/rod power level was chosen as the minimum calibration scan to be included in the regressions. At a nominal 30 kW/rod, the approximate indicated temperature differences between sheath and middle thermocouples are 35 K (63°F) for zone II and 48 K (86.4°F) for zone I.

## 2.2 ORTCAL - Part I

### 2.2.1 Production and description of the "statistics" tape read by ORTCAL - Part I

During the approach to test power in the THTF, the operating checklist given in Appendix B is applicable (effective for tests after 166S for bundle 1); the checklist applies to the sequence, the type, and the number of computer scans to be taken. The operation log and/or T/C scan files are used for steady-state calibration points.

The steady-state files on the raw data tape are processed by a series of conversion codes and finally by a statistics code; the end product from data management is a statistics tape of the steady-state calibration points which consists of 1000-word block files (one file per calibration point). The first 500 words of each block contain the mean engineering-units responses of the instruments monitored by the CCDAS, and the second 500 words contain the standard deviations of those responses.

More flexibility is allowed in the FCTF operations. The calibration checklist for the FCTF is shown in Appendix B. However, the data processing is the same as for the THTF, and the end product is again a statistics tape which is read and processed by the FCTF version of ORTCAL - Part I.

The following discussion on Part I of ORTCAL pertains to the bundle 1 THTF configuration and the CCDAS; however, the code logic, structure, and purpose are independent of the loop configurations and are readily adaptable for instrumentation changes, loops, pin designs, etc.

### 2.2.2 Code logic and methods used

Given a statistics tape containing a number of steady-state calibration points, ORTCAL (Part I) reads one file at a time. The code computes the core coolant flow rate from a core heat balance and the local fluid conditions (i.e., bulk temperature, saturation temperature, and pressure) for each thermocouple level; subsequently, the heat transfer coefficient, heat transfer regime, pin radial gap, and pin temperature profile are determined for each bundle thermocouple position. All this information is accumulated on an updated ORTCAL thermocouple history tape (i.e., the

information from the tape is added to the information on an old ORTCAL thermocouple history tape). The information flow is shown in Fig. 2.4. The information contained on the history tapes is shown in Table 2.1, and examples of the abbreviated output (for thermocouple positions TE-318BG and TE-301DJ) are presented in Appendix C.

Given the precision of the flow measurements in the THTF,<sup>26</sup> it is fortunate that there are redundant measurements of the electric core coolant inlet-outlet temperatures. This redundancy allows the computation of the mean fluid core inlet temperature ( $\bar{T}_{in}$ ) from up to 7 sensor responses and the mean fluid core outlet temperature ( $\bar{T}_{out}$ ) from up to 35 sensor responses. The core plenum pressures ( $P_{in}$  and  $P_{out}$ ) can be determined from PE-201 and PDE-200 (or PE-201 and PE-156, or PE-156 and PDE-200). Therefore, knowing that the fluid is subcooled and knowing the temperature and pressure at the core inlet and outlet, one can determine the fluid core inlet and outlet enthalpies ( $H_{in}$  and  $H_{out}$ ) by a simple state search. The total power input to the core can be calculated from

$$TP_{core} = \sum_{i=1,49} I_{S_i} V_{G_i} . \quad (2.7)$$

Thus, the core flow rate is

$$F_{core} = TP_{core} / (H_{out} - H_{in}) . \quad (2.8)$$

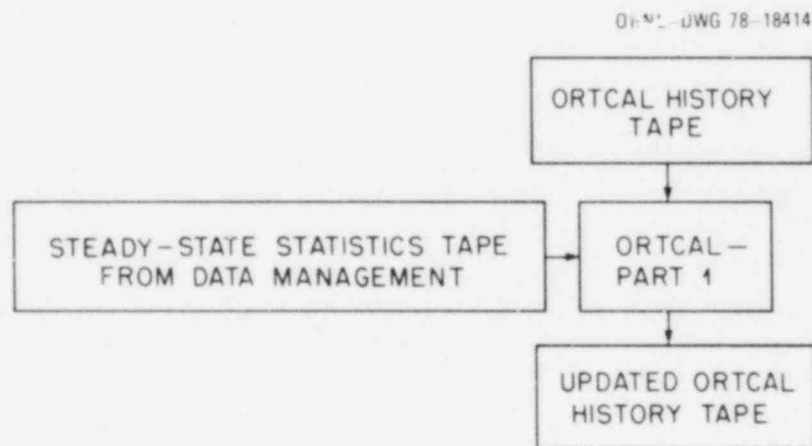


Fig. 2.4. Updated ORTCAL thermocouple history tape.

Table 2.1. Information contained on an ORTCAL thermocouple history tape<sup>a</sup>

Entry <sup>b</sup>	Description
IT(1)	Day of year
IT(2)	Number of hours since last day
IT(3)	Number of minutes since last hour
IT(4)	Number of quarter-seconds since last minute
F(1)*	Nominal power input to electrical pin (kW)
F(2)	Electrical current to pin (A)
F(3)	Generator voltage (V)
F(4)	Average power output (Btu/sec/ft)
F(5)*	Bundle inlet temperature (°F) [averaged from bottom flange TE(4) and TE-162, -24, -172]
F(6)*	Bundle outlet temperature (°F) [averaged from subchannel TE(32) and TE-222, -212, -40]
F(7)*	Upper plenum pressure from PE-201 (psia)
F(8)	Core inlet pressure from PE-156 (psia)
F(9)*	Calculated local bulk fluid pressure (psia)
F(10)*	Calculated local bulk fluid temperature (°F)
F(11)*	Calculated local saturation temperature (°F)
F(12)*	Core coolant flow rate (lb <sub>m</sub> /sec) (calculated from heat balance on core)
F(13)*	Core coolant flow rate at inlet (gpm) [calculated from F(12) and fluid specific volume]
F(14)	Core coolant flow rate at inlet (gpm) (observed on either FE-19 or FE-166)
F(15)	Core coolant flow rate at outlet (gpm) [calculated from F(12) and fluid specific volume]
F(16)*	Sheath thermocouple response (°F)
F(17)*	Middle thermocouple response (°F) (if middle T/C is not on CCDAS during given run or does not exist, zero is entered)
F(18)	Calculated last node temperature in inner stainless steel sheath (°F)
F(19)	Calculated first node temperature in outer stainless steel sheath (°F)
F(20)*	Temperature difference across gap between sheaths (°F)
F(21)*	Surface heat transfer coefficient (Btu/hr·ft <sup>2</sup> ·°F)
F(22)*	Surface heat flux (Btu/hr·ft <sup>2</sup> )
F(23)*	Mode of heat transfer at surface (i.e., forced convection or nucleate boiling)
F(24)*	Calculated gap between sheaths (mils of an inch)
F(25)–F(30)	Extra locations, loaded as zeroes

<sup>a</sup>Information available on the tape generated by ORTCAL.

<sup>b</sup>The entries are entered on the tape for each sheath thermocouple on the CCDAS during a given calibration run; the starred items are presented in the subsequent abbreviated paper output.

The local bulk fluid temperature is computed at each thermocouple level from

$$T_{\text{local}} = \bar{T}_{\text{in}} + \left[ \frac{\sum_{i=1,49} \int_0^{\ell_{\text{local}}} \text{PFA}_i(\ell) P_{a_i} d\ell}{\sum_{i=1,49} \int_0^{\ell_{\text{total}}} \text{PFA}_i(\ell) P_{a_i} d\ell} \right] (\bar{T}_{\text{out}} - \bar{T}_{\text{in}}), \quad (2.9)$$

where  $\ell$  is the heated length of the fuel pin simulator referenced to 0 at the ground end. The local fluid pressure is calculated by

$$P_{\text{local}} = P_{\text{in}} - \left( \frac{\ell_{\text{EQIN-LOCAL}}}{\ell_{\text{EQIN-OUT}}} \right) (P_{\text{in}} - P_{\text{out}}), \quad (2.10)$$

where  $\ell_{\text{EQIN-LOCAL}}$  is the equivalent distance from PE-156 to the thermocouple level and  $\ell_{\text{EQIN-OUT}}$  is the equivalent distance from PE-156 to PE-201.<sup>27</sup> The local saturation temperature is determined by interpolation from tables, given the local fluid pressure.

From the local fluid conditions (i.e., bulk temperature and pressure, saturation temperature, and mass flow) at each thermocouple level and the local power generation rate (i.e.,  $\text{PFA}_{\text{local}} \times P_a$ ) at each bundle thermocouple position, one can now determine the local heat transfer coefficient, heat transfer regime (either forced convection or subcooled nucleate boiling), pin radial gap, and pin temperature profile.

Consider the schematic of the fuel pin simulator in Fig. 2.5 with attention to the inset, in which the continuous homogeneous substrates (i.e., outer sheath, inner sheath, BN insulator, etc.) are handled better mathematically if the continuous domains are replaced by a pattern of discrete points (nodes) within the domains. The technique is consistent with the ORINC deviations;<sup>4</sup> briefly, the substrates are divided into a finite number of equal subvolumes and the centers of mass of the subvolumes are defined as the nodal points. The temperature of a subvolume is associated with its center of mass. A clearer understanding of the element notation can be gained by referring to Figs. 2.6 and 2.7.

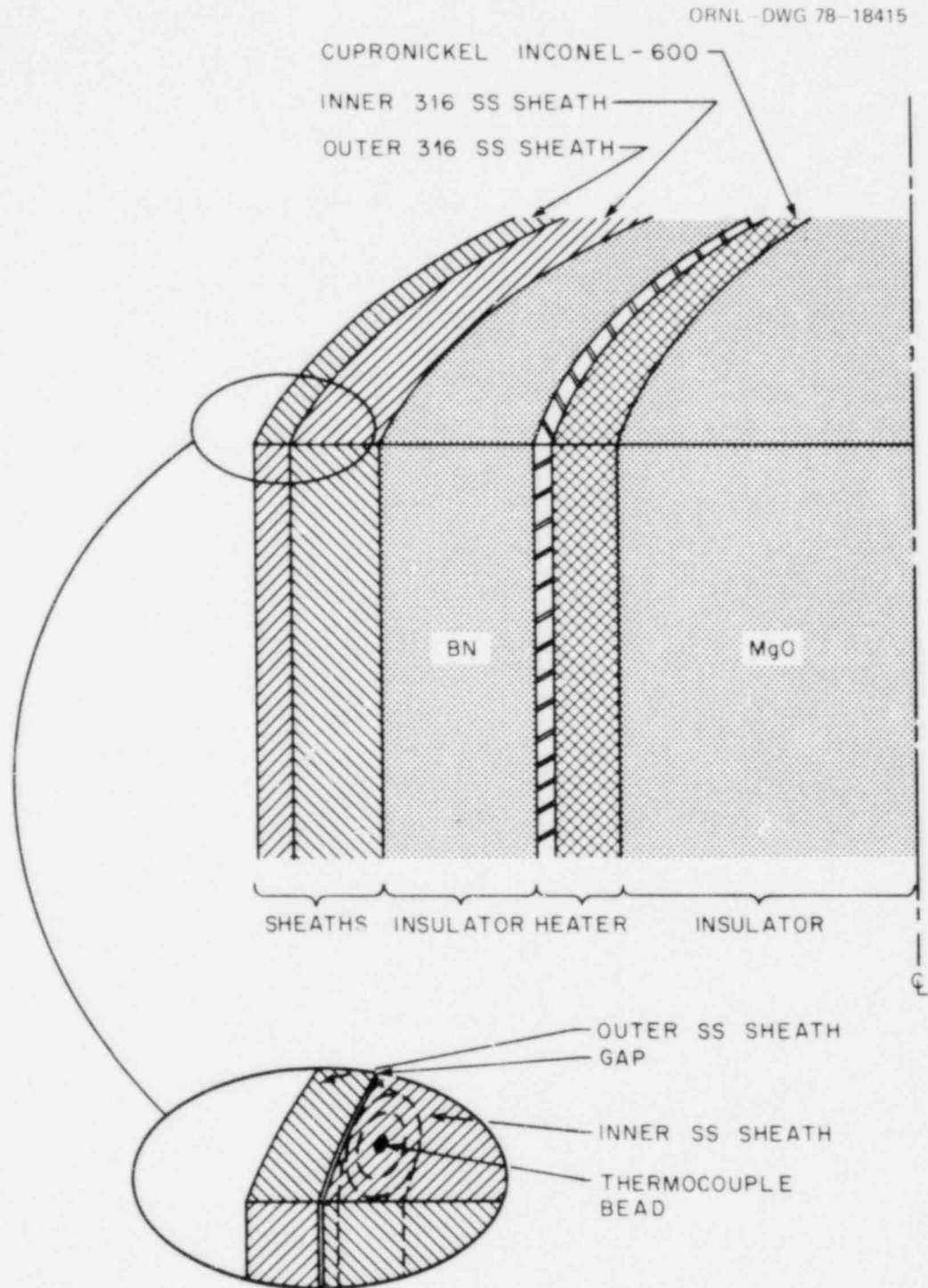


Fig. 2.5. Schematic of fuel pin simulator with inset showing thermocouple and groove superimposed on solid inner stainless steel sheath.

ORNL-DWG 77-12761R2

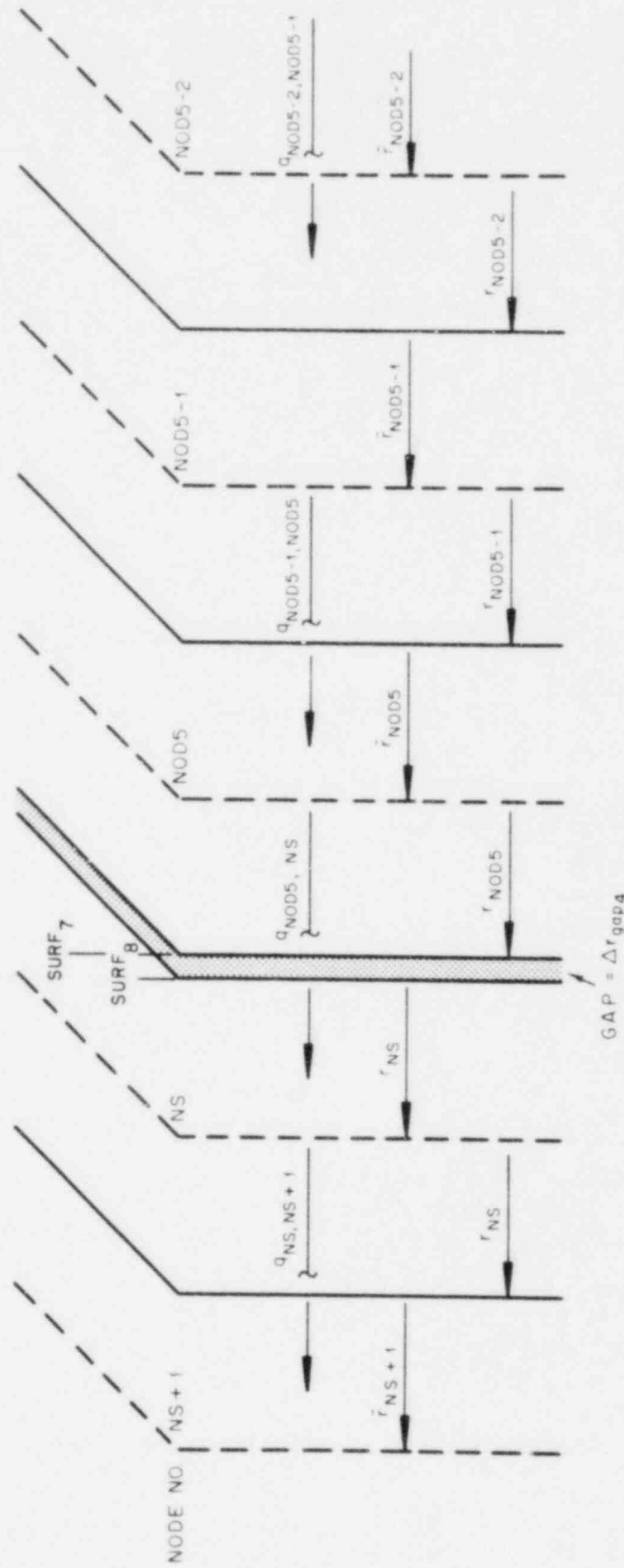


Fig. 2.6. Notation relative to the derivation of the heat transfer model at the interface of the inner and outer stainless steel sheaths.

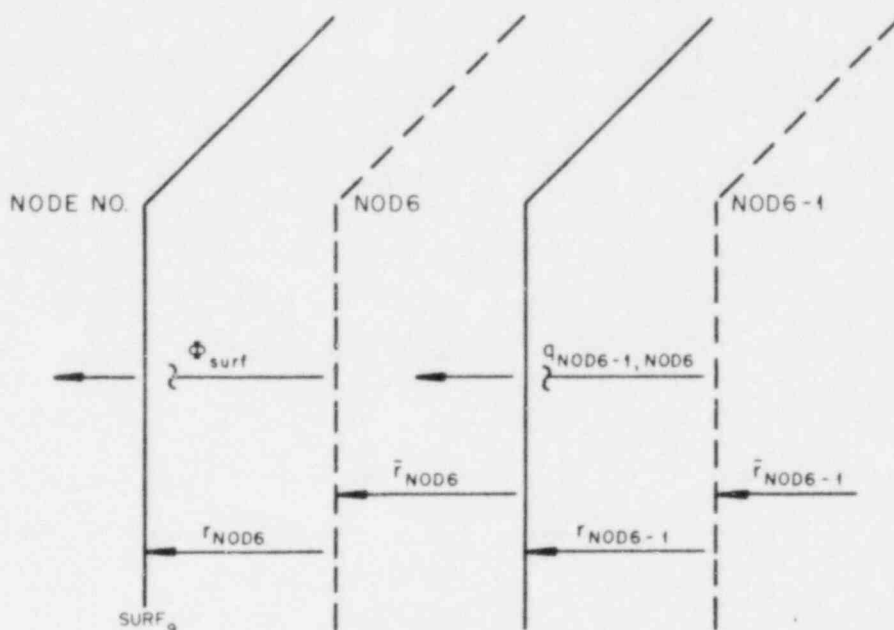


Fig. 2.7. Notation relative to the derivation of the heat transfer model at the heater surface.

The following mathematical derivations for the heat transfer models in the substrates and at the interfaces are based on the same assumptions as the ORINC models. All the ORTCAL mathematical models are one dimensional and no attempt is made to fine-structure the sheath thermocouple; it is treated as part of the solid inner stainless steel sheath (Fig. 2.5). Normally, during the discretizing of the inner sheath, an effort is made to subdivide the inner sheath such that the radial position of the last node ( $\bar{r}_{\text{NOD5}}$ , Fig. 2.6) is at approximately the same radial position as the thermocouple bead (Fig. 2.5).

The following assumptions are given:

1. steady-state conditions exist;
2. heat flow between nodes is constant for any  $r$  between nodes;
3. the thermal conductivity  $k_i$  is evaluated at the nodal temperature  $T_i$ ;
4. a gap exists at the sheath-to-sheath interface and heat can be transferred by conduction, convection, and radiation across the gap;
5. the last node (NOD5, Fig. 2.6) temperature ( $T_{\text{NOD5}}$ ) in the inner sheath is known;



6. the local fluid conditions (i.e., flow rate, bulk and saturation temperature, and pressure) are known;
7. the local power-generation rate is known.

The mathematical model for heat transfer between nodes  $i-1$  and  $i$  within a substrate (e.g., the outer sheath) is

$$q_{i-1,i} = - \left[ \frac{2}{\frac{\ln(r_{i-1}/\bar{r}_{i-1})}{k_{i-1}} + \frac{\ln(\bar{r}_i/r_{i-1})}{k_i}} \right] (T_i - T_{i-1})\pi\ell. \quad (2.11)$$

Similarly, at the surfaces in Figs. 2.6 and 2.7,

Surface 9

$$\begin{aligned} \phi_{\text{surf}_9} = q_{\text{NOD6,fluid}}/\pi\ell &= - \left[ \frac{2}{\frac{\ln(r_{\text{NOD6}}/\bar{r}_{\text{NOD6}})}{k_{\text{NOD6}}}} \right] (T_{\text{surf}_9} - T_{\text{NOD6}}) \\ &= -2r_{\text{NOD6}} h_f (T_{\text{sink}} - T_{\text{surf}_9}) = - \left[ \frac{1}{r_{\text{NOD6}} h_f} + \frac{2}{k_{\text{NOD6}}} \frac{\ln(r_{\text{NOD6}}/\bar{r}_{\text{NOD6}})}{r_{\text{NOD6}}} \right] \\ &\quad \times (T_{\text{sink}} - T_{\text{NOD6}}), \quad (2.12) \end{aligned}$$

Surfaces 7 and 8

$$\begin{aligned} q_{\text{NOD5,NS}} &= - \left[ \frac{2}{\frac{\ln(r_{\text{NOD5}}/\bar{r}_{\text{NOD5}})}{k_{\text{NOD5}}}} \right] (T_{\text{surf}_7} - T_{\text{NOD5}})\pi\ell \\ &= - \left\{ \frac{2}{\frac{1}{k_{\text{gap}_4}} + \frac{\ln[(r_{\text{NOD5}} + \Delta r_{\text{gap}_4})/r_{\text{NOD5}}]}{r_{\text{NOD5}}} + r_{\text{NOD5}} h_{\text{gap}_4} + r_{\text{NOD5}} h_{r_4}} \right\} (T_{\text{surf}_8} - T_{\text{surf}_7})\pi\ell \\ &= - \left[ \frac{2}{\frac{\ln(\bar{r}_{\text{NS}}/r_{\text{NOD5}})}{k_{\text{NS}}}} \right] (T_{\text{NS}} - T_{\text{surf}_8})\pi\ell, \quad (2.13) \end{aligned}$$

where  $h_{\text{gap}_4}$  is the convective heat transfer coefficient and  $h_{r_4}$  is defined by

$$h_{r_4} = \sigma f (T_{\text{surf}_8}^2 + T_{\text{surf}_7}^2)(T_{\text{surf}_8} + T_{\text{surf}_7}) \quad (2.14)$$

Note, at steady state,

$$\begin{aligned} \text{QDPI} &= q_{i-1,i} / \pi \ell = \phi_{\text{surf}_9} = q_{\text{NOD5,NS}} / \pi \ell \\ &= q_{\text{NOD6,fluid}} / \pi \ell \end{aligned} \quad (2.15)$$

Subsequently, knowing  $T_{\text{NOD5}}$  and QDPI allows the calculation of the gap inside surface temperature ( $T_{\text{surf}_7}$ ) from Eq. (2.13) by

$$T_{\text{surf}_7} = T_{\text{NOD5}} - \text{QDPI} / \left[ \frac{2}{\frac{\ln(r_{\text{NOD5}}/\bar{r}_{\text{NOD5}})}{k_{\text{NOD5}}}} \right] \quad (2.16)$$

Also, if QDPI and  $T_{\text{surf}_9}$  are known, the outer stainless steel sheath nodal temperature ( $T_i$ ) and the gap outside surface temperature ( $T_{\text{surf}_8}$ ) can be determined by manipulating Eqs. (2.11) through (2.13):

$$T_{\text{NOD6}} = T_{\text{surf}_9} + \text{QDPI} / \left[ \frac{2}{\frac{\ln(r_{\text{NOD6}}/\bar{r}_{\text{NOD6}})}{k_{\text{NOD6}}}} \right] \quad (2.17)$$

$$T_{i-1} = T_i + \text{QDPI} / \left[ \frac{2}{\frac{\ln(r_{i-1}/\bar{r}_{i-1})}{k_{i-1}} + \frac{\ln(\bar{r}_i/r_{i-1})}{k_i}} \right] \quad (2.18)$$

where  $i - 1 = \text{NOD6} - 1, \text{NS}$  and

$$T_{\text{surf}_8} = T_{\text{NS}} + \text{QDPI} / \left[ \frac{2}{\frac{\ln(\bar{r}_{\text{NS}}/r_{\text{NOD5}})}{k_{\text{NS}}}} \right] \quad (2.19)$$

Since the  $k_i$  values are dependent on the nodal temperatures, an iterative procedure is required to determine the nodal temperatures.

Calculation of the nodal temperatures above requires the knowledge of  $T_{\text{surf}_9}$ . The  $T_{\text{surf}_9}$  value is determined by the following procedure:

1. The pin is assumed to be locally in forced convection in subcooled liquid, and the film heat transfer coefficient ( $h_f$ ) is calculated from the Dittus and Boelter<sup>28</sup> correlation,

$$h_f = 0.023 (k_f/D_h)(Pr_f)^{0.4} (Re_f)^{0.8}, \quad (2.20)$$

where the physical properties are evaluated at  $T_{\text{bulk}}$  (i.e.,  $T_{\text{local}}$ ). Thus, substitution of  $h_f$  into Eq. (2.12) yields

$$T_{\text{surf}_9} = T_{\text{bulk}} + QDPI/2r_{\text{NOD6}} h_f. \quad (2.21)$$

2. The pin is then assumed to be locally in subcooled nucleate boiling, and Thom's<sup>29</sup> correlation yields

$$T_{\text{surf}_9} = T_{\text{SAT}} + 4.32 \left( \frac{QDPI}{2r_{\text{NOD6}}} \right)^{1/2} \exp(-P_{\text{local}}/1260). \quad (2.22)$$

3. A comparison of the  $T_{\text{surf}_9}$  values by Dittus-Boelter and Thom allows the determination of the heat transfer regime, heat transfer coefficient and  $(T_{\text{surf}_9})_{\text{actual}}$  (i.e., determination of mode of heat transfer is based on minimum surface temperature).

The surface temperatures of the gap (Fig. 2.6,  $T_{\text{surf}_7}$  and  $T_{\text{surf}_8}$ ) have been calculated from Eqs. (2.16) and (2.19). Therefore, referring to the following variant of Eq. (2.13),

$$\frac{k_{\text{gap}_4}}{\ln \left[ \frac{(r_{\text{NOD5}} + \Delta r_{\text{gap}_4})}{r_{\text{NOD5}}} \right]} + r_{\text{NOD5}} h_{\text{gap}_4} + r_{\text{NOD5}} h_{r_4} = \frac{QDPI/2}{(T_{\text{surf}_7} - T_{\text{surf}_8})}; \quad (2.23)$$

$T_{\text{surf}_7}$ ,  $T_{\text{surf}_8}$ ,  $r_{\text{NOD5}}$ , and QDPI are known, and  $h_{r_4}$  can be calculated from

Eq. (2.14). Thus, the remaining unknowns in Eq. (2.23) are  $h_{gap_4}$ ,  $k_{gap_4}$ , and  $\Delta r_{gap_4}$ . Since the gaps measured<sup>3,5</sup> by the Y-12 Development Division Metallurgical Department were less than 0.0013 cm wide, the convective heat transfer effect in Eq. (2.23) can be neglected. Also, because of the BDHT heater design,<sup>1</sup> the gap between the sheaths is exposed to the atmosphere (outside the bundle); therefore, the gas in the gap must be air, which has a known thermal conductivity. Thus,  $k_{gap_4}$  is evaluated from  $k_{air}$  at  $(T_{surf_7} + T_{surf_8})/2.0$ . Solving Eq. (2.23) for  $\Delta r_{gap_4}$  yields

$$\Delta r_{gap_4} = r_{NOD5} \left\{ \exp \left[ \frac{k_{gap}}{QDPI/2} \frac{1}{(T_{surf_7} - T_{surf_8})} - r_{NOD5} h_{r_4} \right] - 1.0 \right\}. \quad (2.24)$$

The "aging" of THTF bundle 1 is illustrated in Figs. 2.8 to 2.10 for thermocouple positions TE-318BG and TE-301DJ. These are graphs of the calculated gap thickness ( $\Delta r_{gap_4}$ ) vs the number of times bundle 1 has been brought to power (with the curves drawn through approximately equivalent boundary conditions). White<sup>30-32</sup> noted an upward drift in the indicated sheath thermocouple temperatures in the FCTF during testing of bundle 1 production heaters and conjectured that the shift was caused by an "increase in the thermal resistance from the inner sheath to the outer sheath which probably grows due to the decrease in contact pressure as the outer sheath expands plastically during heatup." The data also indicated that the thermocouple responses stabilized (i.e., no further drift) as the rod "aged." Actually, the increase in the thermal resistance occurs due to an increase in the gap ( $\Delta r_{gap_4}$ ) between the sheaths as shown in Figs. 2.8 and 2.9. Also in the "aged" THTF bundle 1, the gaps have stabilized at thermocouple positions TE-318BG and TE-301DJ (Figs. 2.8 and 2.9) and the thermocouple responses have stabilized.

Figures 2.8 and 2.9 show gap closure when the rod surface temperature is held constant and the rod power-generation rate is increased (i.e., the inner sheath thermally expands, thus closing the gap). Figure 2.10 shows the gap opening when the power-generation rate is held constant

ORNL-DWG 78-18416

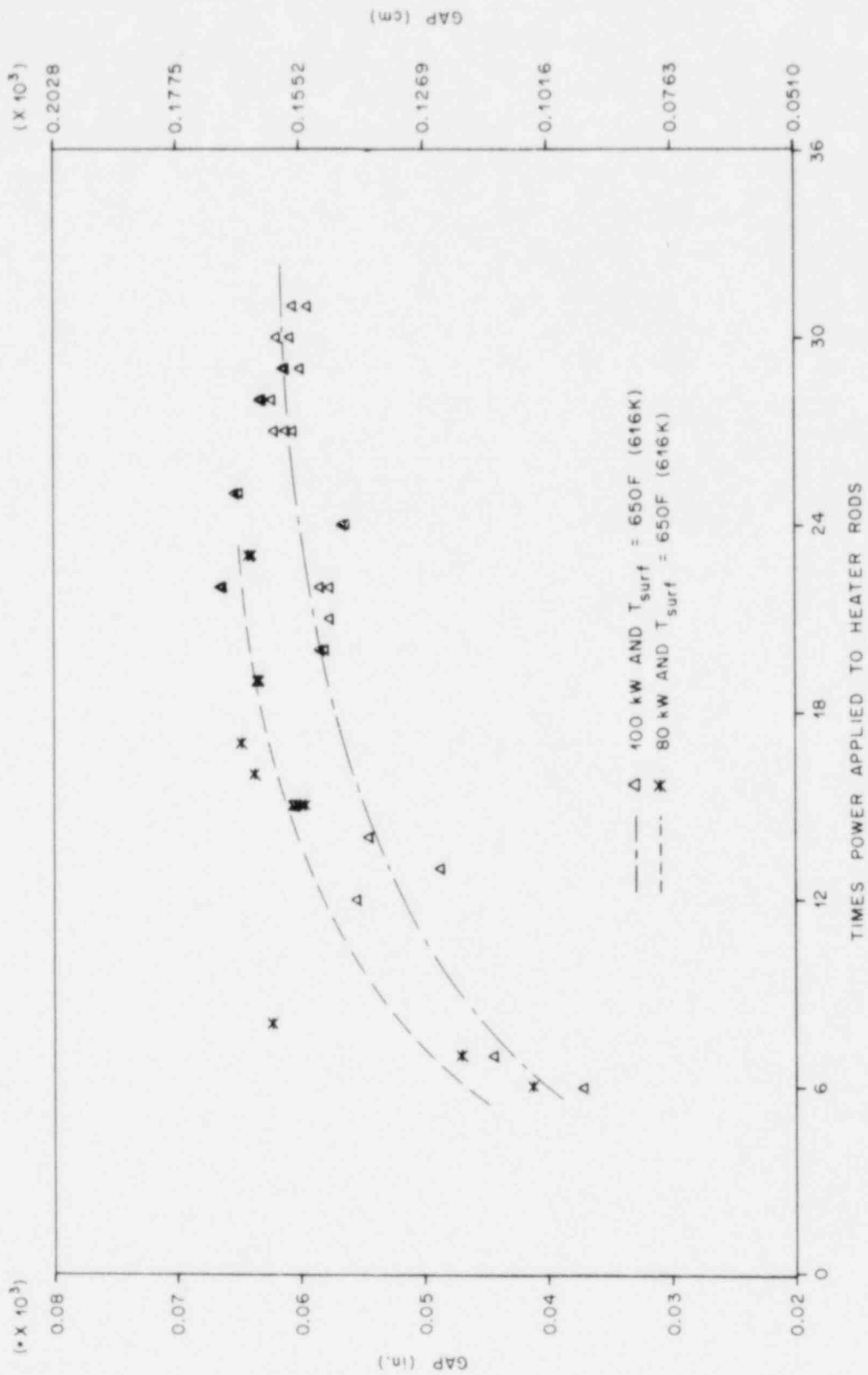


Fig. 2.8. Gap aging history at thermocouple position TE-318BG.

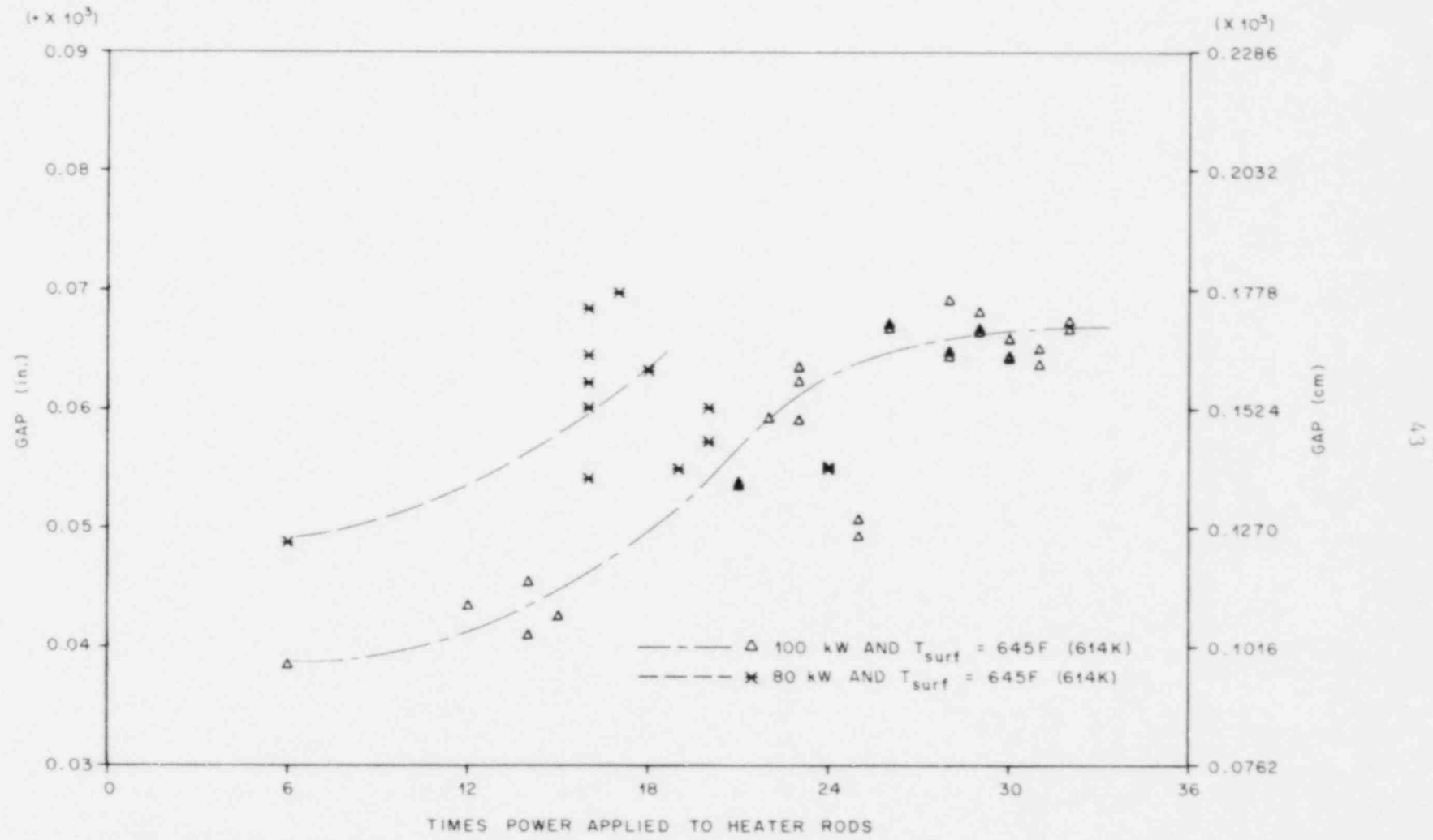


Fig. 2.9. Gap aging history at thermocouple position TE-301DJ (constant surface temperature).

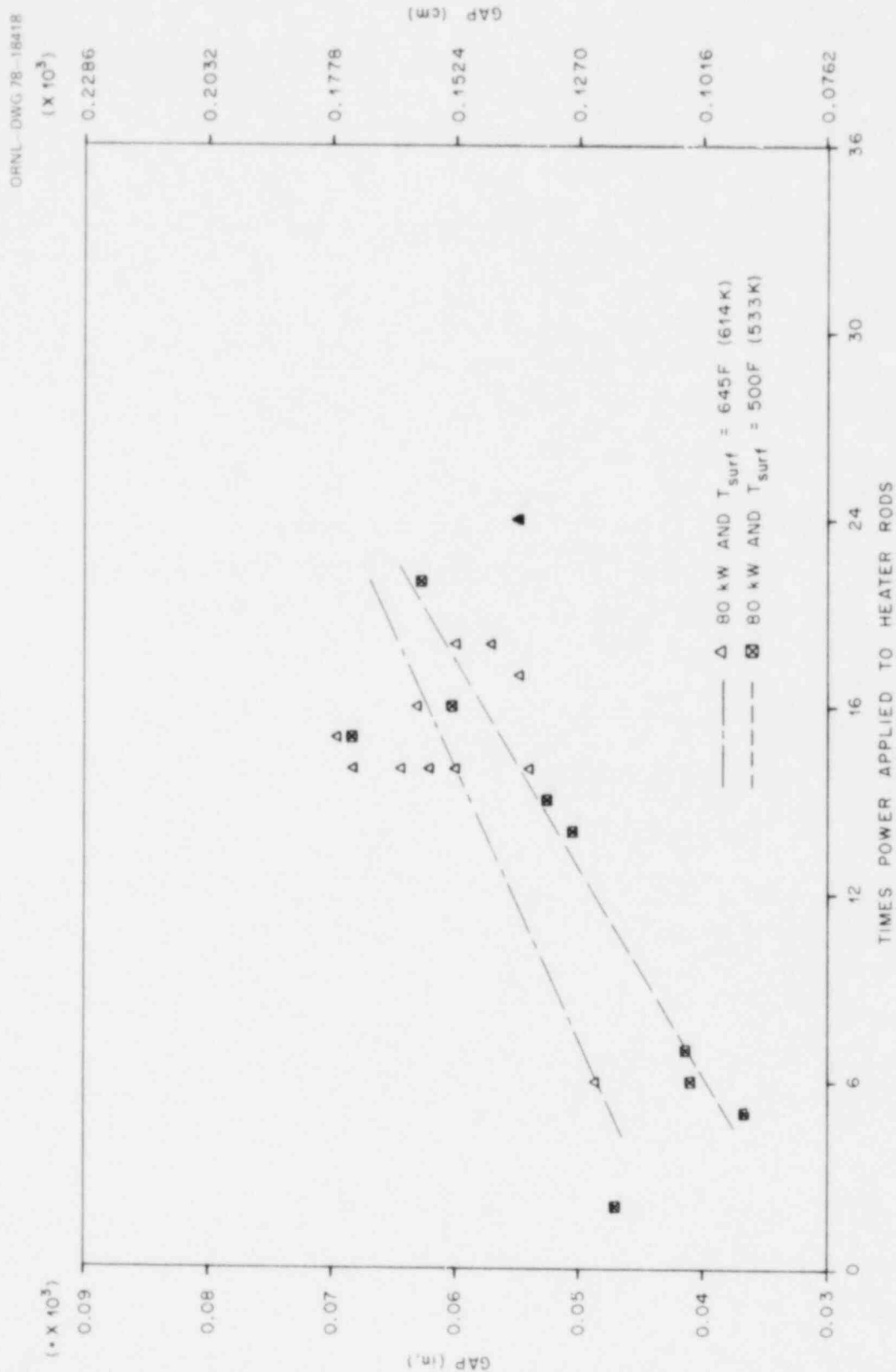


Fig. 2.10. Gap aging history at thermocouple position TE-301DJ  
(constant power-generation rate).

and the surface temperature increases (the outer sheath thermally expands away from the inner sheath).

### 2.3 ORTCAL - Part II

Part II of ORTCAL uses temperatures indicated by the sheath and middle thermocouples along with the power-generation rate [entries F(16), F(17), and F(4) in Table 2.1, respectively, from the thermocouple history tape] to produce the effective thermal conductivity of the BN insulator.

For a simulator with heater eccentricity equal to zero, the typical one-dimensional pin radial temperature profile at steady state is as shown in Fig. 2.11. The temperature gradient within the MgO is zero, since  $\partial T/\partial r|_{r=0} = 0$  and  $\dot{q}_{\text{MgO}} = 0$ ; therefore, if the pin centerline temperature is known (i.e., if the middle thermocouple exists, is good, and is monitored by the CCDAS), the inside surface temperature of the heater sublayer is known. Heat flow within the heater sublayer is proportional to  $r^2$ , which is expressed mathematically<sup>4</sup> as

$$q_{i-1,i} = -\frac{\bar{k}_{i-1,i} 4\pi\lambda r_{i-1}^2}{(r_i^2 - r_{i-1}^2)} (T_i - T_{i-1}), \quad (2.25)$$

to describe the heat flow between nodes  $i-1$  and  $i$  within the heater substrate. Heat flow within the BN and stainless steel sheath substrates is constant (an assumption) between nodes and is modeled mathematically by Eq. (2.11). Therefore, if the temperature dependencies of the substrate thermal conductivities and the power generation rate are known, the pin centerline temperature can be determined from the sheath thermocouple response or the sheath thermocouple temperature can be determined from the middle thermocouple response by using Eqs. (2.11) and (2.25).

The temperature dependencies of the thermal conductivities for 316 stainless steel, Cupronickel, and Inconel-600, presented in Appendix A, represent least-squares fits to literature data. It is assumed that the thermal conductivity of the BN can be approximated by a polynomial in terms of temperature, that is

$$k_{\text{BN}}(T) = C_1 + C_2T + C_3T^2 + C_4T^3, \quad (2.26)$$



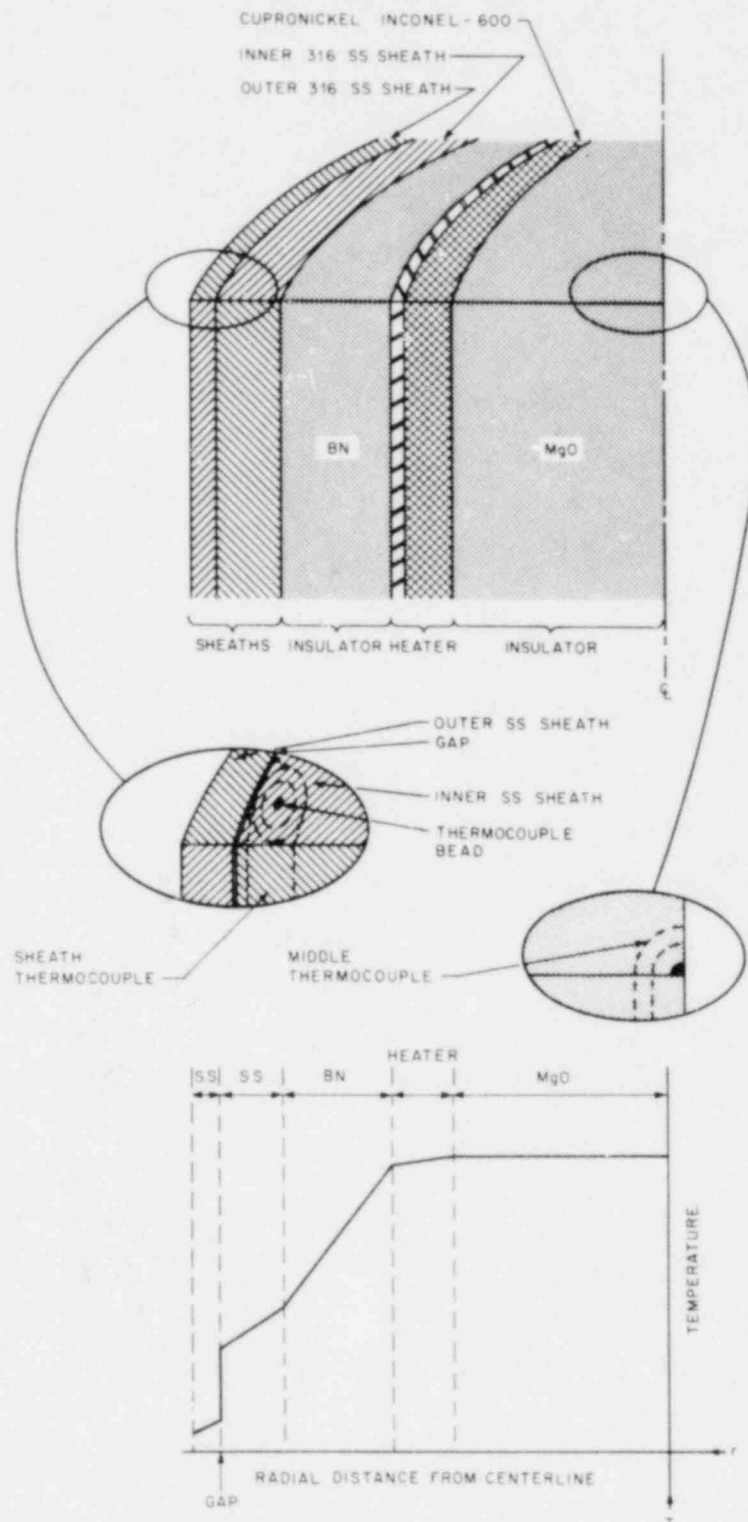


Fig. 2.11. Schematic of fuel pin simulator with sheath and middle thermocouples in insets with typical pin radial temperature profile at steady state.

where  $C_i$  are the polynomial coefficients. Thus, given a set of coefficients ( $C_i$ ) for Eq. (2.26), the simulator centerline temperature ( $T_{\text{center}_j}$ ) can be calculated for each steady-state observation ( $j$ ) given the following boundary conditions (for each observation): (1) the sheath thermocouple response [entry F(16) in Table 2.1] and (2) the linear power-generation rate [entry F(4)].

The regression procedure for determining the temperature dependence of  $k_{\text{BN}}$  [Eq. (2.26)] involves the minimization of the sum-of-squares function

$$F(C_1, C_2, C_3, C_4) = \sum_{j=1}^{\text{No.}} (Y_{\text{center}_j} - T_{\text{center}_j})^2 \quad (2.27)$$

with respect to the  $C_i$  parameters, where  $Y_{\text{center}_j}$  represents the observed middle thermocouple response [entry F(17) in Table 2.1],  $T_{\text{center}_j}$  is the calculated steady-state pin centerline temperature, and  $N$  is number of observations.

The technique employed for optimizing Eq. (2.27) is a numerical search using essentially a pattern search strategy. Pattern search is a direct search procedure which operates on an objective function [i.e., Eq. (2.27)] and proceeds to minimize the function. In general, this method involves the sequential examination of a finite set of trial values of the independent variables to determine whether the objective function can be improved and then changing the independent variables simultaneously in a pattern move based on information acquired in the exploratory search. Each pattern move is followed by a sequence of exploratory moves which revise the pattern. The search continues until the value of the objective function cannot be reduced. The initial work on pattern search was done by James B. Jeeves,<sup>33</sup> but the search technique used by ORTCAL (Part II) is a more improved algorithm developed by Weisman, Wood, and Rivlin.<sup>34</sup>

Examples of the regression output are given in Appendix D for thermocouple positions TE-318BG (Table D.1) and TE-301DJ (Table D.2). The in-situ correlations from Tables D.1 and D.2 and literature values for the

thermal conductivity of BN are compared in Figs. 2.12 and 2.13. [Note: At the end of each table in Appendix D, there is a line stating the "total error" for that individual regression - this value is the minimum objective function, Eq. 2.27, value for the regression.] Also shown are the  $C_i$  parameters [i.e., the best-fit parameters for the temperature polynomial in Eq. (2.26)]. The variance of the fit is defined as

$$\text{VAR} = \sum_{j=1}^{\text{No.}} (Y_{\text{center}_j} - T_{\text{center}_j})^2 / (N - 4) , \quad (2.28)$$

where  $N$  = number of observations and  $N - 4$  is the number of independent determinations of  $(Y_{\text{center}_j} - T_{\text{center}_j})$ ; or, although there are  $N$  different values of  $(Y_{\text{center}_j} - T_{\text{center}_j})$  that can be determined from the data, there are also four constraints [number of parameters ( $C_i$ )] to be determined. The standard deviation of the fit is

$$\delta_{\text{SD}} = \sqrt{\text{VAR}} . \quad (2.29)$$

Therefore, given the fitted parameters from the regression and entries F(16) and F(4) for a steady-state observation, the calculated centerline temperature ( $T_{\text{center}_j}$ ) would be expected to be within  $\pm 3\delta_{\text{SD}}$  of entry F(17) at a 97% confidence level. For thermocouple position TE-318BG, three standard deviations equal  $\sim 7.2$  K ( $12.9^\circ\text{F}$ ), which is about half the combined three standard deviations of the two thermocouple (TE-318BG and TE-318MG) temperature measurements.

Thermocouple positions TE-318BG and TE-301DJ illustrate two of the "better" positions in THTF bundle 1 with regard to the  $k_{\text{BN}}$  regression. There is, of course, the undesirable side of the picture: position TE-322BF (Table D.3), which has a  $3\delta_{\text{SD}}$  of 30.6 K ( $55.1^\circ\text{F}$ ). The "difference" column in Table D.3 shows that there has obviously been a gradual but steady change in the heater thermal performance over the life of the bundle at this position. The difference  $(Y_{\text{center}_j} - T_{\text{center}_j})$  at a nominal 100 kW/rod was 14 K ( $25.1^\circ\text{F}$ ) during run 2.1 (bundle life  $\sim 2$  weeks), 3.9 K ( $7^\circ\text{F}$ ) during run 9.1 (a bundle life of  $\sim 6$  months, 2 weeks), and  $-14.4$  K ( $-25.9^\circ\text{F}$ ) during run 23.3 (a bundle life of  $\sim 20$  months). White has often stated<sup>30, 35-38</sup> that a measure of the thermal performance of a

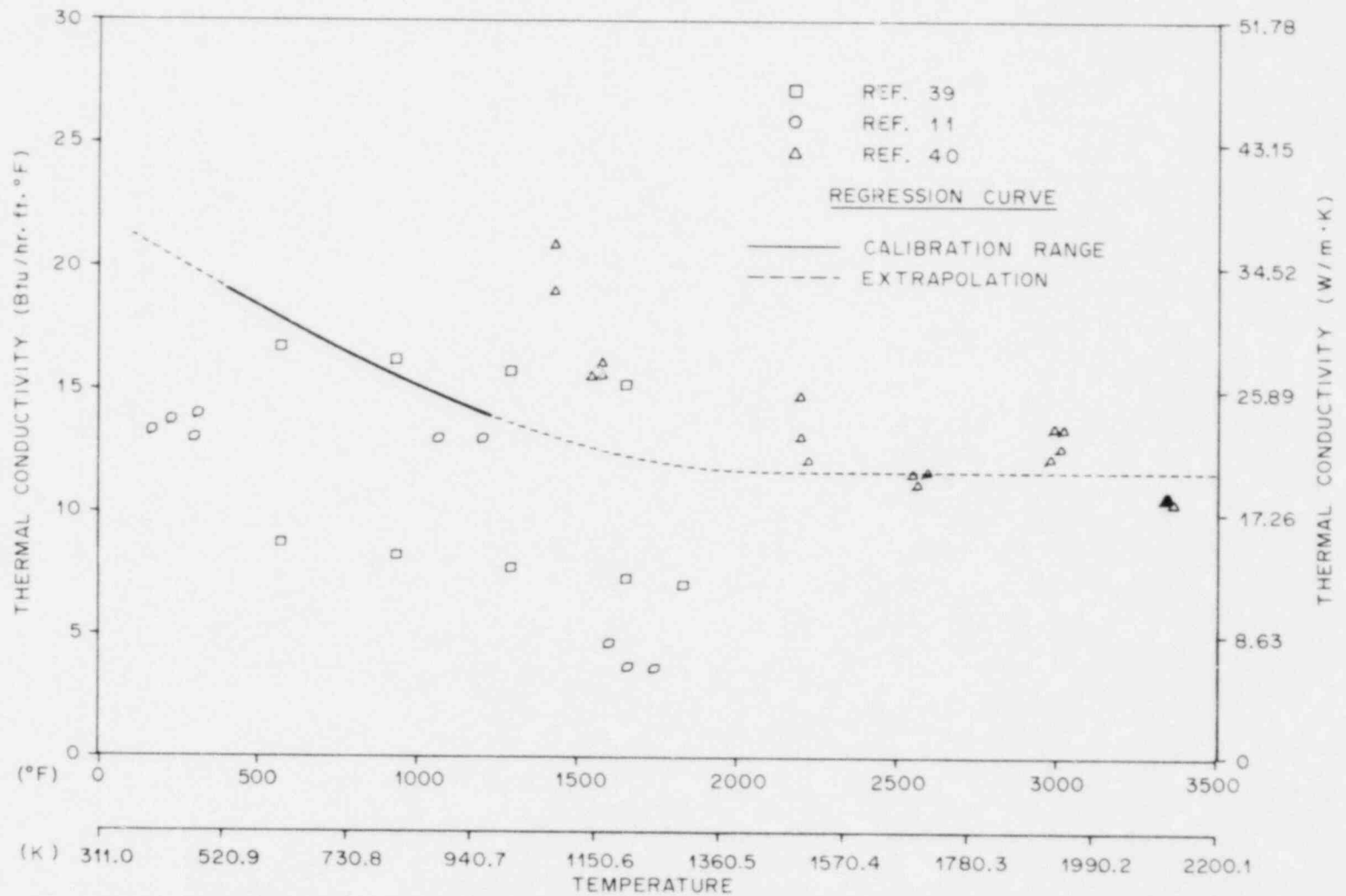


Fig. 2.12. Boron nitride thermal conductivity at 318BG (comparison of regression results with literature data).

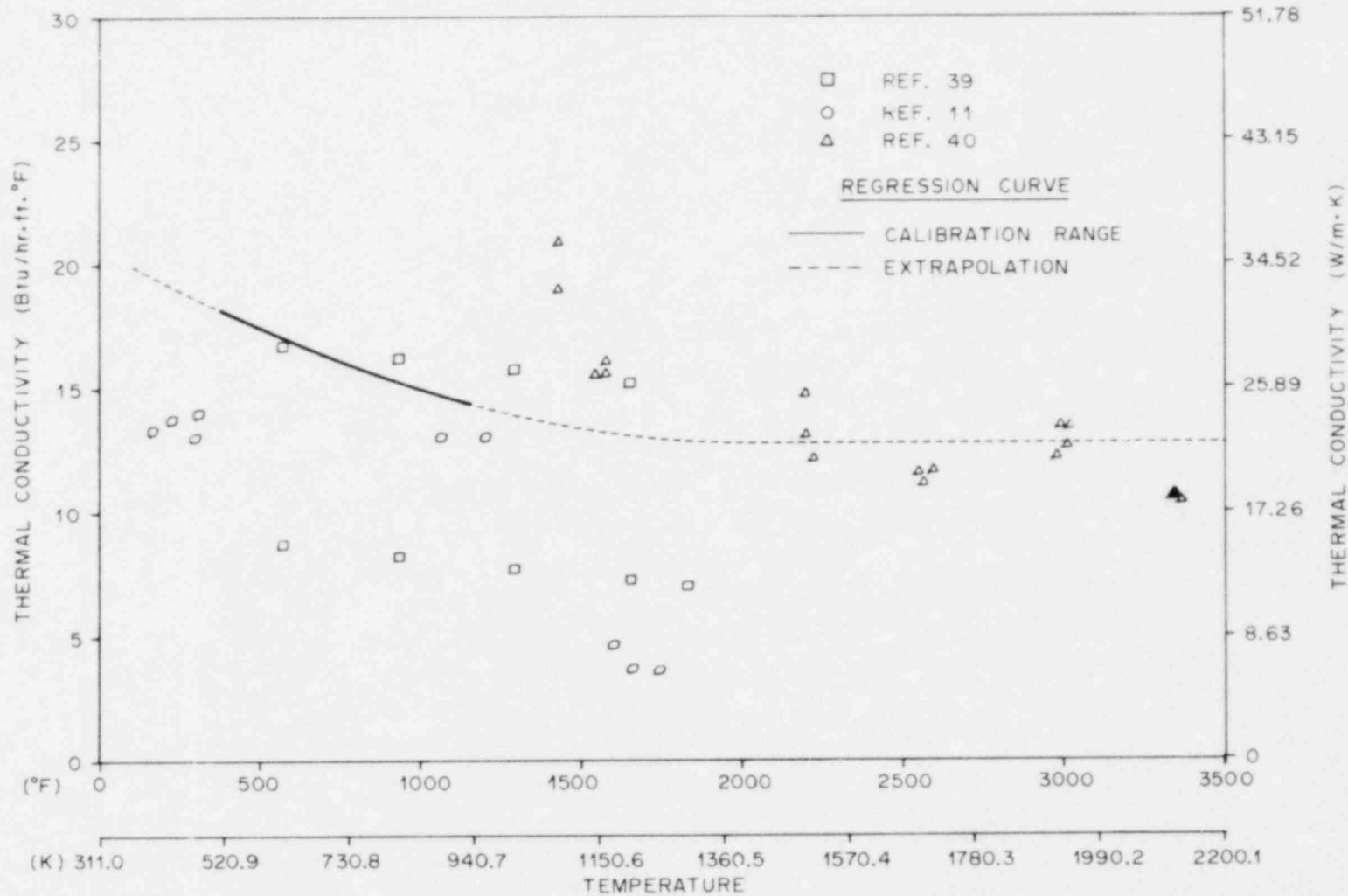


Fig. 2.13. Boron nitride thermal conductivity at 301DJ (comparison of regression results with literature data).

heater is the repeatability of the radial temperature difference between the center and sheath thermocouples. He has also stated that the radial  $\Delta T$  must have diagnostic sensitivity to changes in the internal conditions of the heater. Plots similar to those of White for thermocouple positions 318BG, 301DJ, and 322BF are presented in Figs. 2.14 to 2.16, respectively. The radial temperature difference at positions 318BG and 301DJ remained relatively unchanged after 32 powered runs and ~20 months; however, at position 322BF there was a drastic change between runs 2.1 and 23.3 [at 100 kW the  $\Delta T$  changed 26.1 K (47°F)]. "Since radial  $\Delta T$ 's are insensitive to core flow rate, system pressure, heat transfer coefficient at the surface, and gap resistance between the heater sheaths, possible explanations for the changes are (1) a change in heater thermal properties; (2) a change in generated heat flux profile; (3) distortion of the heater; (4) degradation of the thermocouples;"<sup>38</sup> and (5) changes in the radial position of the heating element relative to the sheaths. Zero power temperature measurements and thermocouple electrical properties measurements discount point 4. The slope of the curves in Fig. 2.16 is approximately the same, thus detracting from point 2. The likely explanations are points 1, 3, and 5, with 5 being the most probable considering the manufacturing process (swaging) for these heaters. Regardless of the reason, analysis of the heat transfer from heater positions with this degree of uncertainty may prove very difficult, except for the determination of the time to CHF.

The primary purpose of ORTCAL (Part II) is to produce the effective thermal conductivity of the BN insulator. In essence, the ORTCAL package creates a coefficient data tape (CDT) which contains all the calibration and regression results for each thermocouple position in the THTF bundle. An example of the information contained on the CDT is shown in Table 2.2 for position TE-318BG. ORTCAL (Part II) supplies the information contained in the dashed block. The basic lines of information flow are illustrated in Fig. 2.17.

It is apparent after a review of Fig. 1.13 that all sheath thermocouples are not paired with middle thermocouples. These positions are

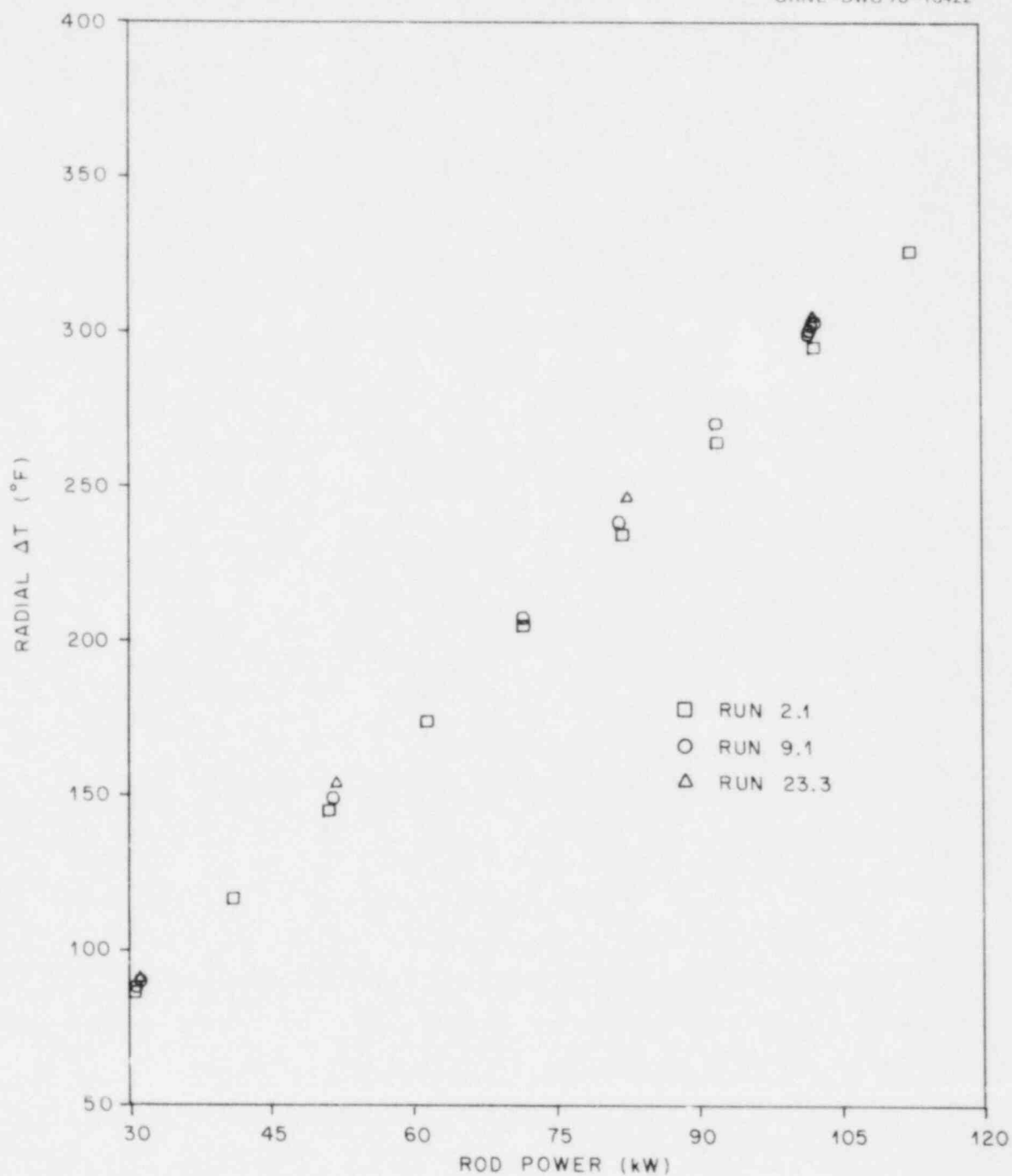


Fig. 2.14. Radial  $\Delta T$  as a function of rod power (thermocouple position 318BG).

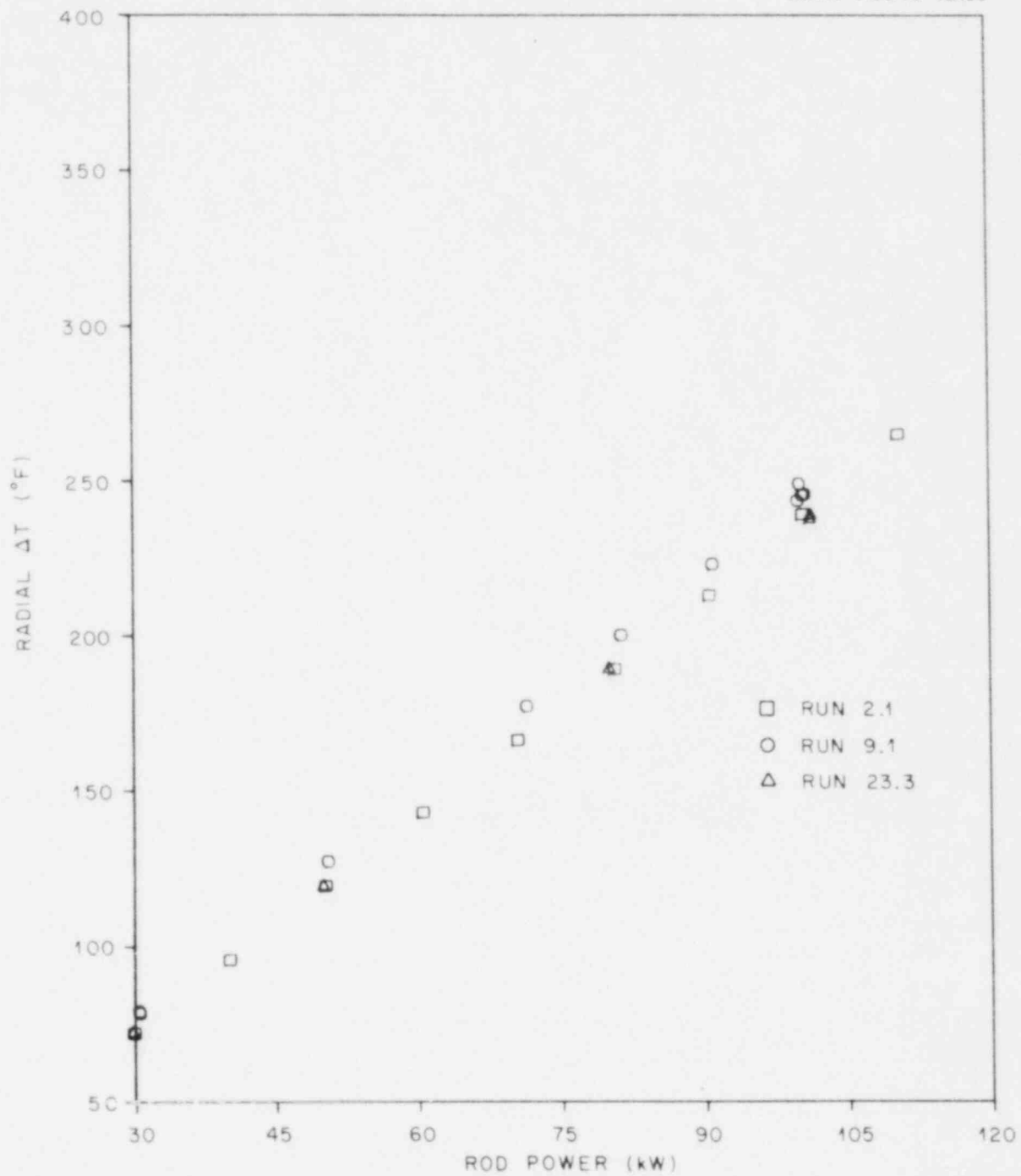


Fig. 2.15. Radial  $\Delta T$  as a function of rod power (thermocouple position 301DJ).



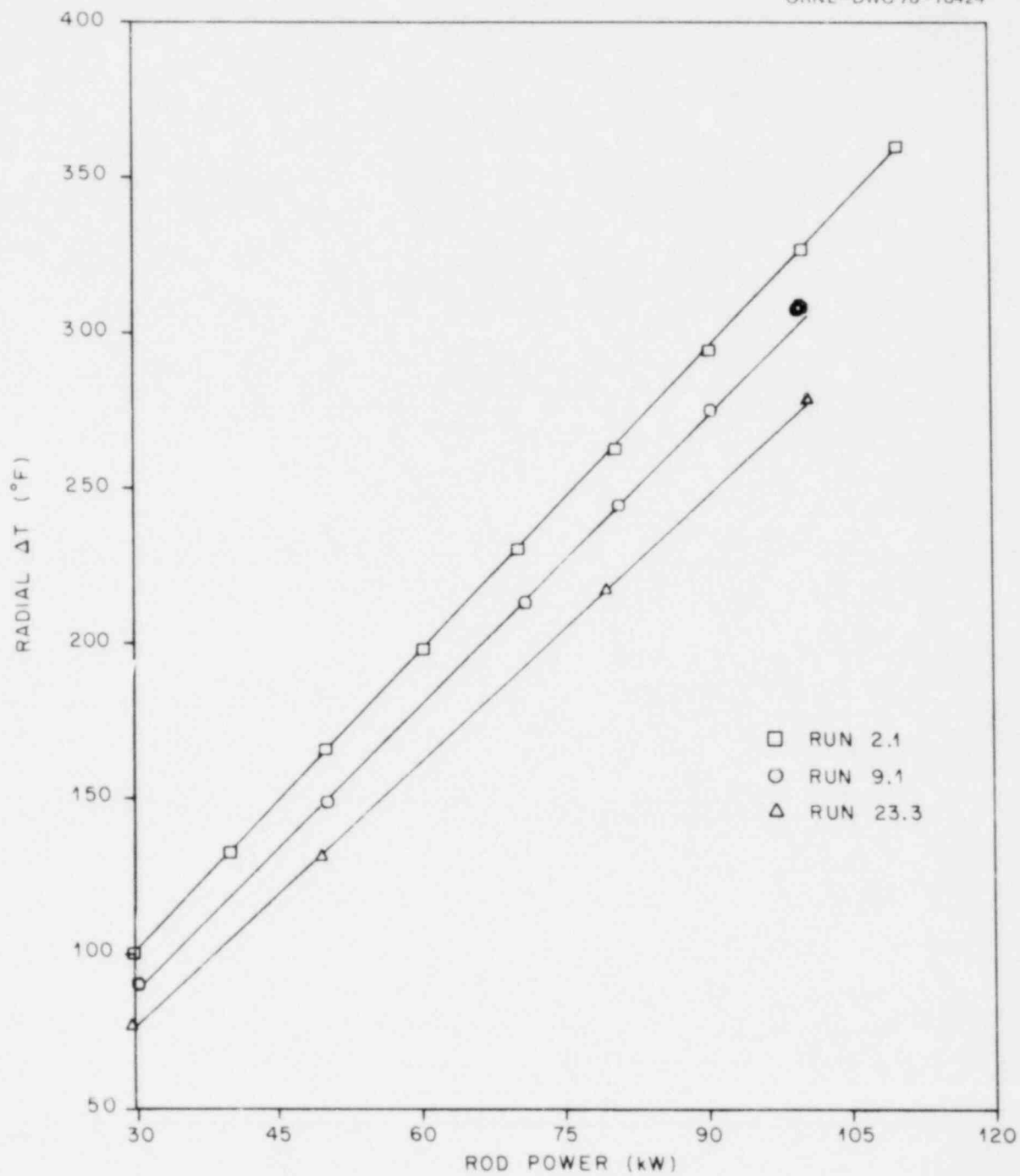


Fig. 2.16. Radial  $\Delta T$  as a function of rod power (thermocouple position 322BF).

Table 2.2. Calibration results for position TE-318BG  
in THTF bundle 1

\*\*\*\*\*  
\*\*\*\*\*  
\*\*\* THERMOCOUPLE NO. J18-BG \*\*\*  
\*\*\*\*\*  
\*\*\*\*\*

\*\*\*\*\* MIDDLE T/C --- J18-MG

\*\*\*\*\* DATE OF LAST MODIFICATION : MAY 1, 1978

\*\*\*\*\* AXIAL POWER PEAKING FACTOR IS : 1.6659  
DETERMINED BY INDIV RESISTANCE CAL.

ØRTCAL - PART II

\*\*\*\*\* COEFFICIENTS FOR TEMPERATURE POLYNOMIAL FIT OF KBN  
DETERMINED FOR THE ABOVE SPECIFIC ITCS/ITCM PAIR  
C(1)= 0.21976151E 02  
C(2)= -0.74225366E-02  
C(3)= -0.73717558E-07  
C(4)= 0.59715699E-09

VARIANCE OF FIT= 0.18624649E 02  
UNITS FOR KBN FIT : BTU/(HR\*FT\*\*2/FT\*F)

\*\*\*\*\* COEFFICIENTS FOR TEMPERATURE POLYNOMIAL FIT FOR KMGO  
DETERMINED FOR THE ABOVE SPECIFIC T/C PAIR  
C(1)= 0.72101289E 01  
C(2)= -0.10450333E-01  
C(3)= 0.79769443E-05  
C(4)= -0.29365270E-08  
C(5)= 0.45424298E-12

VARIANCE OF FIT= 0.43312866E 03  
UNITS FOR KMGO FIT : BTU/(HR\*FT\*\*2/FT\*F)

ACTUAL MGO POROSITY CALCULATED VIA MODIFIED  
RUSSELL EQUATION : 0.18648702E 00

\*\*\*\*\* COEFFICIENTS FOR THE THERMAL EXPANSION GAP MODEL FIT  
DETERMINED FOR THE ABOVE SHEATH T/C

C(1)= 0.52502546E 01 SD= 0.12002551E 02  
C(2)= 0.5059676AE-02 SD= 0.17433237E-01  
C(3)= -0.43716855E-05 SD= 0.27200751E-05

VARIANCE OF FIT= 0.91365113E-04

GAP CALCULATION AT THE BIAS POINT : 0.0547 (MILS)

BIAS TEMP. INSIDE S.S.S. NODAL TEMP. : 815.4 DEG. F  
BIAS TEMP. OUTSIDE S.S.S. NODAL TEMP. : 700.8 DEG. F  
BIAS FLUX : 532344.1 BTU/HR/FT\*\*2

THE MAXIMUM TEMPERATURE FOR WHICH THE ABOVE  
REGRESSION FIT IS APPLICABLE IS 817.17 DEG. F

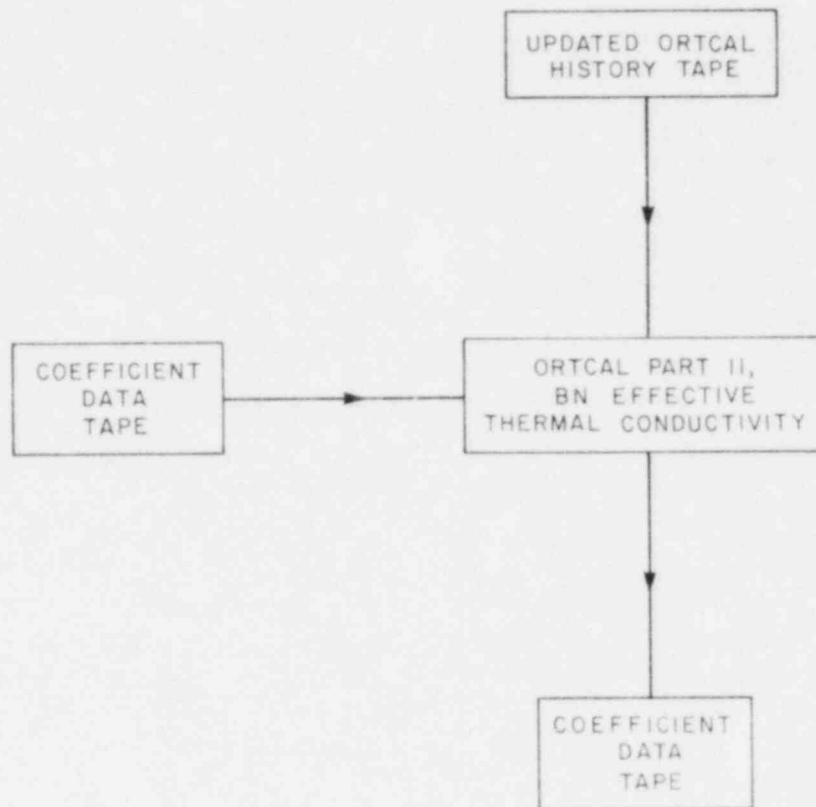


Fig. 2.17. Lines of information flow for ORTCAL - Part II.

classified by the following procedure:

1. For positions in the bundle where a middle thermocouple is paired with a sheath thermocouple, an individual regression is made and the regression coefficients and variance are loaded on the CDT only for that pair of thermocouples.

2. For levels with middle-sheath thermocouple pairs, a level regression is made; that is, the thermocouple pair responses are "lumped" together and an overall regression for the level is performed. The coefficients and variance resulting from this regression are loaded on the CDT for positions not covered by item 1.

3. For levels with no middle-sheath thermocouple pairs (levels D, I, K, L, M, and N in THTF bundle 1), a bundle regression is made. The coefficients and variance resulting from this regression are loaded on the CDT for positions not covered by item 1 or 2.

Figure 2.17 is actually a simplification of the network required to classify the thermal conductivity of the BN insulator. One computer program does the individual and level regressions and a second program handles the bundle regression; lines of information flow required to fully classify the BN thermal conductivity for the entire bundle are shown in Fig. 2.18. For comparison with the individual regressions in Figs. 2.12 and 2.13, a plot of the bundle regression is shown in Fig. 2.19.

#### 2.4 ORTCAL - Part III

The thermal conductivity of MgO is a strong function of its packed density (or porosity) as shown in Fig. 2.20. Since the construction procedure for the THTF heaters involves a series of swaging operations with certain sections of the heater being swaged more than others, the estimated density of the MgO ceramic core ranges from 70 to 90% of the theoretical density.

Part III of ORTCAL uses the temperatures indicated by the sheath and the middle thermocouples along with the power-generation rate to produce the effective thermal diffusivity of the MgO core. [The regressions of ORTCAL - Part II (determination of the effective thermal conductivity of the BN insulator) must precede the regressions of ORTCAL - Part III.]

Power drop tests (i.e., controlled transients) are performed for use by Part III of ORTCAL. These tests involve simply "tripping" power to the bundle with the core mass flow rate and core inlet pressure and temperature remaining essentially constant throughout the test. The CCDAS is on fast scan during the test (duration  $\sim 3$  min); but most of the action is over within  $\sim 10$  sec after power is tripped.

An engineering units tape of the "trip" file is read by preprocessor programs, which determine trip point and mean steady-state instrument responses (prior to trip) and reorganize the information into the input format required by Part III.

It is assumed that the thermal conductivity of MgO can be approximated by a polynomial in terms of temperature, that is

$$k_{\text{MgO}}(T) = C_1 + C_2T + C_3T^2 + C_4T^3 + C_5T^4, \quad (2.30)$$

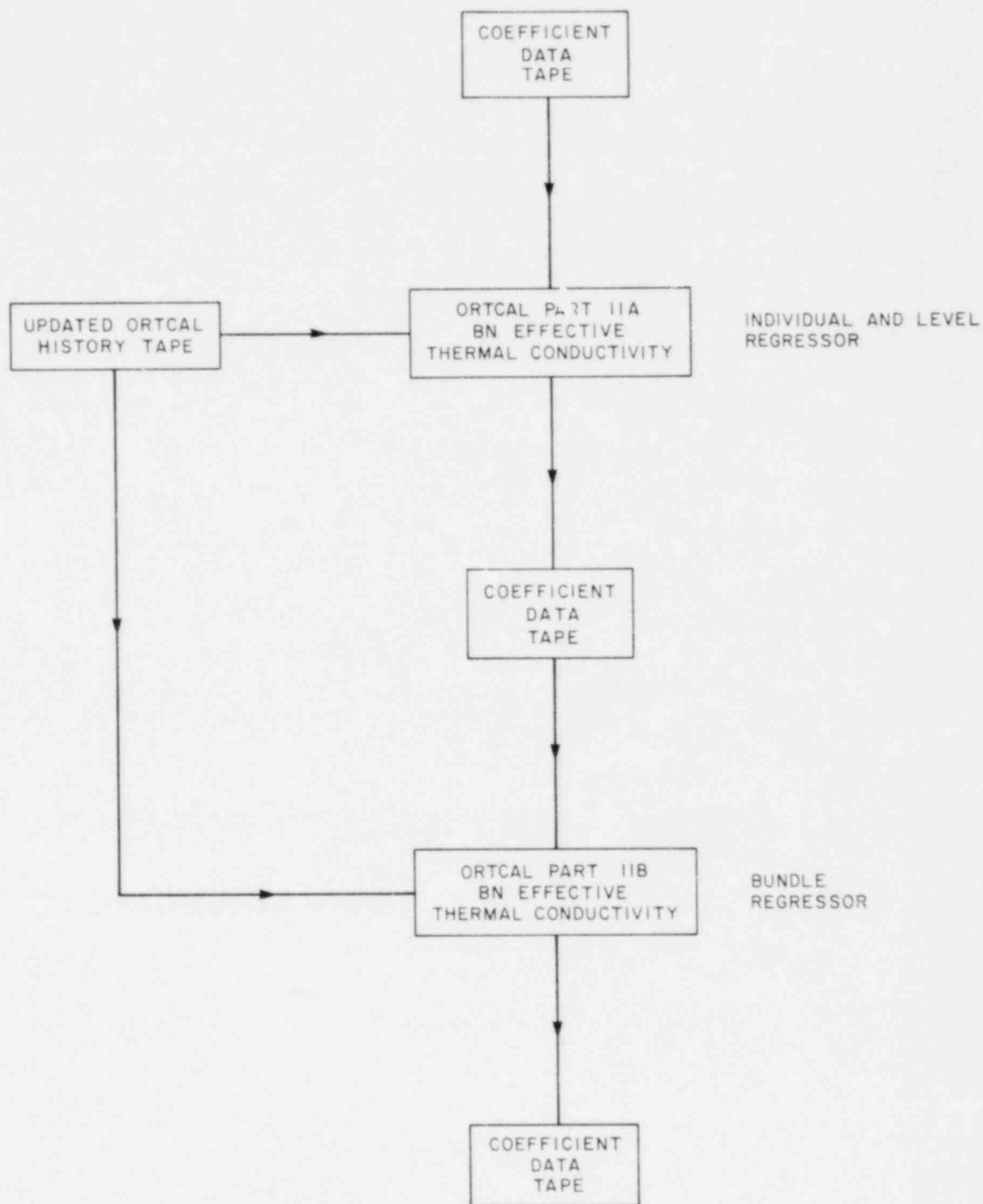


Fig. 2.18. Lines of information flow required for complete  $k_{BN}$  classification at all bundle thermocouple positions.

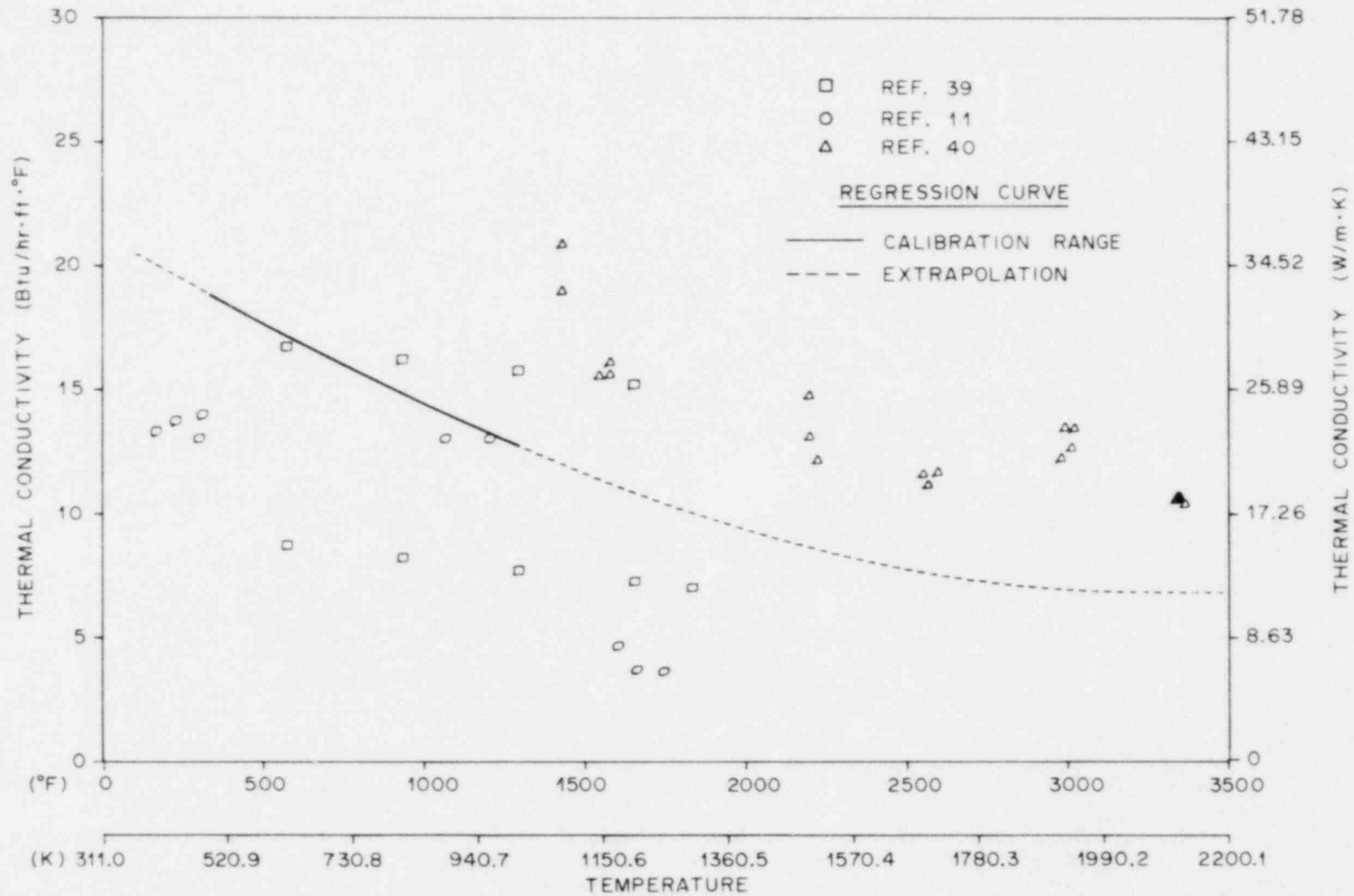


Fig. 2.19. Boron nitride thermal conductivity for bundle 1 (comparison of regression results with literature data).

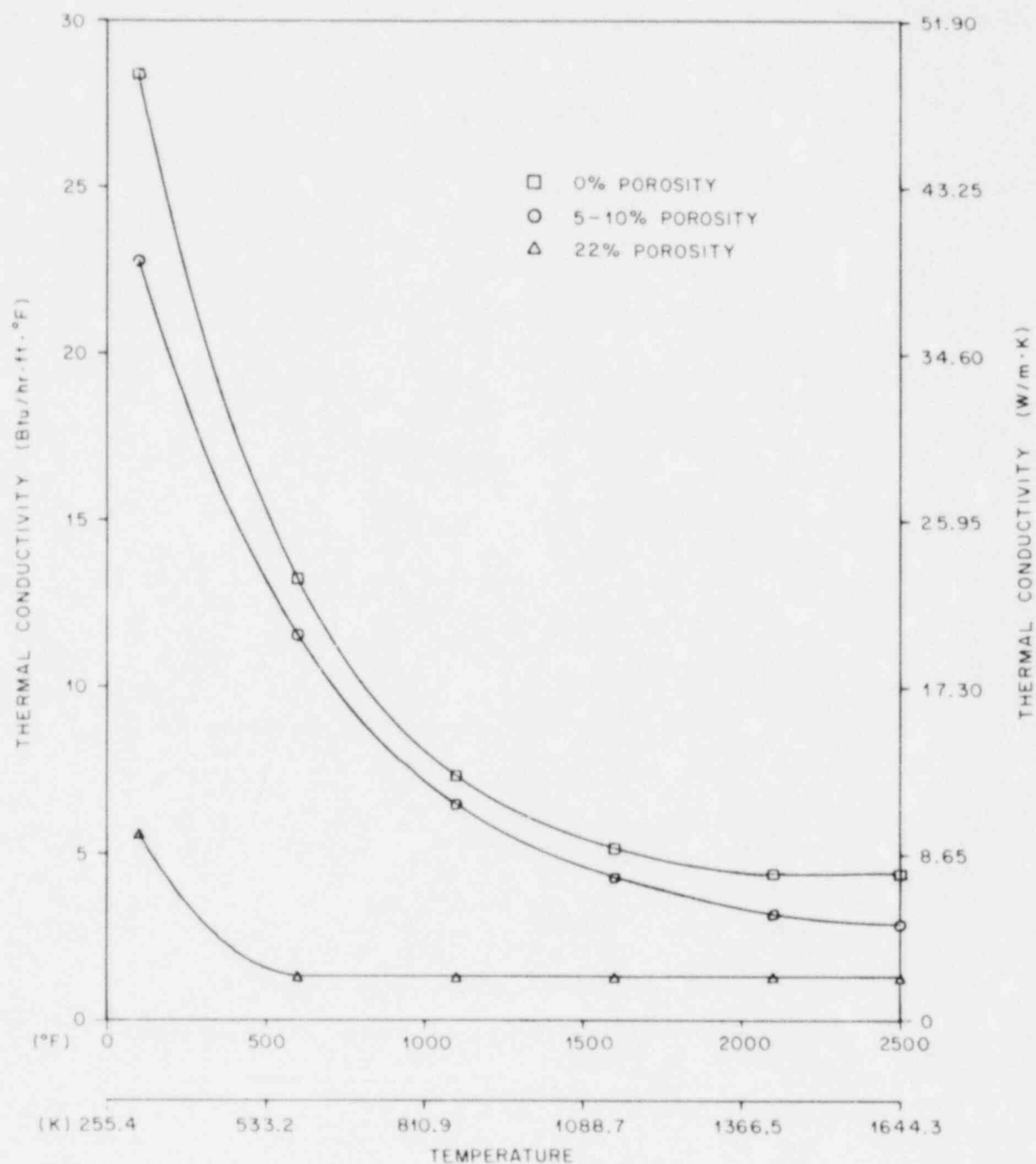


Fig. 2.20. MgO thermal conductivity as a function of temperature and porosity (literature data, Ref. 6).

where  $C_i$  are the polynomial coefficients. The MgO thermal diffusivity regression is based on minimization of the following sum-of-squares function,

$$F(C_1, C_2, C_3, C_4, C_5) = \sum_{j=1}^{N_\phi} \left[ \sum_{i=1}^{\eta_I} (Y_{\text{center}_i} - T_{\text{center}_i})^2 \right]_j, \quad (2.31)$$

with respect to the  $C_i$  parameters. The term  $Y_{\text{center}_i}$  represents the observed middle thermocouple response,  $T_{\text{center}_i}$  is the  $i$  calculated pin centerline temperature,  $\eta_I$  is the number of observations per power drop, and  $N_\phi$  is the total number of power drops.

Part III essentially solves the forward conduction problem given a set of  $C_i$  coefficients and the following boundary conditions: (1) power-generation rate (as a function of time) and (2) sheath thermocouple response (as a function of time). The program runs the inverse package developed for ORINC<sup>4</sup> as a subroutine driven by a numerical pattern search (the same routine used by Part II) for the optimum polynomial coefficients.

Appendix E gives an example of ORTCAL - Part III regression output for thermocouple position TE-301DJ. Line plots which overlay the predicted (i.e., calculated) centerline temperatures and observed middle thermocouple responses for TE-301DJ for five power drops are also presented. The appendix also gives the overall regression results for position TE-301DJ, power trip 1.1 (from 50 kW/rod), power trip 1.2 (from 90 kW/rod), power trip 1.3 (from 122 kW/rod), power trip 1.4 (90 kW/rod), and power trip 8.1 (from 50 kW/rod).

A plot of the regression fits for TE-301DJ and TE-318BG vs literature data for the thermal conductivity of MgO is shown in Fig. 2.21. The "blocked" portion of Table 2.3 represents the contribution of Part III to the CDT file. A simplified flow chart of the information flow required for ORTCAL - Part III is presented in Fig. 2.22.

There are a limited number of locations in THTF bundle 1 that have sheath-middle thermocouple pairs monitored by the CCDAS (see Section 2.3). Therefore, the number of locations in bundle 1 for which the rigorous regressions of Part III can be applied is limited; however, the entire bundle (266 sheath thermocouple locations) must be classified. The



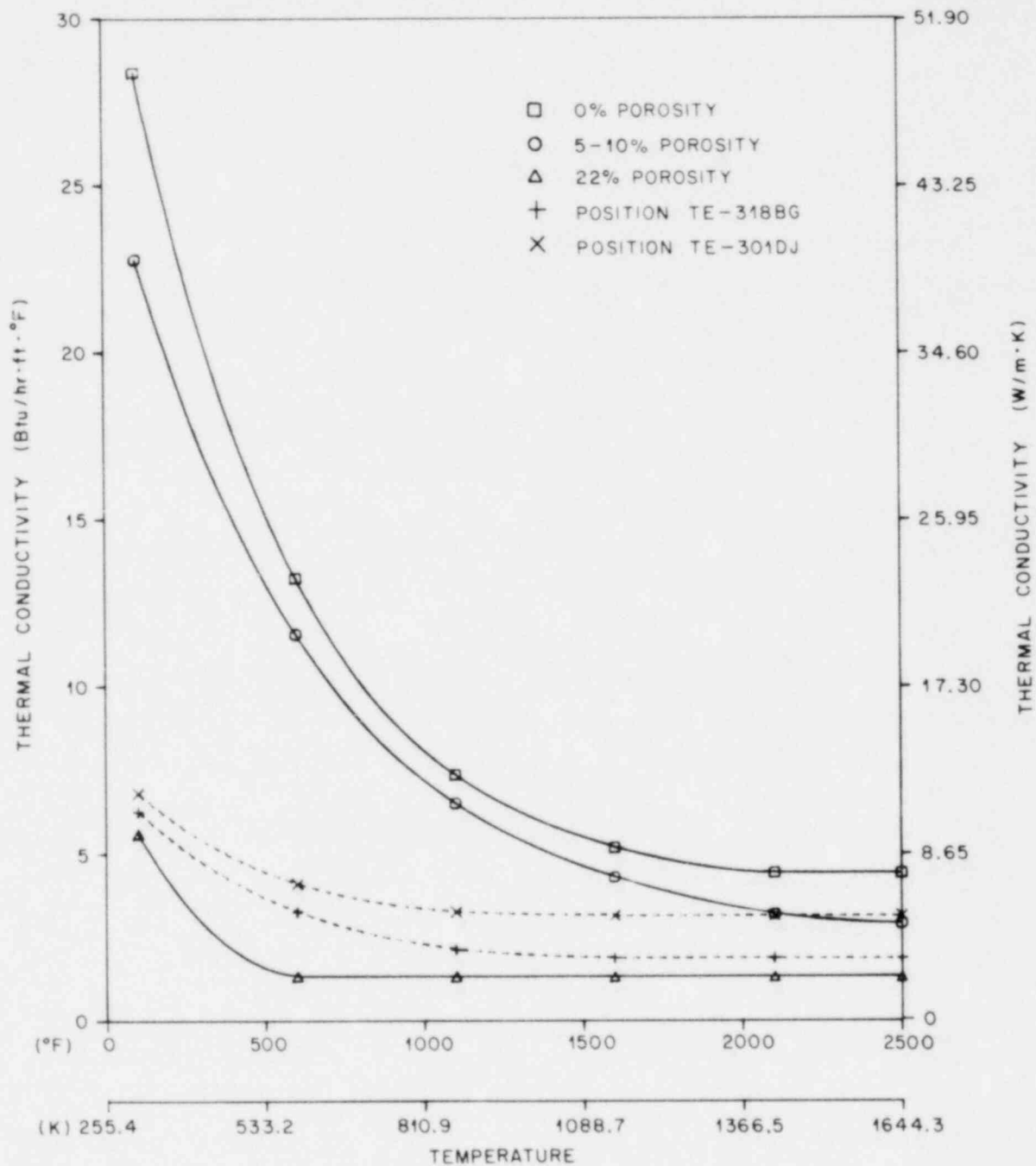


Fig. 2.21. MgO thermal conductivity as a function of temperature and porosity (comparison of regression results at 318BG and 301DJ with literature data, Ref. 6).

Table 2.3. Calibration results for position TE-301DJ  
in THF bundle 1

```
*****
*****
*** THERMOCOUPLE NO. 301-DJ ***
*****
*****
```

\*\*\*\*\* MIDDLE T/C --- 301-MJ

\*\*\*\*\* DATE OF LAST MODIFICATION : MAY 1, 1978

\*\*\*\*\* AXIAL POWER PEAKING FACTOR IS : 1.3012  
DETERMINED BY INDIV RESISTANCE CAL.

\*\*\*\*\* COEFFICIENTS FOR TEMPERATURE POLYNOMIAL FIT OF KBN  
DETERMINED FOR THE ABOVE SPECIFIC ITCS/ITCM PAIR  
C(1)= 0.20594376E 02  
C(2)= -0.71305782E-02  
C(3)= 0.11995689E-05  
C(4)= 0.19595138E-09

VARIANCE OF FIT= 0.15701573E 02  
UNITS FOR KBN FIT : BTU/(HR\*FT\*\*2/FT\*F)

ØRTCAL - PART III

```
***** COEFFICIENTS FOR TEMPERATURE POLYNOMIAL FIT FOR KMGD
DETERMINED FOR THE ABOVE SPECIFIC T/C PAIR
C(1)= 0.77045898E 01
C(2)= -0.99152625E-02
C(3)= 0.79940228E-05
C(4)= -0.28400076E-08
C(5)= 0.37483889E-12
```

VARIANCE OF FIT= 0.23226364E 02  
UNITS FOR KMGD FIT : BTU/(HR\*FT\*\*2/FT\*F)

ACTUAL MGD POROSITY CALCULATED VIA MODIFIED  
RUSSELL EQUATION : 0.16666609E 00

\*\*\*\*\* COEFFICIENTS FOR THE THERMAL EXPANSION GAP MODEL FIT  
DETERMINED BY USING THE BIAS GAP VALUE AS A MEAN GAP

C(1)= 0.0 SD= 0.0  
C(2)= 0.0 SD= 0.0  
C(3)= 0.0 SD= 0.0

VARIANCE OF FIT= 0.0

GAP CALCULATION AT THE BIAS POINT : 0.0547 (MILS)

BIAS TEMP. INSIDE S.S.S. NODAL TEMP. : 780.7 DEG. F  
BIAS TEMP. OUTSIDE S.S.S. NODAL TEMP. : 691.2 DEG. F  
BIAS FLUX : 409356.5 BTU/HR/FT\*\*2

THE MAXIMUM TEMPERATURE FOR WHICH THE ABOVE  
REGRESSION FIT IS APPLICABLE IS 0.0 DEG. F

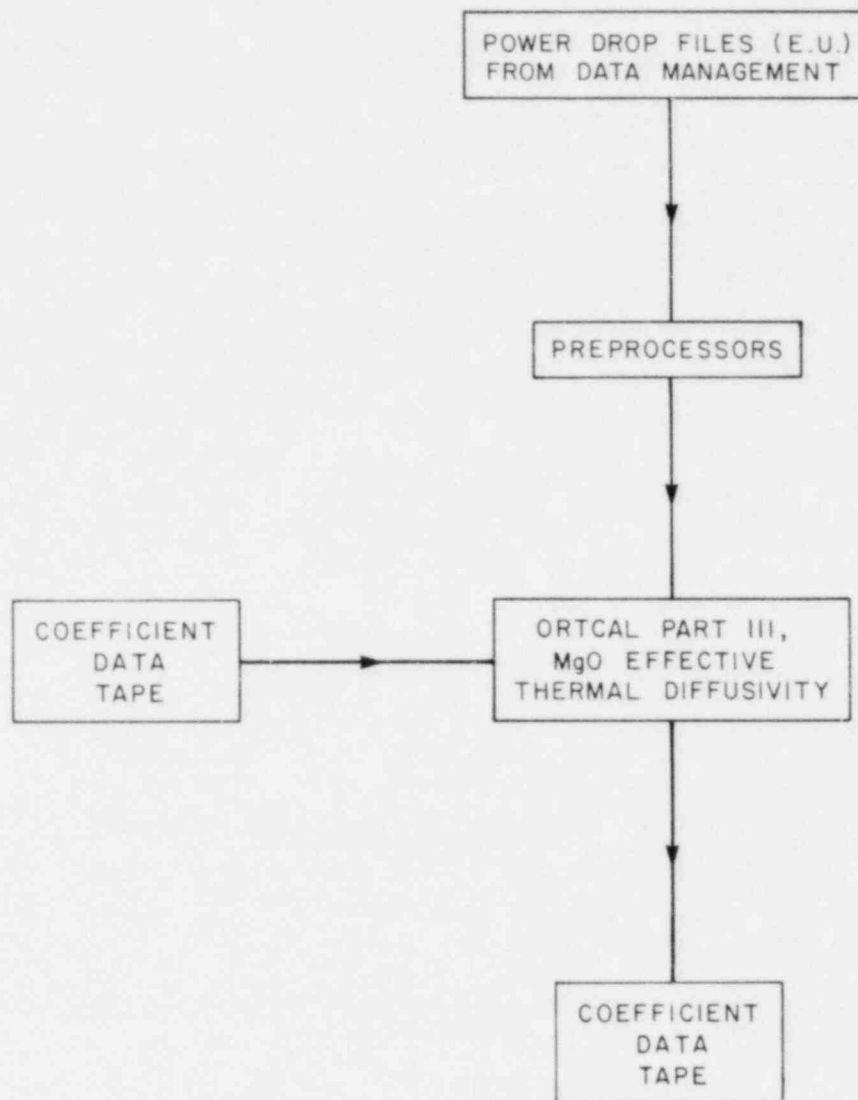


Fig. 2.22. Lines of information flow for ORTCAL - Part III.

following steps comprise the current approach to classifying bundle 1:

1. For positions in the bundle where there is a middle thermocouple paired with a sheath thermocouple, an individual regression is made and the regression coefficients and variance are loaded on the CDT only for that pair of thermocouples. The porosity of the MgO core is estimated from the regression fit and the modified Russell equation (Appendix G) and is entered on the CDT.

2. For levels with middle-sheath thermocouple pairs, a level regression is made; that is, the thermocouple pair responses are "lumped" together and an overall regression for the level is performed. The coefficients and variance resulting from this regression are loaded on the CDT for those positions that are not covered by item 1. The porosity of the MgO core for the levels is estimated from the regression fit and the modified Russell equation and the estimate is entered on the CDT.

3. Unlike the  $K_{BN}$  regressions, a bundle regression *cannot* be made for levels with no middle-sheath thermocouple pairs (levels D, I, K, L, M, and N in bundle 1). A bundle regression was appropriate for the  $k_{BN}$  because the radial dimensions of the BN (Table 1.3) are approximately constant throughout the rod and the expected compaction of the BN would be approximately the same. However, for the MgO core, the radial dimensions (Table 1.3) and degree of compaction vary in a rod depending on the power zone and the amount of swaging required. The thermal conductivity of MgO is estimated for levels D, I, K, L, M, and N by using the modified Russell equation, which contains the functional dependence of  $k_{MgO}$  for both temperature and porosity. All that is needed is an estimate of the porosity for the above levels. The porosity  $p$  of the core is assumed to be proportional to the cross-sectional area of the core or

$$p \propto R_{MgO}^2 \quad (2.32)$$

Figure 2.23 contains a plot of the porosities estimated in items 1 and 2 for E, F, G, H, and J level thermocouples and a least-squares linear fit to the data yields the curve in Fig. 2.23. The estimated porosities for levels D, I, K, L, M, and N in bundle 1 are shown in Table 2.4.

#### 2.5. ORTCAL - Part IV

Part IV of ORTCAL applies regression analysis to the output from Part I to determine the expansion coefficients and proper bias points for the stainless steel annuli forming the gap. The mechanical model chosen to utilize this information is one dimensional, which is consistent with the thermal model used in the inverse calculation. The linear

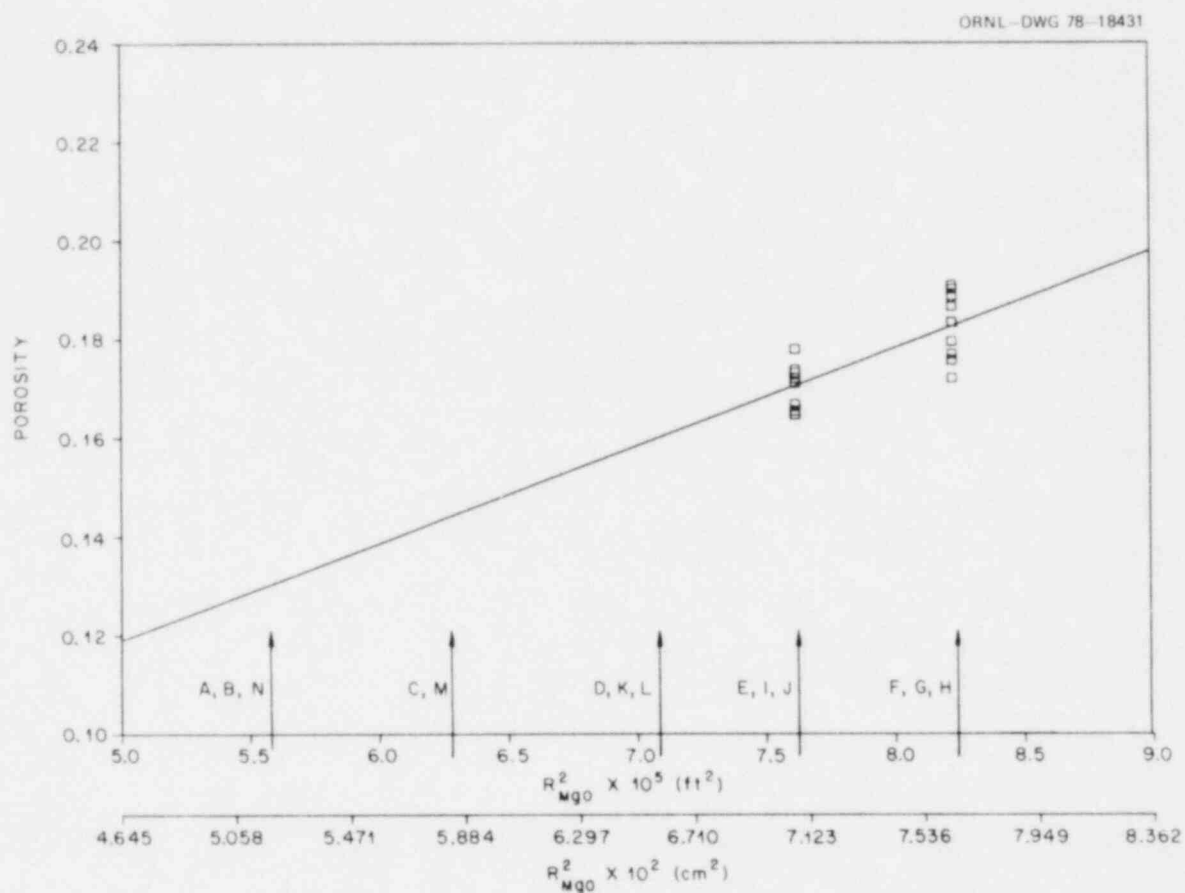


Fig. 2.23. Estimated MgO core porosity for THTF bundle 1.

Table 2.4. Bundle 1 estimated MgO core porosities

Level	Porosity
D	0.1598
I	0.1705
K	0.1598
L	0.1598
M	0.1442
N	0.1303

gap model used in ORINC is

$$\Delta\text{gap} = \Delta\text{gap}_0 + \Delta\bar{r}_{\text{NS}} - \Delta\bar{r}_{\text{NOD5}} , \quad (2.33)$$

where subscript 0 denotes the bias gap and subscripts NS and NOD5 refer to the first node in the outer sheath and the last node in the inner sheath, respectively (see Fig. 2.24). The values of  $\Delta\bar{r}$  in Eq. (2.33) can be expanded by the following equation, which was derived<sup>4</sup> from the definition for the coefficient of linear expansion:

$$L - L_0 = L_0 \{ \exp [C_1(T - T_0) + C_2(T^2 - T_0^2) + C_3(T^3 - T_0^3)] - 1.0 \} . \quad (2.34)$$

Expanding  $\Delta\bar{r}_{\text{NS}}$  and  $\Delta\bar{r}_{\text{NOD5}}$  by using Eq. (2.34) and inserting the expansion in Eq. (2.33) yields

$$\begin{aligned} \Delta\text{gap} = & \Delta\text{gap}_0 + \bar{r}_{\text{NS}} \{ \exp [C_1(T_{\text{NS}} - T_{\text{NS}}|_0) + C_2(T_{\text{NS}}^2 - T_{\text{NS}}|_0^2) \\ & + C_3(T_{\text{NS}}^3 - T_{\text{NS}}|_0^3)] - 1.0 \} - \bar{r}_{\text{NOD5}} \{ \exp [C_1(T_{\text{NOD5}} - T_{\text{NOD5}}|_0) \\ & + C_2(T_{\text{NOD5}}^2 - T_{\text{NOD5}}|_0^2) + C_3(T_{\text{NOD5}}^3 - T_{\text{NOD5}}|_0^3)] - 1.0 \} . \quad (2.35) \end{aligned}$$

The term  $\Delta\text{gap}_0$  is the bias gap and  $T_{\text{NS}}|_0$  and  $T_{\text{NOD5}}|_0$  are the bias nodal temperatures.

Part IV scans the history tape generated in Part I to find a specified thermocouple or thermocouple level and loads the observed gap [entry F(24) in Table 2.1] and nodal temperatures [entries F(18) and F(19)] for each steady-state point for all powered runs for that thermocouple or thermocouple level. The bias points (gap and nodal temperatures) for each powered run are also determined and loaded.

Since the gap behavior can be expressed in one concise mathematical formula [Eq. (2.35)], a nonlinear least-squares routine (rather than the pattern search technique used previously) is employed to determine the coefficients  $C_1$ ,  $C_2$ , and  $C_3$  in Eq. (2.35).

An example of the Part IV thermocouple level regression for the G level in bundle 1 at TE-318BG is given in Table F.1; the individual regression is presented in Table F.2 and a summary is shown in Table F.3.

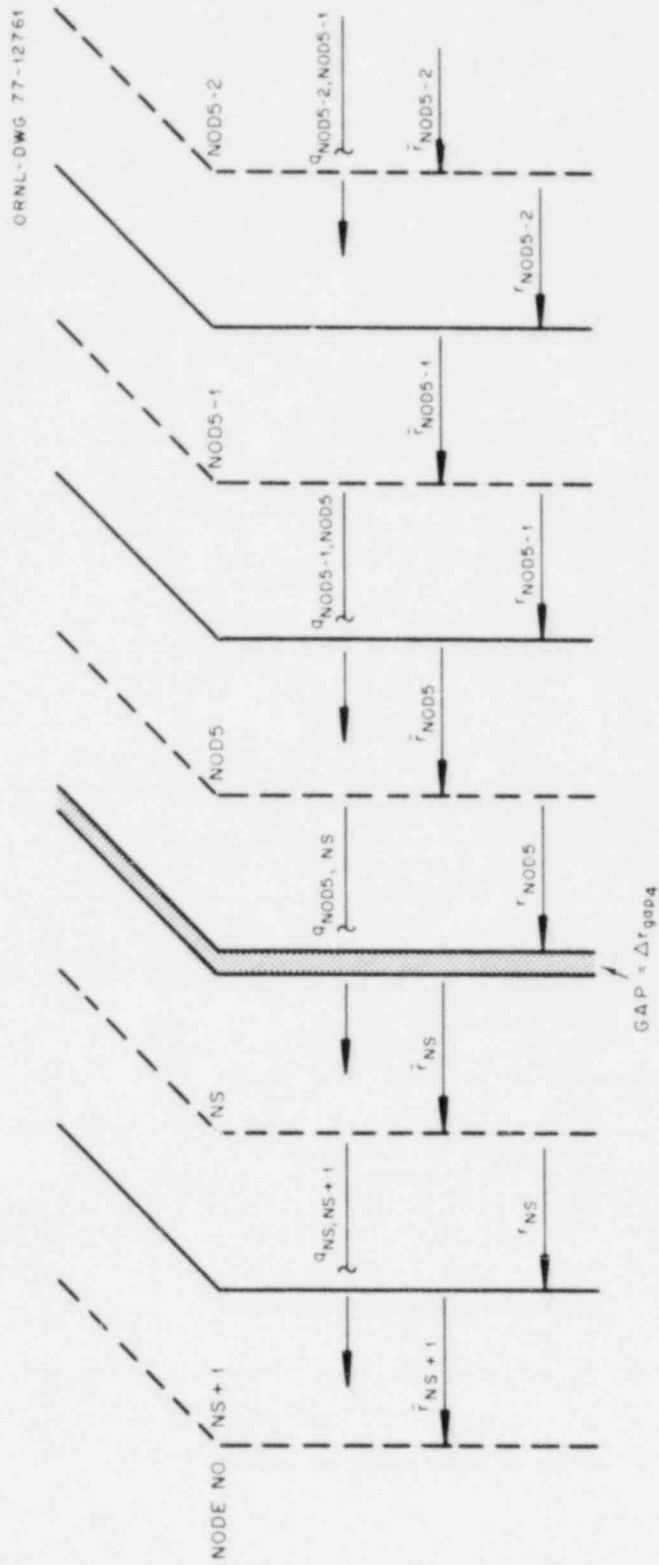


Fig. 2.24. Notation relative to the mathematical model of the thermo-mechanical behavior of the gap between the inner and outer stainless steel sheaths.

The contribution of Part IV to the CDT file is illustrated in the blocked portion of Table 2.5. A simplified flow chart of the information flow to and from Part IV is presented in Fig. 2.25.

Note that the coefficients, standard deviations of the coefficients, and variance of the fit are zeroed in Table 2.3. This indicates that the Part IV regression failed at this position and level. Failure modes for the gap coefficient regression are:

1. the nonlinear least-squares routine diverges in attempting to find a solution;
2. the nonlinear least-squares routine fails to converge (within specified error criterion) to a solution;
3. either or both of the level and individual regressions have negative first derivatives at any of the bias points.

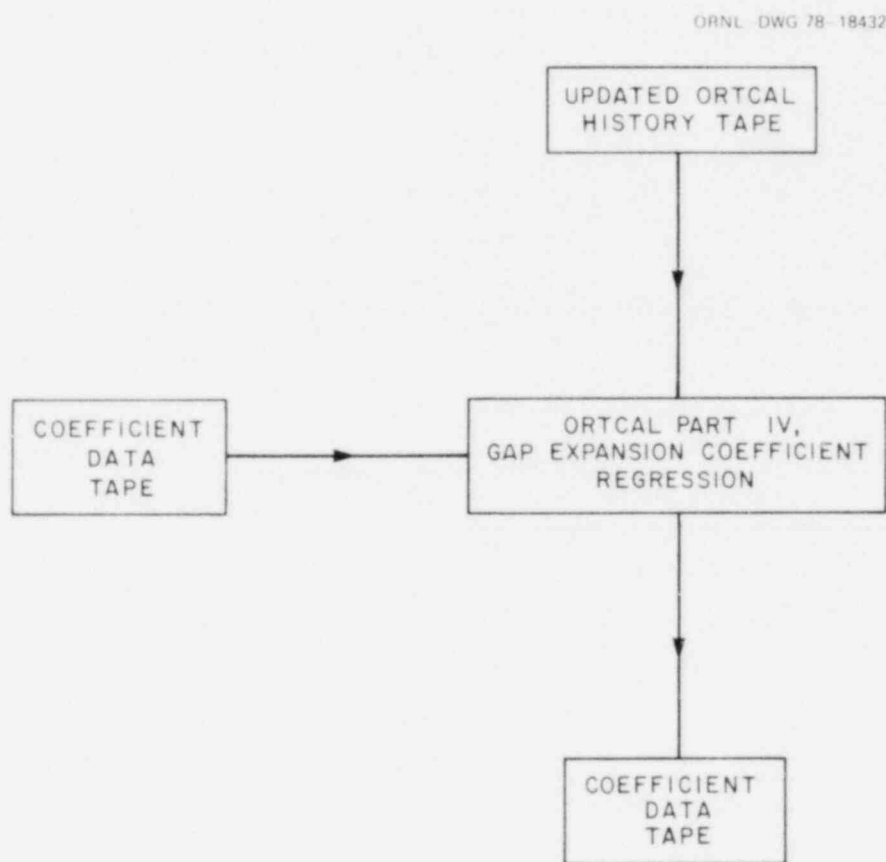


Fig. 2.25. Lines of information flow for ORTCAL - Part IV.



Table 2.5. The ORTCAL - Part IV contribution to the CDT  
file for position TE-318BG in THTF bundle 1

```

*****
*****
*** THERMOCOUPLE NO. 318-RG ***
*****
*****

***** MIDDLE T/C --- 318-MG

***** DATE OF LAST MODIFICATION : MAY 1, 1978

***** AXIAL POWER PEAKING FACTOR IS : 1.6659
        DETERMINED BY INDIV RESISTANCE CAL.

***** COEFFICIENTS FOR TEMPERATURE POLYNOMIAL FIT OF KBN
        DETERMINED FOR THE ABOVE SPECIFIC T/C/S/ITCM PAIR
C(1)= 0.21976151E 02
C(2)= -0.74225366E-02
C(3)= -0.73717558E-07
C(4)= 0.59715699E-09

        VARIANCE OF FIT= 0.18624649E 02
        UNITS FOR KBN FIT : BTU/(HR*FT**2/FT*F)

***** COEFFICIENTS FOR TEMPERATURE POLYNOMIAL FIT FOR KMG0
        DETERMINED FOR THE ABOVE SPECIFIC T/C PAIR
C(1)= 0.72101288E 01
C(2)= -0.10450333E-01
C(3)= 0.79769443E-05
C(4)= -0.29365270E-08
C(5)= 0.45424298E-12

        VARIANCE OF FIT= 0.43312866E 03
        UNITS FOR KMG0 FIT : BTU/(HR*FT**2/FT*F)

        ACTUAL MG0 POROSITY CALCULATED VIA MODIFIED
        RUSSELL EQUATION : 0.18648702E 00

```

ORTCAL - PART IV

```

***** COEFFICIENTS FOR THE THERMAL EXPANSION GAP MODEL FIT
        DETERMINED FOR THE ABOVE SHEATH T/C

C(1)= 0.52502546E 01      SD= 0.12002551E 02
C(2)= 0.50596754E-02      SD= 0.17433237E-01
C(3)= -0.43715855E-05     SD= 0.87200751E-05

        VARIANCE OF FIT= 0.91365113E-04

        GAP CALCULATION AT THE BIAS POINT :                0.0547      (MILS)

        BIAS TEMP. INSIDE S.S.S. NODAL TEMP. :              815.4      DEG. F
        BIAS TEMP. OUTSIDE S.S.S. NODAL TEMP. :             700.8      DEG. F
        BIAS FLUX : 532344.1 BTU/HR/FT**2

        THE MAXIMUM TEMPERATURE FOR WHICH THE ABOVE
        REGRESSION FIT IS APPLICABLE IS 817.17 DEG. F

```

The primary failure mechanism for the Part IV regressions is item 3, which implies that the simple one-dimensional linear thermal expansion model described by Eq. (2.33) is not capable of describing the dynamic gap behavior at those locations where regression failure occurs. A negative first derivative of Eq. (2.35) implies that the thermal expansion coefficient of stainless steel decreases with increasing temperature, but available physical property data<sup>6</sup> refute this behavior. The linear thermal expansion model accounts only for the radial expansion or contraction of the gap and does not allow for other mechanisms of stress relief. For instance, it is conjectured that there are severe torsional stresses imparted to the stainless steel sheaths by the swaging process during construction of the heaters and that these stresses would be worse at levels H and J. (The heaters are swaged in the direction of A to O level, and levels H and J are located in close proximity to power level breaks with significant radial dimensional differences prior to swaging.) The expected relief of these torsional stresses would be azimuthal rotation of the sheaths relative to each other and the heating element; thus, the gap could not be described by Eq. (2.33).

Part IV regressions are summarized in Table F.4 for THTF bundle 1 through run 24.1. Of the available 269 bundle thermocouple positions, approximately 65% (175) can be calibrated by use of Eq. (2.33). Of the 94 regression failures, 75 (80%) are due to the mode 3 failure mechanism and 73 of the failures occur on H and J level.

If the regressions fail for any of the above reasons, the bias gap is used as a mean gap (i.e., constant gap throughout the transient) in the inverse calculations.

### 3. CONSEQUENCES OF NONCALIBRATION OF FUEL PIN SIMULATORS

The effect of not classifying fuel pin simulators can best be illustrated by a series of examples that consist of ORINC runs on THTF test 105, where the points of interest in the rod calibration (i.e., BN thermal conductivity, MgO thermal diffusivity, and gap between the sheaths) were varied to qualitatively assess their effect on the inverse calculations. (For a description of the phenomenological sequences in the THTF during test 105, see Refs. 26 and 41.) These properties were not varied in such a manner that the quantitative sensitivity of the calculated surface temperature and flux (with respect to the properties) could be determined (this analysis is currently being done). At present, the only alternative to the approach described in Chapter 2 is to use temperature fits to the literature data for the BN and MgO thermal conductivities and to assume that there is no gap between the sheaths. Therefore, ORINC case studies were made using the following combinations:

1. Case 1. ORTCAL regressions for BN thermal conductivity and MgO thermal diffusivity and the sheath-gap model;
2. Case 2. ORTCAL regression for  $k_{BN}$  and  $\alpha_{MgO}$  and all gaps zeroed;
3. Case 3. Least-squares fits to literature data for  $k_{BN}$  and  $\alpha_{MgO}$  and ORTCAL regressions for the sheath-gap model;
4. Case 4. Least-squares fits to literature data for  $k_{BN}$  and  $\alpha_{MgO}$  and all gaps zeroed.

Case 1 will be used as the base case; case 4 is the current state-of-the-art practice.

Typical rod surface temperature plots (case 1) for thermocouple levels E and C are presented in Figs. 3.1 and 3.2, respectively. Similar plots for the surface heat flux are shown in Figs. 3.3 and 3.4. The corresponding set of plots for case 2 is presented in Figs. 3.5 to 3.8.

A comparison of Figs. 3.3 and 3.4 and Figs. 3.7 and 3.8 reveals little difference in the computed surface heat fluxes. This is expected, since the inverse solutions of the transient conduction equation for cases 1 and 2 will yield identical results for the computed temperature profile from node 1 to node NOD5 (Figs. 3.9 and 3.10) and for the heat

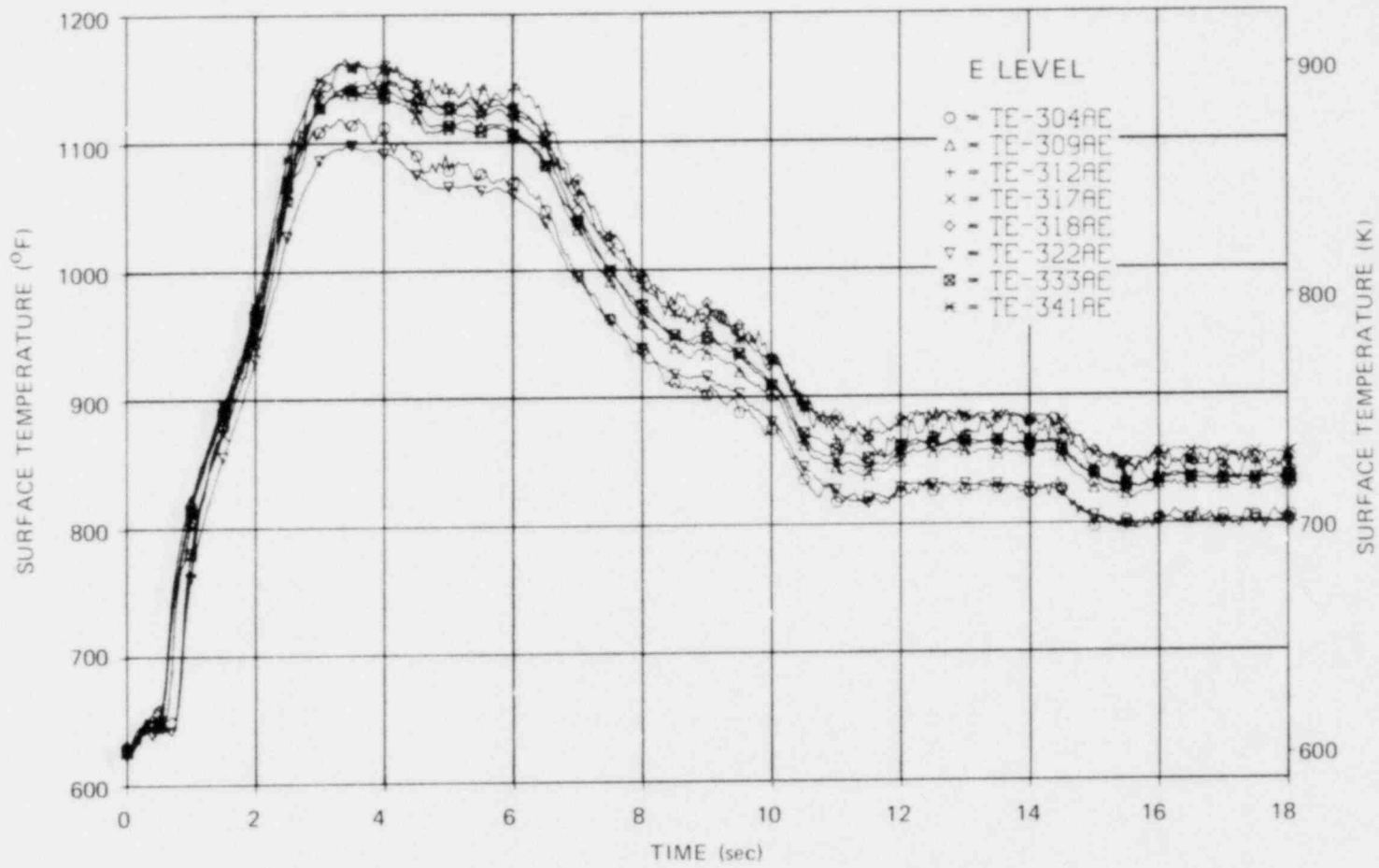


Fig. 3.1. ORINC rod surface temperatures, level E, THTF test 105, case 1.

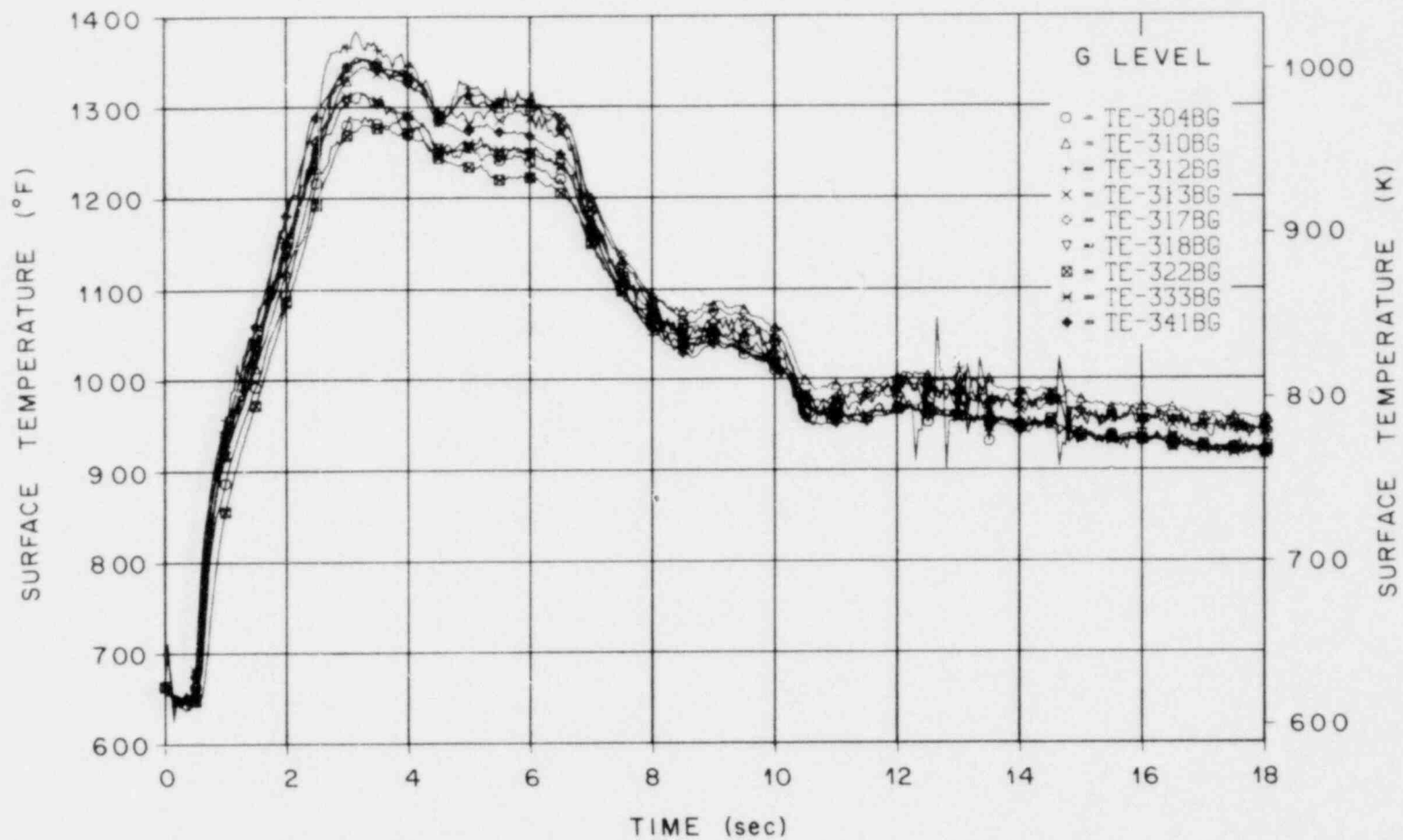


Fig. 3.2. ORINC rod surface temperatures, level G, THTF test 105, case 1.

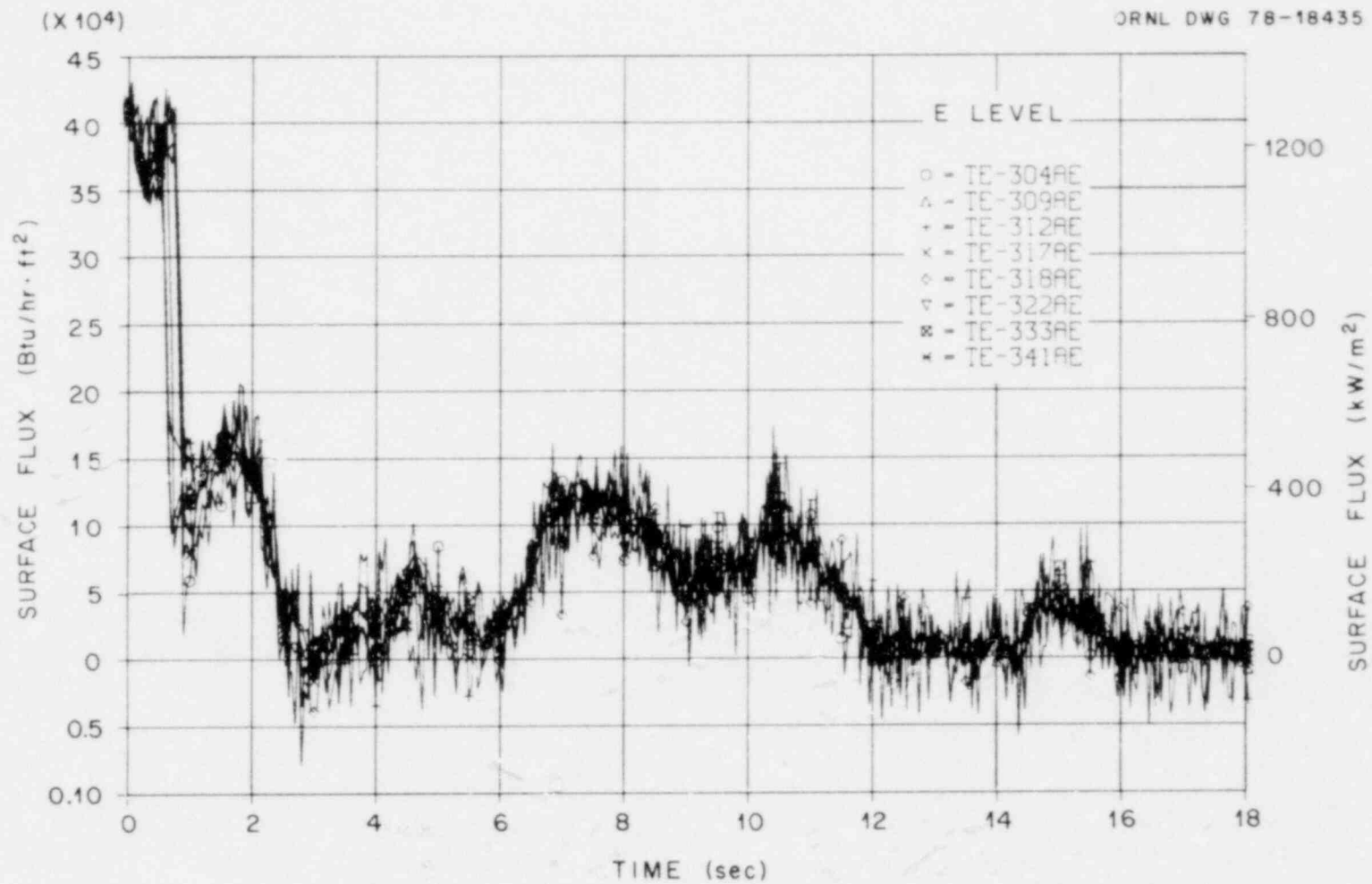


Fig. 3.3. ORINC rod surface heat fluxes, level E, THTF test 105, case 1.

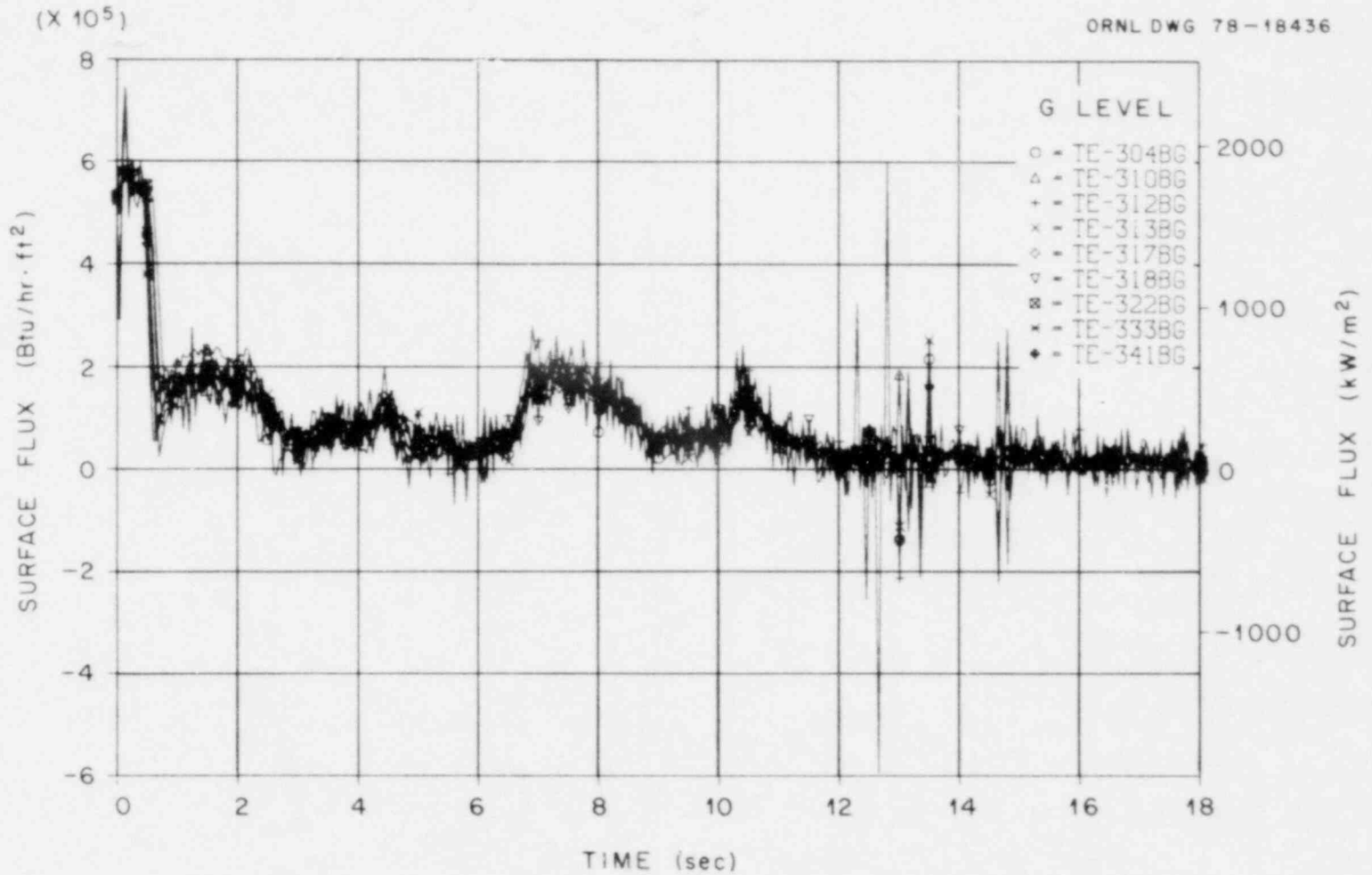


Fig. 3.4. ORINC rod surface heat fluxes, level G, THTF test 105, case 1.

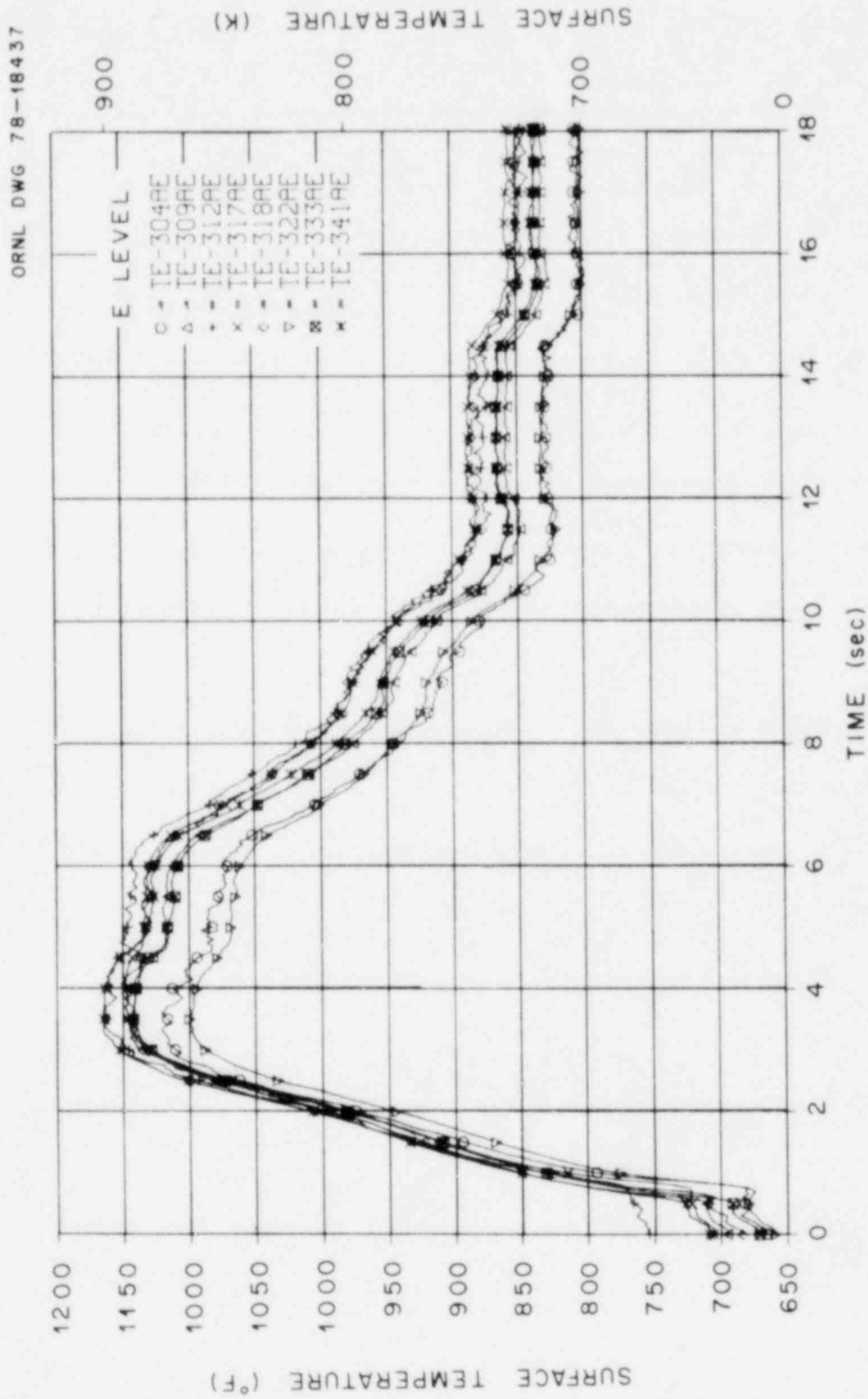


Fig. 3.5. ORINC rod surface temperatures, level E, THF test 105, case 2.



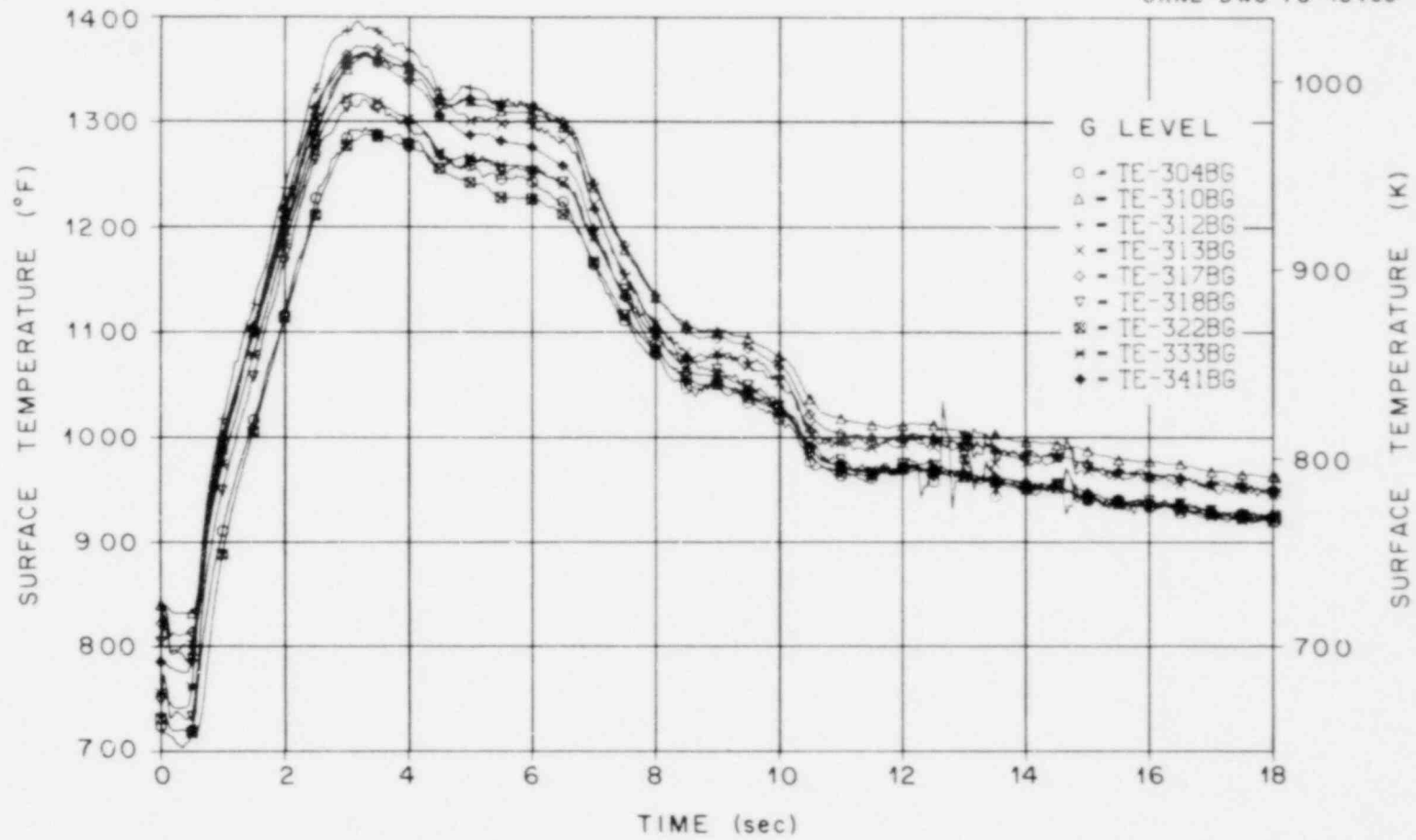


Fig. 3.6. ORINC rod surface temperatures, level G, THTF test 105, case 2.

ORNL DWG 78-18439

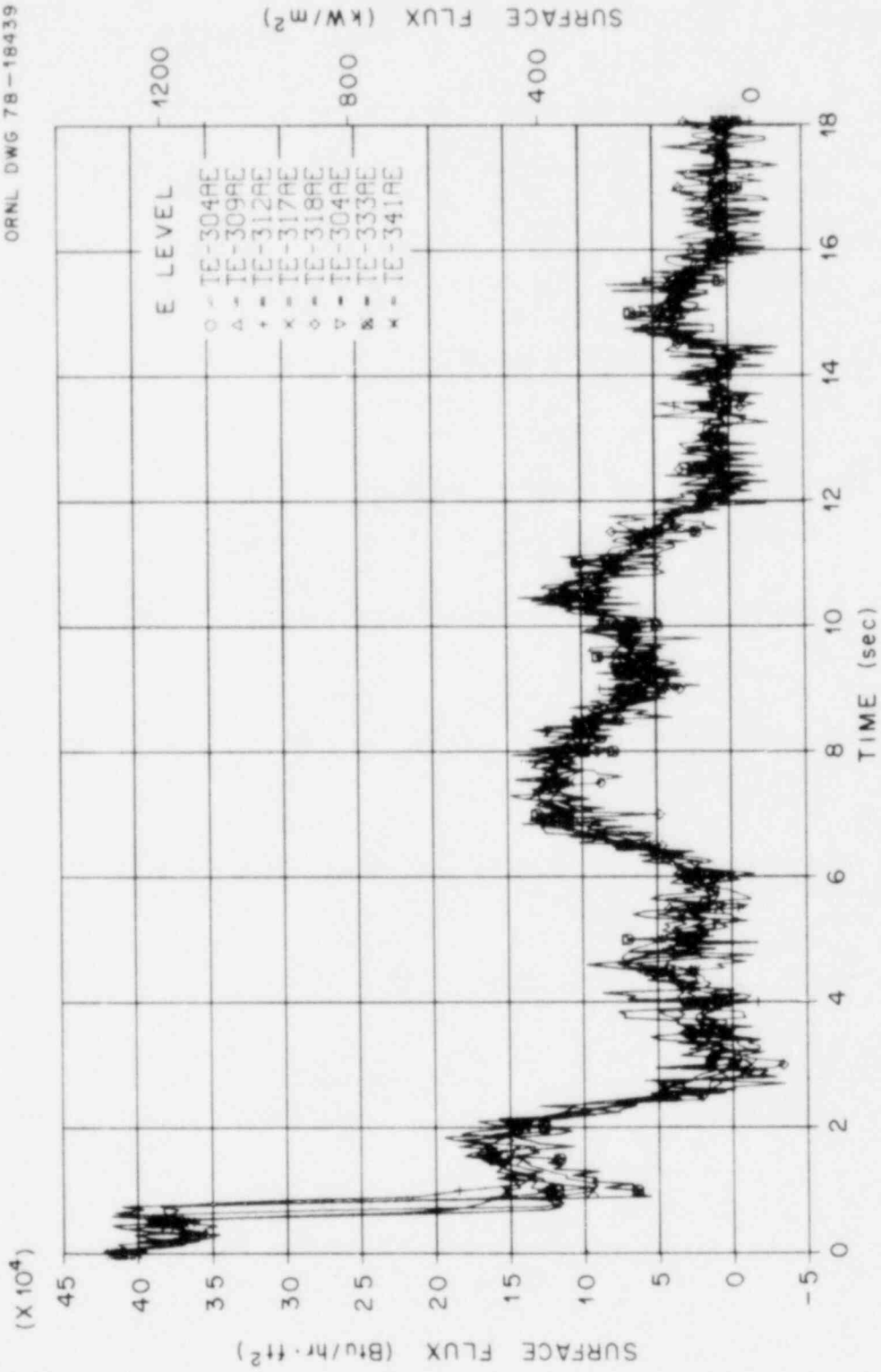


Fig. 3.7. ORING rod surface heat fluxes, level E, THTF test 105, case 2.

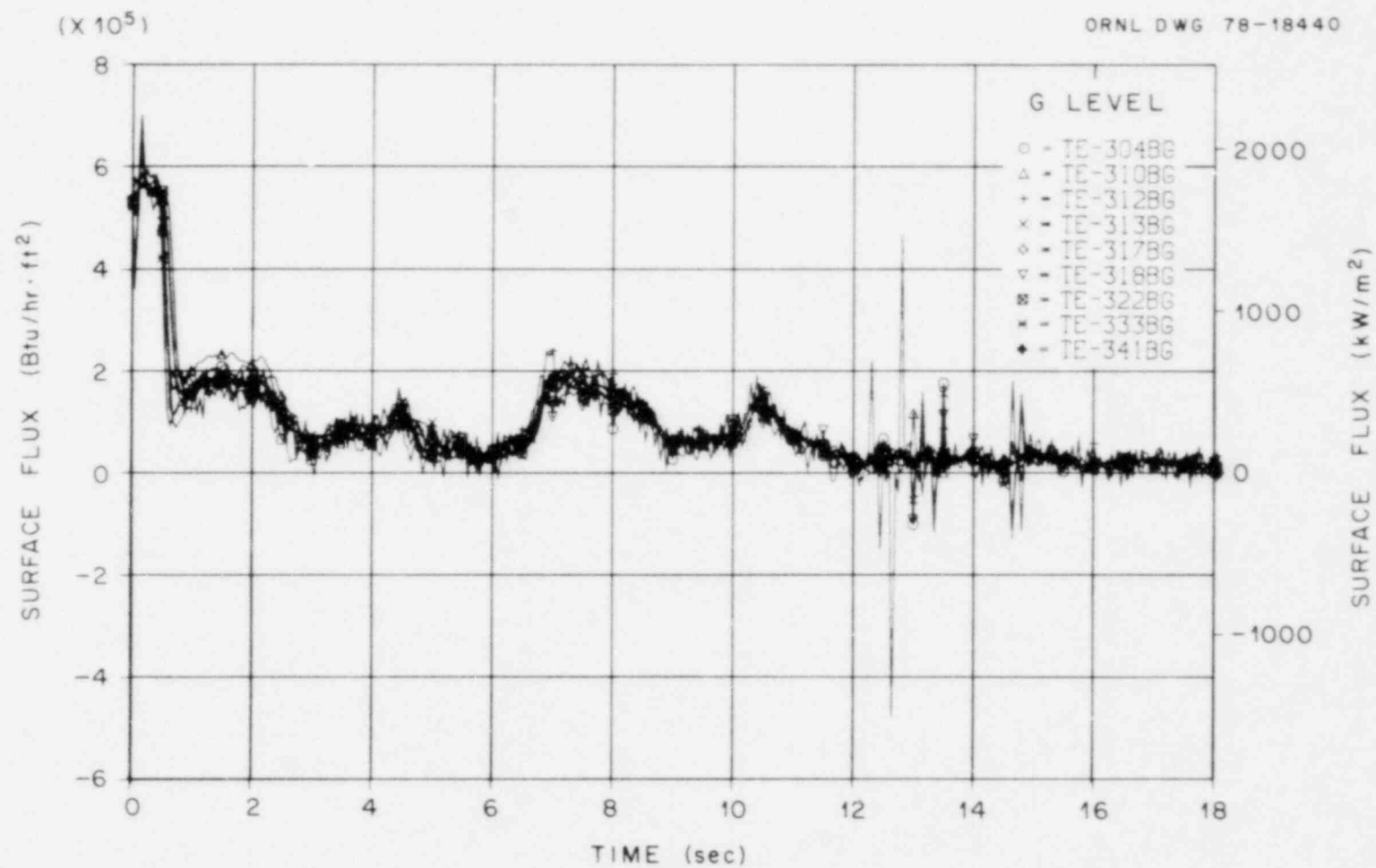


Fig. 3.8. ORINC rod surface heat fluxes, level G, THTF test 105, case 2.

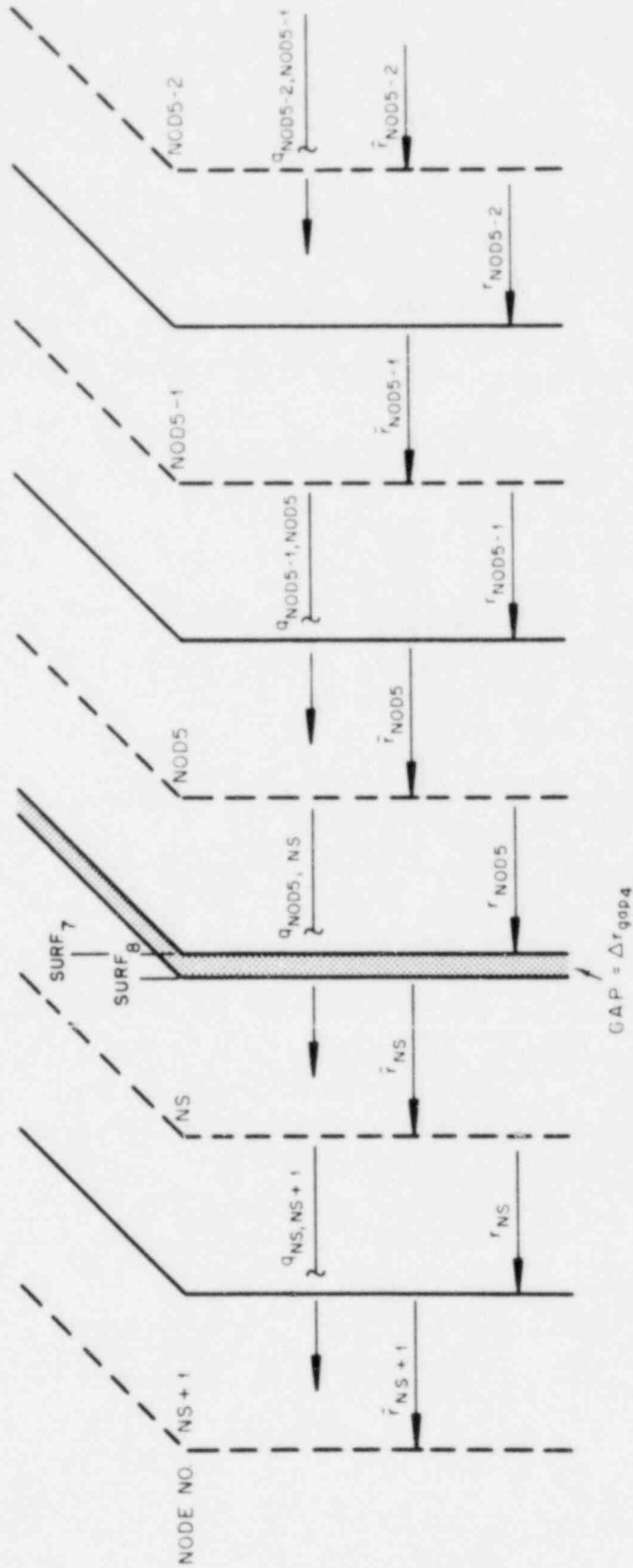


Fig. 3.9. Element notation at the inner stainless steel sheath to the outer stainless steel sheath interface.

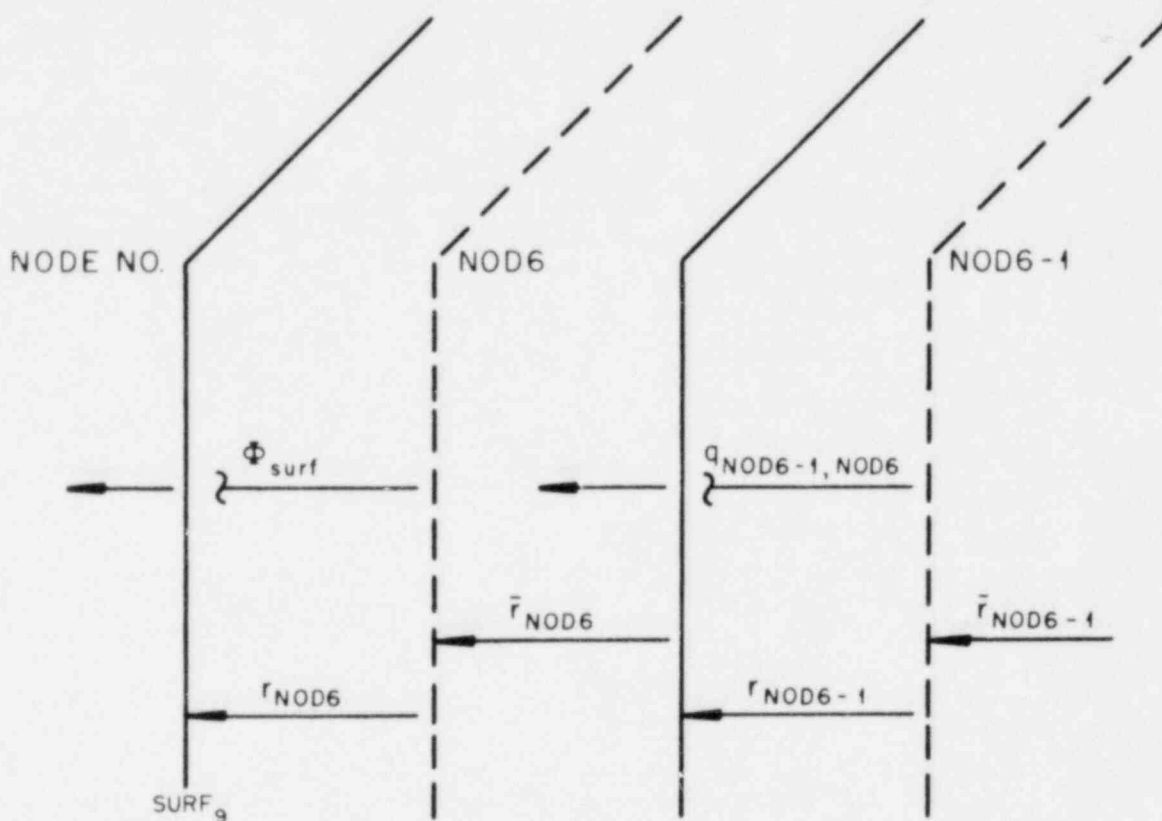


Fig. 3.10. Element notation at the heater surface.

flow from node NOD5 to node NS. Thus, since  $q_{\text{NOD5,NS}}$  is the same for both cases, the temperature for node NS in the outer stainless steel sheath must be higher for case 2 because the thermal resistance of the gap has been removed. Not only will the temperatures in the outer sheath (nodes NS to NOD6) be higher, the computed surface heat flux ( $\phi_{\text{surf}}$ ) will also be slightly different because of the temperature dependence of the specific heat and the thermal conductivity of stainless steel.

The noteworthy difference between cases 1 and 2 is obvious when Figs. 3.1 and 3.2 and 3.5 and 3.6 are compared; there is a significant discrepancy in the surface temperature plots in the pre- and post-CHF regions prior to bundle power trip. The rod surface conditions for two time periods (0 and 2 sec) from Figs. 3.1 and 3.5 are compared in Table 3.1. For case 1 at steady state on level E, the rod surface temperatures

Table 3.1. Comparison of case 1 and case 2 surface conditions for level E at 0 and 2 sec<sup>2</sup>

Thermocouple	Heat transfer mode	Surface flux @ t = 0 [W/m <sup>2</sup> (Btu/hr ft <sup>2</sup> )]	Surface temperature @ t = 0 [K (°F)]	Surface heat transfer coefficient @ t = 0 [W/m <sup>2</sup> K (Btu/hr °F ft <sup>2</sup> )]	Surface flux @ t = 2 [W/m <sup>2</sup> (Btu/hr ft <sup>2</sup> )]	Surface temperature @ t = 2 [K (°F)]
Case 1						
304AE	Forced conv.	1.299(10) <sup>5</sup> [4.1188(10) <sup>5</sup> ]	604.8 [628.9]	3.75(10) <sup>4</sup> [6607]	4.077(10) <sup>5</sup> [1.2926(10) <sup>5</sup> ]	789.8 [962.0]
309AE	Forced conv.	1.287(10) <sup>5</sup> [4.0809(10) <sup>5</sup> ]	604.3 [628.1]	3.76(10) <sup>4</sup> [6625]	4.550(10) <sup>5</sup> [1.4426(10) <sup>5</sup> ]	794.0 [969.4]
312AE	Forced conv.	1.268(10) <sup>5</sup> [4.0210(10) <sup>5</sup> ]	604.5 [628.4]	3.69(10) <sup>4</sup> [6503]	3.710(10) <sup>5</sup> [1.1763(10) <sup>5</sup> ]	791.6 [965.3]
317AE	Forced conv.	1.263(10) <sup>5</sup> [4.0052(10) <sup>5</sup> ]	603.1 [625.8]	3.83(10) <sup>4</sup> [6753]	4.593(10) <sup>5</sup> [1.4565(10) <sup>5</sup> ]	781.0 [946.1]
318AE	Forced conv.	1.310(10) <sup>5</sup> [4.1551(10) <sup>5</sup> ]	605.9 [630.9]	3.66(10) <sup>4</sup> [6458]	4.431(10) <sup>5</sup> [1.4049(10) <sup>5</sup> ]	788.0 [958.7]
322AE	Forced conv.	1.277(10) <sup>5</sup> [4.0478(10) <sup>5</sup> ]	601.7 [623.5]	4.04(10) <sup>4</sup> [7112]	4.183(10) <sup>5</sup> [1.3264(10) <sup>5</sup> ]	773.2 [932.1]
333AE	Forced conv.	1.296(10) <sup>5</sup> [4.1084(10) <sup>5</sup> ]	603.5 [626.6]	3.88(10) <sup>4</sup> [6839]	4.350(10) <sup>5</sup> [1.3794(10) <sup>5</sup> ]	793.6 [968.9]
341AE	Forced conv.	1.317(10) <sup>5</sup> [4.1769(10) <sup>5</sup> ]	605.1 [629.4]	3.77(10) <sup>4</sup> [6640]	4.629(10) <sup>5</sup> [1.4677(10) <sup>5</sup> ]	796.4 [973.8]
Case 2						
304AE	Nucleate boiling	1.299(10) <sup>5</sup> [4.1188(10) <sup>5</sup> ]	625.6 [666.4]	1.98(10) <sup>5</sup> [34830]	4.003(10) <sup>5</sup> [1.2692(10) <sup>5</sup> ]	797.1 [975.2]
309AE	Nucleate boiling	1.287(10) <sup>5</sup> [4.0809(10) <sup>5</sup> ]	641.9 [695.7]	5.64(10) <sup>4</sup> [9932]	4.573(10) <sup>5</sup> [1.4501(10) <sup>5</sup> ]	809.3 [997.1]
312AE	Nucleate boiling	1.268(10) <sup>5</sup> [4.0210(10) <sup>5</sup> ]	674.4 [754.3]	2.29(10) <sup>4</sup> [4035]	3.931(10) <sup>5</sup> [1.2463(10) <sup>5</sup> ]	814.9 [1007.1]
317AE	Nucleate boiling	1.263(10) <sup>5</sup> [4.0052(10) <sup>5</sup> ]	647.5 [705.8]	4.44(10) <sup>4</sup> [7825]	4.582(10) <sup>5</sup> [1.4530(10) <sup>5</sup> ]	800.8 [981.8]
318AE	Nucleate boiling	1.310(10) <sup>5</sup> [4.1551(10) <sup>5</sup> ]	635.7 [684.7]	7.84(10) <sup>4</sup> [13815]	4.665(10) <sup>5</sup> [1.4792(10) <sup>5</sup> ]	800.7 [981.6]
322AE	Nucleate boiling	1.277(10) <sup>5</sup> [4.0478(10) <sup>5</sup> ]	621.8 [659.5]	4.66(10) <sup>4</sup> [82044]	4.266(10) <sup>5</sup> [1.3527(10) <sup>5</sup> ]	780.1 [944.4]
333AE	Nucleate boiling	1.296(10) <sup>5</sup> [4.1084(10) <sup>5</sup> ]	628.3 [671.3]	1.39(10) <sup>5</sup> [24541]	4.417(10) <sup>5</sup> [1.4006(10) <sup>5</sup> ]	801.2 [982.5]
341AE	Nucleate boiling	1.317(10) <sup>5</sup> [4.1769(10) <sup>5</sup> ]	649.0 [708.5]	4.40(10) <sup>4</sup> [7745]	4.652(10) <sup>5</sup> [1.4751(10) <sup>5</sup> ]	815.3 [1007.8]

<sup>2</sup>At t = 0, bulk avg. temp. = 570.1 K (566.5°F); saturation temp. = 619.0 K (654.6°F); local fluid pressure = 1570.2 kPa (2280 psia).

range from 601.7 to 605.9 K with a predicted heat transfer mode of forced convection; however, for case 2 (zero gaps), the heat transfer mode changed to nucleate boiling and the rod surface temperature range became 621.8 to 674.4 K. There are similar results for 2 sec into the transient, with a rod surface temperature range of 773.2 to 796.4 K for case 1 and a rod surface temperature range of 780.1 to 815.3 K for case 2. The calculated surface temperatures for case 2 are higher than those for case 1, and the range is much broader. The question of which case is more accurate must be answered because, as noted earlier, the calculated surface

fluxes do not vary significantly between the cases but the driving potential (i.e.,  $T_{\text{surface}} - T_{\text{sink}}$ ) is drastically different. As a result, the computed surface heat transfer coefficient would be greatly affected.

A study of the steady-state conditions (at  $t = 0$  sec) for cases 1 and 2 at level E gives a reasonable answer to the above question. Case 1 predicts forced convection at level E. Using the local fluid conditions in Table 3.1, the Dittus-Boelter correlation yields a film coefficient of  $3.6 \times 10^4$  W/m<sup>2</sup>-K. The mean of the coefficients determined by ORINC for level E in case 1 is  $3.77 \times 10^4$  W/m<sup>2</sup>-K (17 observations with a standard deviation about the mean of  $0.05 \times 10^4$  W/m<sup>2</sup>-K). At steady-state, the mean surface heat flux for level E is  $1.290 \times 10^6$  W/m<sup>2</sup> (17 observations with a standard deviation about the mean of  $0.020 \times 10^6$  W/m<sup>2</sup>). If the surface temperature for level E is calculated by

$$T_{\text{surf}} = T_{\text{bulk}} + \frac{\bar{\phi} \pm 3\delta_{\bar{\phi}}}{h_{\text{D-B}}}, \quad (3.1)$$

the expected surface temperature range for level E would be 604.2 to 607.5 K, essentially the range determined for case 1. In case 2, for the nucleate boiling regime to be chosen by ORINC, the pin model had to transfer heat to a sink temperature equal to the saturation temperature (619.0 K at 15709.2 kPa). If Thom's correlation is used for the sub-cooled nucleate boiling regime, the expected surface temperature range for level E can be determined by

$$T_{\text{surf}} = T_{\text{sat}} + 0.0406 (\bar{\phi} \pm 3\delta_{\bar{\phi}})^{1/2} e^{-P/8687}. \quad (3.2)$$

The expected range for level E would be 626.4 to 626.7 K if the local fluid pressure in Table 3.1 is used; however, the computed surface temperature range is 621.8 to 674.4 K. If there are pressure fluctuations radially at level E, the local pressures required to produce the computed rod surface temperatures in Table 3.1 for case 2 must be determined. Assuming Thom's correlation is applicable and using the rod surface heat fluxes (at  $t = 0$ ) in Table 3.1, the local pressures shown in Table 3.2 and Fig. 3.11 would be required. From Fig. 3.11, it should be readily apparent that the existence of such radial pressure differences at one

Table 3.2. Local fluid pressure required to achieve surface temperatures for case 2 during nucleate boiling

Thermocouple No.	Surface temperature [K (°F)]	Required local fluid pressure [MPa (psia)]
304AE	625.6 (666.4)	16.23 (2354)
309AE	641.9 (695.7)	20.10 (2916)
312AE	674.4 (754.3)	$\alpha$
317AE	647.5 (705.8)	$\alpha$
318AE	635.7 (684.7)	18.57 (2694)
322AE	621.8 (659.5)	15.41 (2235)
333AE	628.3 (671.3)	16.84 (2442)
341AE	649.0 (708.5)	22.00 (3190)

$\alpha$  Greater than critical pressure.

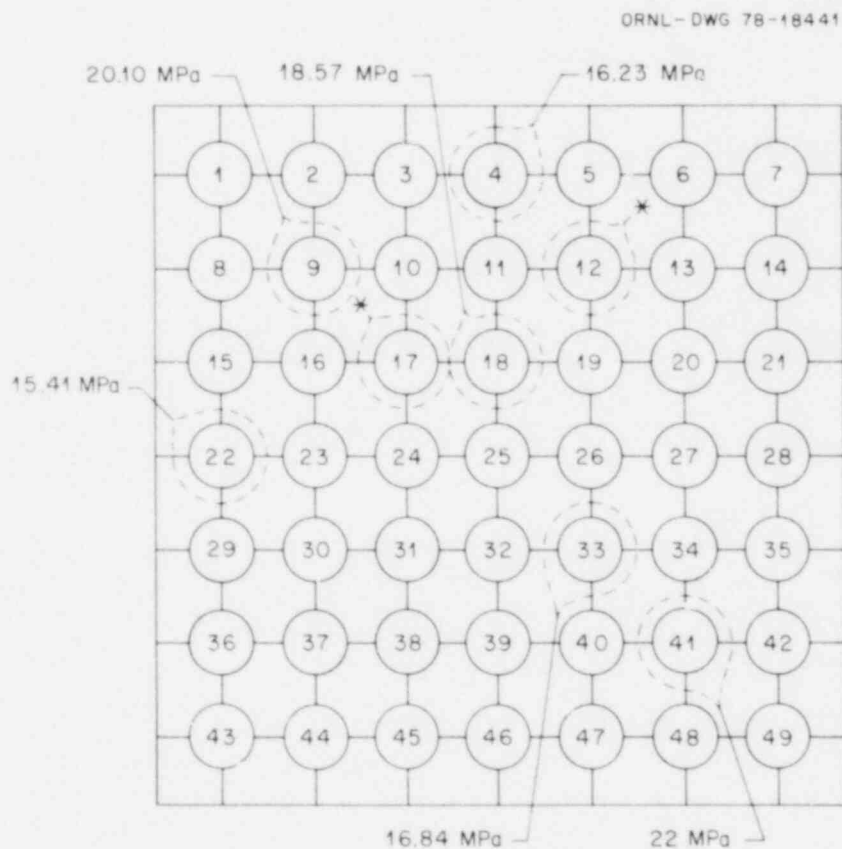


Fig. 3.11. Distribution of pressure superimposed on cross section of bundle 1 core.



axial level in the core is physically impossible. Thus, it could be concluded that case 1 describes the surface conditions at level E best and that case 2 (with the zero gap assumption) grossly miscalculates the surface temperatures.

Case 3 of the ORINC studies was an attempt to determine *only* the effect on the inverse calculations of using literature data for the insulator thermal conductivities; thus, both cases 1 and 3 use the ORTCAL dynamic gap model and gap regressions. The only differences between cases 1 and 3 are the regression fits for  $k_{BN}$  and  $\alpha_{MgO}$  (i.e., ORTCAL regressions on THTF data in case 1 and least-squares fits to literature data in case 3). Fits to the literature data yield *higher* thermal conductivities values for both BN and MgO than those predicted by the ORTCAL regressions. The ORINC results at thermocouple position 318BG for THTF test 105 will be reviewed for cases 1 and 3.

A case result will be defined to be correct if the calculated pin internal thermal response from ORINC matches or closely approximates the actual internal response from a pin centerline thermocouple. The centerline thermocouple provides the means for independently verifying the model results.

The ORINC-calculated surface heat fluxes for cases 1, 3, and 4 are overlaid in Fig. 3.12 for 18 sec of the transient, and the corresponding surface temperatures are presented in Fig. 3.13. There appear to be minimal (if any) differences between cases 1 and 3; however, there is a very deceiving compression effect from the Y-axis scale factor (this will be reviewed later). Figure 3.14 is an overlay of the calculated pin centerline temperature response for cases 1, 3, and 4 with the response from thermocouple TE-318MG (the centerline thermocouple relative to TE-318BG). Note that case 1 very closely approximates the response of 318MG; however, case 3 not only initializes incorrectly at steady state but responds too fast, peaks too high, and rolls off too fast.

The incorrect setup in steady state for case 3 (the centerline temperature is  $\sim 18$  K low) is caused solely by the BN thermal conductivity. As stated earlier, a fit to literature data for the thermal conductivity of BN yields higher values than those predicted by the ORTCAL regressions; therefore, for the same power-generation rate, less thermal gradient is

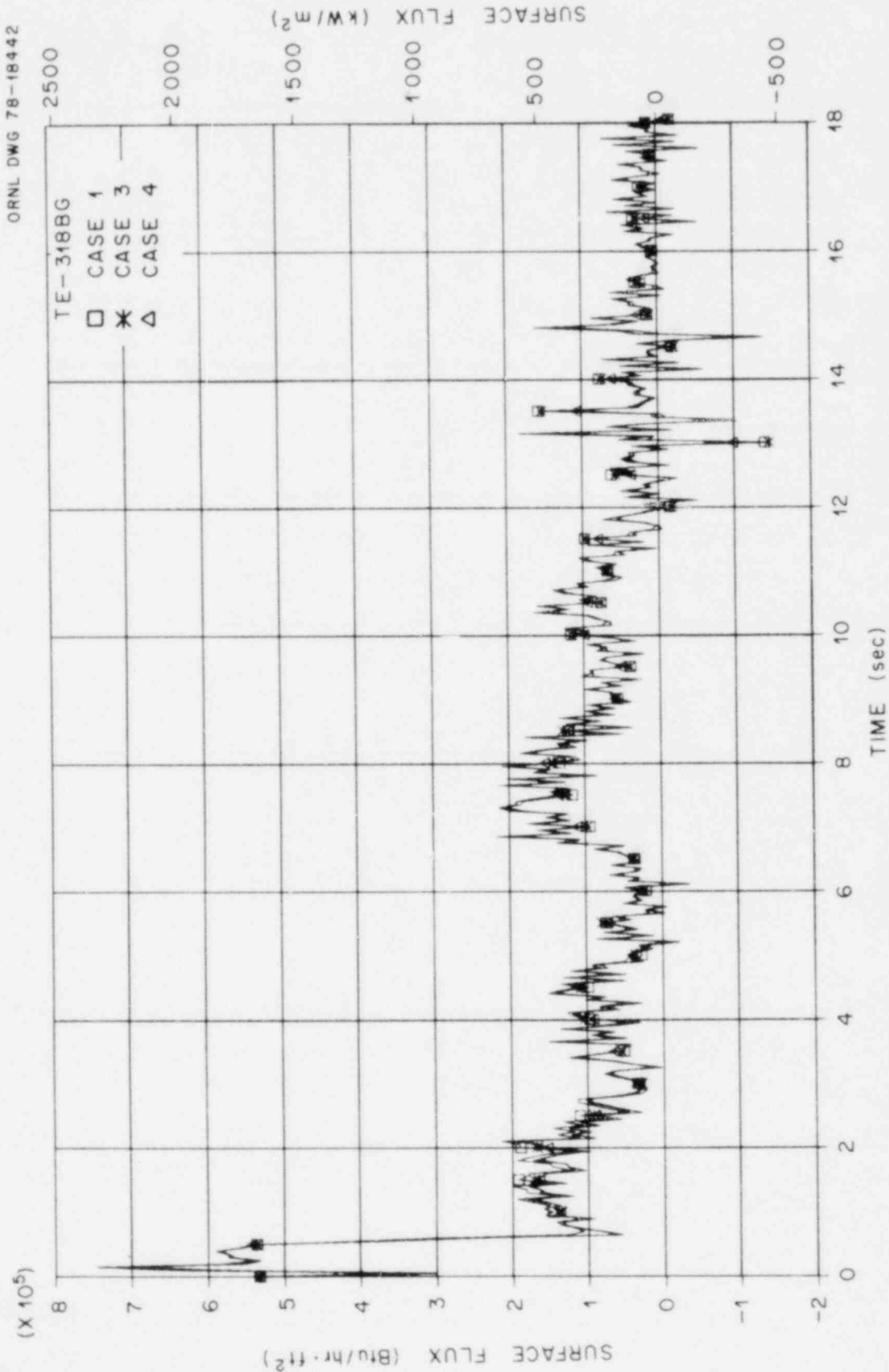


Fig. 3.12. ORINC rod surface heat flux, TE-318BG, THTF test 105, 0-18 sec.

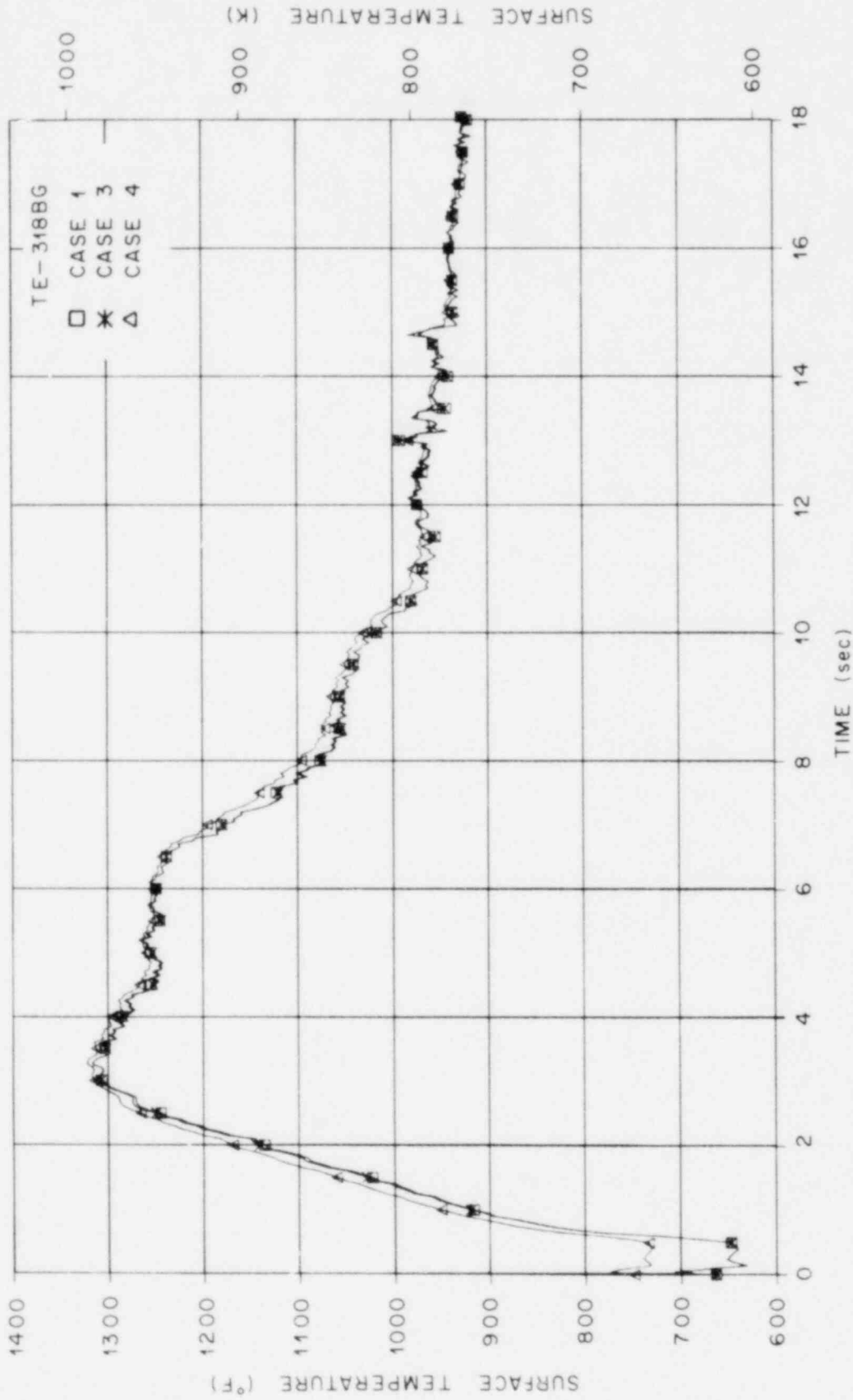


Fig. 3.13. ORINC rod surface temperature, TE-318BG, THTF test 105, 0-18 sec.

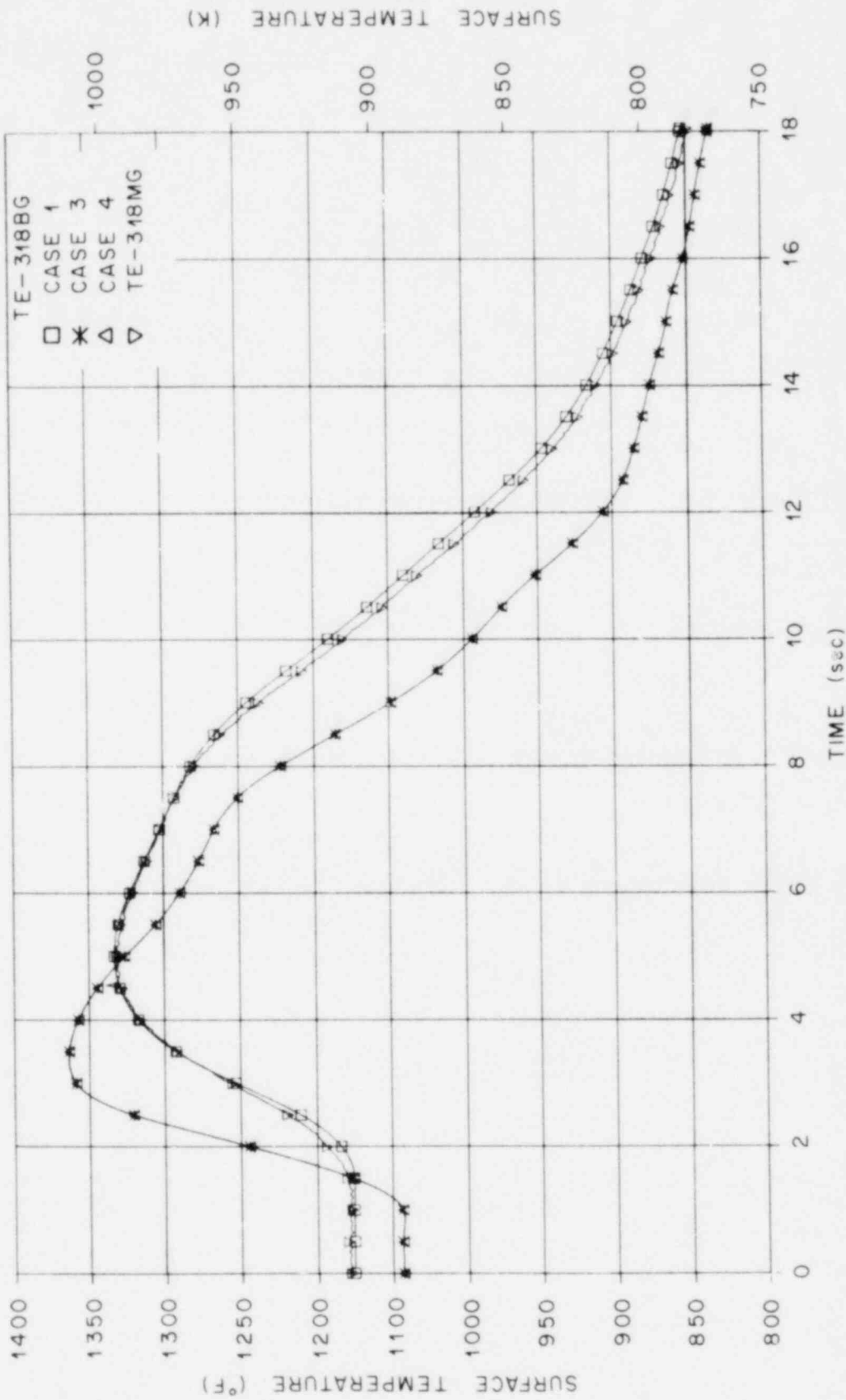


Fig. 3.14. Rod centerline temperature, TE-318BG, THTF test 105, 0-18 sec.

required in case 3 to move the heat through the BN and thus the centerline temperature is lower. As a result of the lower temperature profile, the total heat content of the pin is less at steady state. A comparison of the overall heat balance for cases 1 and 3 shows that the total heat removed per unit length of pin, as defined by

$$2\pi r_{\text{surf}} \int_0^{t_{\text{end}}} \phi_{\text{surf}} dt ,$$

is 1.8% less for case 3 (43.843 W-hr/m for case 1). The total energy input to the pin is the same for both cases (39.944 W-hr/m), but the change in internal energy for case 3 is ~20.3% less than that for case 1 (3.957 W-hr/m for case 1). Since the final temperature profile for cases 1 and 3 is essentially the same (i.e., the final heat content of the pin would be the same), the error is in the steady-state initialization.

Do not assume that the 1.8% error in

$$2\pi r_{\text{surf}} \int_0^{t_{\text{end}}} \phi_{\text{surf}} dt$$

is distributed evenly over the time interval (0- $t_{\text{end}}$ ) because it is not. As noted earlier, Fig. 3.12 is misleading due to the Y-axis scaling.

The time range (0-18 sec) can be broken down into time intervals over which the value of the surface heat flux does not vary orders of magnitude; Figs. 3.15 to 3.18 show breakdowns of the 0-18-sec time range into intervals of 0-0.5, 0.5-2.0, 2.0-8.0, and 5.0-18.0 sec, respectively. The corresponding surface temperature plots are presented in Figs. 3.19 to 3.22. Over the time intervals of 0-0.65 and 3.3-18.0 sec, the calculated surface heat flux and surface temperature for cases 1 and 3 are basically the same. One of the primary forcing functions for the inverse calculations ( $\dot{q}''$ ) drops to 0.0 at ~6.0 sec and drops to ~1/10 of the steady-state value at ~3.3 sec. Also, the pin at this position (318BG) is in nucleate boiling in steady state and remains so until CHF at ~0.5 sec and thus there is little change in the internal response until ~0.65 sec. Over the 0.65- to 3.0-sec interval, the calculated flux for case 3 ranges

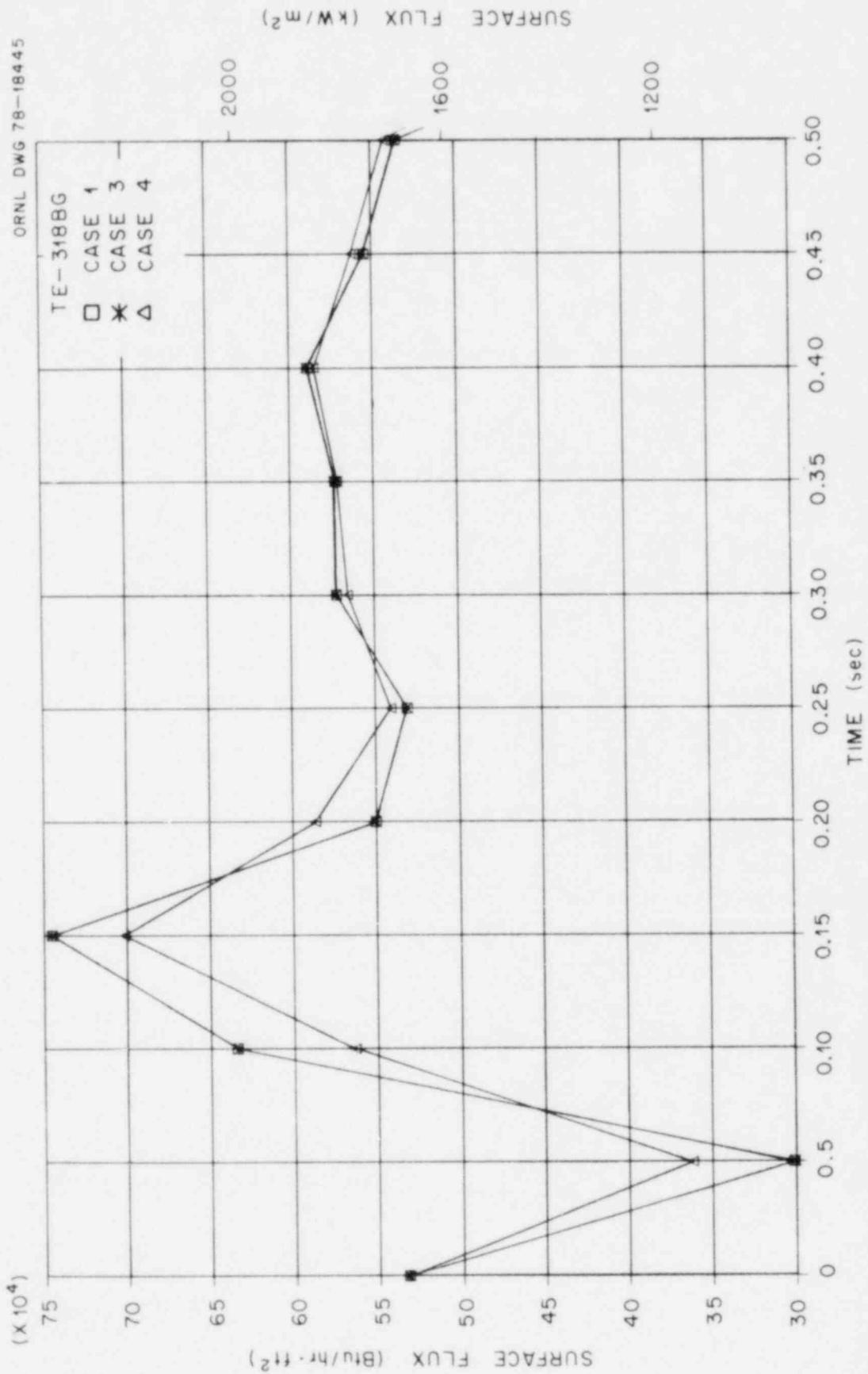


Fig. 3.15. ORINC rod surface heat flux, TE-318BG, THTF test 105, 0-0.5 sec.

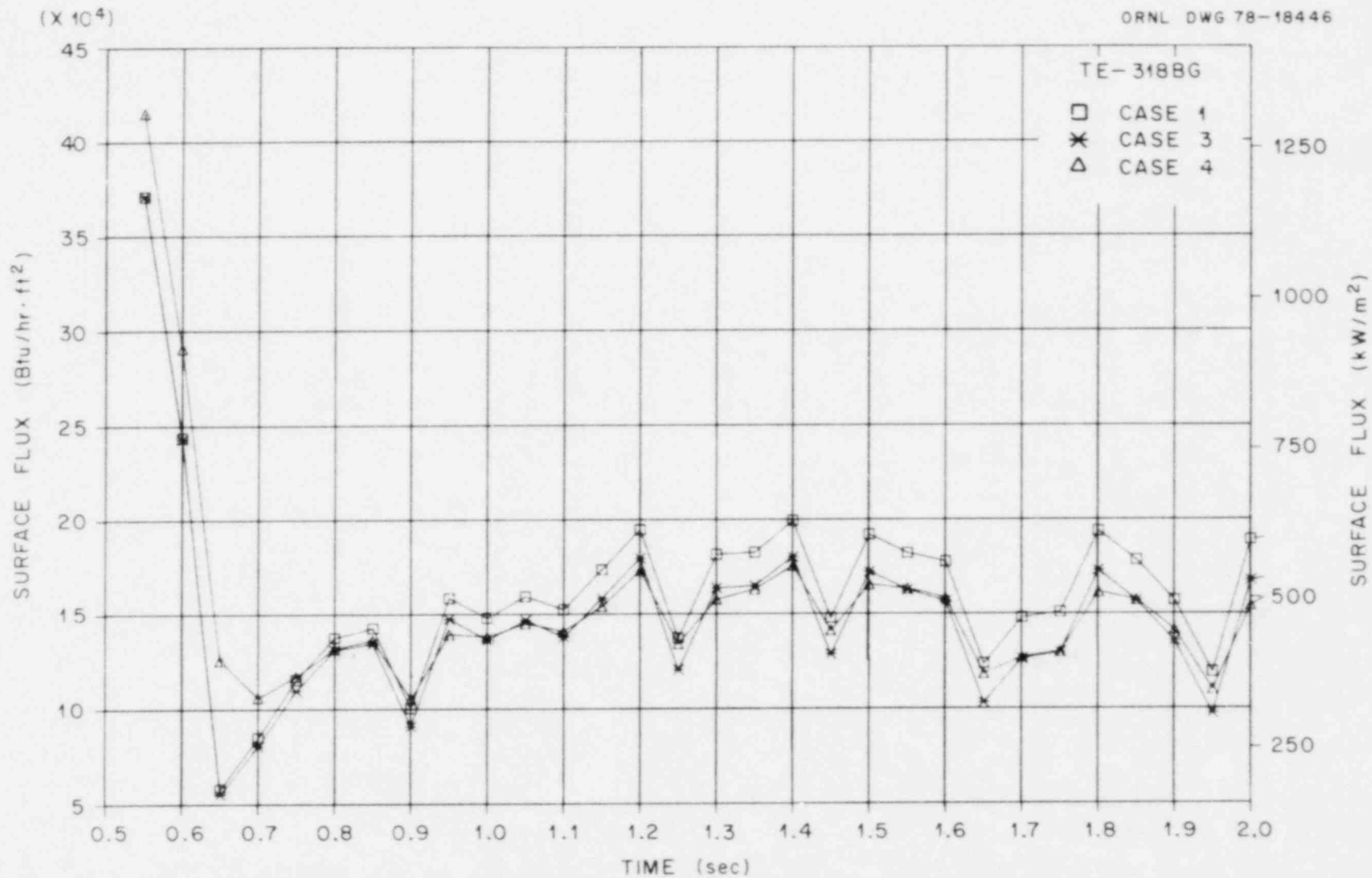


Fig. 3.16. ORINC rod surface heat flux, TE-318BG, THTF test 105, 0.5-2 sec.

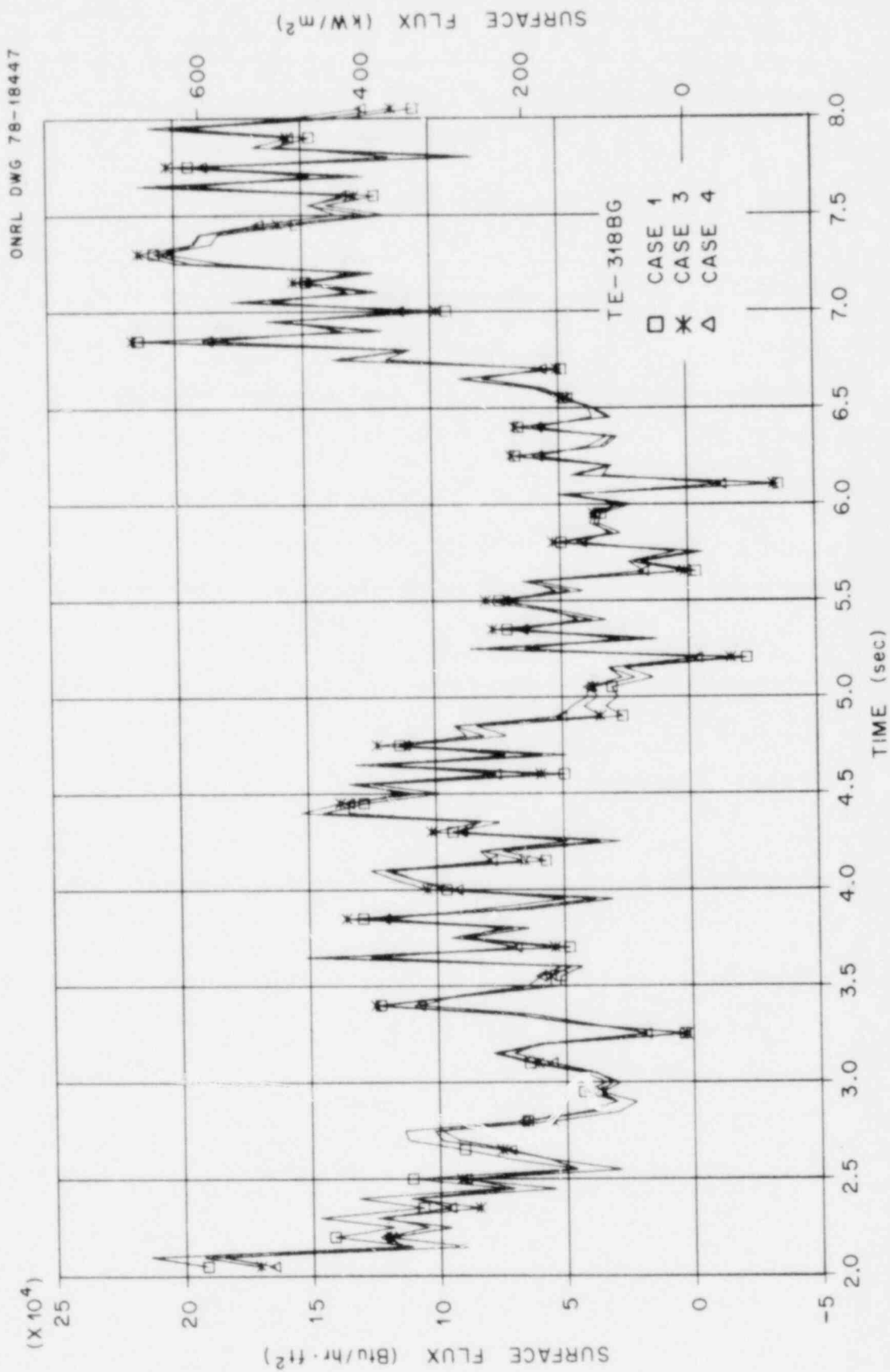


Fig. 3.17. ORINC rod surface heat flux, TE-318BG, THTF test 105, 2.0-8 sec.



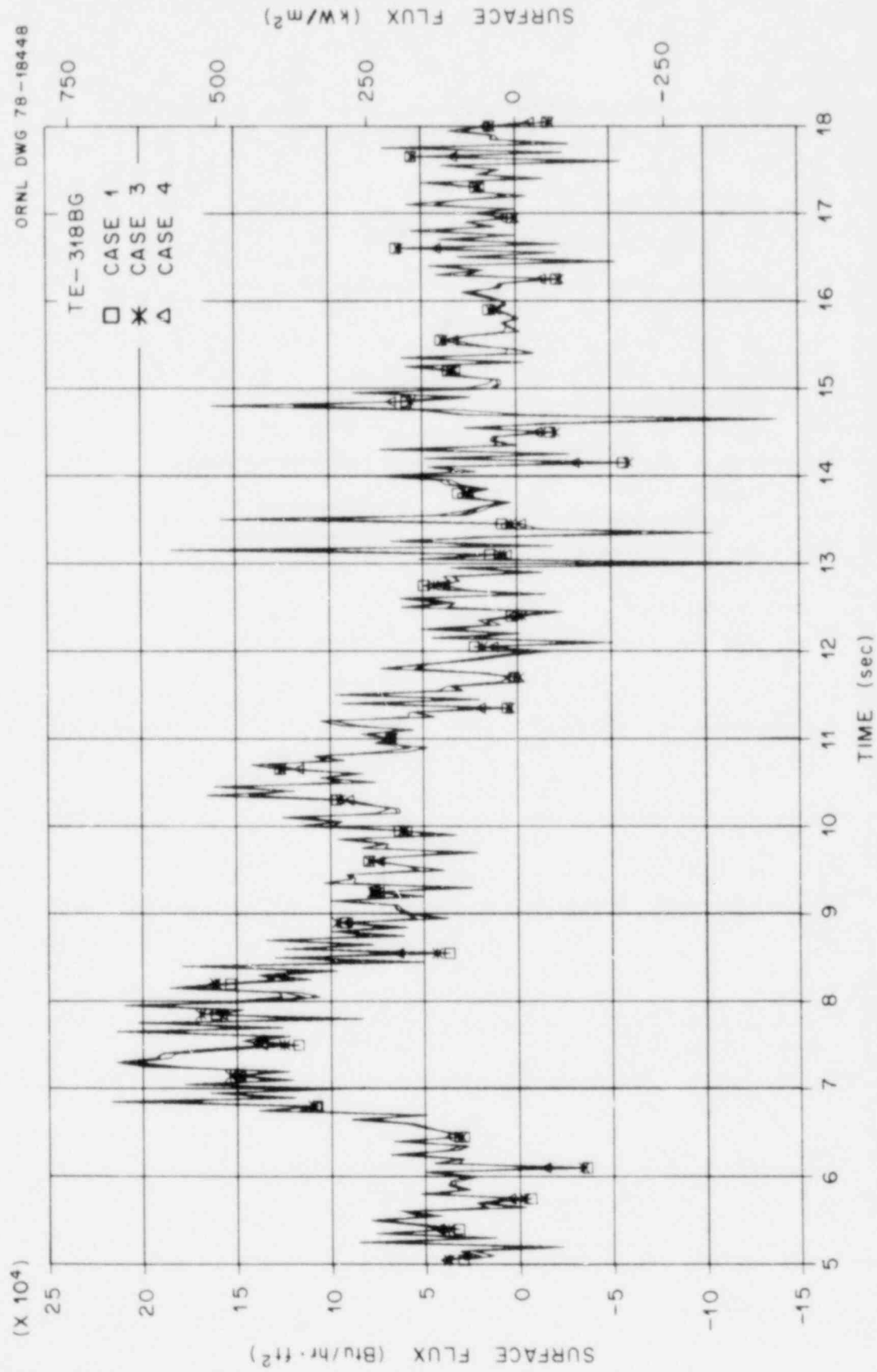


Fig. 3.18. ORINC rod surface heat flux, TE-318BG, THTF test 105, 5.0-18 sec.

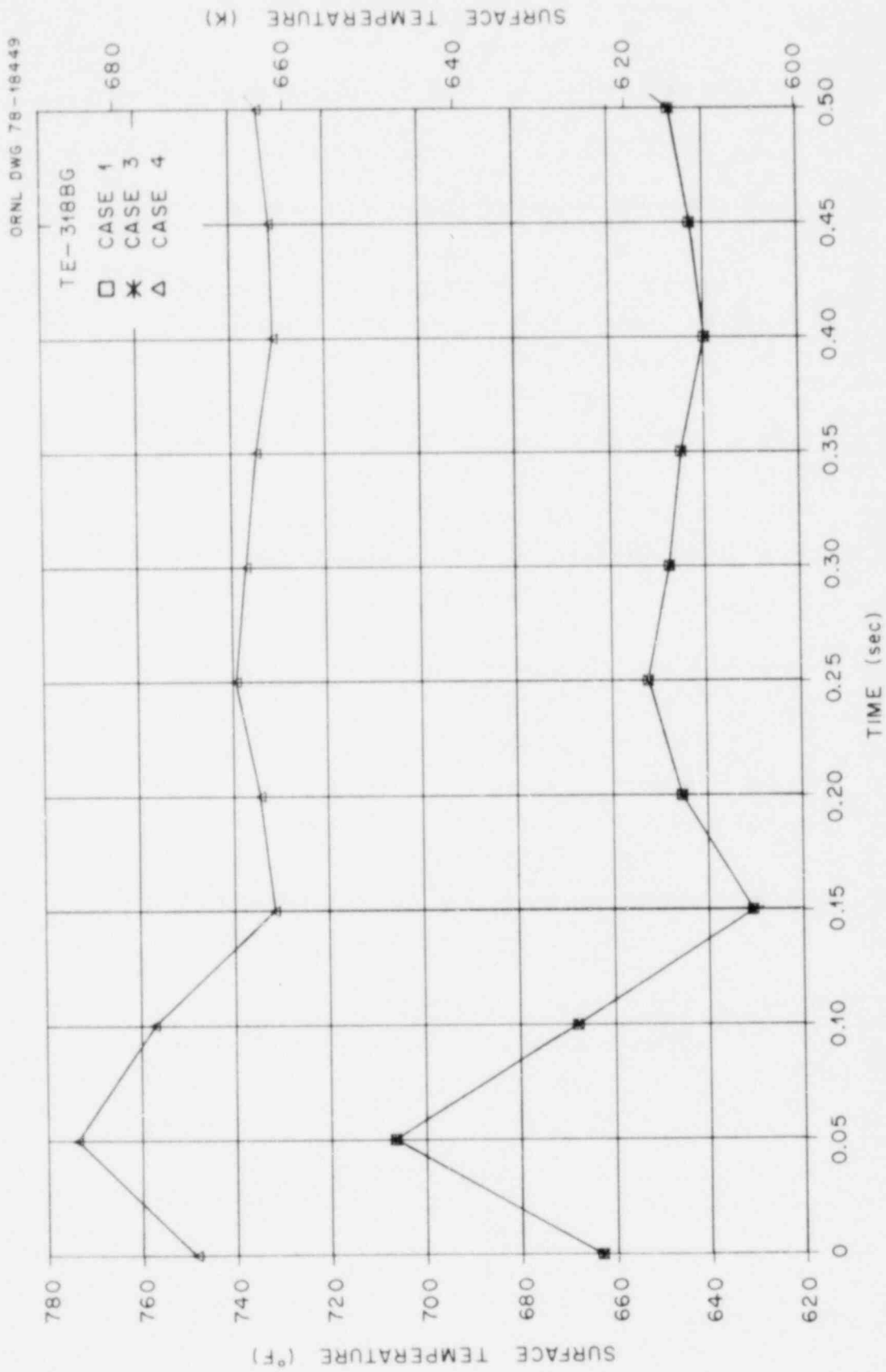


Fig. 3.19. ORINC rod surface temperature, TE-318BG, THF test 105, 0-0.5 sec.

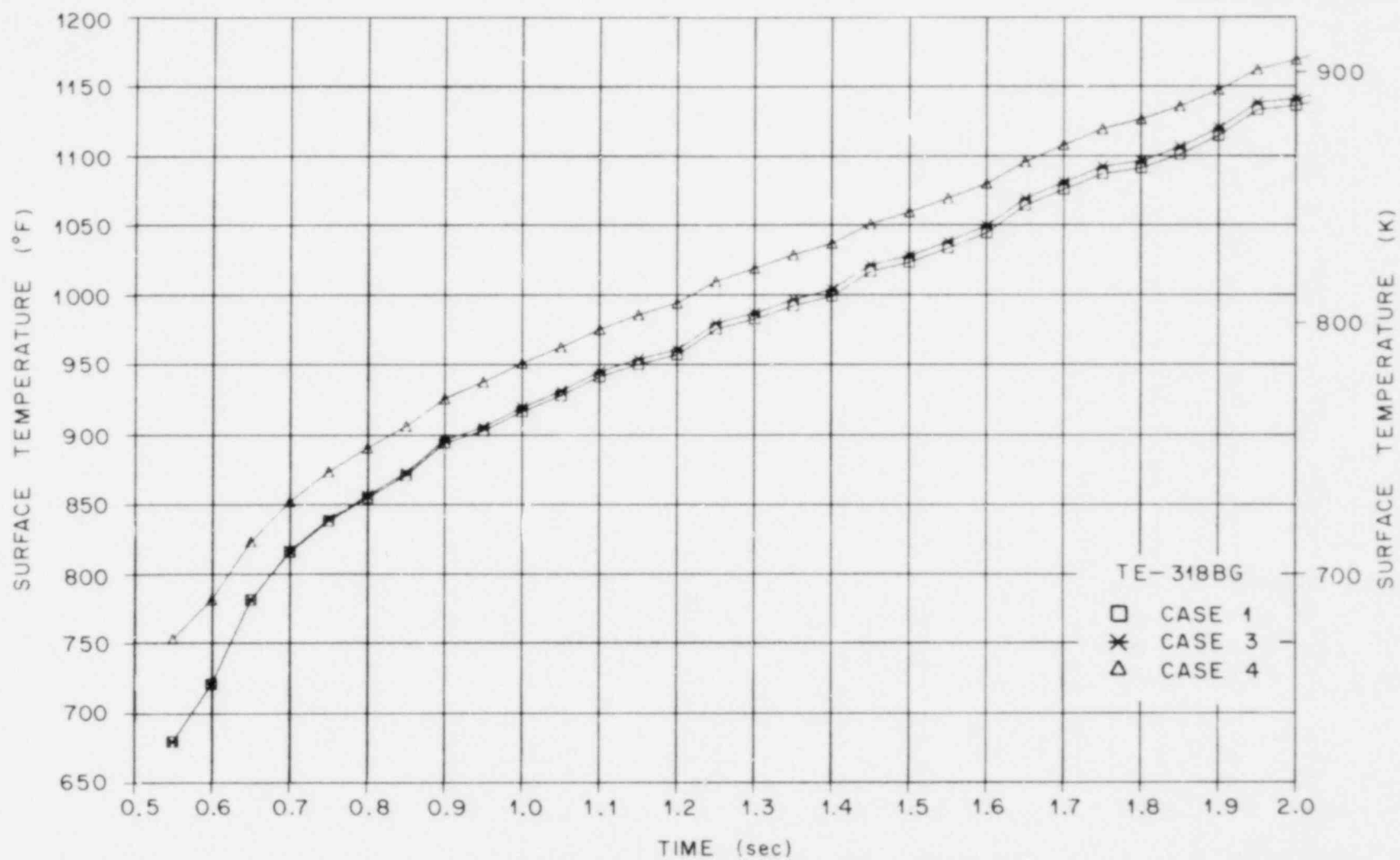


Fig. 3.20. ORINC rod surface temperature, TE-318BG, THTF test 105, 0.5-2 sec.

ORNL DWG 78-18451

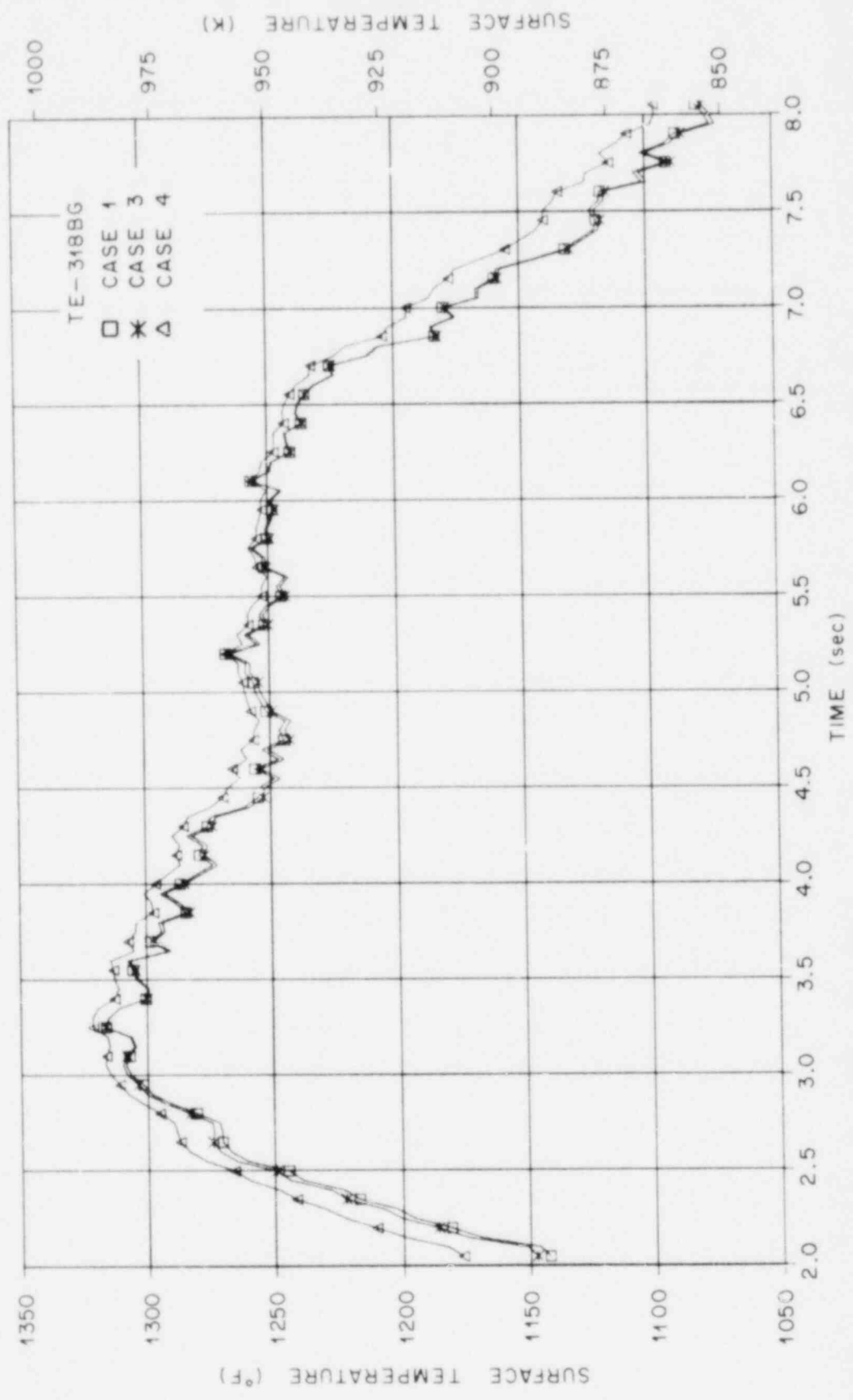


Fig. 3.21. ORINC rod surface temperature, TE-318BG, THTF test 105, 2.0-8 sec.

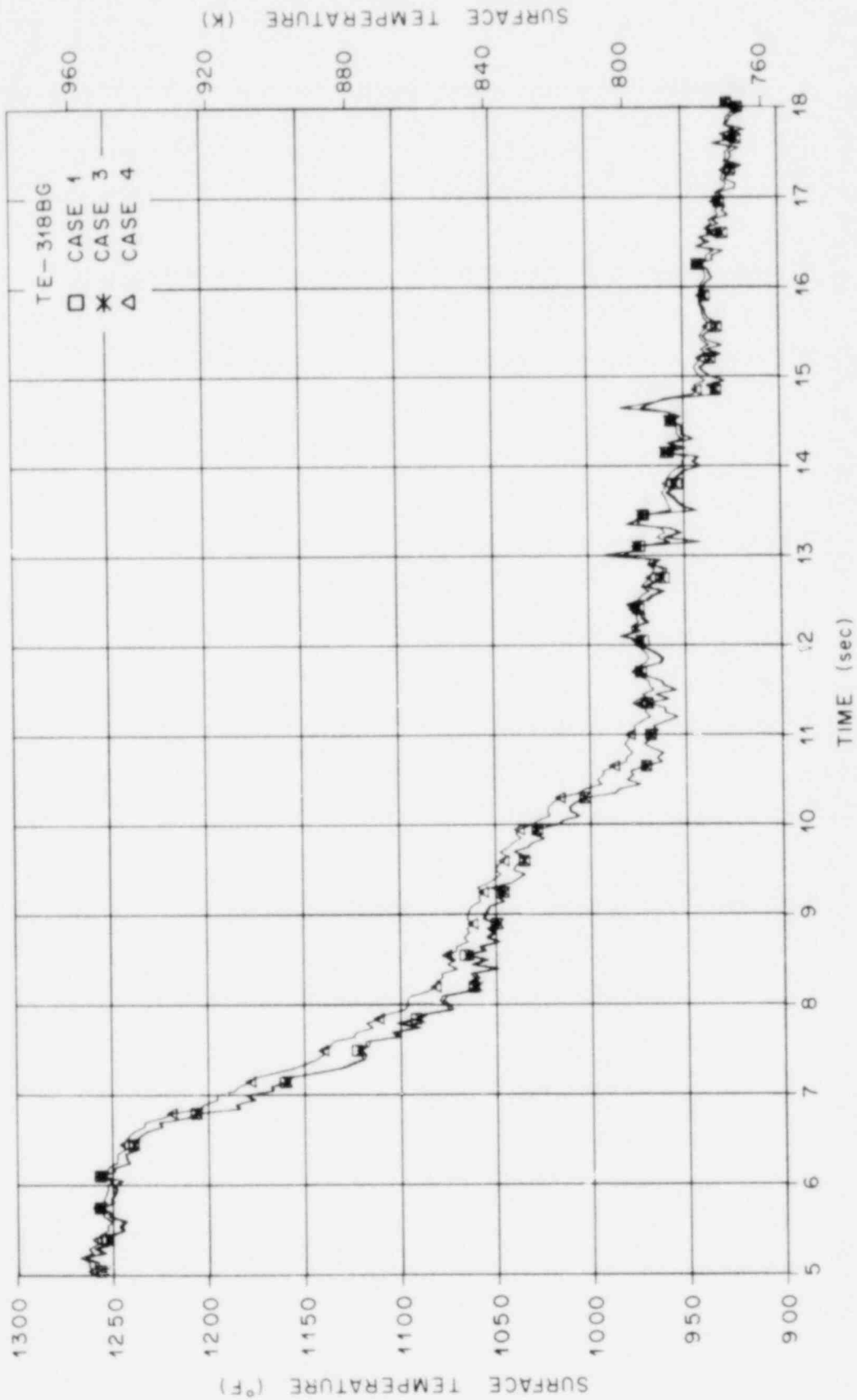


Fig. 3.22. ORINC rod surface temperature, TE-318BG, THF test 105, 5.0-18 sec.

from 0.0 to 40.0% lower than for case 1. Figure 3.23 gives a plot of the surface heat flux ratio (case 3/case 1) for the 0.50- to 3.40-sec time interval. The general conclusion is that the inverse computed surface heat flux can be off by as much as 40% in comparing cases 3 and 1.

The general observation that the interior of the pin responds too fast in case 3 is obvious in Fig. 3.14. A better "feel" for what is occurring within the pin can be gained by referring to the sequence of radial temperature plots for 0-4.75 sec. Figures 3.24 through 3.28 give responses for case 1 and case 3. There is little perceivable difference between the cases through 0.75 sec (Fig. 3.24); however, the differences are very apparent from 1.00 to 4.75 sec. In Fig. 3.25, the active component (Inconel-600) temperature (at  $r = 0.3$  cm) is higher in case 1, eventually peaking at 2.15 sec at 1061 K in case 1 and 1036 K in case 3, but the MgO temperatures (at  $r \leq 0.2764$  cm) are higher in case 3. Since the thermal diffusivity of the MgO is higher in case 3,

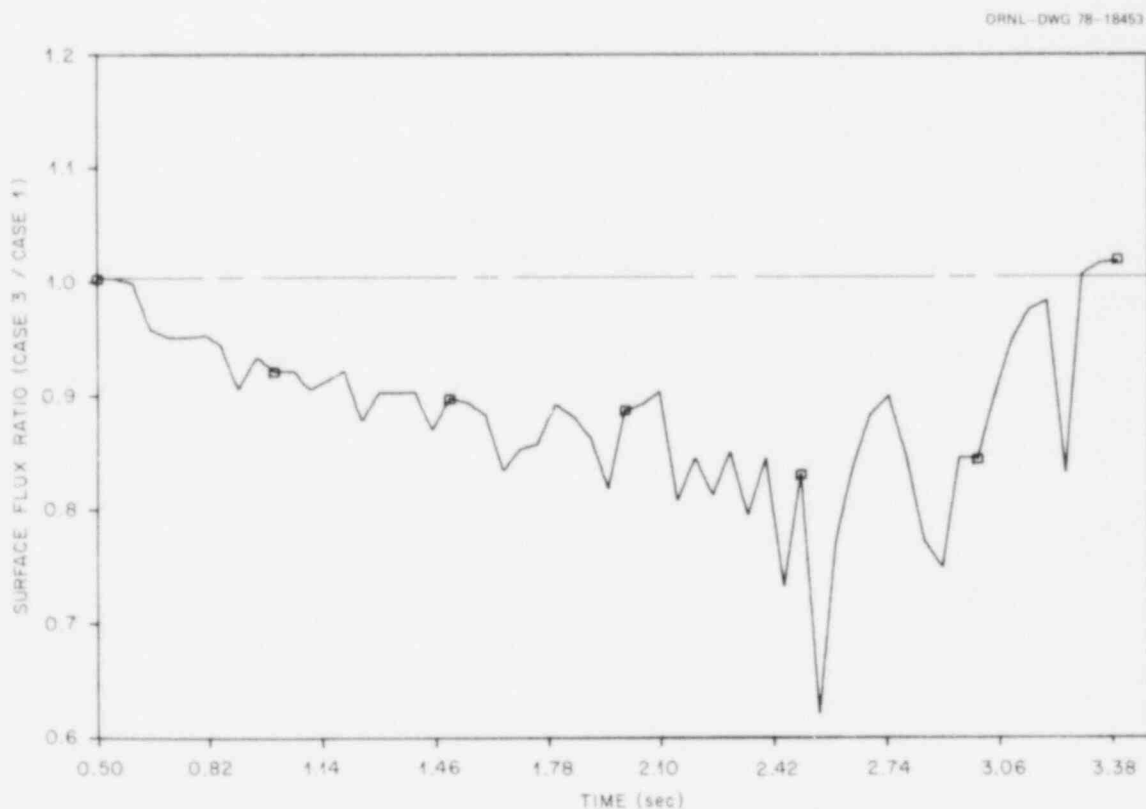


Fig. 3.23. Comparison of surface heat fluxes, cases 1 and 3.

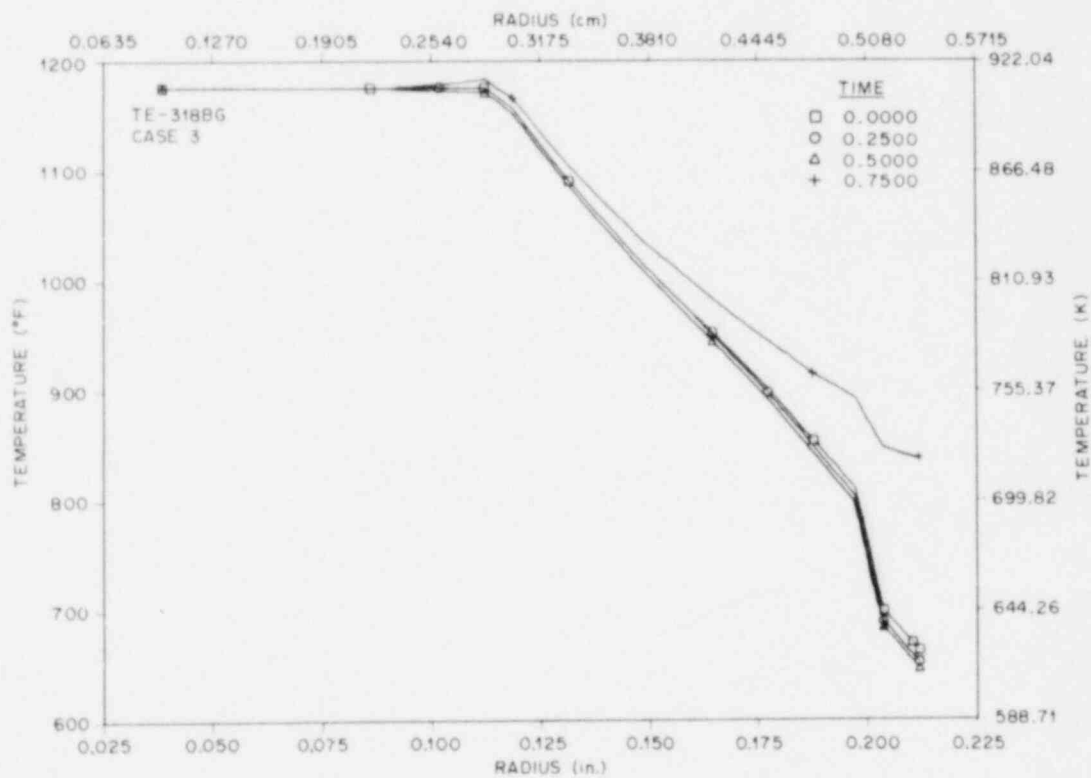
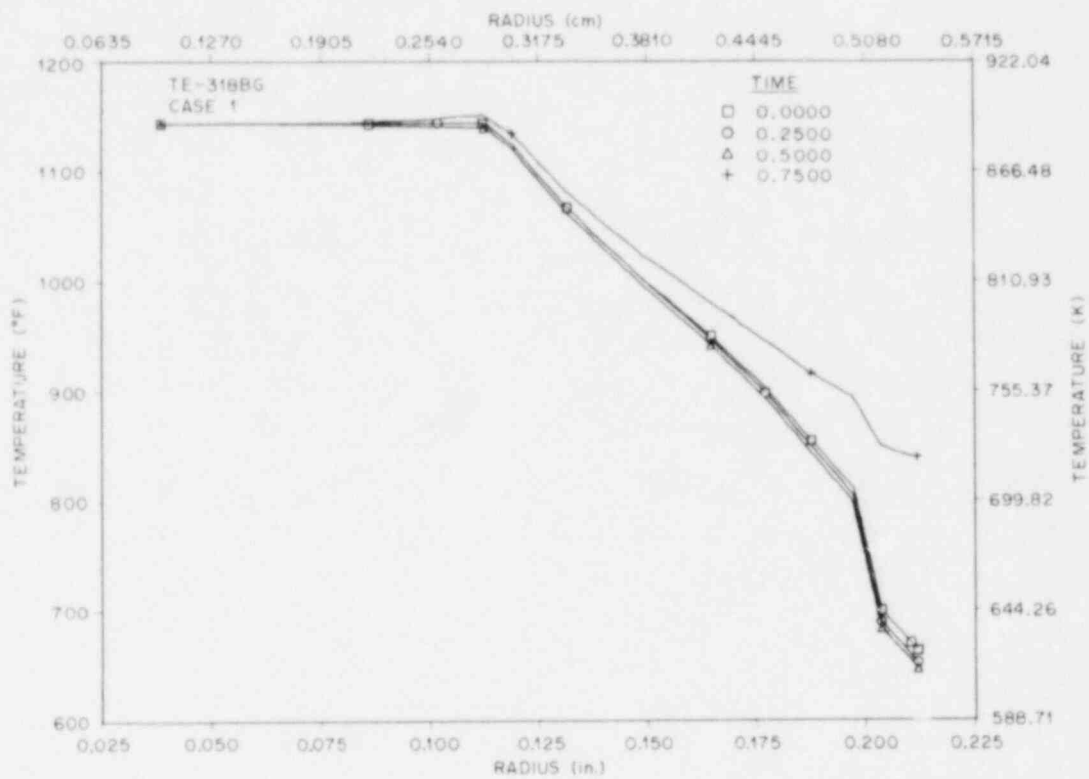


Fig. 3.24. Calculated pin internal thermal response, 0-0.75 sec.

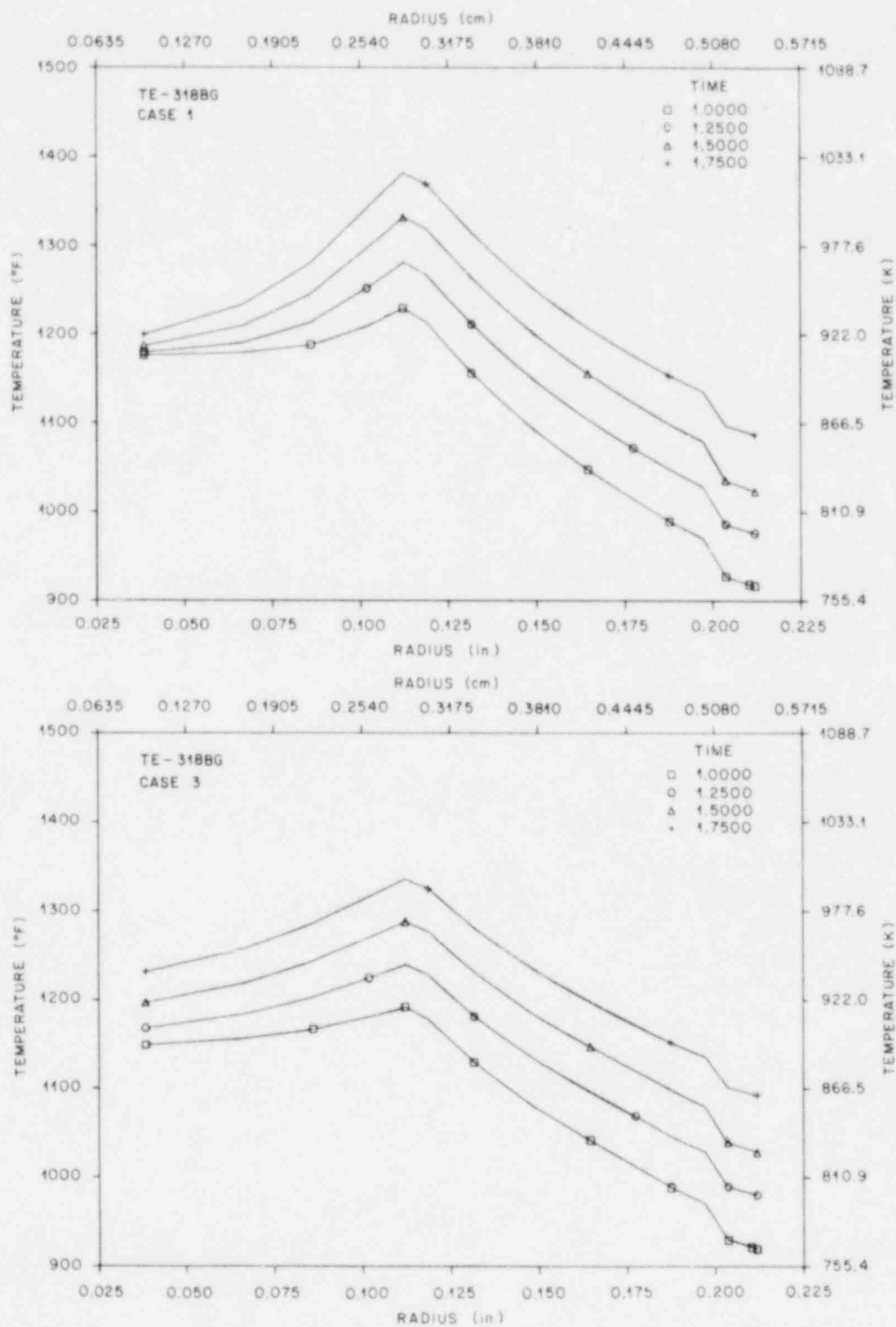


Fig. 3.25. Calculated pin internal thermal response, 1.0-1.75 sec.



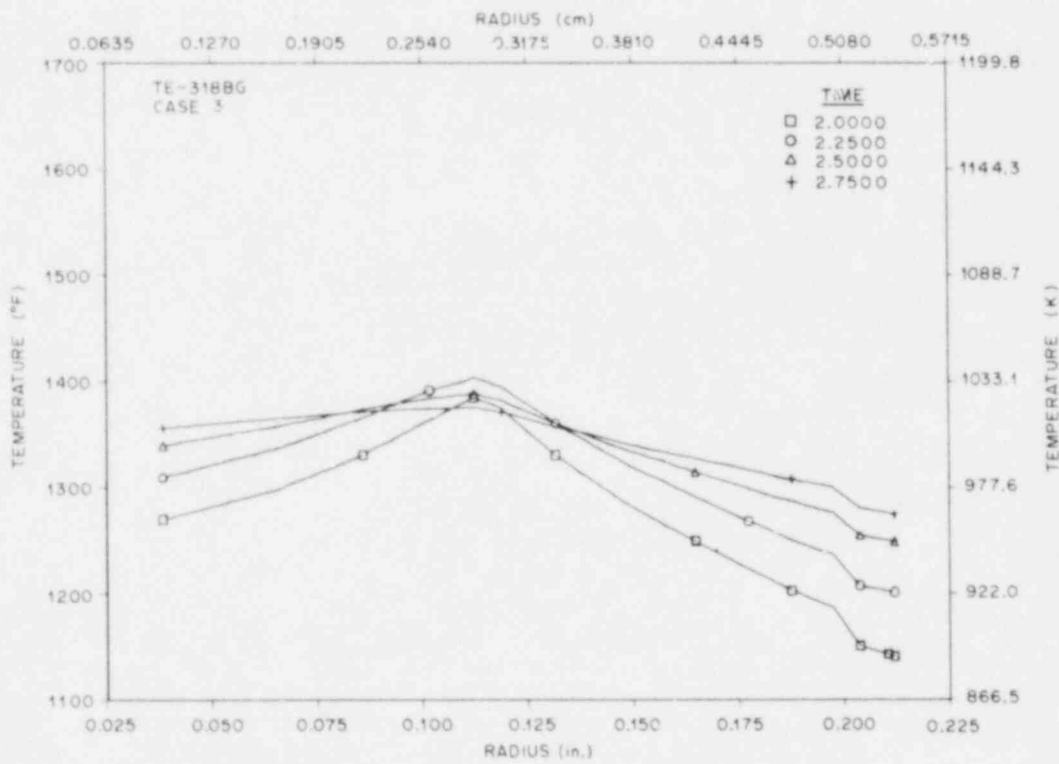
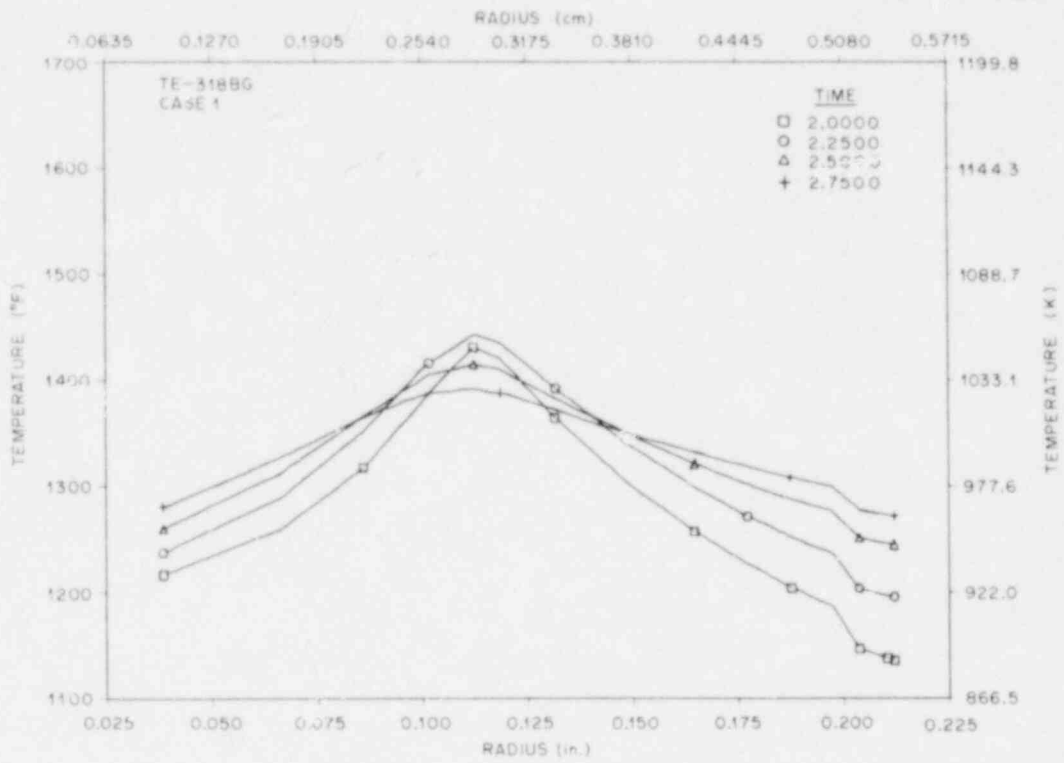


Fig. 3.26. Calculated pin internal thermal response, 2.0-2.75 sec.

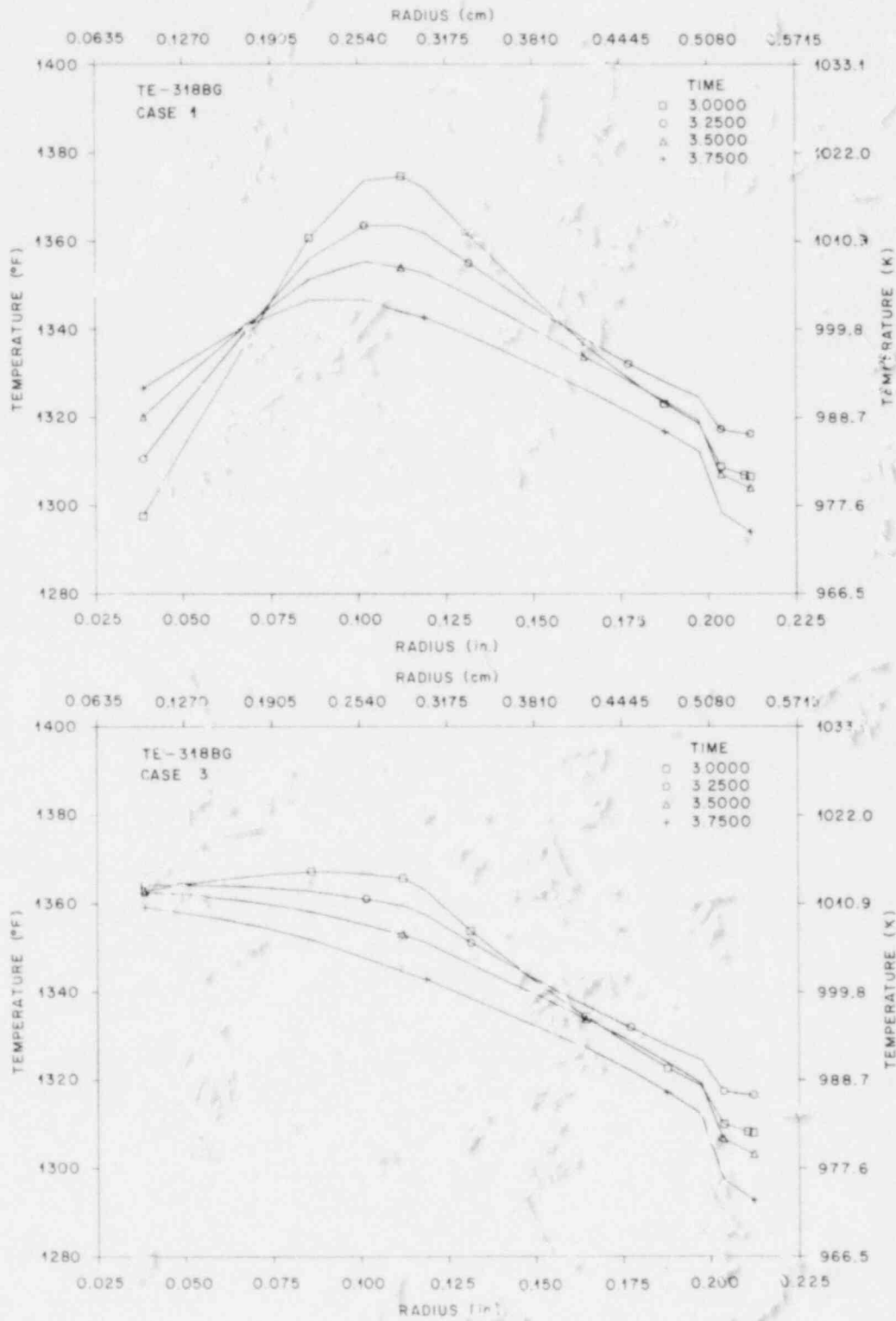


Fig. 3.27. Calculated pin internal thermal response, 3.0-3.75 sec.

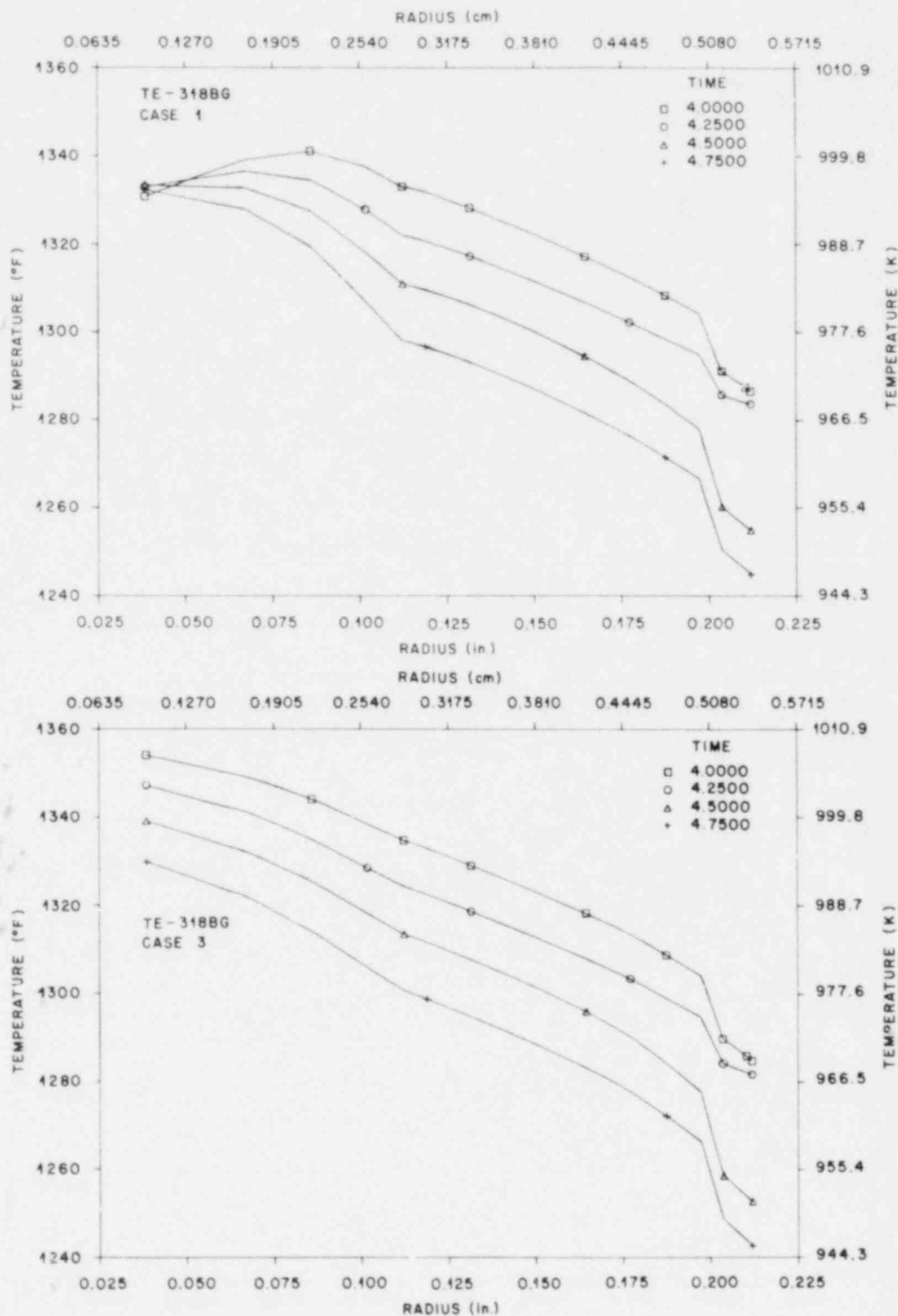


Fig. 3.28. Calculated pin internal thermal response, 4.0-4.75 sec.

the thermal resistance is less and thus more heat goes into the core of the simulator. Therefore, the centerline temperature in case 3 will respond faster and peak higher. The centerline temperature peaks at 1013 K at 3.20 sec and at 996 K at 4.45 sec for cases 3 and 1, respectively. The primary reason that the case 3 surface heat flux is less than that of case 1 in the 0.65- to 3.40-sec time interval is that more heat is being driven into the interior of the simulator rather than to the surface. Note that the temperature profile in case 3 "rolls over" between 3.00 and 3.25 sec, which is  $\approx 1.25$  sec before that of case 1.

Where neglect of the gap between the sheaths (as in case 2) affects the driving potential at the surface of the pin, the use of literature data for  $k_{BN}$  and  $\alpha_{MgO}$  alters the spatial and temporal history of the heat flow within the pin and, as a result, the computed surface heat flux.

Case 4 will not be discussed to any extent other than to say that it represents the superposition of the errors in cases 2 and 3 and the state-of-the-art thermal analysis of fuel pin simulators prior to ORTCAL and ORINC.

## 4. CONCLUSIONS

An experimental thermocouple calibration procedure and a four-part calibration program, ORTCAL (ORNL Thermocouple Calibration), have been developed to supply heater rod performance information to the inverse heat conduction model and program ORINC.

Case studies have shown that failure to fully classify fuel pin simulators (i.e., with regard to component physical properties, gaps, etc.) can result in severe errors (during inverse calculations) in the computed driving potential at the surface of the pin ( $\Delta T$ ), the spatial and temporal history of the heat flow within the pin, and the computed surface heat flux.

## REFERENCES

1. *Project Description ORNL-PWR Blowdown Heat Transfer Separate-Effects Program - Thermal Hydraulic Test Facility (THTF)*, ORNL/NUREG/TM-2 (February 1976).
2. *Anticipated Transients Without Scram for Water-Cooled Power Reactors*, WASH-1270 (September 1973).
3. R. L. Ludwig, *Metallographic Evaluation of Position of Outer Thermocouples in BDHT Heater 150-5*, Y-12 Development Division Metallurgical Department (September 1975).
4. L. J. Ott and R. A. Hedrick, *ORINC - A One-Dimensional Implicit Approach to the Inverse Heat Conduction Problem*, ORNL/NUREG-23 (November 1977).
5. R. L. Ludwig, personal communication, 1975.
6. Y. S. Touloukian, *Thermophysical Properties of High Temperature Solid Materials*, The Macmillan Company, New York, 1967.
7. E. W. Washburn, *International Critical Tables of Numerical Data, Physics, Chemistry, and Technology*, McGraw-Hill, New York.
8. R. E. Kirk and D. F. Othmer, *Encyclopedia of Chemical Technology*, The Interscience Encyclopedia, Inc., New York, 1952.
9. G. R. Finlay and G. H. Fetterley, "Boron Nitride - An Unusual Refractory," *Amer. Ceram. Soc., Bull.* 31, 141-43 (1952).
10. P. Popper, *Special Ceramics*, Heywood and Company Ltd., London, 1960.
11. J. E. Campbell and E. M. Sherwood, *High-Temperature Materials and Technology*, Wiley, New York.
12. J. Wolf, *Aerospace Structural Metals Handbook*, Mechanical Properties Data Center, Traverse City, Mich., 1973.
13. R. C. Weast, *Handbook of Chemistry and Physics*, The Chemical Rubber Company, Cleveland, Ohio, 1967.
14. S. Malang, *HETRAP: A Heat Transfer Analysis Program*, ORNL/TM-4555 (September 1974).
15. *International Nickel Co. Technical Bulletin T-7* (1956).
16. *ASTM Special Technical Publication No. 227* (1958).
17. *Alloy Digest, Cupro-Nickel, 30%-70%*, Engineering Alloys Digest, Inc., Upper Montclair, N.J., 1963.
18. J. D. White, *Recommended Procedures and Tests to Determine the Status of THTF Bundle No. 1*, BDHT-1879.
19. J. D. White, *Status of THTF Bundle*, BDHT-1883 (Nov. 4, 1976).
20. D. J. Fraysier, personal conversation, Mar. 16, 1978.
21. K. V. Childs and L. J. Ott, *Surface Heat Flux Perturbations in BDHT Heaters* (to be published).

22. W. D. Turner, D. C. Elrod, and I. I. Siman-Tov, *HEATING5 - An IBM 360 Heat Conduction Program*, ORNL/CSD/TM-15 (March 1977).
23. *Quarterly Progress Report on Blowdown Heat Transfer Separate-Effects Program for July-September 1977*, ORNL/NUREG/TM-149 (March 1978).
24. R. K. Adams, R. L. Anderson, and M. J. Roberts, *THTF Thermocouple Anomalous Readings*, BDHT-1819 (May 13, 1976).
25. T. G. Kollie et al., "Large Thermocouple Thermometry Errors Caused by Magnetic Fields," *Rev. Sci. Instrum.* 48(5), 501-511 (May 1977).
26. R. A. Hedrick et al., *PWR Blowdown Heat Transfer Separate-Effects Program Data Evaluation Report - System Response for Thermal-Hydraulic Test Facility Test Series 100*, ORNL/NUREG-19 (November 1977).
27. K. G. Turnage, personal communication.
28. M. Jakob, *Heat Transfer*, Vol. 1, Wiley, New York, 1957.
29. J. R. S. Thom et al., "Boiling in Subcooled Water During Flow up Heated Tubes or Annuli," *Proc. Inst. Mech. Engr.* 180, Part 3C, 226-46 (1966).
30. *Quarterly Progress Report on Blowdown Heat Transfer Program for July-September 1975*, ORNL/TM-5117 (November 1975).
31. *Quarterly Progress Report on Reactor Safety Programs Sponsored by the NRC Division of Reactor Safety Research for January-March 1975*, ORNL/TM-4914, Vol. 1 (July 1975).
32. *Quarterly Progress Report on Reactor Safety Programs Sponsored by the NRC Division of Reactor Safety Research for October-December 1974*, ORNL/TM-4808, Vol. 1 (April 1975).
33. R. Hooke and F. A. Jeeves, *J. Assoc. Comput. Mach.* 8, 119 (1961).
34. J. Weisman, C. F. Wood, and L. Rivlin, "Optimal Design of Chemical Process Systems," *Chem. Eng. Prog.* 61, 50-63 (1965).
35. *Quarterly Progress Report on Blowdown Heat Transfer Separate-Effects Program for April-June 1976*, ORNL/NUREG/TM-46 (January 1977).
36. *Quarterly Progress Report on Blowdown Heat Transfer Separate-Effects Program for July-September 1976*, ORNL/NUREG/TM-61 (February 1977).
37. *Quarterly Progress Report on Blowdown Heat Transfer Separate-Effects Program for January-March 1977*, ORNL/NUREG/TM-109 (August 1977).
38. *Quarterly Progress Report on Blowdown Heat Transfer Separate-Effects Program for April-June 1977*, ORNL/NUREG/TM-134 (November 1977).
39. C. D. Pears, Southern Research Inst., USAF ASD-TDR-62-765, 1-402 [AD 298 061].
40. V. Casal et al., KFK-2368, für Kernforschung M.B.H. (September 1976).
41. W. G. Craddick et al., *PWR Blowdown Heat Transfer Separate-Effects Program Data Evaluation Report - Heat Transfer for Thermal-Hydraulic Test Facility Test Series 100*, ORNL/NUREG-45 (1978).

42. H. W. Russell, "Principles of Heat Flow in Porous Insulators," *J. Am. Ceram. Soc.* 18, 1-5 (1935).
43. M. J. Laubitz, "Thermal Conductivity of Powders," *Can. J. Phys.* 37, 798-808 (1959).



Appendix A

PHYSICAL PROPERTIES DATA

Table A.1. Physical property data for Inconel 600<sup>2</sup>

1 Btu/hr ft °F = 1.73 W/m °C  
 1 Btu/lb-°F = 1 cal/g °C  
 1 lb/ft<sup>3</sup> = 0.01602 g/cm<sup>3</sup>  
 °C = 5/9 (°F - 32)  
 Density = 526 lb/ft<sup>3</sup>  
 Melting point = 2500-2600°F

Temperature (°F)	Specific heat, C <sub>p</sub> (Btu/lb °F)	Thermal conductivity, k (Btu/hr ft °F)
0	0.0977	8.4
50	0.1011	8.6
100	0.1041	8.7
150	0.1068	8.9
200	0.1092	9.1
250	0.1113	9.3
300	0.1132	9.5
350	0.1148	9.7
400	0.1163	9.9
450	0.1176	10.2
500	0.1188	10.4
550	0.1199	10.6
600	0.1209	10.9
650	0.1218	11.2
700	0.1228	11.4
750	0.1237	11.7
800	0.1247	12.0
850	0.1254	12.2
900	0.1262	12.5
950	0.1270	12.8
1000	0.1278	13.1
1050	0.1287	13.4
1100	0.1297	13.7
1150	0.1307	14.0
1200	0.1317	14.3
1250	0.1328	14.6
1300	0.1340	14.9
1350	0.1352	15.2
1400	0.1364	15.5
1450	0.1377	15.8
1500	0.1391	16.1
1550	0.1405	16.4
1600	0.1419	16.7
1650	0.1434	17.0
1700	0.1450	17.3
1750	0.1466	17.6
1800	0.1482	17.8

<sup>a</sup> Best polynomial fit to data for C<sub>p</sub> and k:

$$0 \leq T \leq 800$$

$$C_p = 9.77430344 \times 10^{-2} + 7.11642206 \times 10^{-5}T - 7.72415660 \times 10^{-8}T^2 + 3.80815379 \times 10^{-11}T^3$$

$$800 \leq T \leq 2500$$

$$C_p = 12.04458 \times 10^{-2} - 2.680032 \times 10^{-6}T + 1.005603 \times 10^{-8}T^2$$

$$0 \leq T \leq 2500$$

$$k = 8.42944336 + 2.88105011 \times 10^{-3}T + 2.42143869 \times 10^{-6}T^2 - 6.19365892 \times 10^{-10}T^3,$$

where k is given in Btu/hr ft °F, C<sub>p</sub> given in Btu/lb °F, and T in °F.

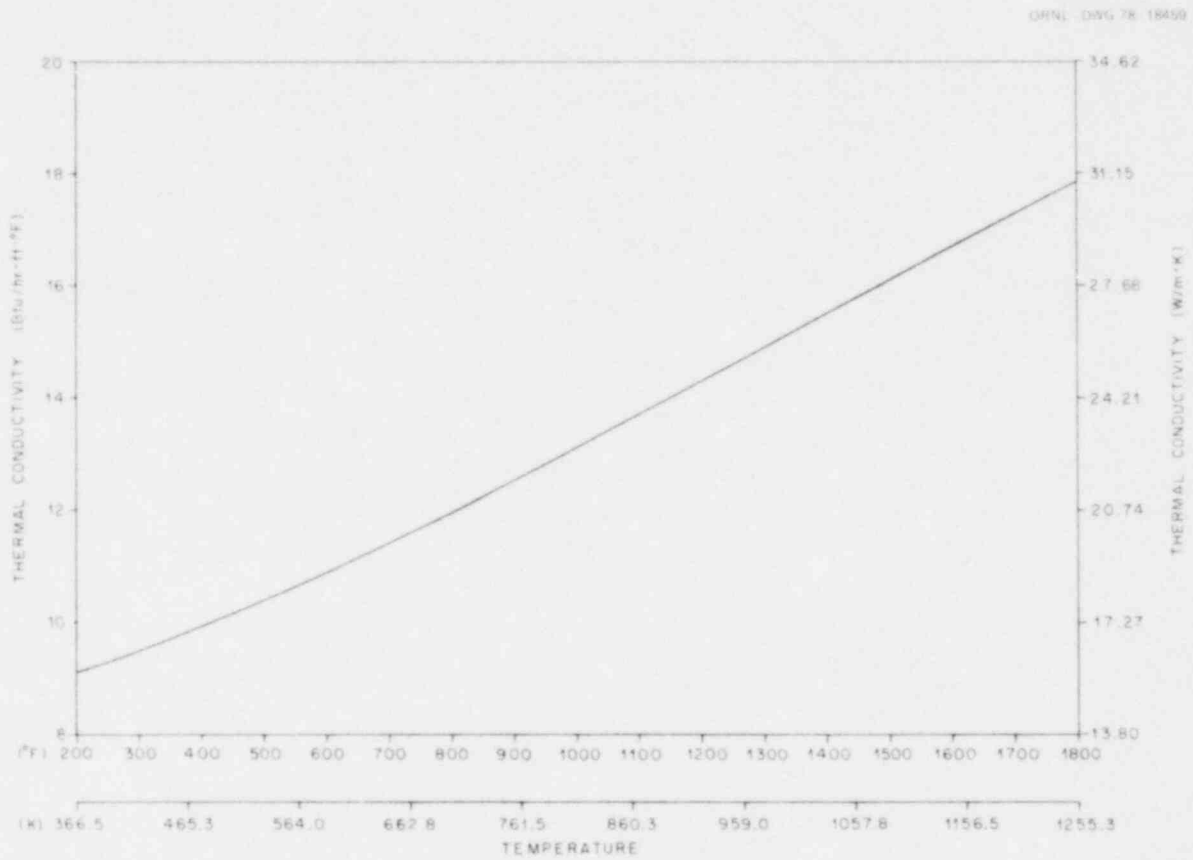


Fig. A.1. Thermal conductivity of Inconel 600.

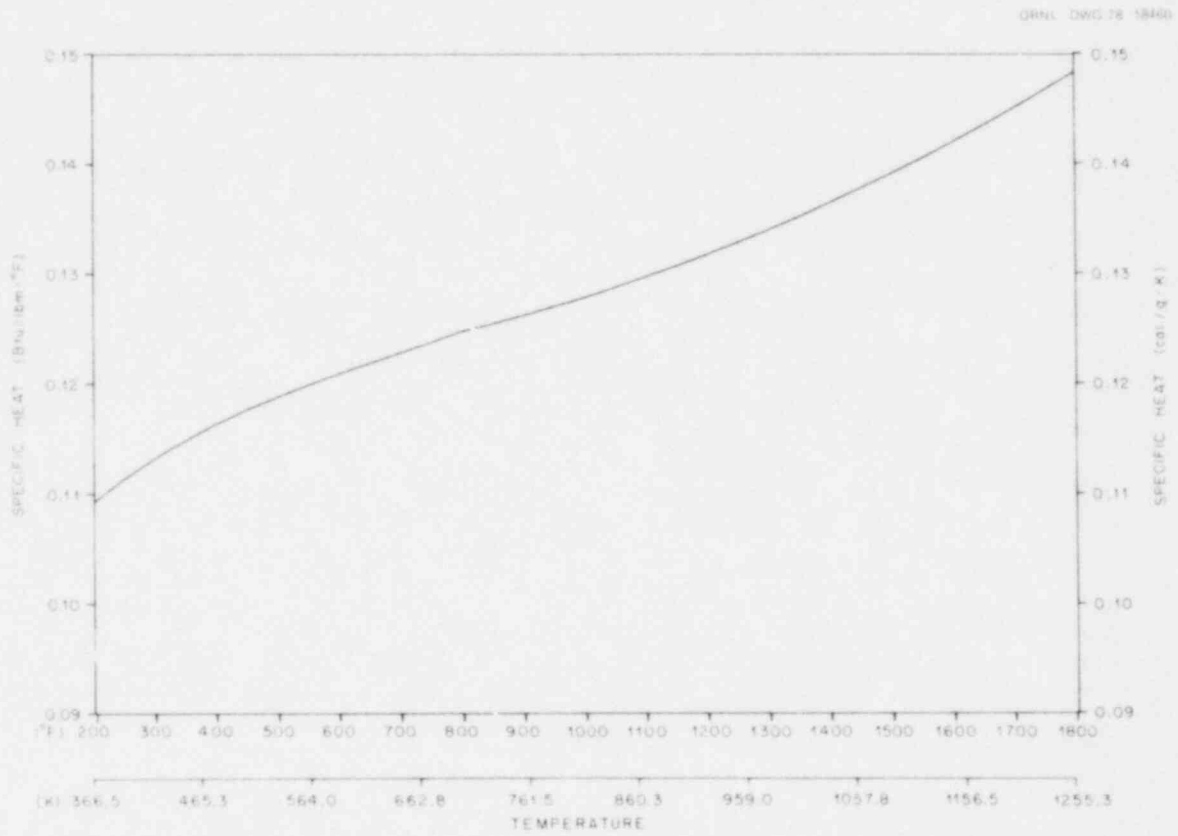


Fig. A.2. Specific heat of Inconel 600.

Table A.2. Physical property data for Cupronickel<sup>a</sup>

1 Btu/hr ft °F = 1.73 W/m °C  
 1 Btu/lb °F = 1 cal/g °C  
 1 lb/ft<sup>3</sup> = 0.01602 g/cm<sup>3</sup>  
 °C = 5/9 (°F - 32)  
 Density = 553 lb/ft<sup>3</sup>  
 Melting point = 2140-2280°F

Temperature (°F)	Specific heat, C <sub>p</sub> (Btu/lb °F)	Thermal conductivity, k (Btu/hr ft °F)
0	0.0950	16.8
50	0.0965	16.8
100	0.0978	17.1
150	0.0991	17.5
200	0.1004	18.0
250	0.1016	18.6
300	0.1027	19.3
350	0.1039	20.1
400	0.1049	21.0
450	0.1060	21.9
500	0.1070	22.8
550	0.1080	23.8
600	0.1090	24.9
650	0.1100	26.1
700	0.1110	27.3
750	0.1119	28.6
800	0.1129	30.0
850	0.1139	31.5
900	0.1149	33.2
950	0.1159	35.1
1000	0.1169	37.2
1050	0.1180	39.5
1100	0.1191	42.2
1150	0.1203	45.2
1200	0.1215	48.6
1250	0.1227	52.4
1300	0.1240	56.8
1350	0.1253	61.7
1400	0.1268	67.2
1450	0.1282	73.4
1500	0.1298	80.4
1550	0.1314	88.3
1600	0.1332	97.0
1650	0.1350	106.8
1700	0.1369	117.6
1750	0.1389	129.6
1800	0.1410	142.9

<sup>a</sup>Best polynomial fit to data for C<sub>p</sub> and k:

$$0 \leq T \leq 2100$$

$$C_p = 9.50193405 \times 10^{-2} + 2.93776393 \times 10^{-5}T - 1.41008059 \times 10^{-8}T^2 + 6.65068001 \times 10^{-12}T^3,$$

$$k = 1.68024902 \times 10^1 - 1.31225586 \times 10^{-3}T + 4.43458557 \times 10^{-5}T^2 - 4.77302819 \times 10^{-8}T^3 + 2.50679477 \times 10^{-11}T^4,$$

where k is in Btu/hr ft °F, C<sub>p</sub> in Btu/lb °F, and T in °F.

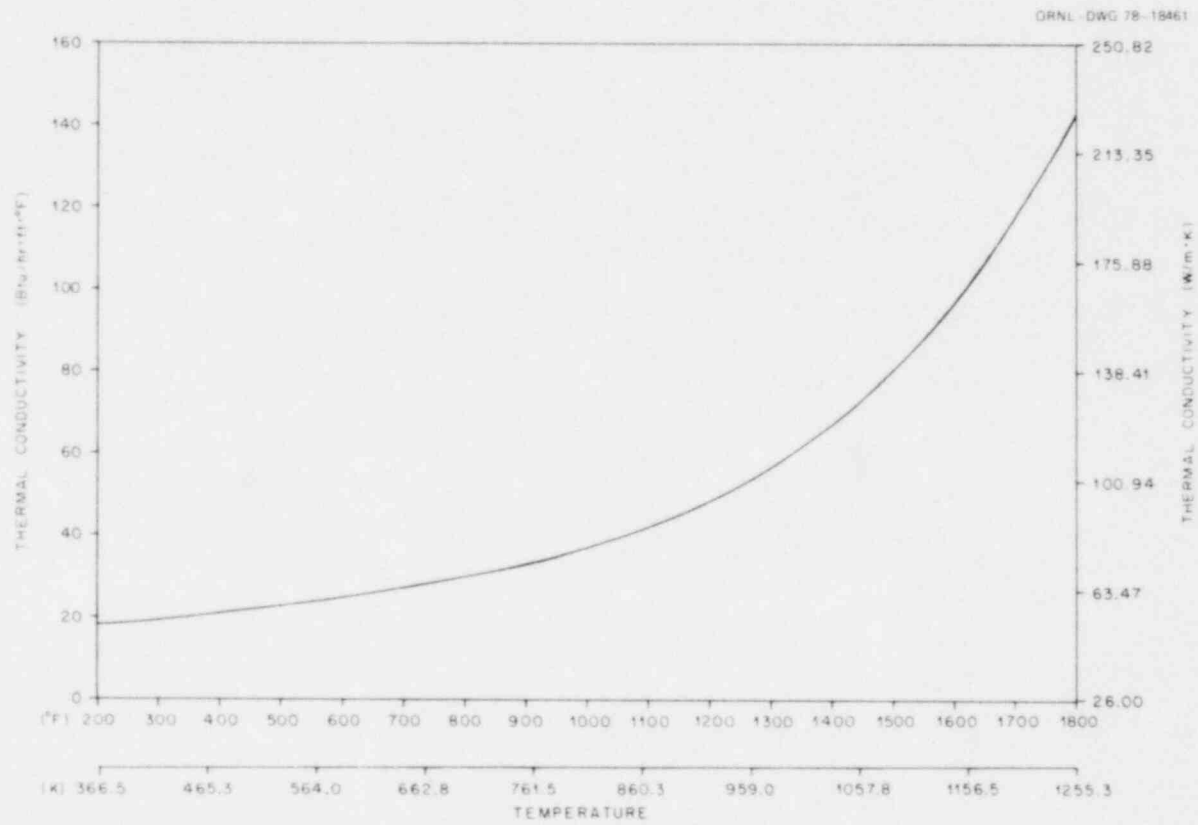


Fig. A.3. Thermal conductivity of Cupronickel.

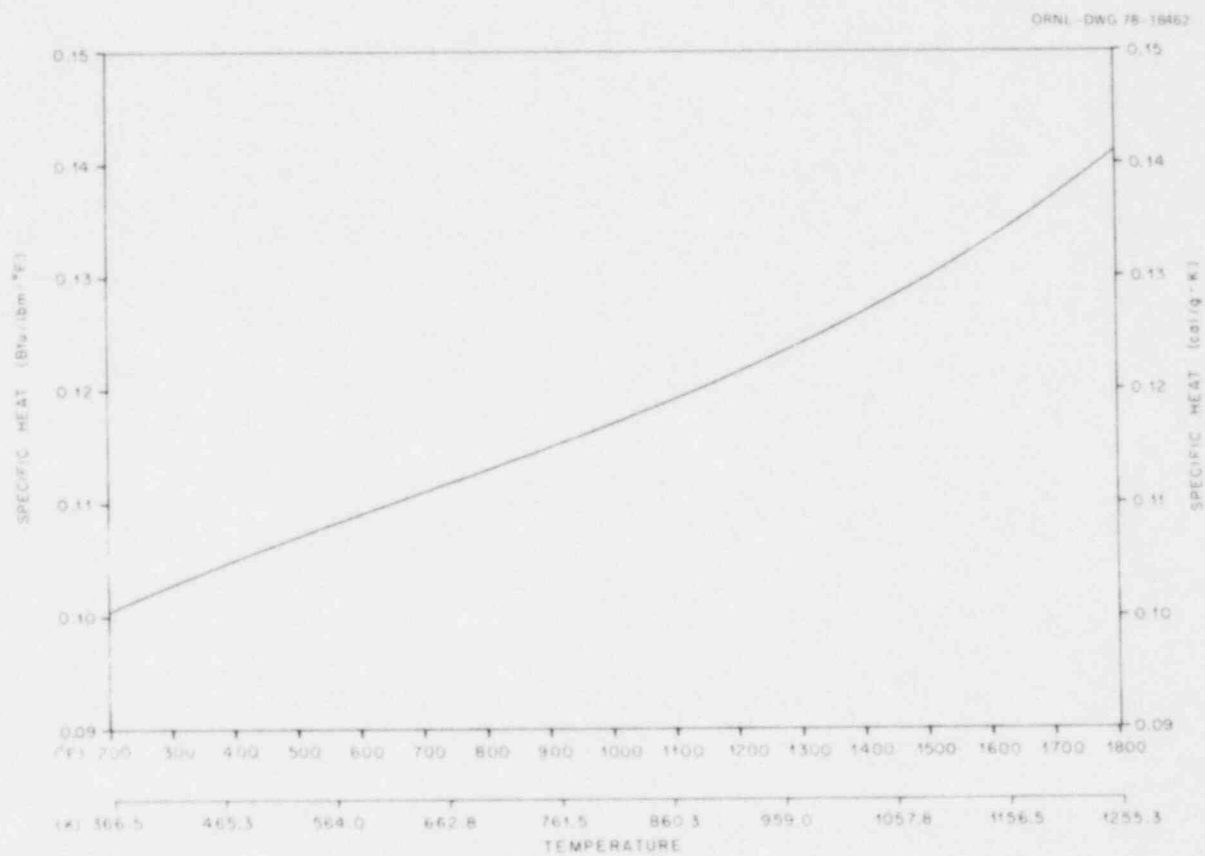


Fig. A.4. Specific heat of Cupronickel.

Table A.3. Physical property data for 316 stainless steel<sup>a</sup>

1 Btu/hr ft °F = 1.73 W/m °C  
 1 Btu/lb °F = 1 cal/g °C  
 1 lb/ft<sup>3</sup> = 0.01602 g/cm<sup>3</sup>  
 °C = 5/9 (°F - 32)  
 Density = 496 lb/ft<sup>3</sup>  
 Melting point = 2500-2550°F

Temperature (°F)	Specific heat, C <sub>p</sub> (Btu/lb °F)	Thermal conductivity, k (Btu/hr ft °F)
0	0.1042	7.2
50	0.1072	7.5
100	0.1099	7.7
150	0.1124	8.0
200	0.1148	8.2
250	0.1170	8.5
300	0.1190	8.7
350	0.1209	8.9
400	0.1227	9.1
450	0.1243	9.4
500	0.1259	9.6
550	0.1274	9.8
600	0.1288	10.0
650	0.1301	10.2
700	0.1313	10.4
750	0.1325	10.7
800	0.1337	10.9
850	0.1348	11.1
900	0.1359	11.3
950	0.1369	11.5
1000	0.1380	11.7
1050	0.1390	11.9
1100	0.1400	12.1
1150	0.1411	12.4
1200	0.1421	12.6
1250	0.1431	12.8
1300	0.1442	13.0
1350	0.1452	13.2
1400	0.1463	13.5
1450	0.1474	13.7
1500	0.1485	13.9
1550	0.1496	14.2
1600	0.1508	14.4
1650	0.1519	14.7
1700	0.1531	14.9
1750	0.1543	15.2
1800	0.1556	15.4

<sup>a</sup>Best polynomial fit to data for C<sub>p</sub> and k:

$$0 \leq T \leq 2500$$

$$C_p = 1.04247093 \times 10^{-1} + 6.05583191 \times 10^{-5}T - 4.37721610 \times 10^{-8}T^2 + 2.01225703 \times 10^{-11}T^3 - 3.16413562 \times 10^{-15}T^4,$$

$$0 \leq T \leq 2050$$

$$k = 7.24584961 + 5.07926941 \times 10^{-3}T - 9.89995897 \times 10^{-7}T^2 + 3.82840426 \times 10^{-10}T^3,$$

where k is in Btu/hr ft °F, C<sub>p</sub> in Btu/lb °F, and T in °F.



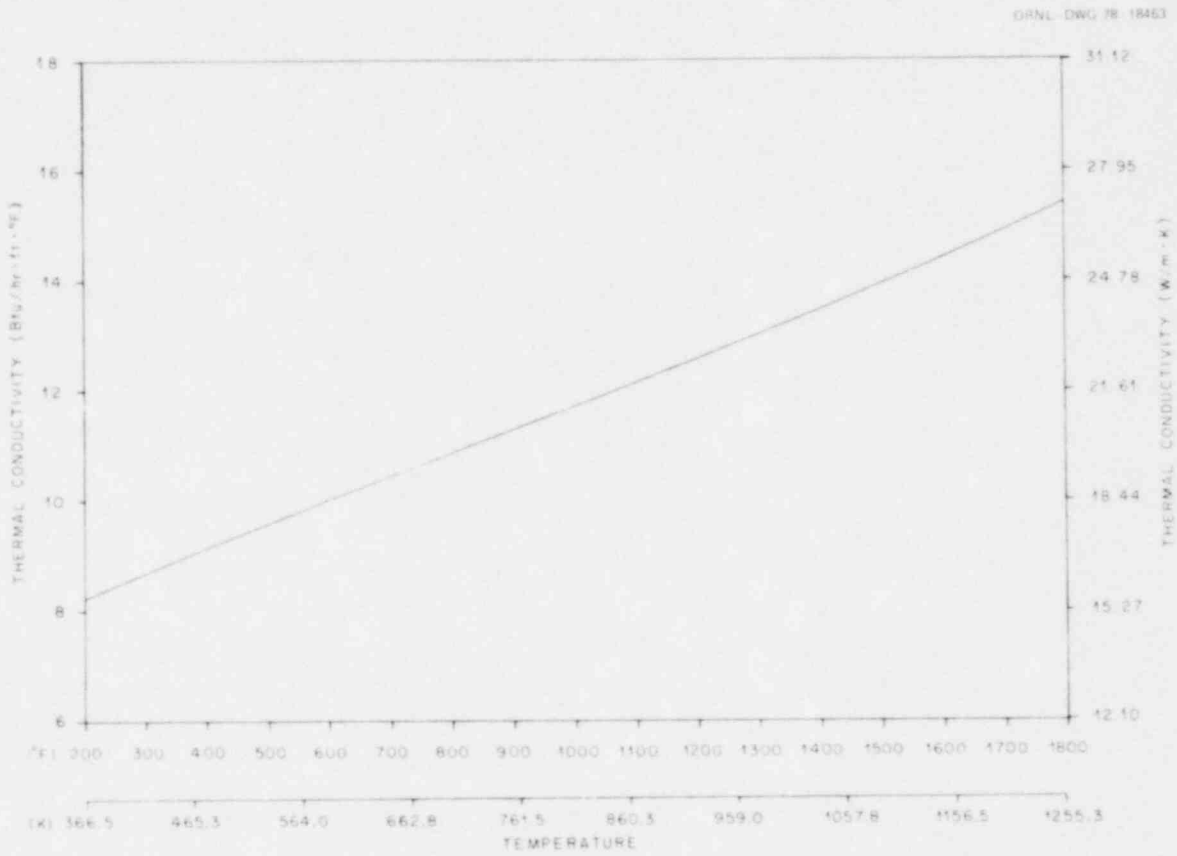


Fig. A.5. Thermal conductivity of 316 stainless steel.

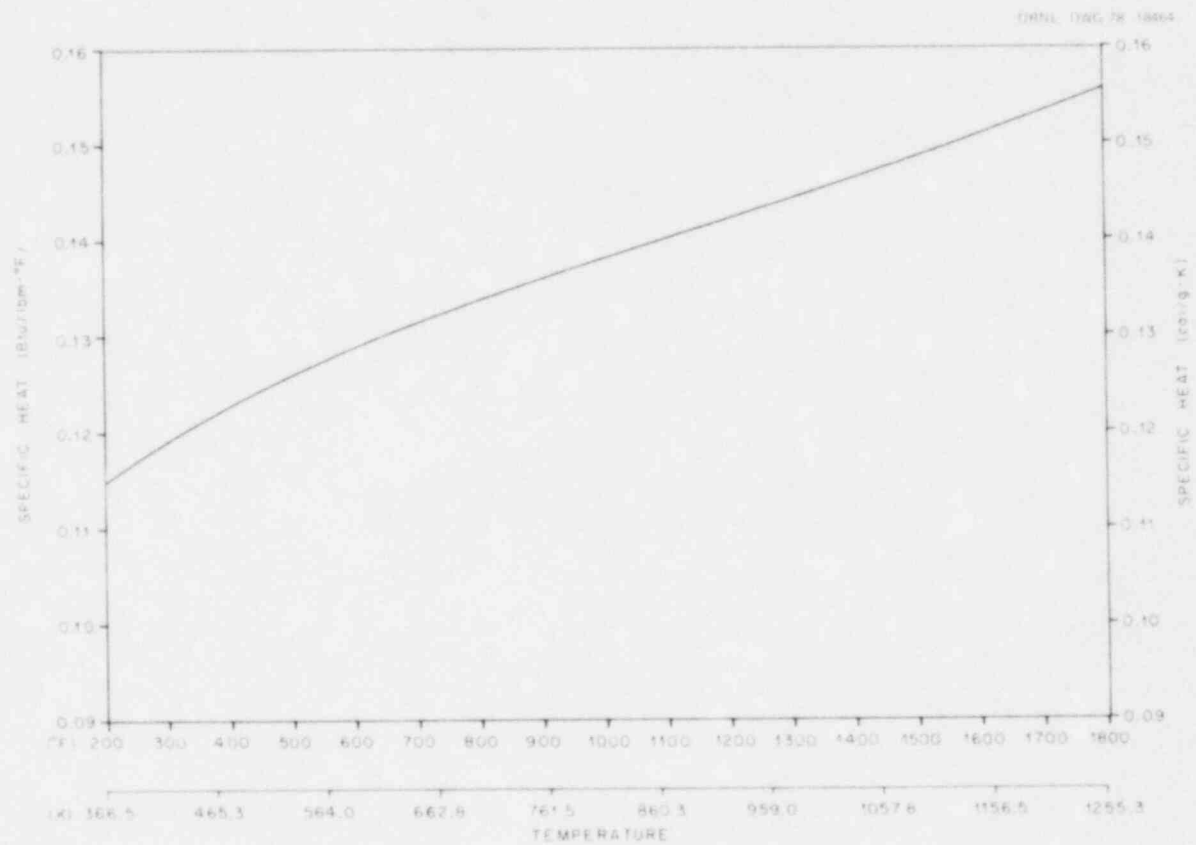


Fig. A.6. Specific heat of 316 stainless steel.

Table A.4. Physical property data  
for magnesium oxide<sup>a</sup>

1 Btu/hr ft °F = 1.73 W/m °C  
 1 Btu/lb °F = 1 cal/g °C  
 1 lb/ft<sup>3</sup> = 0.01602 g/cm<sup>3</sup>  
 °C = 5/9 (°F - 32)  
 Density = 212 lb/ft<sup>3</sup>

Temperature (°F)	Specific heat, C <sub>p</sub> (Btu/lb °F)
0	0.2243
50	0.2302
100	0.2359
150	0.2413
200	0.2463
250	0.2511
300	0.2557
350	0.2599
400	0.2639
450	0.2677
500	0.2712
550	0.2745
600	0.2776
650	0.2805
700	0.2832
750	0.2856
800	0.2879
850	0.2901
900	0.2920
950	0.2938
1000	0.2955
1050	0.2970
1100	0.2984
1150	0.2997
1200	0.3009
1250	0.3020
1300	0.3030
1350	0.3039
1400	0.3047
1450	0.3055
1500	0.3062
1550	0.3069
1600	0.3075
1650	0.3081
1700	0.3087
1750	0.3093
1800	0.3098

<sup>a</sup>Best polynomial fit to data for  
 C<sub>p</sub> :  
 0 ≤ T ≤ 2400

$$C_p = 2.24258423 \times 10^{-3} \\
+ 1.22666359 \times 10^{-6}T \\
- 6.35191100 \times 10^{-9}T^2 \\
+ 1.21040955 \times 10^{-11}T^3,$$

where C<sub>p</sub> is in Btu/lb °F and T in °F.

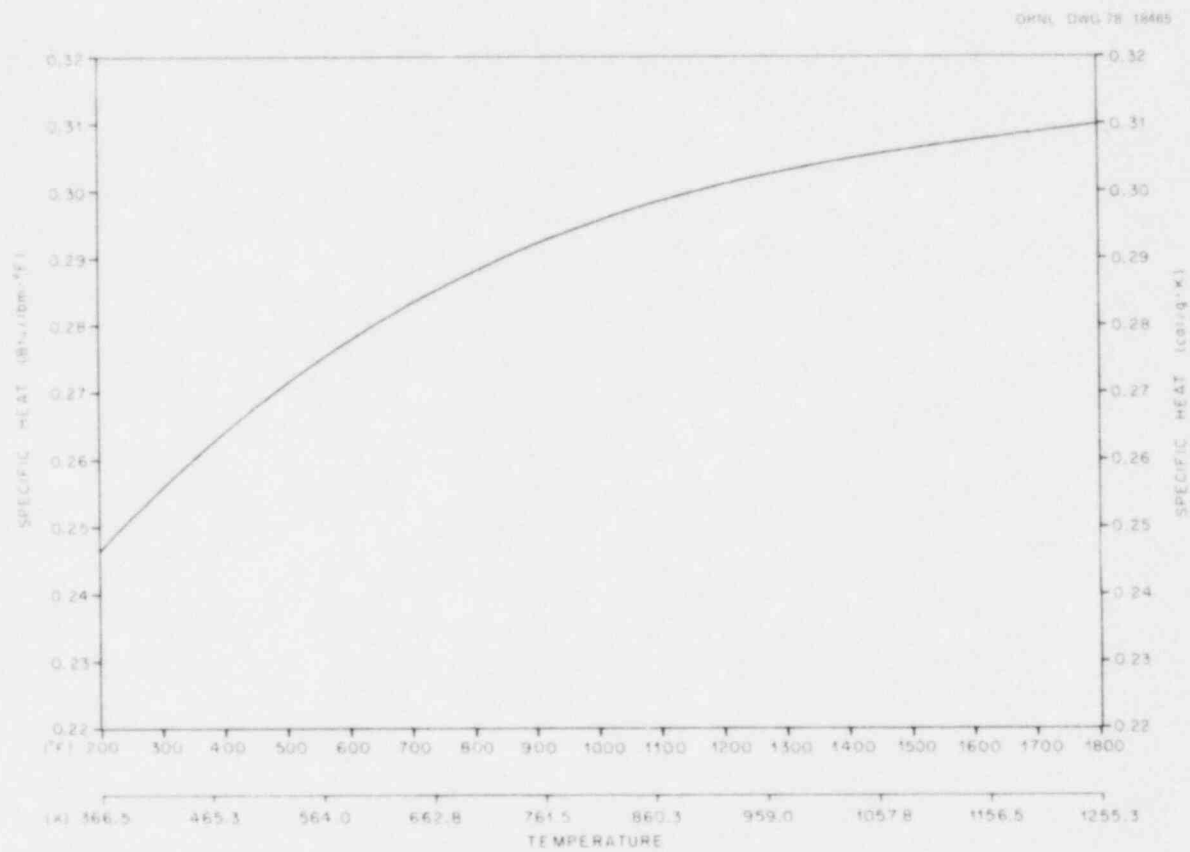


Fig. A.7. Specific heat of magnesium oxide.

Table A.5. Physical property data for boron nitride<sup>a</sup>

1 Btu/hr ft °F = 1.73 W/m °C  
 1 Btu/lb °F = 1 cal/g °C  
 1 lb/ft<sup>3</sup> = 0.01602 g/cm<sup>3</sup>  
 °C = 5/9 (°F - 32)  
 Density = 125 lb/ft<sup>3</sup>

Temperature (°F)	Specific heat, C <sub>P</sub> (Btu/lb °F)
0	0.1678
50	0.1859
100	0.2031
150	0.2195
200	0.2352
250	0.2500
300	0.2641
350	0.2775
400	0.2901
450	0.3021
500	0.3134
550	0.3241
600	0.3342
650	0.3437
700	0.3526
750	0.3610
800	0.3689
850	0.3763
900	0.3832
950	0.3897
1000	0.3957
1050	0.4014
1100	0.4067
1150	0.4116
1200	0.4162
1250	0.4205
1300	0.4245
1350	0.4283
1400	0.4318
1450	0.4352
1500	0.4383
1550	0.4413
1600	0.4441
1650	0.4469
1700	0.4495
1750	0.4521
1800	0.4546

<sup>a</sup>Best polynomial fit to data for

C<sub>P</sub>:

$$0 \leq T \leq 2000$$

$$C_P = 1.67812347 \times 10^{-1} \\ + 3.70264053 \times 10^{-4}T \\ - 1.73793524 \times 10^{-7}T^2 \\ + 3.14486215 \times 10^{-11}T^3,$$

$$2000 \leq T \leq 2600$$

$$C_P = 0.4306064 + 1.70744517 \\ \times 10^{-5}T,$$

where C<sub>P</sub> has units of Btu/lb °F and T has units of °F.

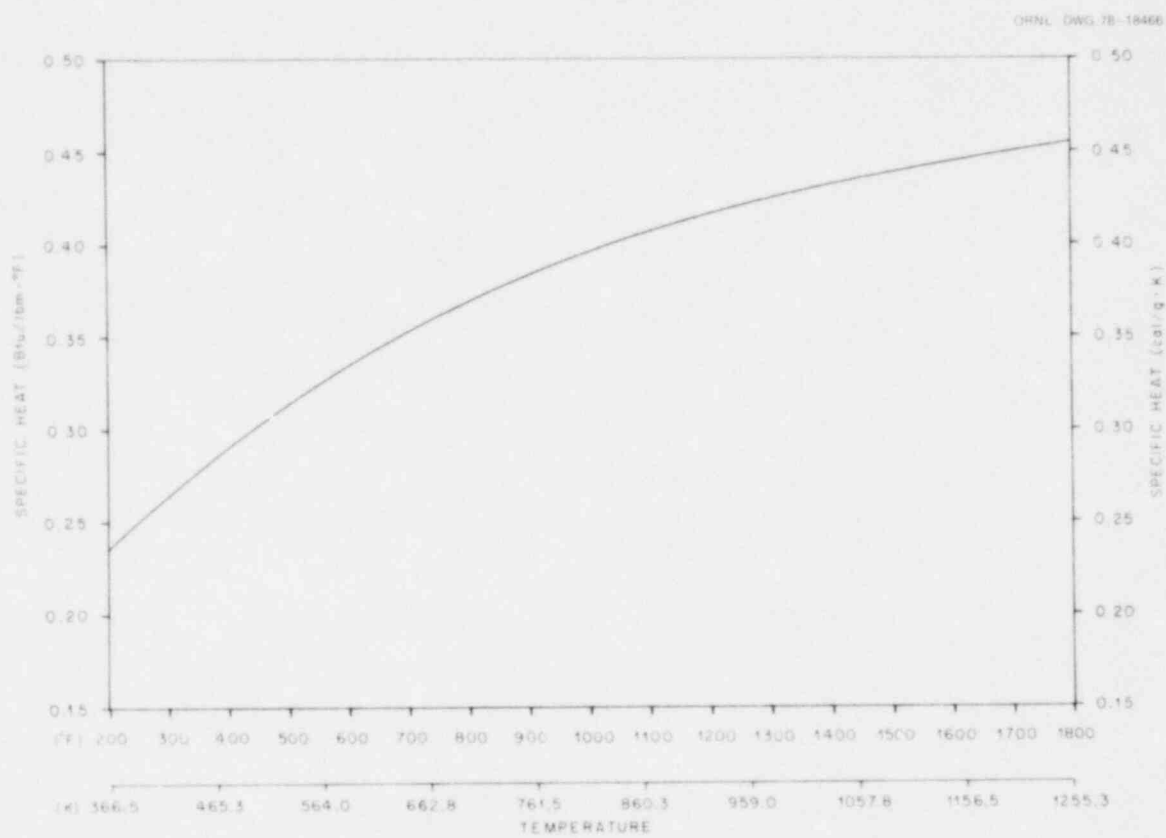


Fig. A.8. Specific heat of boron nitride.

Appendix B

## OPERATING CHECKLIST FOR APPROACH TO POWER

Subject: APPROACH TO POWER	TEST NO.	DATE OF TEST:
		Initial/Time
NOTE		
This section applies to the type and number of computer scans to be taken during a normal approach to test power. If any of the following power levels are to be eliminated for a given test, the entry must be crossed out and initialed by the Analysis Group representative.		
NOTE		
All scans listed for a specific power level must be reviewed and approved by the Analysis Group representative prior to a change in loop conditions or power level.		
1.0 Power level = 0 kW		
_1.1 Operator's log		
_1.2 Long power verification		
_1.3 T/C scan (takes ~15 minutes)		
_1.4 Analog scan (100 ft)		_____
2.0 Power level = 10 volts (rod resistance check)		
_2.1 Long power verification		_____
3.0 Power level = 20 volts (rod resistance check)		
_3.1 Long power verification		_____
4.0 Power level = 45 volts ~5 kW/rod) (rod resistance check)		
_4.1 Long power verification		_____
5.0 Power level = 30 kW/rod		
_5.1 Short power verification (repeat as necessary to verify 30 ± 0.5 kW/rod on all generators)		
_5.2 Long power verification		
_5.3 Operator's log		
_5.4 T/C scan (takes ~15 minutes)		
_5.5 Analog scan (100 feet)		_____
NOTE		
The 30 kW/rod must be taken. The core inlet temperature should be ~400°F for section 5.0 but will be allowed to drift upward for the remaining power levels.		
6.0 Power level = 50 kW/rod		
_6.1 Short power verification (repeat as necessary to verify 50 ± 0.5 kW/rod on all generators).		
_6.2 Long power verification		
_6.3 Operator's log		
_6.4 T/C scan (takes ~15 minutes)		
_6.5 Analog scan (100 feet)		_____



Subject: APPROACH TO POWER	TEST NO.	DATE OF TEST:
		Initial/Time
<p>7.0 Power level = 70 kW/rod</p> <p>_7.1 Short power verification (repeat as necessary to verify <math>70 \pm 0.5</math> kW/rod on all generators).</p> <p>_7.2 Long power verification</p> <p>_7.3 Operator's log</p> <p>_7.4 T/C scan (takes ~15 minutes)</p> <p>_7.5 Analog scan (100 feet)</p>		
NOTE		
I&C should be allowed to take scans required for calibration of densitometers.		
<p>8.0 Power level = 100 kW/rod</p> <p>_8.1 Short power verification (repeat as necessary to verify <math>100 \pm 0.5</math> kW/rod on all generators).</p> <p>_8.2 Long power verification</p> <p>_8.3 Operator's log</p> <p>_8.4 T/C scan (takes ~15 minutes)</p> <p>_8.5 Analog scan (100 feet)</p>		
<p>9.0 Power level = _____ kW/rod (test power level)</p> <p>_9.1 Short power verification (repeat as necessary to verify _____ <math>\pm 0.1</math> kW/rod on all generators).</p> <p>_9.2 Long power verification</p> <p>_9.3 Operator's log (repeat as necessary to verify desired test conditions).</p>		
NOTE		
Make sure I&C personnel and PDP-8 operator are ready for blowdown (i.e., turbine meter range set, fast-scan program loaded and ready, etc.).		
<p>10.0 At <math>t = -15</math> seconds initiate</p> <p>_10.1 Digital fast scan for 5 minutes</p> <p>_10.2 Analog scan (800 feet)</p>		

## FCTF CALIBRATION PROCEDURE

Run No. 1: Steady-state scans starting at 30 kW up to 122 kW in 10-kW increments; power drop from 122 kW at the following conditions

Pressure, ~2250 psig  
Core flow, ~20-25 gpm  
Core inlet temperature, minimum

Run No. 2: Repeat No. 1, except system pressure ~1500 psi.

Run No. 3: Repeat No. 1, except core inlet temperature ~550°F.

Succeeding Runs: Steady-state scans at 30, 60, 90, and 122 kW, pressure 2250 psig, core flow ~20-25 gpm.

Run No. 4      Hold inlet temperature ~400°F until 122 kW data point is taken.

Run No. 5      Hold inlet temperature ~450°F until 122 kW data point is taken.

Run No. 6      Hold inlet temperature ~500°F until 122 kW data point is taken.

Run No. 7      Hold inlet temperature ~550°F until 122 kW data point is taken.

Runs 8 through 10 let inlet temperature float with power.

Appendix C

EXAMPLES OF ORTCAL - PART I OUTPUT

Table C.1. THTF thermocouple calibration runs

Run No.	Date	Approach to BD No.
1.1	May 4, 1976	Calibration only
1.2	May 5, 1976	Calibration only
1.3	May 5, 1976	Calibration only
1.4	May 6, 1976	Calibration only
2.1	May 19, 1976	Calibration only
2.2	May 20, 1976	Calibration only
3.1	May 26-27, 1976	101
4.1	June 17, 1976	Aborted
4.2	June 18, 1976	102
5.1	July 8, 1976	104
6.1	August 4, 1976	103
7.1	August 19, 1976	105
8.1	September 9, 1976	Aborted
8.2	October 9, 1976	Aborted
8.3	November 5, 1976	151
9.1	November 18, 1976	152
10.1	December 8, 1976	153
11.1	January 13, 1977	154
12.1	January 27, 1977	154R
13.1	February 10, 1977	155
14.1	March 10, 1977	156
15.1	March 24, 1977	157
16.1	April 28, 1977	158
17.1	May 27, 1977	160
18.1	June 16, 1977	161
19.1	June 30, 1977	162
20.1	August 23, 1977	163
21.1	September 22, 1977	164R
22.1	October 13, 1977	165
23.1	December 1, 1977	166
23.2	December 16, 1977	166R
23.3	January 19, 1978	166S
24.1	February 16, 1978	167

Table C.1. Example of ORICAL - Part I output for thermocouple TE-318G

TIME	NOMINAL POWER (KW)	BUNDLE INLET TEMP. (F)	BUNDLE EXIT TEMP. (F)	UPPER PLENJN PRESS. (PSIA)	LOCAL BULK PRESS. (PSIA)	LOCAL BULK TEMP. (F)	LOCAL SAT. TEMP. (F)	CORE FLOW RATE (LN/SEC)	CORE FLOW RATE (GPM)	SHEATH T/C READING (F)	MIDDLE T/C READING (F)	SURFACE HEAT COEFF. (F)	SURFACE HEAT FLUX (F)	H.T. MODE	DEL-T GAP (F)	GAP (MILS)
CALIBRATION RUN NUMBER 1.1 MAY 4																
23:36:56	30.3	405.4	429.8	2223.7	2239.8	419.0	652.0	53.36	442.7	477.4	566.2	6419.	130162.	F.C.	20.5	0.0414
23:44:18	40.1	403.1	434.7	2218.2	2234.4	420.8	651.7	54.49	451.3	495.4	613.1	6529.	171816.	F.C.	25.3	0.0391
23:53:20	40.5	401.9	433.3	2216.7	2232.7	419.4	651.5	55.39	458.4	494.8	613.7	6607.	173735.	F.C.	25.7	0.0395
0129: 6	50.7	406.6	445.2	2212.9	2229.9	428.2	651.3	55.83	463.6	520.1	669.8	6700.	217618.	F.C.	30.5	0.0379
CALIBRATION RUN NUMBER 1.2 MAY 5																
14:31:56	40.7	306.2	336.9	2234.9	2254.1	323.3	652.9	59.50	463.4	402.5	522.9	6269.	174455.	F.C.	26.8	0.0374
14:50:53	50.7	350.6	389.9	2209.3	2227.7	372.5	651.2	56.80	454.0	467.3	616.7	6430.	217389.	F.C.	31.3	0.0372
15:19:21	50.6	401.7	439.8	2293.9	2311.9	423.0	656.6	56.63	466.3	516.1	663.5	6745.	216901.	F.C.	32.0	0.0399
15:56:45	60.9	405.0	451.1	2288.9	2307.2	430.7	656.3	58.24	466.3	540.3	719.2	6754.	261115.	F.C.	36.3	0.0383
16:11: 7	71.2	400.4	452.0	2286.4	2305.1	429.2	656.2	58.54	483.7	557.2	765.3	6964.	305271.	F.C.	44.0	0.0461
16:50:43	81.2	401.5	464.0	2222.4	2238.3	436.4	651.9	54.73	452.7	584.5	820.9	6640.	348228.	F.C.	50.2	0.0408
17:13:10	91.6	402.6	473.8	2192.2	2208.1	442.3	650.0	53.92	446.5	606.7	875.7	6594.	392785.	F.C.	53.9	0.0395
CALIBRATION RUN NUMBER 1.3 MAY 5																
19:21:26	102.2	404.2	480.4	2210.0	2226.4	446.7	651.1	55.88	463.3	627.9	927.7	6810.	438562.	F.C.	60.3	0.0403
19:53:59	112.1	403.7	483.6	2251.1	2267.7	447.0	653.8	56.23	464.8	644.7	970.4	6844.	480673.	F.C.	65.9	0.0405
20:22:51	124.5	401.2	498.8	2217.3	2231.7	455.7	651.5	52.66	435.6	675.6	1037.0	6540.	534211.	F.C.	70.5	0.0399
21: 41:19	124.6	440.3	536.8	2216.2	2229.6	494.2	651.4	51.32	437.6	715.7	1075.0	6582.	534540.	F.C.	73.7	0.0430
CALIBRATION RUN NUMBER 1.4 MAY 6																
12:35:24	91.6	291.6	356.2	2239.8	2259.7	327.7	653.3	63.00	486.8	494.5	757.1	6603.	392913.	F.C.	53.7	0.0356
12:57:41	91.5	293.3	357.0	2225.6	2245.6	328.8	652.4	63.83	493.6	496.6	757.6	6683.	392560.	F.C.	55.5	0.0368
13:35:46	91.4	306.2	370.6	2275.5	2295.0	342.2	655.6	62.81	489.0	507.2	769.1	6716.	391958.	F.C.	53.5	0.0358
13:48:44	91.3	322.2	386.5	2258.1	2277.6	358.1	654.3	62.59	491.7	522.3	783.4	6833.	391688.	F.C.	54.1	0.0370
CALIBRATION RUN NUMBER 2.1 MAY 19																
41: 51: 2	30.6	400.7	426.1	2259.4	2271.0	414.9	654.0	49.97	413.1	474.7	560.9	6059.	131236.	F.C.	20.4	0.0408
42:28:22	41.0	400.8	434.0	2302.9	2314.6	419.3	656.8	51.36	424.5	496.9	613.4	6218.	175076.	F.C.	25.7	0.0389
51: 51:39	51.1	400.1	441.1	2250.8	2262.2	423.0	653.5	51.56	426.0	518.3	663.2	6258.	219187.	F.C.	31.1	0.0383
53:37:54	61.4	400.7	450.0	2303.4	2315.1	429.2	656.8	51.41	424.8	540.3	714.0	6271.	263206.	F.C.	35.3	0.0368
61: 01: 0	71.5	400.7	457.4	2231.6	2242.7	432.3	652.2	51.90	429.1	559.1	763.8	6343.	305650.	F.C.	38.2	0.0347
64:45:11	81.9	400.2	464.5	2219.3	2230.0	436.1	651.4	52.14	431.0	580.5	814.9	6387.	351304.	F.C.	43.5	0.0351
71: 51:50	91.8	400.8	473.0	2234.6	2245.9	441.1	652.4	51.95	429.5	600.6	864.9	6394.	393694.	F.C.	46.9	0.0343
73:51:54	102.0	401.0	480.2	2220.9	2212.6	445.2	650.3	52.40	433.4	623.3	918.3	6461.	437530.	F.C.	54.1	0.0360
81:37: 4	112.1	401.4	488.1	2220.4	2231.0	449.8	651.4	52.49	434.2	644.9	971.0	6492.	480711.	F.C.	59.6	0.0368
CALIBRATION RUN NUMBER 2.2 MAY 19																
22:42:55	30.7	400.0	425.6	2231.1	2243.0	414.3	652.2	49.82	411.7	474.6	562.9	6041.	131859.	F.C.	20.6	0.0408
23:10:47	40.9	400.3	433.3	2218.3	2230.2	418.8	651.4	51.48	425.5	497.3	614.1	6228.	175610.	F.C.	26.8	0.0406
23:32:51	51.1	400.7	441.6	2206.6	2217.9	423.5	650.6	51.73	427.7	519.8	665.7	6276.	219333.	F.C.	32.1	0.0397
23:57:45	61.3	400.2	449.1	2198.9	2210.1	427.5	650.1	51.81	428.3	540.6	716.0	6309.	263081.	F.C.	36.6	0.0383
01:31: 6	71.5	399.8	457.1	2220.8	2232.3	431.8	651.5	51.39	424.6	562.2	766.1	6290.	306696.	F.C.	41.4	0.0378
01:55:49	81.8	400.6	465.6	2250.4	2261.9	436.9	653.4	51.56	426.2	582.8	817.6	6334.	350685.	F.C.	44.8	0.0362
11:23: 3	91.9	400.4	472.5	2236.2	2247.3	440.7	652.5	52.10	430.6	603.3	867.7	6406.	394175.	F.C.	50.1	0.0366
21:30:44	102.2	400.6	480.6	2293.1	2305.3	445.2	656.2	51.97	429.5	624.0	920.7	6416.	438512.	F.C.	53.9	0.0358
21:55:20	112.3	400.9	488.4	2256.6	2268.1	449.7	653.8	52.09	430.7	643.6	970.4	6452.	481816.	F.C.	57.6	0.0354
31:47:32	124.3	400.3	496.0	2247.9	2259.5	453.7	653.3	52.60	434.7	665.4	1027.1	6523.	533154.	F.C.	62.2	0.0351
42:51:42	124.2	449.5	545.2	2275.0	2285.5	503.0	655.0	50.06	430.0	712.2	1072.6	5488.	532716.	F.C.	60.8	0.0356
71: 51:39	124.4	499.2	591.8	2280.9	2290.3	550.9	655.3	48.15	433.7	755.9	1117.5	6474.	533511.	F.C.	57.4	0.0349
71:51:40	124.6	545.7	633.3	2281.0	2288.3	594.6	655.1	45.15	429.6	789.4	1149.0	62413.	534287.	N.B.	61.3	0.0379
81:51:29	112.2	544.7	625.5	2301.4	2308.5	589.8	656.4	44.97	427.2	773.8	1099.0	60184.	481123.	N.B.	51.3	0.0351
81:41: 8	102.3	544.1	618.9	2324.3	2331.7	585.9	657.8	44.92	426.4	759.1	1054.4	6258.	438625.	F.C.	49.9	0.0372
91:19:59	92.0	544.5	612.7	2321.5	2329.0	582.5	657.7	44.81	425.5	743.4	1006.1	6231.	364713.	F.C.	49.4	0.0405
91:43:39	81.9	544.9	606.3	2306.8	2313.9	579.2	656.7	44.58	423.6	724.4	958.7	6193.	351302.	F.C.	45.4	0.0412
101: 71:36	71.5	544.5	599.0	2297.7	2305.4	574.9	656.2	44.49	422.6	703.5	907.6	6166.	306781.	F.C.	40.9	0.0420
101:31:29	61.3	544.1	591.8	2311.1	2318.2	570.6	657.0	44.35	421.0	683.3	856.9	6133.	262928.	F.C.	37.2	0.0439
101:55:49	50.5	543.1	583.1	2302.7	2310.1	565.4	656.5	43.91	416.3	660.1	802.5	6065.	216693.	F.C.	31.9	0.0451
11:19:26	40.7	542.7	576.2	2319.4	2327.6	561.4	657.6	42.62	403.8	639.0	753.5	5908.	174544.	F.C.	26.0	0.0449
11:44:10	30.3	542.4	567.6	2307.5	2315.3	556.5	656.8	42.42	401.8	615.1	699.8	5869.	129951.	F.C.	20.0	0.0457
CALIBRATION RUN NUMBER 3.1 MAY 27																
11:41:13	30.7	401.6	426.6	2221.7	2234.8	415.6	651.7	52.14	431.4	478.6	565.5	6273.	131900.	F.C.	24.1	0.0482
11:36: 0	40.9	398.8	432.3	2235.6	2248.4	417.5	652.6	51.73	427.0	498.5	615.3	6244.	175505.	F.C.	29.4	0.0445
21: 21:32	51.1	402.3	443.2	2258.9	2271.9	425.1	654.1	52.72	436.3	524.1	669.6	6383.	219355.	F.C.	35.4	0.0439
21:23:56	61.4	402.2	450.9	2258.6	2271.6	429.4	654.1	53.02	438.8	545.5	720.7	6435.	263409.	F.C.	40.4	0.0424
21:45:31	71.6	401.9	458.9	2263.4	2282.4	433.7	654.8	52.69	435.9	567.9	771.9	6426.	306975.	F.C.	46.1	0.0422
31:11:21	81.8	403.9	468.5	2271.1	2288.2	440.0	654.9	52.78	437.3	589.8	824.2	6469.	350952.	F.C.	49.9	0.0405
31:32:41	92.0	403.8	475.8	2255.7	2268.9	444.0	653.9	53.17	440.5	609.3	874.7	6529.	394542.	F.C.	53.8	0.0393
41: 11:10	102.0	403.6	483.3	2269.5	2282.7	448.1	654.8	53.13	440.1	629.6	925.1	6540.	437431.	F.C.	58.5	0.0391
42:51:28	112.3	403.0	491.1	2268.9	2282.2	452.2	654.7	52.73	436.6	651.5	976.8	6527.	481708.	F.C.	64.0	0.0395
44:41:45	124.5	404.5	501.6	2249.4	2262.6	458.7	653.5	52.71	437.0	678.9	1038.9	6559.	534182.	F.C.	71.1	0.0403
51:17: 8	124.4	404.6	505.6	2258.5	2271.3	503.7	654.0	51.46	442.6	724.5	1082.7					

Table C.2. (continued)

TIME	NOMINAL POWER (KW)	BUNDLE INLET TEMP. (F)	BUNDLE EXIT TEMP. (F)	UPPER PLENUM PRESS. (PSIA)	LOCAL BULK TEMP. (F)	LOCAL BULK TEMP. (F)	LOCAL SAT. TEMP. (F)	CORE FLOW RATE (LB/SEC)	CORE FLOW RATE (GPM)	SHEATH T/C READING (F)	MIDDLE T/C READING (F)	SURFACE H-T, COEFF, FLUX	SURFACE HEAT FLUX	H-T, MODE	DEL-T GAP (F)	GAP (MILS)
CALIBRATION RUN NUMBER 4.1 JUNE 17																
171411.8	30.7	401.8	424.9	2235.9	2249.3	414.7	652.6	55.51	487.6	478.4	566.7	6685.	131844.	F.C.	26.2	0.0520
14136124	61.3	504.6	550.5	2292.5	2304.7	530.2	655.2	50.86	450.9	546.8	825.6	6684.	262905.	F.C.	44.0	0.0503
1417187	92.0	531.3	599.0	2297.1	2309.1	569.1	656.4	47.90	447.4	735.8	1006.5	6517.	394846.	F.C.	57.7	0.0468
CALIBRATION RUN NUMBER 4.2 JUNE 18																
9112126	30.7	400.2	424.1	2283.4	2276.1	413.5	653.6	54.58	450.9	410.5	563.4	6493.	131554.	F.C.	24.9	0.0497
9153133	61.4	457.0	504.8	2276.7	2278.8	483.7	654.5	51.48	445.2	599.5	775.4	6581.	263530.	F.C.	40.6	0.0445
10127142	92.1	500.5	569.2	2214.3	2276.1	538.8	651.1	49.95	450.8	1054.0	973.4	6622.	395092.	F.C.	57.4	0.0455
1115118	112.3	547.2	625.4	2240.4	2279.1	590.9	652.8	47.10	449.3	773.7	1100.7	57577.	481602.	N.B.	54.3	0.0372
11140133	124.3	547.4	632.8	2274.9	2284.2	595.1	655.0	47.06	448.8	793.7	1175.7	62251.	533240.	N.B.	65.0	0.0410
CALIBRATION RUN NUMBER 5.1 JULY 8																
9151154	30.8	405.4	431.3	2265.8	2279.1	419.9	654.5	50.76	417.8	491.2	580.0	6125.	132075.	F.C.	31.9	0.0641
10141125	61.3	422.4	472.1	2280.0	2293.2	450.1	655.5	51.26	430.7	580.5	754.5	6571.	263003.	F.C.	54.7	0.0568
11135117	92.0	455.4	527.2	2232.1	2244.9	495.5	652.3	50.86	439.	677.0	947.9	6540.	394430.	F.C.	71.4	0.0549
1114111	91.9	456.6	528.4	2256.5	2269.3	496.7	653.9	50.71	438.1	679.4	948.5	6529.	394057.	F.C.	70.7	0.0561
1311015	124.3	548.8	635.6	2302.9	2314.4	597.2	656.8	45.92	436.6	817.2	1180.0	6365.	533146.	N.B.	53.0	0.0553
CALIBRATION RUN NUMBER 6.1 AUG. 4																
3150110	30.8	398.8	425.1	2284.4	2297.5	413.5	655.7	49.63	439.6	482.0	572.7	6077.	131968.	F.C.	28.8	0.0574
1115114	62.0	499.1	547.6	2281.6	2293.7	426.2	655.5	48.82	439.7	653.0	833.3	6451.	266125.	F.C.	51.9	0.0576
11139136	91.9	497.8	568.0	2284.2	2296.6	537.0	655.7	49.11	441.9	717.9	990.8	6526.	394015.	F.C.	71.6	0.0570
12113136	124.2	545.5	632.0	2237.1	2249.1	593.8	652.6	46.56	443.1	814.6	1175.9	60416.	532758.	N.B.	89.1	0.0530
1311917	124.1	546.9	634.0	2291.7	2303.2	595.5	656.1	46.04	436.7	815.4	1178.7	63045.	532344.	N.B.	86.9	0.0547
CALIBRATION RUN NUMBER 7.1 AUG. 19																
16144127	30.6	401.1	426.6	2211.3	2224.3	415.4	651.0	51.12	422.8	484.3	574.5	6174.	131399.	F.C.	30.1	0.0613
17151135	61.0	481.6	522.4	2263.7	2275.4	504.4	654.3	48.91	432.8	610.2	760.3	6375.	218870.	F.C.	43.4	0.0578
14153130	91.5	466.3	524.9	2265.4	2278.1	495.0	654.2	52.85	459.2	666.8	907.3	6739.	349525.	F.C.	71.6	0.0618
1511716	91.1	510.8	567.2	2308.9	2316.9	542.8	656.9	50.44	460.0	708.5	949.0	6686.	347818.	F.C.	70.4	0.0632
15127152	91.0	530.4	586.9	2304.7	2311.6	542.9	656.6	49.21	459.1	726.8	966.6	6634.	341313.	F.C.	69.6	0.0631
15136142	80.9	545.3	601.2	2225.4	2231.9	574.5	651.5	47.71	454.1	741.1	950.7	6531.	347000.	F.C.	68.9	0.0636
CALIBRATION RUN NUMBER 12.1 JAN. 27																
11120134	30.7	400.2	425.2	2294.5	2217.3	414.2	650.6	50.08	414.0	489.0	580.7	6057.	131837.	F.C.	36.2	0.0726
11144122	61.0	409.2	449.0	2216.5	2204.3	431.4	649.7	51.80	431.1	549.2	699.4	6329.	218751.	F.C.	54.2	0.0684
1211116	91.6	404.3	467.4	2231.4	2241.9	439.5	652.1	51.93	430.5	614.9	856.2	6384.	350065.	F.C.	75.1	0.0618
1223315	91.6	460.5	523.9	2282.5	2291.0	495.9	655.3	49.08	425.7	659.0	911.0	6351.	349881.	F.C.	73.8	0.0636
12250152	91.2	525.2	588.0	2308.9	2316.9	542.8	656.9	47.22	437.8	727.2	969.3	6402.	348271.	F.C.	71.2	0.0647
1319119	91.8	543.5	600.8	2274.2	2282.5	575.5	654.8	47.33	449.1	743.5	987.4	6463.	350892.	F.C.	70.8	0.0647
1912142	101.4	538.6	611.4	2219.5	2229.5	579.3	651.3	47.67	449.0	772.5	1075.7	6539.	434848.	F.C.	73.9	0.0555
2014122	124.5	546.7	633.0	2257.1	2266.6	594.9	653.7	46.55	443.7	811.0	1178.6	6137.	534042.	N.B.	84.0	0.0528
CALIBRATION RUN NUMBER 8.3 NOV. 5																
1314133	31.5	416.8	441.9	2247.9	2257.8	430.8	653.2	47.37	396.3	470.0	592.8	5688.	135008.	F.C.	27.8	0.0551
1419110	52.5	410.1	450.7	2253.8	2262.9	432.8	653.6	49.03	408.1	541.8	697.6	6042.	225220.	F.C.	42.1	0.0514
14229159	73.9	412.4	468.3	2257.8	2265.1	443.6	653.8	49.54	413.1	591.9	811.3	6167.	317058.	F.C.	54.6	0.0491
14409141	84.0	413.2	476.6	2246.3	2257.1	448.6	653.1	49.67	414.5	613.2	864.6	6206.	367333.	F.C.	59.8	0.0480
14153135	94.0	413.6	484.7	2246.8	2257.4	453.3	653.1	49.94	416.9	636.6	922.1	6256.	405510.	F.C.	65.8	0.0474
1510148	105.4	411.2	489.5	2248.4	2259.1	454.9	653.3	50.38	419.8	656.3	973.3	6307.	452095.	F.C.	72.0	0.0474
15144127	104.6	534.2	605.6	2251.7	2260.1	574.1	653.3	46.15	432.9	766.7	1080.3	6348.	448761.	F.C.	67.0	0.0487
1619110	109.1	541.6	614.8	2300.4	2308.7	582.5	656.4	45.95	434.8	780.0	1108.0	6359.	468055.	F.C.	67.2	0.0472
16118135	113.8	539.8	615.7	2278.8	2286.7	582.2	655.0	46.16	435.9	786.1	1127.8	6361.	488046.	F.C.	69.3	0.0470
1719114	124.3	546.8	635.1	2293.5	2299.8	595.1	655.9	41.71	397.5	810.1	1178.3	62918.	533163.	N.B.	71.6	0.0512
CALIBRATION RUN NUMBER 9.1 NOV. 18																
13251118	30.6	412.2	437.0	2254.1	2265.2	426.0	653.6	48.27	402.5	497.0	585.0	5953.	131390.	F.C.	31.2	0.0634
1320159	31.1	408.4	433.1	2245.1	2256.2	422.2	653.1	48.57	403.9	494.6	584.6	5942.	133578.	F.C.	32.0	0.0638
13152135	61.5	413.3	453.1	2226.7	2238.2	435.5	651.9	49.43	412.6	545.1	697.1	6117.	221107.	F.C.	47.2	0.0589
14116133	71.4	412.3	467.1	2266.6	2299.1	442.9	655.8	50.00	417.4	591.3	798.6	6216.	306211.	F.C.	59.3	0.0551
14138136	81.5	415.0	475.1	2276.2	2287.2	447.7	654.1	50.16	418.4	614.1	852.5	6249.	349656.	F.C.	65.2	0.0539
14147136	91.6	416.9	486.1	2253.6	2264.4	455.8	653.6	50.25	420.7	678.4	958.8	6298.	393126.	F.C.	70.0	0.0524
1512129	102.0	412.3	491.9	2283.4	2293.5	456.7	655.5	48.52	404.3	660.0	963.1	6128.	437585.	F.C.	76.0	0.0518
15121134	101.6	464.5	542.0	2315.8	2324.9	507.8	657.4	47.22	411.0	758.5	1010.4	6210.	435817.	F.C.	76.2	0.0543
15138127	101.4	509.8	584.3	2315.0	2324.0	551.4	657.4	45.81	417.7	749.5	1049.9	6222.	434769.	F.C.	74.8	0.0553
15153139	101.2	547.4	619.0	2331.8	2340.0	597.3	658.3	43.46	414.	782.8	1082.0	6100.	434264.	F.C.	71.8	0.0545
CALIBRATION RUN NUMBER 10.1 DEC. 8																
11129118	31.3	406.3	437.8	2297.2	2301.5	433.9	656.0	37.82	313.9	502.3	592.2	4887.	134445.	F.C.	32.9	0.0655
11147124	41.5	415.9	457.2	2298.3	2302.4	439.4	656.0	35.27	320.0	536.7	655.5	4996.	178047.	F.C.	40.6	0.0626
1219136	61.6	408.0	464.8	2264.3	2291.0	438.4	655.3	39.44	327.1	579.1	756.8	5418.	264380.	F.C.	54.5	0.0582
1323916	82.1	406.5	486.4	2294.1	2294.9	451.1	655.8	38.88	322.8	631.4	873.0	5111.	352067.	F.C.	66.2	0.0551
1327712	81.7	523.5	595.0	2267.6	2270.9	463.4	654.0	37.40	347.5	738.4	981.2	5336.	350439.	F.C.	66.3	0.0605
13232152	81.6	534.1	604.6	2259.5	2262.2	473.9	653.5	35.97	341.8	747.7	990.1	5314.	350195.	F.C.	65.5	0.0603
1314114	81.5	537.6	611.5	2314.0	2316.2	478.9	656.9	34.91	328.1	755.2	957.0	5084.	349788.	F.C.	64.9	0.0603
1314613	81.5	541.2	615.0	2314.4	2320.3	482.4	657.1	34.53	326.6	758.6	1001.8	5049.	349788.	F.C.	64.5	0.0599
13152147	81.5	546.0	619.9													

Table C.2. (continued)

TIME	NOMINAL POWER (KW)	BUNDLE INLET TEMP. (F)	BUNDLE EXIT TEMP. (F)	UPPER PLENUM PRESS. (PSIA)	LOCAL BULK PRESS. (PSIA)	LOCAL BULK TEMP. (F)	LOCAL SAT. TEMP. (F)	CORE FLOW RATE (LB/SEC)	CORE FLOW RATE (GPM)	SHEATH T/C READING (F)	MIDDLE T/C READING (F)	SURFACE H.T. COEFF. (F)	SURFACE HEAT FLUX	H.T. NODE	DEL-T GAP (F)	GAP (MILS)
CALIBRATION RUN NUMBER 13.1 FEB. 10																
10133:25	30.8	410.8	435.8	2282.0	2294.1	424.8	555.5	47.99	399.7	498.2	589.7	5918.	132192.	F.C.	33.3	0.0672
10154:5	51.4	419.9	460.5	2265.3	2278.3	442.6	554.5	48.42	406.1	556.4	709.9	6051.	220294.	F.C.	48.4	0.0611
11141:1	61.0	426.6	474.1	2254.2	2266.2	453.1	553.7	48.93	412.5	584.5	766.6	6152.	261705.	F.C.	54.7	0.0593
11125:44	71.3	436.9	491.8	2249.6	2261.6	467.5	553.4	48.81	415.0	617.8	831.3	6208.	305972.	F.C.	61.5	0.0586
11140:22	81.7	446.7	509.2	2238.6	2250.3	481.6	552.7	48.34	414.4	649.9	895.2	6221.	350466.	F.C.	67.3	0.0572
12151:2	81.3	501.5	564.1	2227.7	2238.0	536.4	551.9	44.76	404.4	703.5	948.6	6056.	348557.	F.C.	66.1	0.0591
13147:8	81.6	550.8	633.1	2265.6	2270.1	596.7	554.0	29.31	281.0	769.7	1012.4	49782.	349838.	N.B.	66.4	0.0622
CALIBRATION RUN NUMBER 14.1 MAR. 9																
11117:50	30.9	422.6	451.2	2269.0	2273.4	438.6	554.2	41.21	346.4	519.2	607.5	5302.	132615.	F.C.	38.0	0.0776
11140:1	51.2	420.1	468.0	2265.7	2270.2	446.9	554.0	40.79	342.2	569.7	718.9	5294.	219438.	F.C.	52.6	0.0676
12: 2:29	81.7	423.5	499.7	2261.3	2265.7	466.1	553.7	40.25	338.5	648.2	891.0	5314.	350279.	F.C.	71.4	0.0605
12125:4	81.4	460.4	532.7	2251.6	2255.7	500.7	553.0	40.78	353.8	679.4	921.9	5500.	349212.	F.C.	71.2	0.0620
12149:10	81.1	500.6	571.8	2306.2	2310.4	540.3	556.5	39.13	353.0	717.6	959.6	5450.	348015.	F.C.	70.2	0.0634
13118:51	81.0	548.0	616.2	2314.3	2317.4	586.1	557.0	36.73	350.5	761.2	1004.1	5328.	347386.	F.C.	67.7	0.0634
13134:23	81.5	546.1	619.0	2320.9	2322.4	586.8	557.3	34.46	328.0	765.8	1007.3	5066.	349549.	F.C.	67.6	0.0632
CALIBRATION RUN NUMBER 15.1 MAR. 23																
10132:1	30.6	402.2	423.5	2307.0	2324.4	414.1	557.4	56.43	466.9	485.2	574.5	6673.	131433.	F.C.	33.6	0.0674
10155:54	51.2	403.6	437.1	2306.3	2324.0	422.3	557.4	59.51	492.8	533.6	683.3	7014.	219729.	F.C.	50.7	0.0628
11140:1	81.8	479.7	531.2	2306.4	2322.2	508.4	557.3	57.05	503.7	670.8	911.1	7228.	349536.	F.C.	69.8	0.0605
12121:39	101.9	534.0	595.8	2277.8	2291.5	568.5	556.3	53.51	501.5	762.2	1064.9	7120.	437291.	F.C.	78.8	0.0584
131: 8:45	101.9	544.2	602.8	2346.1	2361.4	576.9	559.6	55.30	524.6	767.9	1069.4	7345.	437264.	F.C.	78.1	0.0580
CALIBRATION RUN NUMBER 16.1 APR. 27																
12128:55	70.7	420.0	442.7	2199.9	2211.7	432.7	550.2	52.25	438.4	508.0	595.6	6379.	131703.	F.C.	37.0	0.0755
12155:12	51.2	418.6	456.4	2215.8	2227.4	439.7	551.2	52.00	435.8	554.8	703.8	6392.	219723.	F.C.	51.7	0.0653
13121:11	87.8	420.8	481.3	2177.8	2189.4	454.6	553.7	52.22	438.5	635.1	896.4	6491.	376463.	F.C.	74.0	0.0576
141: 0:52	102.0	484.3	556.7	2194.4	2204.5	524.7	549.7	49.60	440.4	725.0	1031.7	5529.	437417.	F.C.	78.9	0.0566
14142:58	101.8	544.5	603.6	2333.6	2347.5	577.5	558.8	54.66	518.9	768.0	1071.9	7280.	436537.	F.C.	77.3	0.0576
CALIBRATION RUN NUMBER 17.1 MAY 26																
11123:1	30.7	423.5	448.8	2196.3	2205.9	437.6	549.8	46.56	391.7	515.6	603.7	5641.	131802.	F.C.	37.9	0.0776
11145:13	51.1	422.8	464.1	2311.7	2321.8	445.8	557.2	47.37	398.0	564.2	711.1	5960.	219822.	F.C.	52.8	0.0674
12: 9:15	89.4	449.2	519.1	2202.8	2212.1	488.2	550.2	47.04	404.2	674.3	939.2	6116.	383424.	F.C.	74.8	0.0591
12135:46	101.8	497.9	589.6	2235.6	2240.5	549.1	552.1	37.49	337.4	762.7	1069.5	5295.	436862.	F.C.	77.7	0.0576
12152:17	101.6	528.8	620.2	2267.7	2271.4	579.8	554.0	34.88	324.9	791.4	1095.8	5573.	436668.	N.B.	76.9	0.0584
13110:40	101.7	545.8	639.6	2295.0	2297.7	598.1	555.7	31.89	303.5	802.9	1101.2	5627.	436304.	N.B.	80.9	0.0663
13113:25	101.8	545.7	639.2	2282.5	2285.3	597.9	554.9	32.01	304.7	802.5	1100.8	5628.	436471.	N.B.	87.2	0.0660
CALIBRATION RUN NUMBER 18.1 JUNE 15																
16153:51	30.6	424.2	450.3	2271.3	2281.6	438.8	554.7	45.20	380.4	515.6	604.7	5709.	131138.	F.C.	36.4	0.0751
1717:18	51.0	474.7	515.7	2262.7	2272.0	497.6	554.1	45.24	397.7	613.9	762.7	5464.	218718.	F.C.	51.5	0.0688
17136:32	81.7	517.7	579.6	2258.1	2266.5	552.3	553.7	44.31	407.4	723.7	969.1	6063.	350579.	F.C.	70.3	0.0634
17154:39	81.8	544.9	606.4	2221.2	2226.0	579.3	551.2	41.58	395.6	751.0	996.1	5861.	349470.	F.C.	69.4	0.0641
18: 7:50	81.5	545.3	606.8	2231.8	2238.2	579.6	551.9	41.55	395.5	750.9	996.1	5859.	349404.	F.C.	68.9	0.0638
CALIBRATION RUN NUMBER 19.1 JUNE 29																
121: 8:50	30.6	418.4	445.7	2218.4	2225.4	433.6	551.1	43.50	364.5	511.0	601.2	5513.	131172.	F.C.	36.0	0.0740
12131:59	51.0	467.3	511.0	2245.3	2251.6	491.7	552.8	42.79	373.6	610.4	760.5	5682.	218783.	F.C.	52.1	0.0693
15: 6:26	81.7	489.2	555.1	2281.1	2287.8	526.0	555.1	43.58	388.5	699.0	944.3	5890.	360316.	F.C.	69.8	0.0616
13131:46	101.8	542.1	617.9	2299.4	2305.1	584.4	556.2	41.70	394.9	786.1	1092.5	5891.	436505.	F.C.	74.9	0.0566
13140:39	101.8	548.0	622.1	2322.6	2328.6	588.5	557.6	41.02	390.3	790.4	1095.9	5830.	436780.	F.C.	74.3	0.0563
CALIBRATION RUN NUMBER 20.1 AUG. 22																
11141:52	30.5	449.1	470.8	2246.1	2256.8	461.3	553.1	53.17	456.8	538.3	624.6	6617.	130825.	F.C.	40.0	0.0844
12: 5:46	51.9	474.6	503.0	2308.9	2326.6	490.5	557.5	45.81	378.1	606.7	753.6	6009.	222753.	F.C.	59.7	0.0774
12135:35	81.6	523.0	588.9	2268.9	2284.4	548.6	554.9	60.03	555.3	715.7	954.4	7713.	349818.	F.C.	78.2	0.0699
13: 1:53	101.8	543.7	602.1	2369.7	2383.1	578.3	561.0	55.71	528.0	776.1	1075.1	7384.	436668.	F.C.	87.5	0.0653
13121:45	101.8	544.4	603.1	2346.2	2359.3	577.2	559.5	55.20	523.9	776.8	1075.4	7336.	436671.	F.C.	86.9	0.0649
CALIBRATION RUN NUMBER 21.1 SEP. 21																
11: 9:140	30.9	438.5	465.2	2213.3	2224.1	453.4	551.0	43.83	373.3	536.0	627.7	5637.	132524.	F.C.	41.5	0.0861
121: 5:145	51.4	469.0	511.3	2237.5	2247.5	492.6	552.5	43.93	384.2	617.0	769.8	5807.	220634.	F.C.	58.0	0.0769
12153:56	71.9	526.5	580.7	2310.1	2319.9	556.7	557.1	43.66	405.3	716.6	933.1	6006.	305631.	F.C.	70.3	0.0717
18120:14	91.8	544.7	615.3	2287.1	2295.7	584.1	555.6	40.33	383.3	778.4	1054.0	5736.	393935.	F.C.	77.8	0.0649
18122:1	91.8	545.3	615.6	2269.6	2277.8	584.5	554.5	40.47	385.0	778.6	1054.2	5754.	393702.	F.C.	77.9	0.0649
CALIBRATION RUN NUMBER 22.1 OCT. 12																
11148:45	31.1	438.5	463.5	2216.7	2224.9	452.5	551.0	45.95	391.3	531.1	625.6	5849.	133244.	F.C.	38.2	0.0786
12117:55	51.8	483.3	542.2	2235.5	2243.2	516.2	552.2	47.88	424.5	690.0	933.1	6313.	345976.	F.C.	75.6	0.0670
12129:23	101.9	504.3	584.0	2237.7	2243.8	551.0	552.3	45.98	418.9	758.9	1066.0	6241.	437269.	F.C.	84.2	0.0620
12159:23	102.0	546.3	621.9	2308.1	2313.1	588.5	556.7	41.31	393.3	795.6	1103.8	5864.	437492.	F.C.	79.7	0.0605
13: 0:25	102.0	548.1	623.2	2307.4	2312.5	590.1	556.7	41.44	395.5	797.5	1104.9	5780.	437588.	N.B.	80.5	0.0611
CALIBRATION RUN NUMBER 23.1 NOV. 30																
11122:1	31.1	428.9	450.1	2267.4	2276.4	439.4	554.4	48.27	406.7	517.1	608.7	6020.	133572.	F.C.	37.7	0.0765
11141:15	51.8	441.1	480.9	2298.0	2306.4	463.3	556.3	48.23	411.4	582.6	735.4	6129.	222288.	F.C.	54.0	0.0690
11158:35	72.4	478.1	531.9	2265.6	2263.5	508.1	553.5	47.73	421.0	644.6	879.1	6266.	310757.	F.C.	67.5	0.0655
12119:17	101.9	521.0	594.5	2235.0	2240.9	562.0	552.1	45.62	421.3	767.9	1072.3	6244.	436953.	F.C.	82.5	0.0613
12138:																

Table C.2. (continued)

TIME	NOMINAL POWER (KW)	BUNDLE INLET TEMP. (F)	BUNDLE EXIT TEMP. (F)	UPPER PLENUM PRESS. (PSIA)	LOCAL BULK PRESS. (PSIA)	LOCAL BULK TEMP. (F)	LOCAL SAT. TEMP. (F)	CORE FLOW RATE (LB/SEC)	CORE FLOW RATE (GPM)	SHEATH T/C READING (F)	MIDDLE T/C READING (F)	SURFACE H.T. COEFF. (F)	SURFACE HEAT FLUX	H.T. MODE	DEL-T GAP (F)	GAP (MILS)
CALIBRATION RUN NUMBER 23.2 DEC. 15																
101 5118	31.0	429.5	454.8	2210.7	2218.4	443.8	450.0	45.02	389.1	520.4	615.5	5815.	132900.	F.C.	36.2	0.0742
10127117	61.5	471.1	518.8	2211.7	2218.8	497.7	450.7	46.86	410.7	634.2	819.3	6135.	263909.	F.C.	59.7	0.0670
101391 4	61.6	484.3	530.4	2225.9	2233.7	510.1	451.6	47.73	423.7	645.1	830.4	6275.	264070.	F.C.	59.3	0.0670
111 9120	102.1	542.0	614.5	2276.8	2284.0	582.5	454.9	45.85	415.3	788.0	1095.9	6127.	438096.	F.C.	81.0	0.0611
111181 15	102.2	550.2	623.1	2290.3	2295.5	590.9	455.6	42.50	406.9	795.2	1103.5	58851.	438222.	N.B.	79.1	0.0599
11123126	102.1	549.5	622.7	2271.4	2276.4	590.4	454.4	42.29	404.6	795.8	1103.6	55990.	438145.	N.B.	80.8	0.0613
CALIBRATION RUN NUMBER 23.3 JAN. 19																
151 71 0	31.0	476.6	499.9	2113.6	2119.4	489.6	444.1	47.53	419.2	565.6	656.9	6174.	132852.	F.C.	37.2	0.0792
15128151	51.9	513.9	551.3	2209.0	2215.0	534.8	450.4	47.20	432.4	650.5	804.7	6313.	222708.	F.C.	52.2	0.0797
15148134	82.4	531.4	589.9	2178.0	2182.7	564.1	448.3	45.42	425.0	736.5	983.4	6231.	353548.	F.C.	72.1	0.0651
16113141	101.8	551.0	622.6	2246.2	2250.2	591.0	452.7	43.10	413.4	794.8	1100.0	54749.	436747.	N.B.	81.4	0.0618
16117113	101.9	549.8	621.9	2276.5	2280.8	590.1	454.7	43.06	412.1	794.8	1100.1	6075.	437296.	F.C.	80.1	0.0607
CALIBRATION RUN NUMBER 24.1 FEB. 16																
101421 1	39.5	441.3	467.1	2255.8	2261.7	455.7	453.4	44.45	379.3	529.9	621.3	5709.	130739.	F.C.	33.9	0.0713
111 8140	51.2	492.2	533.5	2252.7	2257.7	515.3	453.2	43.97	393.3	629.9	782.0	5895.	219567.	F.C.	49.4	0.0667
11128120	72.1	512.4	568.4	2276.5	2280.7	543.7	454.7	43.55	397.9	697.2	913.2	5949.	309283.	F.C.	63.0	0.0634
121291 8	102.0	544.4	618.8	2192.3	2195.2	585.9	449.1	42.04	400.0	789.0	1097.6	52466.	437687.	N.B.	78.7	0.0593
12150111	102.0	545.9	619.7	2186.8	2190.0	587.1	448.8	42.13	401.6	790.2	1098.6	52247.	437597.	N.B.	80.2	0.0605



Table E.3. Example of ORCAL - Part I output for thermocouple TR-3010.

TIME	NOMINAL POWER	BUNDLE INLET TEMP.	BUNDLE EXIT TEMP.	UPPER PLENUM PRESS.	LOCAL BULK PRESS.	LOCAL BULK TEMP.	LOCAL SAT. TEMP.	CORE FLOW RATE	CORE FLOW RATE	SHEATH T/C READING	MIDDLE T/C READING	SURFACE H.T. COEFF.	SURFACE HEAT FLUX	H.T. MODE	DEL-T GAP	GAP (MILS)
	(KW)	(F)	(F)	(PSIA)	(PSIA)	(F)	(F)	(LB/SEC)	(GPM)	(F)	(F)	(F)	(BTU/HR)		(F)	(MILS)
CALIBRATION RUN NUMBER 1.1 MAY 4																
23136156	30.0	405.4	429.8	2223.7	2235.5	425.1	651.7	53.30	442.7	465.3	538.0	6445.	100764.	F.C.	11.0	0.0285
23144118	39.7	403.1	434.7	2218.2	2230.0	428.6	651.4	54.49	451.3	481.0	577.0	6574.	133079.	F.C.	14.2	0.0261
23153120	40.2	401.9	433.3	2216.7	2228.3	427.7	651.3	55.39	458.4	480.4	577.4	6653.	134708.	F.C.	14.8	0.0291
01291 6	50.1	406.8	445.2	2212.9	2224.5	437.8	651.0	55.83	463.6	503.4	623.4	6755.	168028.	F.C.	18.3	0.0293
CALIBRATION RUN NUMBER 1.2 MAY 5																
14131156	40.3	396.2	336.9	2234.9	2248.9	331.0	652.6	59.50	463.4	390.5	486.1	6336.	135238.	F.C.	19.1	0.0341
14150153	50.2	390.4	389.9	2209.3	2227.7	382.3	650.9	56.80	454.0	450.8	571.5	6500.	168439.	F.C.	19.5	0.0297
14159121	50.0	401.7	439.8	2293.9	2307.0	432.5	656.3	56.63	468.3	501.2	622.2	6801.	167862.	F.C.	21.6	0.0345
14156148	60.3	405.0	451.1	2288.9	2302.3	442.2	656.0	56.24	466.3	524.2	670.7	6819.	202097.	F.C.	25.5	0.0345
141181 7	70.2	402.4	452.0	2286.4	2300.0	442.0	655.9	58.54	483.7	540.0	710.0	7040.	235351.	F.C.	33.4	0.0391
14150142	80.0	401.5	464.0	2222.4	2234.0	451.9	651.6	54.73	452.7	571.7	765.5	6724.	268465.	F.C.	44.7	0.0470
17113110	90.	402.6	473.8	2192.2	2203.8	460.1	649.7	53.92	446.5	598.7	820.2	6616.	302718.	F.C.	54.1	0.0512
CALIBRATION RUN NUMBER 1.3 MAY 5																
19121126	100.6	404.2	480.4	2210.0	2221.0	465.7	650.9	55.88	463.3	535.5	882.1	6909.	337585.	F.C.	77.5	0.0672
19153159	110.2	400.7	483.6	2251.1	2263.2	467.6	653.5	56.23	464.8	666.2	933.2	6952.	369598.	F.C.	98.2	0.0792
20122151	122.3	401.2	498.8	2217.3	2227.8	480.0	651.2	57.56	435.6	716.9	1007.1	3656.	410557.	F.C.	123.5	0.0927
211 4119	122.4	440.3	535.8	2216.2	2226.0	518.2	651.1	51.32	437.6	752.1	1042.5	6883.	410410.	F.C.	121.5	0.0936
CALIBRATION RUN NUMBER 1.4 MAY 6																
12135124	90.4	291.6	356.2	2239.8	2254.2	343.8	652.9	63.00	486.8	498.1	712.8	6747.	303290.	F.C.	67.9	0.0584
12157141	90.3	293.3	357.0	2225.6	2240.2	344.7	652.0	63.83	493.6	498.3	712.0	6827.	303002.	F.C.	67.8	0.0584
13135144	90.3	316.2	370.6	2275.5	2289.8	358.2	655.2	62.81	489.0	509.3	724.8	6853.	302752.	F.C.	65.8	0.0572
13148144	90.1	322.2	386.5	2258.1	2272.3	374.1	654.1	62.59	491.7	522.8	739.1	6961.	302373.	F.C.	64.5	0.0568
CALIBRATION RUN NUMBER 2.1 MAY 19																
41 41 2	30.0	400.7	426.1	2250.4	2267.0	411.2	653.8	49.97	413.1	464.5	536.5	6094.	100638.	F.C.	13.1	0.0339
4129122	40.1	400.8	434.0	2302.9	2311	475.6	656.6	51.36	424.5	485.2	580.9	6263.	134590.	F.C.	18.1	0.0356
51 4130	50.2	400.1	441.1	2250.5	2259	432.6	653.3	51.56	426.0	504.6	624.1	6314.	168456.	F.C.	22.2	0.0394
6137184	60.4	402.7	450.0	2303.4	2312	492.5	656.6	51.41	424.8	525.3	668.3	6336.	202569.	F.C.	25.9	0.0351
61 01 0	70.4	400.7	457.4	2231.6	2239	434.5	652.0	51.90	429.1	545.0	711.2	6417.	236087.	F.C.	30.7	0.0360
6145111	80.5	400.2	464.5	2219.3	2227	437.1	651.2	52.14	431.0	564.4	753.5	6470.	270079.	F.C.	35.1	0.0366
71 4150	90.4	400.8	473.0	2234.8	2242	437.1	652.2	51.95	429.5	587.3	800.2	6484.	303195.	F.C.	42.1	0.0397
7135154	100.2	401.8	483.2	2201.9	2209	437.0	650.1	52.40	433.4	616.9	855.9	6559.	335973.	F.C.	57.4	0.0497
81371 4	110.2	401.4	488.1	2220.4	2228	437.4	651.1	52.49	434.2	660.0	924.8	6598.	369724.	F.C.	65.4	0.0688
CALIBRATION RUN NUMBER 2.2 MAY 19																
22142155	30.1	400.0	426.6	2231.7	2239.8	420.7	652.0	49.82	411.7	465.9	539.2	6076.	101090.	F.C.	14.9	0.0385
23110147	40.1	400.3	433.3	2218.3	2227.0	427.0	651.2	51.48	425.5	486.9	583.4	6273.	134612.	F.C.	20.4	0.0401
23132151	50.3	400.7	441.6	2206.6	2214.8	433.7	650.4	51.73	427.7	507.7	628.2	6334.	168579.	F.C.	24.9	0.0397
23157145	60.3	400.2	449.1	2198.9	2207.1	439.7	649.9	51.81	428.3	527.6	672.5	6374.	202310.	F.C.	29.4	0.0397
01311 6	70.2	399.8	457.1	2220.8	2229.2	446.0	651.3	51.39	424.6	548.2	715.3	6365.	235432.	F.C.	34.2	0.0403
0155149	80.4	400.6	465.6	2250.4	2258.8	453.1	653.2	51.96	426.2	569.6	761.1	6417.	26792.	F.C.	39.2	0.0410
11231 3	90.2	400.4	472.5	2236.2	2244.3	458.6	652.3	52.10	430.6	590.6	805.1	6519.	336575.	F.C.	53.6	0.0462
0130144	100.3	400.6	480.6	2293.1	2302.0	465.2	656.0	51.97	429.5	613.8	852.6	6515.	371018.	F.C.	61.8	0.0493
2155120	110.3	400.9	488.4	2256.6	2265.0	471.5	653.6	52.09	430.7	637.2	900.5	6558.	410060.	F.C.	74.9	0.0549
3118132	122.3	400.3	496.0	2247.9	2256.4	477.6	653.1	52.60	434.7	666.4	959.3	6638.	407859.	F.C.	73.2	0.0559
4135152	122.2	449.5	545.2	2275.0	2282.6	526.8	654.8	50.96	430.0	713.2	1009.0	6584.	407859.	F.C.	73.2	0.0559
71 5139	122.5	499.2	591.8	2280.9	2287.8	574.0	655.1	48.15	433.7	743.5	1027.1	6565.	410918.	F.C.	56.6	0.0443
82411 8	100.3	544.1	618.9	2324.3	2327.7	604.5	657.7	44.92	426.4	738.4	966.8	6373.	336486.	F.C.	40.2	0.0385
9119159	90.0	544.5	612.7	2321.5	2327.0	599.5	657.5	44.81	425.5	725.2	934.5	6327.	301970.	F.C.	41.0	0.0435
9143139	80.1	544.9	606.3	2308.8	2312.0	594.5	656.6	44.58	423.6	711.8	901.1	6271.	268840.	F.C.	41.4	0.0487
101 7136	70.2	544.5	599.0	2297.7	2303.3	588.5	656.1	44.49	422.6	697.0	867.6	6222.	235512.	F.C.	41.0	0.0430
10131129	60.2	544.1	591.5	2311.1	2316.3	582.4	656.9	44.35	421.0	681.2	831.4	6180.	201946.	F.C.	41.5	0.0553
10155149	49.7	543.1	583.1	2302.7	2308.1	575.4	656.4	43.91	414.3	660.8	785.4	6103.	166619.	F.C.	37.3	0.0486
1119126	40.1	542.7	576.2	2319.4	2324.4	569.8	657.4	42.62	403.8	639.7	740.0	5938.	134499.	F.C.	30.3	0.0482
11144110	29.8	542.4	567.6	2307.5	2313.2	562.8	656.7	42.42	401.8	614.9	689.0	5891.	99864.	F.C.	22.5	0.0468
CALIBRATION RUN NUMBER 3.1 MAY 27																
1114113	30.2	401.6	426.6	2221.7	2231.1	421.8	651.5	52.14	431.4	467.3	540.8	6309.	101403.	F.C.	15.7	0.0405
11361 0	40.2	398.8	432.3	2235.6	2245.0	425.8	652.3	51.73	427.0	485.5	582.7	6291.	134756.	F.C.	20.1	0.0395
21 2132	50.3	402.3	443.2	2258.9	2268.4	435.3	653.9	52.72	436.3	509.3	629.6	6439.	168552.	F.C.	25.3	0.0405
2123156	60.3	402.2	450.9	2258.6	2268.1	441.5	653.8	53.02	438.8	529.8	673.2	6501.	202372.	F.C.	30.3	0.0410
2145131	70.5	401.9	458.9	2269.3	2278.8	447.9	654.5	52.69	435.9	550.4	717.6	6501.	236479.	F.C.	35.0	0.0410
3111121	80.4	403.9	468.5	2271.1	2280.7	456.1	654.6	52.78	437.3	572.0	763.0	6552.	26727.	F.C.	39.5	0.0414
3132141	90.4	403.8	475.8	2255.7	2265.4	462.0	653.7	53.17	440.5	594.8	810.1	6620.	303134.	F.C.	47.8	0.0453
41 1110	100.2	403.6	483.3	2259.5	2270.1	468.0	654.5	53.13	440.1	623.8	864.7	6646.	336137.	F.C.	62.0	0.0539
4125128	110.5	403.0	491.1	2268.9	2278.6	474.1	654.5	52.73	436.6	656.3	922.9	6635.	373663.	F.C.	79.0	0.0634
4148145	122.3	404.5	501.6	2249.4	2259.0	482.9	653.3	52.71	437.0	694.7	994.1	6674.	410250.	F.C.	98.4	0.0730
51171 8	122.2	450.6	545.6	2258.5	2267.8	527.4	653.8	51.46	442.6	747.1	1040.6	6734.	409938.	F.C.	108.1	0.0836
6120158	122.3	547.0	633.6	2253.4	2261.9	616.9	653.4	46.29	441.4	815.9	1118.9	53552.	410110.	N.B.	105.4	0.0859
6149148	110.2	545.8	625.5	2271.5	2280.0	610.1	654.6	46.33	440.9							

Table C.1. (continued)

TIME	NOMINAL POWER (KW)	BUNHOLE INLET (F)	BUNDLE EXIT (F)	UPPER PLENUM (PSIA)	LOCAL BULK (PSIA)	LOCAL BULK (F)	LOCAL SAT. (F)	CORE FLOW RATE (LP/SEC)	CORE FLOW RATE (GPM)	SHEATH T/C (F)	MIDDLE T/C (F)	SURFACE H.T. COEFF. (F)	SURFACE HEAT FLUX	H.T. MODE	DEL-T GAP (F)	GAP (MILS)
CALIBRATION RUN NUMBER 4.1 JUNE 17																
131411 R	30.2	401.8	424.9	2235.9	2245.7	420.4	652.4	56.51	467.6	469.5	544.0	6720.	101253.	F.C.	20.3	0.0524
14136124	60.5	504.6	550.5	2292.5	2301.4	541.7	656.0	50.88	460.9	640.0	789.2	6729.	202997.	F.C.	42.5	0.0628
181 7157	90.6	571.3	599.0	2297.1	2305.8	585.9	656.2	47.9R	447.4	720.7	937.3	6589.	304006.	F.C.	51.2	0.0536
CALIBRATION RUN NUMBER 4.2 JUNE 18																
9112126	30.3	400.2	424.1	2283.4	2292.7	419.5	655.4	54.58	450.9	469.7	544.1	6529.	101607.	F.C.	20.9	0.0537
9153133	60.3	457.0	504.8	2266.7	2275.5	495.6	654.3	51.48	445.2	591.9	736.0	6604.	202112.	F.C.	39.6	0.0564
10127142	90.3	500.5	569.2	2214.3	2222.9	555.9	650.9	49.95	450.8	698.7	920.4	6689.	302948.	F.C.	59.8	0.0615
111 5115	109.9	547.2	625.4	2240.4	2248.9	610.3	652.6	47.10	449.3	742.0	996.0	50251.	368662.	N.B.	37.2	0.0327
CALIBRATION RUN NUMBER 5.1 JULY 8																
9151154	30.2	405.4	431.3	2265.0	2275.5	426.3	653.3	50.36	417.8	474.5	549.8	6160.	101149.	F.C.	18.1	0.0470
10141125	60.3	422.4	472.1	2230.3	2239.7	462.5	655.2	51.26	430.7	558.0	703.6	6432.	202359.	F.C.	37.5	0.0518
11135117	90.4	455.4	527.2	2232.1	2241.4	513.3	652.1	50.86	439.3	651.1	867.0	6614.	303133.	F.C.	53.5	0.0530
1114111	1	90.3	456.6	528.4	2265.8	514.6	653.7	50.71	436.4	652.0	868.1	6604.	302873.	F.C.	53.2	0.0528
131101 5	122.1	546.8	635.6	2302.8	2311.3	618.9	656.6	45.92	436.6	769.5	1055.6	55655.	409626.	N.B.	96.0	0.0449
CALIBRATION RUN NUMBER 6.1 AUG. 4																
9159110	30.2	398.8	425.1	2284.4	2293.9	420.0	655.5	49.63	409.6	468.0	543.1	6053.	101253.	F.C.	17.6	0.0453
111 51 4	60.9	499.1	547.6	2281.6	2290.4	538.3	655.3	48.82	439.7	632.2	779.7	6497.	204196.	F.C.	36.6	0.0536
11139136	90.3	497.8	568.0	2284.2	2293.2	554.5	655.5	49.14	441.9	693.0	912.6	6594.	302763.	F.C.	54.9	0.0563
12113136	122.3	545.5	632.0	2237.1	2245.9	615.3	652.4	46.56	443.1	777.0	1080.3	52887.	410336.	N.B.	67.2	0.0539
131191 7	122.0	546.9	634.0	2291.7	2300.1	617.3	655.9	46.04	438.7	780.7	1083.3	55148.	409357.	N.B.	67.9	0.0547
CALIBRATION RUN NUMBER 7.1 AUG. 19																
16144127	30.5	401.1	426.6	2211.3	2220.8	421.7	650.8	51.12	422.8	470.5	546.5	6209.	102229.	F.C.	18.5	0.0474
17155135	60.1	481.6	522.4	2263.7	2272.2	514.6	654.1	48.91	432.8	591.5	714.3	6415.	168079.	F.C.	29.0	0.0501
191 2142	100.5	538.6	611.4	2219.5	2228.8	597.4	651.2	47.67	449.9	735.0	973.5	6644.	337092.	F.C.	45.7	0.0435
201 6122	122.4	546.7	633.0	2257.1	2264.0	616.4	653.6	46.55	443.7	762.0	1048.4	53674.	410613.	N.B.	51.0	0.0406
CALIBRATION RUN NUMBER 8.2 OCT. 9																
2133152	30.3	401.5	424.3	2286.9	2294.9	419.9	655.6	51.32	424.4	468.3	544.9	6217.	101744.	F.C.	18.2	0.0468
2157141	60.5	456.5	493.0	2310.4	2317.9	486.0	657.0	50.77	413.7	564.0	688.4	6489.	169390.	F.C.	29.9	0.0499
3121126	70.7	503.7	554.4	2313.4	2320.0	544.6	657.1	48.06	434.8	650.4	823.5	6439.	237066.	F.C.	39.1	0.0499
CALIBRATION RUN NUMBER 8.3 NOV. 5																
13141133	30.3	416.8	441.9	2247.9	2255.1	437.1	653.0	47.37	396.3	485.4	562.0	5919.	101495.	F.C.	17.6	0.0458
141 91 0	50.5	410.1	450.7	2253.8	2261.2	442.9	653.4	49.03	408.1	523.4	647.7	6113.	169375.	F.C.	30.3	0.0487
14129159	71.3	412.4	468.3	2257.8	2265.3	457.6	653.7	49.54	413.1	569.2	743.5	6236.	239151.	F.C.	42.0	0.0495
14149141	81.2	413.2	476.6	2246.3	2254.2	464.4	652.9	49.67	414.5	591.1	787.5	6281.	272246.	F.C.	48.0	0.0505
14153135	91.7	413.6	484.7	2248.8	2254.5	471.0	653.0	49.94	416.9	612.5	834.1	6339.	307600.	F.C.	53.3	0.0503
151 9145	101.7	411.2	489.5	2246.4	2256.2	474.4	653.1	50.38	410.8	630.0	875.3	6398.	341029.	F.C.	58.6	0.0505
15144112	101.0	534.2	605.6	2251.7	2257.9	591.8	653.2	46.15	432.9	733.4	977.7	6435.	338924.	F.C.	47.9	0.0455
161 51 0	105.3	541.6	614.8	2300.4	2304.4	600.7	656.3	45.95	434.8	743.2	996.2	6466.	353336.	F.C.	44.9	0.0410
1618135	109.9	539.8	615.7	2278.8	2284.6	601.1	654.9	46.16	435.9	747.2	1009.3	6493.	368470.	F.C.	44.6	0.0393
171 51 4	122.8	546.8	635.1	2293.5	2298.1	618.1	655.8	41.71	397.5	763.6	1053.0	55226.	411861.	N.B.	50.5	0.0401
CALIBRATION RUN NUMBER 9.1 NOV. 18																
12151118	30.5	412.2	437.0	2254.1	2262.2	432.2	653.5	48.27	402.5	482.8	561.2	5984.	102224.	F.C.	19.8	0.0512
13129159	30.4	408.4	433.1	2245.1	2253.2	428.4	652.9	48.57	403.9	478.1	557.2	5995.	102087.	F.C.	18.9	0.0489
13152135	50.4	415.3	453.1	2226.7	2235.1	445.4	651.7	49.43	412.6	526.5	653.9	6167.	169069.	F.C.	31.3	0.0508
14116133	71.3	412.3	467.1	2286.6	2295.0	456.5	655.6	50.06	417.4	569.7	746.9	6283.	239186.	F.C.	43.8	0.0516
14138136	81.1	413.0	475.1	2276.2	2284.2	463.2	654.9	50.16	418.4	590.9	791.1	6324.	272054.	F.C.	49.4	0.0520
14147136	90.7	416.9	486.1	2253.6	2261.5	472.8	653.4	50.25	420.5	614.4	837.4	6378.	304363.	F.C.	54.6	0.0522
151 2129	100.4	412.3	491.9	2283.4	2290.8	476.6	655.3	48.52	404.5	634.0	879.5	6217.	336854.	F.C.	60.2	0.0526
15121134	100.1	464.5	542.0	2315.0	2322.4	527.0	657.3	47.22	411.0	680.9	926.1	6284.	335662.	F.C.	58.3	0.0534
15138127	99.8	509.8	584.3	2315.0	2321.6	570.0	657.2	45.81	417.3	722.3	971.1	6292.	334804.	F.C.	57.9	0.0549
15153139	99.6	547.4	619.0	2331.8	2337.8	605.2	658.2	43.46	414.1	743.5	986.9	6211.	334220.	F.C.	53.9	0.0426
CALIBRATION RUN NUMBER 10.1 DEC. 8																
11125118	30.2	406.3	437.8	2297.2	2300.3	431.7	655.9	37.82	313.9	493.0	567.3	4920.	101131.	F.C.	27.1	0.0715
11147124	40.6	415.9	457.2	2298.3	2301.3	449.2	656.0	38.27	320.0	530.6	629.8	5040.	136149.	F.C.	36.3	0.0732
121 9136	60.6	405.0	464.8	2286.3	2289.9	453.3	655.2	39.44	327.1	570.8	717.9	5179.	203247.	F.C.	51.7	0.0717
121591 8	80.5	406.5	486.4	2294.1	2297.6	471.0	655.7	38.88	322.8	622.9	817.7	5188.	270368.	F.C.	64.9	0.0701
131271 2	80.6	523.5	595.0	2267.6	2270.0	581.2	654.0	37.46	346.8	722.6	919.4	5397.	270319.	F.C.	58.1	0.0684
13121252	80.6	534.1	604.6	2259.5	2261.5	591.0	653.4	36.97	346.8	729.0	925.2	5385.	270342.	F.C.	54.6	0.0645
13143116	80.5	537.7	611.5	2314.0	2315.6	597.3	656.8	34.84	328.1	734.0	930.7	5163.	270037.	F.C.	52.3	0.0622
131461 3	80.5	541.2	615.0	2318.4	2319.8	600.8	657.1	34.53	326.6	736.5	931.9	5144.	270100.	F.C.	50.3	0.0601
13152147	80.5	546.0	619.9	2304.9	2306.2	605.7	656.3	33.83	322.0	737.0	931.9	5089.	270115.	F.C.	45.3	0.0541
CALIBRATION RUN NUMBER 11.1 JAN. 13																
13149136	30.4	428.6	451.9	2255.0	2264.2	447.4	653.6	52.92	446.9	504.0	577.2	6522.	101814.	F.C.	27.4	0.0726
14112127	50.6	425.0	463.2	2307.4	2314.0	455.8	656.7	53.48	450.2	546.9	668.0	6619.	169821.	F.C.	43.0	0.0793
14134140	80.8	426.3	485.9	2291.7	2298.8	474.5	655.8	54.05	455.6	613.4	806.0	6768.	271008.	F.C.	63.8	0.0684
14153130	80.4	466.3	524.9	2265.4	2271.7	513.6	654.1	52.65	459.2	650.4	841.9	6801.	269781.	F.C.	62.8	0.0697
151171 5	80.1	510.8	566.2	2308.9	2314.8	557.1	656.8	50.44	460.0	691.3	882.5	6743.	268560.	F.C.	60.9	0.0703
15127152	79.9	530.4	585.9	2304.7	2309.9	576.0	656.5	49.21	459.1	709.3	900.4	6686.	268120.	F.C.	60.0	0.0703
15136142	79.9	545.3	601.2	2225.4	2230.1	590.5	651.4	47.71	454.1	722.8	914.3	6602.	267971.	F.C.	58.8	0.0697

Table C.3. (continued)

TIME	NOMINAL POWER (KW)	BUNDLE INLET TEMP. (F)	BUNDLE EXIT TEMP. (F)	UPPER PRESS. (PSIA)	LOCAL BULK PRESS. (PSIA)	LOCAL BULK TEMP. (F)	LOCAL SAT. TEMP. (F)	CORE FLOW RATE (LB/SEC)	CORE FLOW RATE (GPM)	SHEATH T/C READING (F)	MIDDLE T/C READING (F)	SURFACE H.T. COEFF. (F)	SURFACE HEAT FLUX (F)	H.T. MODE	DEL-T GAP (F)	GAP (MILS)
CALIBRATION RUN NUMBER 12.1 JAN. 27																
11120138	30.1	400.2	425.2	2204.5	2214.3	420.4	550.4	50.08	414.0	473.9	552.0	6101.	101125.	F.C.	23.3	0.0603
11144122	50.5	409.2	449.0	2193.8	2201.4	441.3	549.5	51.80	431.1	527.8	655.8	6382.	169282.	F.C.	37.4	0.0603
121 8116	81.6	404.3	467.4	2231.4	2239.0	455.3	652.0	51.3	430.5	591.1	793.6	6464.	273573.	F.C.	57.8	0.0603
121331 8	81.6	405.5	523.9	2282.5	2289.1	511.7	655.2	49.08	425.7	646.1	848.2	6421.	273716.	F.C.	57.0	0.0622
12159150	41.4	525.2	587.0	2308.9	2314.9	573.5	656.8	47.22	437.8	704.9	906.2	6461.	272929.	F.C.	55.4	0.0638
131 9119	80.5	543.5	600.8	2274.2	2280.3	589.7	654.6	47.33	449.1	718.0	917.9	6546.	270081.	F.C.	53.8	0.0632
CALIBRATION RUN NUMBER 13.1 FEB. 10																
10133325	30.4	410.8	435.8	2282.0	2290.8	431.0	655.3	47.99	399.7	486.4	564.1	5950.	102025.	F.C.	24.6	0.0640
101541 8	50.7	419.9	460.5	2266.3	2275.0	452.7	654.3	48.42	406.1	541.9	670.0	6100.	170011.	F.C.	38.9	0.0632
111141 1	80.4	405.6	474.1	2254.2	2262.9	464.9	653.5	48.93	412.5	569.0	721.0	6208.	202471.	F.C.	45.6	0.0636
11125144	70.4	436.9	491.8	2249.4	2258.4	481.2	653.2	48.81	415.0	601.8	777.8	6266.	232425.	F.C.	52.3	0.0640
11140122	80.8	444.7	509.2	2238.6	2247.2	497.1	652.5	48.34	414.4	633.0	828.0	6280.	271083.	F.C.	58.3	0.0636
12115112	80.4	501.5	564.1	2227.7	2235.2	552.0	651.7	44.76	404.4	687.1	887.0	6113.	269825.	F.C.	57.3	0.0657
131471 8	80.7	570.8	633.1	2245.6	2268.9	617.2	653.9	29.31	281.0	739.0	935.1	43735.	270537.	N.B.	46.0	0.0549
CALIBRATION RUN NUMBER 14.1 MAR. 9																
11117155	30.4	422.8	451.2	2269.0	2272.2	445.7	654.1	41.21	346.4	505.6	580.0	5332.	101803.	F.C.	27.2	0.0720
111401 0	50.7	476.1	468.0	2285.7	2269.0	458.8	653.9	40.79	372.2	554.1	678.5	5343.	169965.	F.C.	41.2	0.0676
121 2129	80.8	423.5	499.7	2261.3	2244.5	485.1	653.6	40.25	338.5	631.4	828.0	5386.	270985.	F.C.	61.4	0.0628
121251 4	80.6	460.4	532.7	2251.6	2254.6	518.7	653.0	40.78	353.8	662.0	857.6	5562.	270234.	F.C.	60.5	0.0678
12149110	80.3	500.6	571.8	2304.2	2309.2	588.1	656.5	39.13	353.0	699.2	894.0	5507.	269432.	F.C.	58.7	0.0680
13141151	80.2	548.0	616.2	2314.3	2314.6	603.1	656.9	36.73	350.5	735.7	930.7	5418.	268939.	F.C.	50.2	0.0691
13134123	80.6	546.1	619.0	2320.9	2322.0	604.9	657.2	34.46	328.0	738.2	933.4	5159.	270491.	F.C.	47.9	0.0572
CALIBRATION RUN NUMBER 15.1 MAR. 22																
101321 1	30.4	402.2	423.5	2307.0	2319.7	419.4	657.1	56.43	466.9	464.7	547.0	6705.	101979.	F.C.	20.2	0.0518
10155154	50.4	403.6	437.1	2306.3	2319.2	430.7	657.1	59.51	492.8	510.9	638.5	7065.	169560.	F.C.	33.5	0.0532
111401 2	80.9	479.7	531.2	2306.4	2317.9	521.3	657.0	57.05	503.7	642.4	842.9	7285.	271306.	F.C.	49.5	0.0545
12121179	100.9	534.0	595.8	2277.8	2287.8	583.0	655.1	53.51	501.5	729.8	980.1	7191.	338596.	F.C.	57.2	0.0539
131 8145	100.8	544.2	602.8	2346.1	2357.2	591.5	659.4	55.30	524.6	734.9	983.4	7425.	338162.	F.C.	56.4	0.0536
CALIBRATION RUN NUMBER 16.1 APR. 27																
10128155	30.5	420.0	442.7	2199.9	2208.5	438.3	650.0	52.25	436.4	496.5	569.8	6499.	102146.	F.C.	28.6	0.0747
12155112	50.7	418.6	456.4	2215.8	2224.3	469.1	651.0	52.00	435.8	540.5	663.2	6441.	170145.	F.C.	42.5	0.0688
13121111	81.0	420.8	481.3	2177.8	2187.3	469.7	648.5	52.22	436.5	605.3	802.6	6564.	271717.	F.C.	51.1	0.0628
141 0152	101.1	484.3	564.7	2194.4	2201.7	542.8	649.6	49.60	440.4	704.3	950.5	6600.	339174.	F.C.	67.9	0.0624
141A2158	101.0	544.5	603.6	2333.8	2343.8	592.2	658.6	54.66	518.9	742.1	987.8	7362.	338611.	F.C.	62.4	0.0593
CALIBRATION RUN NUMBER 17.1 MAY 26																
111231 5	30.3	423.5	448.8	2196.3	2203.3	444.0	649.7	46.56	391.7	502.6	575.7	5872.	101586.	F.C.	27.7	0.0734
11145113	50.7	422.8	464.1	2311.7	2319.1	456.1	657.1	47.37	398.0	548.7	669.8	6098.	170054.	F.C.	41.9	0.0884
121 0115	80.5	440.2	519.1	2202.8	2205.6	505.6	650.1	47.04	404.2	653.4	865.1	6185.	297007.	F.C.	62.1	0.0624
12135146	100.9	497.9	589.6	2235.6	2239.1	571.9	652.0	37.49	337.4	742.1	984.7	5369.	338484.	F.C.	65.7	0.0624
12152117	100.8	528.8	620.2	2267.7	2270.4	602.6	654.3	34.88	324.9	763.1	1001.3	48950.	338108.	N.B.	61.2	0.0591
13110140	100.8	545.8	639.6	2295.0	2297.0	621.5	655.7	31.89	303.5	769.0	1003.4	49966.	338108.	N.B.	65.5	0.0636
13113125	100.8	545.7	639.2	2282.5	2284.6	621.2	654.9	32.01	304.7	768.2	1002.7	49505.	338108.	N.B.	65.5	0.0636
CALIBRATION RUN NUMBER 18.1 JUNE 15																
16153151	30.4	424.2	450.3	2271.3	2278.8	445.3	654.5	45.20	380.4	498.4	574.7	5740.	101984.	F.C.	21.7	0.0570
17117118	50.6	474.7	515.7	2262.7	2269.5	507.8	653.9	45.24	397.7	592.3	716.5	6003.	169881.	F.C.	34.3	0.0584
17136132	80.9	517.7	579.2	2258.1	2264.2	567.7	653.6	44.31	407.4	694.6	891.0	6120.	271299.	F.C.	48.9	0.0563
17154119	80.9	544.9	606.4	2221.2	2227.1	594.6	651.1	41.58	395.6	720.5	917.0	5938.	271452.	F.C.	46.9	0.0551
181 7150	80.9	545.3	606.8	2231.8	2234.5	595.0	651.8	41.55	395.5	720.7	917.5	5937.	271309.	F.C.	46.7	0.0549
CALIBRATION RUN NUMBER 19.1 JUNE 29																
121 8150	33.5	418.4	445.7	2218.4	2223.5	440.5	651.0	43.50	364.5	494.6	570.9	5545.	102371.	F.C.	22.0	0.0574
12131150	50.7	467.3	511.0	2245.3	2249.9	502.6	652.7	42.79	373.6	587.7	712.3	5722.	169943.	F.C.	33.5	0.0568
131 4126	80.8	499.2	555.1	2281.1	2286.0	542.4	656.0	43.58	388.5	671.3	867.7	5947.	271029.	F.C.	49.3	0.0557
13131146	100.9	547.1	617.9	2299.4	2303.5	603.3	656.1	41.70	394.9	753.4	998.8	5999.	338384.	F.C.	52.6	0.0507
13140135	100.9	546.0	622.1	2322.6	2327.0	607.5	657.5	41.02	390.3	756.2	1000.6	51218.	338355.	N.B.	51.1	0.0493
CALIBRATION RUN NUMBER 20.1 AUG. 22																
11141150	30.4	449.1	470.8	2246.1	2253.9	466.7	652.0	53.17	456.8	526.0	596.1	6644.	101968.	F.C.	30.4	0.0819
121 5146	50.4	474.6	503.0	2304.9	2311.8	497.6	647.2	45.81	378.1	586.5	701.7	8046.	168952.	F.C.	46.0	0.0780
12135135	80.5	523.0	584.9	2280.9	2280.2	560.1	654.6	46.03	355.3	691.1	876.6	7766.	269943.	F.C.	62.6	0.0719
131 1153	100.9	543.7	602.1	2349.7	2379.5	590.8	650.7	55.71	528.0	748.3	983.3	7462.	338996.	F.C.	70.7	0.0672
1321145	100.8	544.4	603.1	2348.2	2355.7	591.8	659.3	55.20	523.9	748.9	983.4	7416.	338179.	F.C.	70.1	0.0668
CALIBRATION RUN NUMBER 21.1 SEP. 21																
11140140	30.5	438.5	465.2	2213.3	2221.1	460.1	650.8	43.83	373.3	521.7	595.0	5665.	102152.	F.C.	30.1	0.0803
12110148	50.5	459.0	511.3	2237.5	2244.8	503.2	652.3	43.93	384.2	598.4	716.8	5846.	167705.	F.C.	44.9	0.0776
12143154	80.9	466.6	580.7	2310.1	2317.3	570.2	656.9	43.64	405.3	694.5	859.5	6055.	234463.	F.C.	56.4	0.0749
14120114	80.9	544.7	615.3	2287.1	2293.3	601.7	655.5	40.33	383.3	756.1	971.4	5833.	304733.	F.C.	65.1	0.0693
141221 8	90.8	545.3	615.6	2289.6	2275.6	602.0	654.3	40.47	385.0	756.4	971.3	5852.	304678.	F.C.	65.2	0.0695
CALIBRATION RUN NUMBER 22.1 OCT. 12																
11141140	30.1	438.6	463.5	2216.7	2222.7	458.7	650.9	45.95	391.3	516.0	591.9	5877.	100827.	F.C.	26.7	0.0720
12117148	77.6	463.3	542.7	2235.5	2241.1	530.8	652.1	47.88	424.5	644.8	851.3	6370.	260147.	F.C.	60.3	0.0703
12129123	101.2	509.3	584.0	2237.7	2242.2	569.6	652.2	45.98	418.9	738.5	980.6	6312.	339400.	F.C.	73.4	0.0692
12143123	101.1															

Table C.3. (continued)

TIME	NOMINAL POWER (KW)	BUNDLE INLET TEMP. (F)	BUNDLE EXIT TEMP. (F)	UPPER PLENUM PRESS. (PSIA)	LOCAL BULK PRESS. (PSIA)	LOCAL BULK TEMP. (F)	LOCAL SAT. TEMP. (F)	CORE PLDW RATE (LB/SEC)	CORE FLOW RATE (GPM)	SHEATH T/C READING (F)	MIDDLE T/C READING (F)	SURFACE H.T. COEFF. (F)	SURFACE HEAT FLUX	H.T. MODE	DEL-T GAP (F)	GAP (MILS)
CALIBRATION RUN NUMBER 23.1 NOV. 30																
111221 7	29.9	425.9	450.1	2267.7	2274.1	445.5	654.2	48.27	406.7	502.0	575.7	605C.	100458.	F.C.	26.5	0.0709
11141115	50.2	441.1	480.9	2298.0	2304.1	473.2	656.1	48.23	411.4	564.0	684.0	6173.	168226.	F.C.	41.5	0.0693
11158135	70.4	478.1	531.9	2256.1	2261.5	521.5	653.4	47.73	421.0	643.7	811.8	6318.	236142.	F.C.	50.8	0.0693
12119117	101.0	521.0	594.5	2235.0	2239.3	580.3	652.0	45.62	421.3	747.2	987.8	6317.	338991.	F.C.	71.7	0.0682
12138144	100.9	548.9	623.6	2267.2	2270.1	609.2	654.0	41.39	395.7	770.4	1009.3	48959.	338387.	N.B.	68.5	0.0685
12144128	100.9	549.2	624.1	2262.6	2265.2	609.6	653.7	41.22	394.3	770.5	1009.3	48774.	338414.	N.B.	68.9	0.0688
CALIBRATION RUN NUMBER 23.2 DEC. 15																
101 8118	29.9	420.5	454.8	2210.7	2216.3	449.9	650.5	46.02	389.1	505.9	581.2	5845.	100406.	F.C.	25.5	0.0684
10127117	50.8	471.1	518.8	2211.7	2216.0	509.6	650.5	46.86	410.7	617.2	763.7	6181.	203931.	F.C.	48.5	0.0699
101391 4	60.8	484.3	530.4	2225.9	2231.6	521.6	651.5	47.73	423.7	627.5	774.1	6319.	203775.	F.C.	47.7	0.0693
111 9120	101.1	542.0	614.6	2278.5	2282.5	600.6	654.8	43.85	415.3	764.6	1005.9	6230.	338983.	F.C.	68.4	0.0659
11116118	101.0	550.2	623.1	2290.3	2294.1	609.1	655.5	42.50	406.9	769.8	1010.1	49940.	338912.	N.B.	66.3	0.0643
11123126	101.0	549.5	622.7	2271.4	2275.0	608.6	654.3	42.29	404.5	768.9	1008.5	49174.	338695.	N.B.	66.8	0.0685
CALIBRATION RUN NUMBER 23.3 JAN. 19																
151 71 0	29.8	476.6	499.9	2113.6	2117.8	495.4	643.9	47.53	419.2	550.3	623.1	6198.	100015.	F.C.	25.7	0.0720
15128151	49.9	513.9	551.3	2209.0	2213.3	544.1	650.3	47.20	432.4	631.0	751.0	6348.	167444.	F.C.	39.3	0.0701
15048134	79.9	531.4	589.9	2178.0	2181.4	578.7	648.2	45.42	425.0	711.6	901.4	6290.	268045.	F.C.	57.2	0.0674
15113141	101.0	551.0	622.6	2246.2	2249.1	608.8	652.6	43.19	413.4	768.0	1006.0	48181.	338831.	N.B.	67.3	0.0651
15117113	101.0	549.8	621.9	2276.5	2279.7	608.0	654.5	43.08	412.1	768.4	1007.7	49367.	338855.	N.B.	65.9	0.0674
CALIBRATION RUN NUMBER 24.1 FEB. 16																
101421 1	30.1	441.3	467.1	2255.8	2260.1	462.1	653.3	44.45	379.3	522.1	593.7	5737.	100928.	F.C.	29.0	0.0786
111 8140	50.7	492.2	533.5	2252.7	2256.3	525.5	653.1	43.97	393.3	619.5	738.6	5931.	170145.	F.C.	43.6	0.0755
11128120	70.8	512.4	568.4	2276.5	2279.6	557.6	654.6	43.55	397.9	682.6	849.7	5998.	237371.	F.C.	55.8	0.0724
121291 8	101.0	544.4	616.8	2192.3	2194.4	604.5	649.1	42.04	400.0	766.7	1003.3	46135.	338835.	N.B.	69.1	0.0667
12150111	101.0	545.9	619.7	2186.8	2189.2	605.5	648.7	42.13	401.6	767.0	1003.1	46933.	338691.	N.B.	69.8	0.0674

Appendix D

EXAMPLES OF ORTCAL -- PART II OUTPUT

Table D.1. Example of ORCAL - Part II output  
for thermocouple TE-3189G

\*\*\*\*\*  
 \*\*\* THERMOCOUPLE NUMBER: TE-3189G \*\*\*  
 \*\*\*\*\*

## NOMENCLATURE:

Q(KW)/ROD = NOMINAL POWER INPUT PER ROD IN KW  
 TCS = OBSERVED SHEATH T/C READING (DEG F)  
 TCSM = OBSERVED MIDDLE T/C READING (DEG F)  
 TCSMC = CALCULATED MIDDLE T/C READING, USING THE BEST FIT PARAMETERS (DEG F)  
 DIFFERENCE = TCSM - TCSMC

TOTAL RUNS = 31

IF THERE IS A DISCREPANCY BETWEEN THE TOTAL RUNS AND THE NUMBER OF RUNS SHOWN  
 BELOW, IT IS BECAUSE TE-3189G HAS ONLY BEEN ON THE CCDAS DURING THE FOLLOWING RUNS.

RUN NO.	DATE TIME	Q(KW)/ROD	TCS	TCSM	TCSMC	DIFFERENCE
* 1.1	*****MAY	4*				
	23:36:56	30.3	477.4	566.2	565.7	0.51
	23:44:18	40.1	495.4	613.1	612.0	1.09
	23:53:20	40.5	494.8	613.7	612.7	1.03
	0:29: 6	50.7	520.1	569.8	567.8	1.95
* 1.2	*****MAY	5*				
	14:31:56	40.7	402.5	522.9	521.4	1.48
	14:50:53	50.7	467.3	616.7	615.2	1.53
	15:39:21	50.6	516.1	663.5	663.4	0.07
	15:56:45	60.9	540.3	719.2	717.7	1.46
	16:18: 7	71.2	557.2	765.3	764.9	0.44
	16:50:43	81.2	584.5	820.9	821.7	-0.71
	17:13:10	91.6	606.7	875.7	874.8	0.93
* 1.3	*****MAY	5*				
	19:21:26	102.2	627.9	927.7	927.9	-0.21
	19:53:59	112.1	644.7	970.4	974.2	-3.76
	20:22:51	124.5	675.6	1037.6	1043.1	-5.51
	21: 4:15	124.6	715.7	1075.0	1084.1	-9.06
* 1.4	*****MAY	6*				
	12:35:24	91.6	494.5	757.1	762.7	-5.62
	12:57:41	91.5	456.6	757.6	764.5	-6.96
	13:35:46	91.4	507.2	769.1	774.6	-5.52
	13:46:44	91.3	522.3	783.4	789.5	-6.10
* 2.1	*****MAY	19*				
	4: 6: 2	30.6	474.7	560.9	563.8	-2.88
	4:28:22	41.0	456.9	613.4	616.1	-2.65
	5: 8:30	51.1	518.3	663.2	667.1	-3.88
	5:37:54	61.4	540.3	714.0	719.1	-5.09
	5: 0: 0	71.5	559.1	763.8	767.7	-3.85
	6:45:11	81.9	580.5	814.9	819.8	-4.91
	7: 5:50	91.8	600.6	864.9	869.2	-4.33
	7:35:54	102.0	623.3	918.3	922.6	-4.25
	8:37: 4	112.1	644.9	971.0	974.5	-3.50
* 2.2	*****MAY	19*				
	22:42:55	30.7	474.6	562.9	564.0	-1.13
	23:10:47	40.9	457.3	614.1	616.5	-2.43
	23:32:51	51.1	519.8	665.7	668.7	-3.03
	23:57:45	61.3	540.6	716.0	719.3	-3.37
	0:31: 6	71.5	562.2	766.1	770.8	-4.67
	0:55:49	81.8	582.8	817.6	821.7	-4.05
	1:23: 3	91.9	603.3	867.7	872.3	-4.60
	2:30:44	102.2	624.0	920.7	923.9	-3.14
	2:55:20	112.3	643.6	970.4	973.9	-3.48
	3:18:32	124.3	665.4	1027.1	1032.0	-4.83
	4:35:52	124.2	712.2	1072.6	1079.2	-6.58
	7: 5:39	124.4	755.9	1117.5	1124.2	-6.72

Table D.1. (continued)

RUN NO.	DATE TIME	Q(KW)/ROD	TCS	TCSM	TCSMC	DIFFERENCE
	7:51:40	124.6	789.4	1149.0	1159.0	-10.05
	8:18:29	112.2	773.8	1099.0	1105.4	-6.40
	8:41: 8	102.3	759.1	1054.4	1060.6	-6.16
	9:19:59	92.0	743.4	1006.1	1013.9	-7.79
	9:43:39	81.9	724.4	958.7	964.5	-5.74
	10: 7:36	71.5	703.5	907.6	912.6	-4.94
	10:31:29	61.3	683.3	856.9	862.1	-5.14
	10:55:49	50.5	660.1	802.5	807.1	-4.66
	11:19:26	40.7	639.0	753.5	757.3	-3.73
	11:44:10	30.3	615.1	699.8	703.0	-3.21
* 3.1 *****MAY	27*					
	1:14:13	30.7	478.6	585.5	588.0	-2.51
	1:36: 0	40.9	498.5	615.3	617.6	-2.29
	2: 2:32	51.1	524.1	669.6	673.0	-3.40
	2:23:56	61.4	545.5	720.7	724.5	-3.78
	2:45:31	71.6	567.9	771.9	776.7	-4.86
	3:11:21	81.8	589.8	824.2	828.9	-4.76
	3:32:41	92.0	609.3	874.7	878.6	-3.90
	4: 1:10	102.0	629.6	925.1	928.8	-3.70
	4:25:28	112.3	651.5	976.8	981.8	-4.93
	4:48:45	124.5	678.9	1038.9	1046.4	-7.57
	5:17: 6	124.4	724.5	1082.7	1092.4	-9.68
	6:22:58	124.4	797.9	1156.7	1167.3	-10.60
	6:49:48	111.9	782.5	1106.0	1113.6	-7.58
	7:31:58	101.9	766.9	1061.1	1067.3	-6.24
	8: 0:56	91.8	750.1	1013.2	1019.9	-6.74
	8:23:50	81.7	730.6	962.9	970.1	-7.15
	8:46:21	71.4	711.4	913.7	920.3	-6.62
	9: 5:52	61.4	689.9	863.2	869.9	-5.69
	9:42: 8	51.0	668.7	811.2	817.2	-6.04
	10: 4:17	40.8	645.8	759.7	764.4	-4.65
	10:26:10	30.7	623.8	707.9	713.0	-5.11
* 4.1 *****JUNE	17*					
	13:41: 8	30.7	478.4	566.7	567.9	-1.18
	14:36:24	61.3	646.8	825.6	825.5	0.07
	15: 7:57	92.0	735.8	1004.5	1006.3	0.22
* 4.2 *****JUNE	18*					
	9:12:26	30.7	476.5	563.4	565.8	-2.41
	9:53:33	61.4	598.6	775.4	777.6	-2.22
	10:27:42	92.1	705.0	973.4	975.4	-1.93
	11: 5:15	112.3	773.7	1100.7	1105.7	-4.99
	11:40:33	124.3	793.7	1155.2	1162.6	-7.47
* 5.1 *****JULY	8*					
	9:51:54	30.8	491.2	580.0	580.7	-0.72
	10:41:25	61.3	580.5	756.5	759.1	-2.60
	11:35:17	92.0	677.0	947.9	946.6	1.30
	11:41: 1	91.9	679.4	948.5	948.8	-0.30
	13:10: 5	124.3	817.2	1180.0	1186.6	-6.60
* 6.1 *****AUG.	4*					
	9:59:10	30.8	482.0	572.9	571.5	1.39
	11: 5: 4	62.0	653.0	833.3	833.9	-0.64
	11:39:36	91.9	717.9	990.8	987.6	3.19
	12:13:36	124.2	814.6	1179.9	1183.7	-3.81
	13:19: 7	124.1	815.4	1178.7	1184.2	-5.52
* 7.1 *****AUG.	19*					
	16:44:27	30.6	484.5	574.5	573.6	0.94
	17:55:35	51.0	610.2	760.3	758.6	1.64
	19: 2:42	101.4	772.5	1075.7	1071.5	4.22
	20: 6:22	124.5	811.0	1178.6	1180.9	-2.38
* 8.3 *****NOV.	5*					
	13:41:33	31.5	499.6	592.8	591.1	1.69
	14: 9: 0	52.5	541.8	697.6	694.7	2.90
	14:29:59	73.9	590.9	811.3	806.7	4.65
	14:49:41	84.0	613.2	864.6	858.9	5.72

Table D.1. (continued)

RUN NO.	DATE	Q(KW)/ROD	TCS	TCSM	TCSMC	DIFFERENCE
14:53:35		95.0	636.6	922.1	915.0	7.11
15: 9:45		105.4	655.3	973.5	965.9	7.59
15:44:12		104.6	765.3	1080.3	1075.0	5.26
16: 5: 0		109.1	780.0	1108.0	1102.5	5.48
16:18:35		113.8	786.9	1127.8	1123.7	4.06
17: 5: 4		124.3	810.1	1178.3	1179.3	-1.08
* 9.1 *****NOV. 18*						
12:31:18		30.6	497.0	585.0	586.0	-1.02
13:29:59		31.1	494.6	584.6	585.2	-0.54
13:52:35		51.5	548.1	697.1	698.1	-1.03
14:16:33		71.4	591.3	758.6	799.6	-1.04
14:38:36		81.5	614.1	852.5	852.3	0.17
14:47:35		91.6	638.4	908.8	905.9	1.93
15: 2:29		102.0	660.0	963.1	959.5	3.64
15:21:34		101.6	708.5	1010.4	1007.3	3.06
15:38:27		101.4	749.5	1049.9	1048.1	1.84
15:53:39		101.2	782.8	1082.0	1081.5	0.46
*10.1 *****DEC. 8*						
11:25:18		31.3	502.3	592.2	593.4	-1.26
11:47:24		41.5	538.7	659.5	659.4	0.14
12: 9:36		61.6	579.1	758.8	753.5	0.12
12:39: 8		82.1	631.4	873.0	871.4	1.58
13:27: 2		81.7	738.4	981.2	975.0	3.15
13:32:52		81.6	747.7	990.3	987.2	3.15
13:43:15		81.5	755.2	997.2	994.5	2.60
13:46: 3		81.5	758.6	1000.8	998.0	2.88
13:52:47		81.5	753.4	1004.8	1002.7	2.07
*11.1 *****JAN. 13*						
13:49:36		30.8	515.1	603.7	604.6	-0.93
14:12:27		51.3	560.2	709.6	709.5	0.08
14:34:40		81.7	629.5	870.2	868.6	1.63
14:53:30		81.5	666.8	907.3	905.2	2.13
15:17: 6		81.1	708.5	949.0	946.0	3.01
15:27:52		81.0	726.8	966.6	964.2	2.40
15:36:42		80.9	741.1	980.7	978.5	2.29
*12.1 *****JAN. 27*						
11:20:34		30.7	489.9	580.7	579.3	1.42
11:44:22		51.0	549.2	699.4	697.6	1.84
12: 8:16		81.6	614.9	856.2	853.5	2.78
12:33: 5		81.6	669.0	911.0	907.7	3.34
12:55:52		81.2	727.2	969.3	965.2	4.14
13: 9:19		81.8	743.5	987.4	983.4	3.95
*13.1 *****FEB. 10*						
10:33:25		30.8	458.2	589.7	587.8	1.92
10:54: 5		51.4	556.4	709.9	705.9	4.02
11:14: 1		61.0	584.5	766.6	762.2	4.44
11:25:44		71.3	617.8	831.3	826.0	5.35
11:40:22		81.7	649.9	895.2	888.9	6.34
12:15:12		81.3	703.5	948.6	941.5	7.07
13:47: 8		81.6	769.7	1012.4	1009.3	3.14
*14.1 *****MAR. 9*						
11:17:50		30.9	519.2	607.5	609.1	-1.59
11:40: 0		51.2	569.7	718.9	718.5	0.43
12: 2:29		81.7	648.2	891.0	887.0	4.01
12:25: 4		81.4	679.4	921.9	917.7	4.25
12:49:10		81.1	717.6	959.6	955.3	4.24
13:16:51		81.0	761.2	1004.1	998.9	5.19
13:34:23		81.5	765.8	1007.3	1005.1	2.24
*15.1 *****MAR. 23*						
10:32: 1		30.6	485.2	574.5	574.4	0.14
10:58:54		51.2	533.6	683.3	682.7	0.54
11:40: 2		91.5	670.8	911.1	909.2	1.96
12:21:39		101.9	762.2	1064.9	1062.7	2.23
13: 8:45		101.6	767.9	1069.4	1068.5	0.85



Table D.1. (continued)

RUN NO.	DATE		TCS	TCSM	TCSMC	DIFFERENCE
	TIME	Q(KW)/ROD				
*16.1	*****	APR. 27*				
	12:28:55	30.7	508.0	595.6	597.2	-1.65
	12:55:12	51.2	554.8	703.8	703.8	-0.05
	13:21:11	87.8	635.1	896.4	891.9	4.45
	14:01:52	102.0	725.0	1031.7	1025.1	6.64
	14:42:58	101.8	765.0	1071.9	1068.1	3.79
*17.1	*****	MAY 26*				
	11:23:05	30.7	515.6	603.7	604.9	-1.27
	11:45:13	51.1	564.2	711.1	712.8	-1.77
	12:01:15	81.4	674.3	939.2	936.2	2.95
	12:35:46	101.8	762.7	1089.5	1063.0	6.48
	12:52:17	101.8	751.4	1095.8	1092.0	3.74
	13:10:40	101.7	802.9	1101.2	1103.5	-2.25
	13:13:25	101.8	802.5	1100.8	1103.1	-2.26
*18.1	*****	JUNE 15*				
	15:53:51	30.6	515.6	604.7	604.5	0.18
	17:17:18	51.0	613.9	763.7	762.3	1.43
	17:36:32	81.7	723.7	969.1	963.3	5.84
	17:54:39	81.5	751.0	996.1	990.1	6.00
	18:07:50	81.8	750.9	996.1	989.9	6.18
*19.1	*****	JUNE 29*				
	12:01:50	30.6	511.0	601.2	599.9	1.33
	12:31:55	51.0	610.4	760.5	758.8	1.65
	13:01:26	81.7	659.0	944.3	938.2	6.10
	13:31:46	101.8	786.1	1092.5	1086.5	6.04
	13:40:39	101.8	790.4	1095.9	1091.0	4.90
*20.1	*****	AUG. 22*				
	11:41:52	30.5	538.3	624.6	626.9	-2.28
	12:01:46	51.9	606.7	753.6	757.8	-4.19
	12:35:35	81.6	715.7	954.4	954.7	-0.30
	13:01:53	101.8	776.1	1075.1	1076.5	-1.37
	13:21:45	101.8	776.8	1075.4	1077.1	-1.74
*21.1	*****	SEP. 21*				
	11:49:40	30.9	536.0	627.7	625.7	1.98
	12:10:45	51.4	617.0	769.8	766.6	3.17
	12:43:39	71.9	716.6	953.1	927.1	6.02
	13:20:14	91.8	778.4	1054.0	1048.8	5.25
	13:22:06	91.8	778.6	1054.2	1048.9	5.28
*22.1	*****	OCT. 12*				
	11:48:40	31.1	531.1	625.6	621.3	4.33
	12:17:55	80.7	650.0	933.1	926.2	6.92
	12:29:23	101.9	758.9	1066.0	1059.3	6.64
	12:50:23	102.0	795.6	1103.8	1096.8	7.03
	13:01:25	102.0	797.5	1104.9	1098.8	6.05
*23.1	*****	NOV. 30*				
	11:22:07	31.1	517.1	605.7	607.6	1.90
	11:41:15	51.8	582.6	735.4	733.4	2.00
	11:58:35	72.4	664.6	879.1	876.2	2.85
	12:19:17	101.9	767.9	1072.3	1068.3	4.05
	12:38:44	101.7	796.2	1100.8	1096.7	4.10
	12:44:28	101.7	797.0	1101.3	1097.5	3.82
*23.2	*****	DEC. 15*				
	10:01:18	31.0	520.4	615.5	610.4	5.10
	10:27:17	61.5	634.2	819.3	813.5	5.83
	10:39:04	61.6	645.1	830.4	824.5	5.89
	11:09:20	102.1	788.0	1095.9	1089.6	6.30
	11:16:15	102.2	795.2	1103.4	1097.0	6.42
	11:23:26	102.1	795.8	1103.6	1097.5	6.08
*23.3	*****	JAN. 19*				
	15:07:00	31.0	565.6	656.9	655.5	1.40
	15:28:51	51.9	650.5	804.7	801.6	3.15
	15:48:34	82.4	736.5	983.4	978.2	5.22
	16:13:41	101.8	794.8	1100.0	1095.5	4.54
	16:17:13	101.9	794.8	1100.1	1095.9	4.27

Table D.1. (continued)

RUN NO.	DATE	Q(K*)/500	TCS	TCSM	TCSMC	DIFFERENCE
TIME						
*24.1	*****FEB. 16*					
10:42:1		30.5	529.9	621.3	618.4	2.95
11: 6:40		51.2	629.9	782.0	779.8	3.23
11:28:20		72.1	697.2	913.2	908.0	5.23
12:29: 8		102.0	789.0	1097.6	1090.3	7.27
12:30:11		102.0	790.2	1098.6	1091.5	7.13

BEST FIT PARAMETERS FOR AKRN:

WHERE:

$$AKRN = C(1) + C(2)*T + C(3)*T**2 + C(4)*T**3$$

$$C(1) = 0.21976151E-02$$

$$C(2) = -0.74225366E-02$$

$$C(3) = -0.73717558E-07$$

$$C(4) = 0.59715699E-09$$

TOTAL ERROR (SUM OF SQUARED DIFFERENCES) = 0.38925518E 04

VARIANCE OF FIT = 0.18624649E 02

Table D.2. Example of ORTCAL - Part II output  
for thermocouple TE-301DJ

\*\*\*\*\*  
 \*\*\* THERMOCOUPLE NUMBER: TE-301DJ \*\*\*  
 \*\*\*\*\*

## NOMENCLATURE:

Q(KW)/ROD = NOMINAL POWER INPUT PER ROD IN KW  
 TCS = OBSERVED SHEATH T/C READING (DEG F)  
 TCSM = OBSERVED MIDDLE T/C READING (DEG F)  
 TCSMC = CALCULATED MIDDLE T/C READING, USING THE BEST FIT PARAMETERS (DEG F)  
 DIFFERENCE = TCSM - TCSMC

TOTAL RUNS = 32

IF THERE IS A DISCREPANCY BETWEEN THE TOTAL RUNS AND THE NUMBER OF RUNS SHOWN  
 BELOW, IT IS BECAUSE TE-301DJ HAS ONLY BEEN ON THE CCDAS DURING THE FOLLOWING RUNS.

RUN NO.	DATE TIME	Q(KW)/ROD	TCS	TCSM	TCSMC	DIFFERENCE
* 1.1	*****MAY	4*				
	23:36:56	30.0	465.3	538.0	538.4	-0.32
	23:44:19	39.7	481.0	577.0	577.3	-0.28
	23:53:20	40.2	480.4	577.4	578.0	-0.60
	0:29: 6	50.1	503.4	623.4	624.8	-1.45
* 1.2	*****MAY	5*				
	14:31:56	40.3	390.5	486.1	489.2	-3.06
	14:50:53	50.2	450.8	571.5	573.0	-1.48
	15:39:21	50.0	501.2	622.2	622.5	-0.33
	15:56:45	60.3	524.2	670.7	670.1	0.68
	16:18: 7	70.2	540.0	710.0	709.7	0.32
	16:50:43	80.0	571.7	765.5	765.0	0.49
	17:13:10	90.3	598.7	820.2	816.5	3.64
* 1.3	*****MAY	5*				
	19:21:26	100.6	635.5	882.1	878.1	3.97
	19:53:59	110.2	666.2	933.2	931.7	1.49
	20:22:51	122.3	716.9	1007.1	1011.2	-4.11
	21: 4:19	122.4	752.1	1042.5	1046.4	-3.95
* 1.4	*****MAY	6*				
	12:35:24	90.4	498.1	712.8	717.4	-4.59
	12:57:41	90.3	498.3	712.9	717.4	-4.46
	13:35:46	90.3	509.3	724.8	728.1	-3.28
	13:48:44	90.1	522.8	739.1	741.1	-2.02
* 2.1	*****MAY	19*				
	4: 6: 2	30.0	464.5	536.5	537.4	-0.86
	4:28:22	40.1	485.2	580.9	582.6	-1.72
	5: 8:30	50.2	504.6	624.1	626.3	-2.26
	5:37:54	60.4	525.3	668.3	671.5	-3.19
	6: 0: 0	70.4	545.0	711.2	715.3	-4.12
	6:49:11	80.5	564.4	753.5	758.9	-5.45
	7: 5:50	90.4	587.3	800.2	805.5	-5.31
	7:35:54	100.2	616.9	855.9	858.5	-2.59
	8:37: 4	110.2	660.0	924.8	925.6	-0.83
* 2.2	*****MAY	19*				
	22:42:55	30.1	465.5	539.2	539.2	0.02
	23:10:47	40.1	486.9	583.4	584.3	-0.88
	23:32:51	50.3	507.7	628.2	629.5	-1.31
	23:57:45	60.3	527.6	672.5	673.6	-1.17
	0:11: 6	70.2	548.2	715.3	717.9	-2.63
	0:55:49	80.4	569.6	761.1	763.9	-2.78
	1:23: 3	90.2	590.6	805.1	808.4	-3.32
	2:30:44	100.3	613.8	852.6	855.9	-3.35
	3:55:20	110.3	637.2	900.5	903.2	-2.76
	3:18:32	122.3	666.4	959.3	961.0	-1.71
	4:35:52	122.2	713.2	1009.6	1007.3	2.24
	7: 5:39	122.5	743.5	1027.1	1038.2	-11.08
	8:41: 8	100.3	738.4	968.8	979.5	-10.76

Table D.2. (continued)

RUN NO.	DATE TIME	Q(KW)/ROD	TCS	TCSM	TCSMC	DIFFERENCE
	9:19:35	90.0	725.2	934.5	941.6	-7.11
	9:43:35	80.1	711.8	701.1	904.4	-3.28
	10: 7:26	70.2	667.0	817.6	865.7	1.95
	10:31:27	60.2	691.2	831.4	925.9	5.49
	10:55:49	40.7	660.8	785.4	780.3	5.08
	11:19:26	40.1	629.7	740.0	735.2	3.84
	11:44:10	29.8	614.9	689.0	685.6	2.42
* 3.1 *****MAY	27*					
	1:14:13	30.2	467.3	540.8	647.8	-0.04
	1:36: 0	40.2	485.5	582.7	583.0	-3.27
	2: 2:32	50.3	505.3	629.6	631.0	-1.42
	2:23:55	60.3	525.8	673.2	675.8	-2.59
	2:45:31	70.5	550.4	717.6	720.9	-3.24
	3:11:21	80.4	572.0	763.0	765.3	-3.25
	3:32:41	90.4	594.8	810.1	813.0	-2.89
	4: 1:10	100.2	623.8	864.7	865.5	-0.82
	4:25:29	110.5	656.3	922.9	922.5	0.25
	4:48:45	120.3	694.7	994.1	999.2	4.86
	5:17: 8	122.2	747.1	1043.5	1041.2	2.40
	5:22:58	122.3	815.9	1118.9	1109.7	9.19
	6:49:49	110.2	802.2	1075.4	1066.3	9.57
	7:31:58	100.1	785.3	1038.1	1029.6	8.51
	8: 0:55	90.2	774.5	999.2	991.0	8.15
	8:23:50	80.2	753.1	953.2	945.7	7.58
	8:46:21	70.1	716.3	887.6	884.8	2.84
	9: 9:52	60.4	690.4	837.3	835.5	1.77
	9:42: 8	50.1	670.6	796.2	791.1	5.11
	10: 4:17	40.2	648.2	747.7	744.8	2.89
	10:26:10	30.2	623.1	698.2	695.0	2.21
* 4.1 *****JUNE	17*					
	13:41: 8	30.2	489.5	544.0	542.9	1.12
	14:36:24	60.5	540.0	789.2	785.7	3.40
	15: 7:57	90.8	720.7	937.3	934.5	-1.25
* 4.2 *****JUNE	18*					
	9:12:24	30.3	489.7	544.1	543.3	0.72
	9:53:33	50.3	501.9	738.0	737.3	0.72
	10:27:42	90.3	668.7	920.4	915.9	4.51
	11: 5:15	100.9	742.0	966.0	1006.3	-10.23
* 5.1 *****JULY	8*					
	9:51:54	30.2	474.5	549.8	547.3	1.99
	10:41:25	60.3	558.0	703.5	703.8	-0.19
	11:35:17	90.4	651.1	867.0	868.8	-1.73
	11:41: 1	90.3	652.0	868.1	869.5	-1.36
	13:10: 5	122.1	769.5	1055.6	1063.2	-7.55
* 5.1 *****AUG.	4*					
	9:55:10	30.2	468.0	543.1	541.4	1.56
	11: 5: 4	60.6	622.2	779.7	778.8	0.90
	11:39:36	90.3	693.0	912.6	910.1	2.49
	12:13:36	122.3	777.0	1080.3	1071.2	9.09
	13:19: 7	122.0	780.7	1083.3	1074.1	9.16
* 7.1 *****AUG.	19*					
	16:44:27	30.5	470.5	546.5	544.6	1.91
	17:55:35	50.1	591.5	714.3	712.3	1.96
	19: 2:42	100.5	735.0	973.5	976.6	-3.07
	20: 6:22	122.4	762.0	1048.4	1056.4	-8.02
* 8.2 *****OCT.	9*					
	2:33:52	30.3	468.3	544.9	542.0	2.96
	2:57:41	50.5	564.0	688.4	686.0	2.35
	3:21:26	70.7	650.4	823.5	820.5	2.99
* 8.3 *****NOV.	5*					
	13:41:33	30.3	485.4	562.0	559.9	3.14
	14: 9: 0	50.5	523.4	647.7	645.6	2.14
	14:29:59	71.3	569.2	743.5	741.4	2.11

Table D.2. (continued)

RUN NO.	DATE		TCS	TCSM	TCSMC	DIFFERENCE
	TIME	Q(KW)/ROD				
	14:49:41	81.2	591.1	787.5	787.0	0.44
	14:53:35	91.7	612.5	834.1	833.7	0.40
	15: 0:45	101.7	630.0	875.3	875.2	0.14
	15: 4:12	101.0	733.8	977.7	976.7	0.96
	16: 5: 2	105.3	743.2	956.2	955.5	-0.26
	16:18:38	109.0	747.2	1009.3	1011.3	-2.07
	17: 5: 4	122.8	763.6	1053.0	1053.9	-5.91
* 9.1 *****NOV. 18*						
	12:31:16	30.5	482.8	561.2	559.8	4.39
	13:29:59	30.4	478.1	587.2	582.0	5.12
	13:32:35	50.4	526.5	653.0	648.5	5.39
	14:16:23	71.3	569.7	746.9	741.9	4.96
	14:38:36	81.1	590.9	791.1	786.7	4.45
	14:47:36	90.7	614.4	807.4	833.2	4.19
	15: 2:29	100.4	634.0	879.5	876.1	3.39
	15:21:34	100.1	680.9	926.1	921.8	4.35
	15:38:27	99.8	722.3	971.1	962.3	8.77
	15:53:35	99.6	743.5	986.9	983.0	3.97
*10.1 *****DEC. 8*						
	11:25:18	30.2	492.0	567.3	566.1	1.15
	11:47:28	43.6	530.6	629.8	628.8	3.93
	12: 4:36	60.6	570.8	717.9	717.2	0.74
	12:39: 8	80.6	622.9	817.7	817.1	0.58
	13:27: 2	80.6	722.6	919.4	916.2	3.17
	13:32:52	80.6	729.0	925.2	922.5	2.63
	13:53:15	80.5	734.9	930.7	928.3	2.46
	13:46: 3	80.5	736.5	931.9	929.9	1.94
	13:52:47	80.5	737.0	931.9	930.4	1.50
*11.1 *****JAN. 13*						
	13:49:36	30.4	504.0	577.2	577.6	-0.44
	14:12:27	50.6	546.9	668.0	669.3	-1.30
	14:34:40	80.8	613.4	806.0	804.2	-2.12
	14:53:00	80.4	650.4	841.9	843.0	-2.16
	15:17: 5	80.1	691.3	882.5	883.8	-1.36
	15:27:52	79.9	709.3	900.4	901.4	-0.98
	15:36:42	79.9	722.8	914.3	914.7	-0.40
*12.1 *****JAN. 27*						
	11:20:34	30.1	473.9	552.0	547.2	4.80
	11:44:22	50.5	527.8	655.8	647.9	5.84
	12: 8:16	81.6	591.1	753.6	787.9	5.53
	12:33: 5	81.6	646.1	848.2	842.6	5.54
	12:59:52	81.4	704.9	906.2	900.5	5.68
	13: 9:19	80.5	718.0	917.9	911.5	6.36
*13.1 *****FEB. 10*						
	10:33:25	30.4	486.4	564.1	560.3	3.81
	10:54: 5	50.7	541.9	670.0	664.5	5.58
	11:14: 1	60.4	569.6	721.0	715.4	5.54
	11:25:44	70.4	601.8	777.8	771.6	6.14
	11:40:22	80.8	633.3	834.0	828.0	6.00
	12:15:12	80.4	687.1	887.0	880.6	6.43
	13:47: 9	80.7	736.0	935.1	932.7	2.35
*14.1 *****MAR. 9*						
	11:17:50	30.4	505.6	580.0	579.2	0.80
	11:40: 0	50.7	554.1	678.5	676.6	1.92
	12: 2:29	80.8	631.4	828.0	826.1	1.90
	12:25: 4	80.6	662.0	857.6	855.9	1.75
	12:49:10	80.3	699.2	894.6	892.3	2.29
	13:18:51	80.2	735.7	930.7	928.3	2.49
	13:34:23	80.2	738.2	933.4	931.9	1.49
*15.1 *****MAR. 23*						
	10:32: 1	30.4	468.7	547.0	542.6	4.38
	10:55:54	50.6	510.9	638.5	633.4	5.05
	11:40: 2	80.9	642.4	842.9	837.2	5.69
	12:21:39	100.9	729.8	960.1	972.5	7.60
	13: 8:45	100.8	734.9	983.4	977.3	6.06

Table D.2. (continued)

RUN NO.	DATE	Q(KW)/ROD	TCS	TCSM	TCSMC	DIFFERENCE
TIME						
*16.1	*****APR. 27*					
12:28:55		30.5	456.5	569.8	570.4	-0.63
12:55:12		50.7	640.5	663.2	663.2	-0.02
13:21:11		81.0	605.3	602.6	603.7	1.83
14: 0:52		101.1	704.3	950.5	947.5	3.01
14:42:59		101.0	742.1	757.8	984.7	3.11
*17.1	*****MAY 26*					
11:23: 5		30.3	502.6	575.7	576.0	-0.26
11:45:13		50.7	549.7	689.8	671.3	-1.54
12: 9:15		84.5	653.4	865.1	865.6	-1.52
12:35:46		100.9	742.1	984.7	984.7	-0.02
12:52:17		100.8	763.1	1001.3	1005.3	-3.93
13:10:40		100.8	758.0	1003.4	1011.1	-7.73
13:13:25		100.8	768.2	1002.7	1010.4	-7.69
*18.1	*****JUNE 15*					
16:53:51		30.4	453.4	574.7	572.2	2.50
17:17:18		50.6	592.3	716.5	714.5	2.01
17:36:32		80.9	694.6	891.0	889.0	1.93
17:54:39		80.9	720.5	917.0	915.0	2.07
18: 7:50		80.9	720.7	917.5	915.0	2.44
*19.1	*****JUNE 29*					
12: 8:50		30.5	494.6	570.9	568.6	2.23
12:31:59		50.7	587.7	712.3	710.0	2.30
13: 6:26		80.8	671.3	867.7	865.7	1.98
13:31:46		100.9	753.4	958.8	958.8	2.99
13:40:39		100.9	756.2	1000.6	998.6	1.93
*20.1	*****AUG. 22*					
11:41:52		30.4	526.0	596.1	599.5	-3.44
12: 5:46		50.4	586.5	701.7	708.0	-6.28
12:35:35		80.5	691.1	876.6	884.6	-8.00
13: 1:53		100.9	748.3	983.3	990.9	-7.56
13:21:45		100.9	748.9	983.4	991.1	-7.69
*21.1	*****SEP. 21*					
11:49:40		30.5	521.7	595.0	595.4	-0.47
12:10:45		50.0	598.4	716.8	713.9	-2.09
12:43:59		69.9	694.5	859.5	862.5	-2.97
15:20:14		90.9	756.1	971.4	974.3	-2.88
15:22: 5		90.9	756.4	971.3	974.5	-3.22
*22.1	*****OCT. 12*					
11:48:40		30.1	516.0	591.9	583.8	3.10
12:17:55		77.6	664.8	851.3	851.4	-0.11
12:29:23		101.2	738.5	980.6	981.7	-1.12
12:50:23		101.1	771.0	1011.7	1013.9	-2.19
13: 0:25		101.1	771.4	1011.5	1014.4	-2.89
*23.1	*****NOV. 30*					
11:22: 7		29.9	502.0	575.7	574.6	1.12
11:41:15		50.2	564.0	684.5	685.1	-0.59
11:58:35		70.4	643.7	811.8	813.2	-1.43
12:19:17		101.0	747.2	987.8	990.0	-2.18
12:38:44		100.9	770.4	1009.3	1012.7	-3.45
12:44:28		100.9	770.5	1009.3	1012.9	-3.63
*23.2	*****DEC. 15*					
10: 5:18		29.9	505.9	581.2	578.5	2.74
10:27:17		60.8	617.2	763.7	763.7	-0.03
10:39: 4		60.8	627.5	774.1	773.8	0.33
11: 9:20		101.1	764.6	1005.9	1007.4	-1.44
11:16:15		101.0	769.8	1010.1	1012.5	-2.45
11:23:26		101.0	768.9	1008.5	1011.4	-2.87
*23.3	*****JAN. 19*					
15: 7: 0		29.8	550.3	623.1	622.4	0.73
15:28:31		49.9	631.0	751.0	751.2	-0.21
15:46:34		79.9	711.6	901.4	903.7	-2.24
16:13:41		101.0	768.0	1006.0	1010.7	-4.70
16:17:13		101.0	768.4	1007.7	1011.1	-3.37

Table D.2. (continued)

RUN NO.	DATE	Q(KW)/ROD	TCS	TCSM	TCSMC	DIFFERENCE
TIME						
*24.1	*****FEB.	18*				
10:42:1		30.1	522.1	593.7	595.0	-1.30
11: 8:40		53.7	619.5	738.9	741.7	-2.91
11:28:20		70.8	682.6	849.7	852.8	-3.09
12:29: 8		101.0	766.7	1003.3	1009.4	-6.05
12:50:11		101.0	767.0	1003.1	1009.6	-6.55

BEST FIT PARAMETERS FOR AKBN:

WHERE,

$$AKBN = C(1) + C(2)*T + C(3)*T**2 + C(4)*T**3$$

$$C(1) = 0.20594376E-02$$

$$C(2) = -0.71305782E-02$$

$$C(3) = 0.11995689E-05$$

$$C(4) = 0.19595139E-09$$

TOTAL ERROR (SUM OF SQUARED DIFFERENCES) = 0.32816289E-04

VARIANCE OF FIT = 0.15701573E-02

Table D.3. Example of ORICAL - Part II output  
for thermocouple TE-322BF

\*\*\*\*\*  
 \*\*\* THERMOCOUPLE NUMBER: TE-322BF \*\*\*  
 \*\*\*\*\*

## NOMENCLATURE:

Q(KW)/ROD = NOMINAL POWER INPUT PER ROD IN KW  
 TCS = OBSERVED SHEATH T/C READING (DEG F)  
 TCSM = OBSERVED MIDDLE T/C READING (DEG F)  
 TCSMC = CALCULATED MIDDLE T/C READING, USING THE BEST FIT PARAMETERS (DEG F)  
 DIFFERENCE = TCSM - TCSMC

TOTAL RUNS = 32

IF THERE IS A DISCREPANCY BETWEEN THE TOTAL RUNS AND THE NUMBER OF RUNS SHOWN  
 BELOW, IT IS BECAUSE TE-322BF HAS ONLY BEEN ON THE CCDAS DURING THE FOLLOWING RUNS.

RUN NO.	DATE TIME	Q(KW)/ROD	TCS	TCSM	TCSMC	DIFFERENCE
* 1.1	*****MAY	4*				
	23:36:56	29.7	470.2	573.6	559.6	13.95
	23:44:18	39.2	486.6	622.0	604.6	17.40
	23:53:20	39.7	486.8	623.0	606.3	16.73
	0:29: 6	49.6	509.5	678.7	658.7	19.99
* 1.2	*****MAY	5*				
	14:31:56	39.9	397.0	532.0	517.4	14.61
	14:50:53	49.7	457.4	626.4	607.1	19.32
	15:39:21	49.5	505.8	673.0	654.9	18.09
	15:56:45	59.7	527.3	728.9	706.9	21.95
	16:18: 7	69.5	540.0	772.5	749.4	23.04
	16:50:43	79.4	562.6	826.5	802.1	24.41
	17:13:10	89.5	581.4	879.9	852.0	27.93
* 1.3	*****MAY	5*				
	19:21:26	99.9	597.4	928.2	899.9	28.36
	19:53:59	109.6	609.6	959.2	941.3	27.48
	20:22:51	121.7	634.3	1030.9	1003.9	27.00
	21: 4:19	121.9	670.8	1067.5	1041.2	26.31
* 1.4	*****MAY	6*				
	12:35:24	90.1	472.9	763.9	745.5	18.37
	12:57:41	90.0	473.7	764.4	745.1	18.31
	13:35:46	90.0	485.1	776.2	757.2	19.00
	13:48:44	89.9	459.5	790.8	771.3	19.53
* 2.1	*****MAY	19*				
	4: 6: 2	29.9	468.2	568.3	558.1	10.16
	4:28:22	40.0	488.5	621.1	608.7	12.39
	5: 8:30	50.0	507.4	673.1	658.0	15.11
	5:37:54	60.2	527.2	725.2	709.5	15.70
	6: 0: 0	70.1	545.8	776.1	757.3	18.78
	6:45:11	80.3	563.5	826.1	805.8	20.26
	7: 5:50	90.1	581.2	875.7	853.3	22.35
	7:35:54	99.8	599.0	925.0	899.9	25.12
	8:37: 4	109.8	615.1	975.1	947.9	27.20
* 2.2	*****MAY	19*				
	22:42:55	30.0	468.5	569.5	558.8	10.83
	23:10:47	40.0	489.2	621.8	609.5	12.38
	23:32:51	50.1	509.1	674.7	659.8	14.90
	23:57:45	60.1	527.7	725.4	708.6	16.78
	0:31: 6	69.9	546.0	775.3	756.7	18.64
	0:55:49	80.1	564.7	827.1	806.4	20.65
	1:23: 3	89.9	581.5	875.7	853.2	22.49
	2:30:44	99.9	598.9	926.6	901.3	25.25
	2:55:20	109.9	615.8	975.9	948.9	27.00
	3:18:32	121.8	634.5	1031.7	1004.4	27.30
	4:35:52	121.7	679.9	1076.6	1050.0	26.57
	7: 5:39	122.1	725.9	1122.9	1097.6	25.27
	7:51:40	122.2	767.6	1162.7	1140.0	22.63



Table D.3. (continued)

RUN NO.	DATE TIME	QIKW/ROD	TCS	TCSM	TCSMC	DIFFERENCE
	8:15:29	110.0	749.3	1105.6	1083.5	22.02
	8:41:18	100.0	732.5	1056.5	1035.7	21.05
	9:15:55	89.7	716.3	1007.4	987.8	19.65
	9:43:35	79.8	699.9	959.8	941.1	18.69
	10:17:38	69.6	682.1	910.3	893.0	17.27
	10:51:29	63.0	664.2	860.3	844.7	15.59
	10:59:49	49.5	644.5	805.3	793.1	13.15
	11:19:16	39.9	626.6	755.3	745.4	11.33
	11:44:10	29.6	606.4	703.9	693.3	6.59
* 3.1 *****MAY	27*					
	1:14:12	30.1	472.4	573.2	563.0	10.24
	1:36:16	40.0	489.7	623.5	610.1	13.43
	2:12:32	50.1	512.9	678.5	663.5	14.86
	2:23:56	60.1	532.3	730.0	713.3	16.65
	2:45:31	70.3	550.8	781.9	752.6	19.24
	3:11:21	80.1	570.7	833.4	812.5	20.96
	3:32:41	90.1	589.2	883.2	860.4	22.85
	4:11:13	99.9	604.5	931.7	905.8	24.91
	4:28:28	110.1	621.6	982.7	955.5	27.23
	4:46:45	121.9	642.6	1040.3	1012.9	27.43
	5:17:18	121.6	664.1	1080.8	1054.4	26.41
	6:22:58	121.9	770.7	1165.9	1142.1	23.83
	6:46:46	109.8	751.7	1108.9	1085.5	23.43
	7:31:58	99.8	735.2	1059.8	1037.7	22.08
	8:10:58	89.9	720.0	1013.6	992.1	21.55
	8:25:50	80.0	703.9	964.8	945.4	19.39
	8:46:21	69.9	686.6	915.0	897.3	17.69
	9:19:52	60.2	668.9	866.0	850.0	16.04
	9:42:18	50.0	650.5	814.3	800.7	13.67
	10:14:17	40.0	631.4	763.8	751.5	12.31
	10:26:10	30.1	612.8	712.1	703.1	9.08
* 4.1 *****JUNE	17*					
	13:41:18	30.0	476.0	573.3	566.3	7.01
	14:36:24	60.2	637.9	831.6	819.3	12.35
	15:17:57	90.3	718.8	1005.7	992.0	16.64
* 4.2 *****JUNE	18*					
	9:12:28	30.2	473.8	570.1	564.6	5.55
	9:53:33	60.1	589.8	781.6	770.6	11.08
	10:27:42	90.0	687.8	975.0	959.9	15.15
	11:15:15	109.5	752.9	1113.1	1095.8	17.28
	11:40:33	121.8	780.9	1169.3	1152.1	17.21
* 5.1 *****JULY	8*					
	9:51:54	30.0	498.0	582.7	588.3	-5.57
	10:41:25	60.1	585.4	759.1	766.3	-7.19
	11:35:17	90.0	675.6	945.7	947.7	-1.99
	11:41:11	89.9	675.6	947.2	948.4	-1.28
	13:10:15	121.6	810.6	1184.0	1181.7	2.31
* 6.1 *****AUG.	4*					
	9:59:10	30.0	481.6	573.6	571.8	1.76
	11:15:14	60.0	546.0	831.7	828.3	3.42
	11:39:36	89.9	703.5	985.1	975.4	9.71
	12:13:36	121.6	800.8	1182.5	1172.4	10.12
	13:19:17	121.6	802.9	1183.0	1173.7	9.28
* 7.1 *****AUG.	19*					
	16:44:27	30.3	482.3	577.0	573.3	3.74
	17:55:35	49.8	604.3	760.0	754.1	5.95
	19:12:42	100.0	757.8	1074.6	1061.3	13.32
	20:16:22	121.9	799.9	1185.4	1171.7	13.67
* 8.2 *****OCT.	9*					
	2:33:52	30.1	480.1	573.8	570.6	3.21
	2:57:41	50.2	578.2	734.0	729.1	4.97
	3:21:26	70.3	665.2	884.6	877.0	7.56

Table D.3. (continued)

HUN NO.	DATE TIME	Q(KW)/ROD	TCS	TCSM	TCSMC	DIFFERENCE
* 8.3	***NOV.	5*				
	13:41:53	30.0	495.3	590.5	585.3	5.23
	14: 9: 0	50.1	534.6	692.3	685.4	7.48
	14:29:59	70.9	581.1	804.2	794.7	9.52
	14:49:41	80.7	601.6	856.2	845.1	11.09
	14:53:35	91.2	622.9	911.4	898.5	12.91
	15: 9:45	101.1	639.7	961.1	945.9	15.23
	15:44:12	100.5	750.6	1069.4	1055.6	13.77
	16: 5: 0	104.6	765.2	1098.3	1083.4	14.83
	16:18:35	109.3	771.9	1118.3	1104.2	14.12
	17: 5: 4	122.2	804.7	1191.1	1177.4	13.67
* 9.1	*****NOV.	18*				
	12:51:18	30.2	457.8	567.9	588.6	-0.71
	13:29:59	30.2	453.6	584.0	584.4	-0.37
	13:52:35	50.1	548.9	695.8	697.4	-1.60
	14:16:33	70.8	550.6	803.7	804.1	-0.42
	14:38:36	80.6	610.9	855.4	854.1	1.22
	14:47:36	90.2	633.5	908.7	906.1	2.63
	15: 2:29	99.8	650.8	959.3	953.1	6.19
	15:21:34	99.5	657.6	1006.6	999.1	7.52
	15:36:27	99.3	738.4	1046.3	1039.5	6.80
	15:53:39	99.1	772.2	1079.7	1073.1	6.67
*10.1	*****DEC.	8*				
	11:25:18	29.9	506.2	569.1	595.8	-6.70
	11:47:24	40.3	545.0	658.4	656.0	-2.55
	12: 9:36	60.2	583.8	767.5	764.9	-2.39
	12:39: 8	80.1	632.1	869.1	873.9	-4.78
	13:27: 2	80.1	738.4	978.9	980.5	-1.52
	13:32:52	80.1	748.4	989.3	990.6	-1.21
	13:43:16	80.0	755.8	996.1	997.8	-1.64
	13:46: 3	80.0	758.9	1000.0	1000.9	-0.87
	13:52:47	80.0	764.6	1005.2	1006.7	-1.43
*11.1	*****JAN.	13*				
	13:49:36	30.0	527.7	605.4	617.9	-12.46
	14:12:27	50.2	575.7	711.5	725.7	-15.19
	14:34:40	80.3	642.9	869.9	885.2	-15.23
	14:53:30	79.9	679.1	906.3	920.3	-13.99
	15:17: 6	79.6	720.1	947.9	960.5	-12.55
	15:27:52	79.4	738.2	966.3	978.2	-11.91
	15:36:42	79.3	752.5	980.6	992.4	-11.40
*12.1	*****JAN.	27*				
	11:20:34	29.9	503.6	581.0	593.3	-12.30
	11:44:22	50.1	566.6	699.8	717.1	-17.30
	12: 8:16	81.0	632.4	859.0	876.9	-17.92
	12:33: 5	81.0	685.2	913.2	930.0	-16.82
	12:59:52	80.8	743.6	972.6	988.0	-15.40
	13: 9:19	80.0	756.9	983.9	998.9	-14.99
*13.1	*****FEB.	10*				
	10:33:25	30.1	509.1	592.4	599.6	-7.20
	10:54: 5	50.3	569.8	712.1	720.9	-8.77
	11:14: 1	59.9	599.8	770.3	780.0	-9.76
	11:25:44	69.9	632.6	833.8	843.3	-9.48
	11:40:22	80.2	664.1	897.2	906.4	-9.21
	12:15:12	79.9	716.3	950.1	957.6	-7.44
	13:47: 8	80.1	785.7	1021.1	1028.3	-7.20
*14.1	*****MAR.	9*				
	11:17:50	30.0	529.9	605.2	620.1	-14.90
	11:40: 0	50.3	586.1	717.3	737.2	-19.86
	12: 2:29	80.3	665.6	885.3	908.0	-22.63
	12:25: 4	80.0	656.5	916.5	938.1	-21.56
	12:49:10	79.7	733.3	954.2	974.4	-20.13
	13:18:51	79.7	777.6	1000.5	1018.7	-18.10
	13:34:23	80.1	781.5	1003.7	1024.0	-20.33

Table D.3. (continued)

RUN NO.	DATE TIME	Q(KW)/RUD	TCS	TCSM	TCSHC	DIFFERENCE
*15.1	*****MAY, 23*					
	10:32:1	30.1	494.7	577.0	585.2	-8.15
	10:55:54	50.2	547.2	685.0	698.2	-13.21
	11:40:2	80.4	686.7	913.4	929.5	-16.03
	12:21:39	100.3	774.0	1005.7	1082.6	-16.87
	13: 8:45	100.2	784.2	1071.7	1088.6	-16.93
*16.1	*****APR, 27*					
	12:28:55	30.2	520.6	596.2	611.2	-15.04
	12:55:12	50.4	574.0	704.5	725.4	-20.90
	13:21:11	80.5	547.4	865.1	890.4	-25.24
	14: 0:52	100.5	749.9	1031.3	1054.0	-22.74
	14:42:58	100.4	791.8	1070.7	1095.7	-23.00
*17.1	*****MAY, 26*					
	11:23: 5	30.0	529.2	604.5	619.3	-14.81
	11:48:13	50.4	585.2	714.4	736.6	-22.19
	12: 9:15	88.0	703.5	940.5	969.7	-29.15
	12:35:46	100.3	789.5	1007.8	1094.3	-26.51
	12:52:17	100.3	819.1	1097.5	1123.9	-26.35
	13:10:40	100.2	834.7	1111.6	1139.6	-28.03
	13:13:25	100.2	834.2	1111.3	1139.1	-27.71
*18.1	*****JUNE, 15*					
	16:53:51	30.1	529.3	606.4	619.7	-13.31
	17:17:18	50.2	533.4	765.2	784.3	-19.19
	17:35:32	80.3	748.1	967.3	990.9	-23.59
	17:54:39	80.4	775.4	996.9	1018.8	-21.90
	18: 7:50	80.4	775.7	997.3	1018.8	-21.59
*19.1	*****JUNE, 29*					
	12: 8:50	30.2	527.8	605.9	618.5	-12.60
	12:31:59	50.3	531.7	764.3	782.8	-18.45
	13: 6:26	80.3	726.9	945.8	969.5	-23.69
	13:31:46	100.3	817.2	1096.3	1122.2	-25.85
	13:40:39	100.3	821.3	1100.4	1126.3	-25.88
*20.1	*****AUG., 22*					
	11:41:52	30.0	552.9	625.9	643.0	-17.11
	12: 5:46	49.9	626.1	749.9	775.9	-26.05
	12:35:35	79.9	743.3	952.6	984.7	-32.04
	13: 1:53	100.3	808.2	1077.1	1113.1	-35.98
	13:21:45	100.2	809.2	1078.4	1113.9	-35.47
*21.1	*****SEP., 21*					
	11:49:40	30.2	545.0	625.1	635.6	-10.50
	12:10:45	49.6	629.9	762.3	778.9	-16.62
	12:43:59	69.4	733.0	922.2	942.5	-20.34
	15:20:14	90.3	802.2	1051.7	1076.0	-24.31
	15:22: 6	90.2	803.1	1052.1	1076.8	-24.74
*22.1	*****OCT., 12*					
	11:48:40	29.8	545.8	622.9	635.1	-12.14
	12:17:55	77.0	716.0	921.4	948.6	-27.23
	12:29:23	100.6	794.2	1068.8	1099.8	-31.03
	12:50:23	100.5	830.6	1106.8	1136.2	-29.48
	13: 0:25	100.5	832.4	1108.0	1138.1	-30.03
*23.1	*****NOV., 30*					
	11:22: 7	29.6	527.3	605.5	616.3	-10.76
	11:41:15	49.7	598.7	731.1	748.1	-16.95
	11:58:35	69.9	685.3	873.6	896.1	-22.48
	12:19:17	100.4	795.5	1074.1	1100.6	-26.57
	12:38:44	100.3	823.7	1103.0	1128.7	-25.74
	12:44:28	100.3	824.4	1104.1	1129.4	-25.38
*23.2	*****DEC., 15*					
	10: 5:18	29.7	532.9	612.1	621.9	-9.85
	10:27:17	60.4	657.2	819.0	838.9	-19.93
	10:39: 4	60.3	667.5	830.2	849.2	-18.95
	11: 9:20	100.5	815.1	1095.8	1120.6	-24.76
	11:16:15	100.5	823.3	1104.0	1128.8	-24.78
	11:23:26	100.4	823.2	1104.0	1128.6	-24.63

Table D.3. (continued)

RUN NO.	DATE		TCS	TCSM	TCSMC	DIFFERENCE
TIME	Q(KW)/ROD					
*23.3 *****JAN, 19*						
15: 7: 0	29.5		577.5	554.9	565.1	-11.17
15:28:51	46.5		567.5	799.4	816.4	-16.99
15:48:34	79.3		758.4	976.1	998.3	-22.24
16:13:41	100.4		923.2	1102.5	1128.4	-25.94
16:17:13	100.4		822.5	1101.9	1127.8	-25.92
*24.1 *****FEB, 16*						
10:42: 1	29.8		543.5	524.8	532.9	-9.13
11: 8:40	50.3		549.3	786.2	800.5	-14.41
11:28:20	70.3		719.6	913.7	931.5	-17.87
12:29: 8	100.4		817.9	1100.3	1123.2	-22.91
12:50:11	100.4		819.6	1101.8	1124.8	-22.99

BEST FIT PARAMETERS FOR AKBN:

WHERE,

$$AKBN = C(1) + C(2)*T + C(3)*T**2 + C(4)*T**3$$

$$C(1) = 0.21235206E 02$$

$$C(2) = -0.77911189E-02$$

$$C(3) = 0.81915749E-06$$

$$C(4) = 0.43554058E-09$$

TOTAL ERROR (SUM OF SQUARED DIFFERENCES) = 0.71583063E 05

VARIANCE OF FIT = 0.33765576E 03

Appendix E

EXAMPLE OF ORICAL - PART III OUTPUT

\*\*\*\*\*  
 \*\*\*\*\* CASE INFORMATION \*\*\*\*\*  
 \*\*\*\*\*

THERMOCOUPLES NO. TE-3010J AND TE-301MJ

A. CALIBRATION RUNS NO. 1.1 DATE: MAY 5 TIME: 013215Z  
 1.2 MAY 5 171321Z  
 1.3 MAY 5 211431Z  
 1.4 MAY 6 141511Z  
 0.1 SEP. 9 191 21Z

B. RADIAL NODING STRUCTURE FOR THIS RUN:

TOTAL NUMBER OF NODES = 12

NODING BREAK-DOWN:

MAGNESIUM OXIDE CORE NODES 1 THROUGH 4  
 INCONEL-600 HEATER NODES 5 THROUGH 6  
 BORON NITRIDE INSUL. NODES 7 THROUGH 9  
 INNER S.S. SHEATH NODES 10 THROUGH 12

C. FIT PARAMETERS FOR THE EFFECTIVE THERMAL CONDUCTIVITY OF MAGNESIUM OXIDE WHERE,

$KMGD(T) = C(1) + C(2)T + C(3)T^2 + C(4)T^3 + C(5)T^4$

REGRESSION RESULTS:

(SPECIFICALLY FOR TE-3010J AND TE-301MJ)

C(1) = 0.77072439E-01  
 C(2) = -0.99114478E-02  
 C(3) = 0.79930423E-05  
 C(4) = -0.28395633E-08  
 C(5) = 0.37459565E-12

TOTAL NUMBER OF DATA POINTS = 605

VARIANCE OF FIT (I.E., SUM OF SQUARED ERROR) = 0.13066104E-05

VARIANCE OF FIT DIVIDED BY TOTAL NO. OF DATA POINTS = 0.21776926E-08

D. MAGNESIUM CORE POROSITY (AS ESTIMATED BY THE MODIFIED RUSSELL EQN) = 0.16652718E-00

\*\*\*\*\*  
 \*\*\*\*\* TRANSIENT RESULTS \*\*\*\*\*  
 \*\*\*\*\*

TE-3010J AND TE-301MJ

CALIBRATION RUN NO. 1.1 DATE: MAY 5 TIME: 013215Z

TIME-TEMPERATURE-NODE TABLE:

TIME HAS UNITS OF SEC

Q HAS UNITS OF BTU/SEC/FT (XPPFA\*GAVG)

TEMPERATURE HAS UNITS OF DEG F

INTERFACE FLUX (PHI) HAS UNITS OF BTU/HR/FT\*\*2

TCSM IS THE OBSERVED CENTER TC TEMPERATURE IN DEG F

TCTR IS THE CALCULATED CENTER TC TEMPERATURE

TIME--	0.0	0.0500	0.1000	0.1500	0.2000	0.2500	0.3000	0.3500	0.4000	0.4500	0.5000	0.5500
NODE												
1	623.0283	622.9988	622.8105	622.3330	621.4807	620.2168	618.5403	616.4736	614.0032	611.3200	608.3179	605.0884
2	623.0283	622.8577	621.8645	619.9255	617.1836	613.6477	610.3267	606.1323	601.9358	597.6793	593.3767	589.0620
3	623.0283	622.3596	618.8931	613.8337	608.1431	602.3188	595.9789	591.0071	585.4822	580.4436	575.4441	570.5167
4	623.0283	620.9026	611.0759	601.3157	592.6899	585.3752	578.2312	571.9695	566.1139	560.7439	555.5328	550.7933
5	623.0283	618.5225	599.8608	587.8719	578.5925	570.9536	564.2059	558.0780	552.4424	547.1958	542.2701	537.6320
6	612.7756	608.6392	591.4028	580.2202	571.5382	564.1623	557.5903	551.6174	546.1160	540.9910	536.1877	531.6525
7	590.4243	588.2983	578.4587	569.5487	561.9106	555.1426	549.0007	543.3489	538.1211	533.2319	528.6418	524.3033
8	568.5586	567.5452	562.1270	555.8445	549.7593	543.9446	538.4707	533.3092	528.4048	523.7209	519.2710	515.0517
9	551.1790	550.7515	547.5515	543.1042	538.3123	533.3436	529.5037	523.8533	519.5540	515.4136	511.4949	507.7573
10	534.3118	534.3330	532.5007	529.4555	525.8195	521.6516	517.8372	513.3357	509.0210	505.7868	502.4581	498.9832
11	517.1152	517.6008	516.5322	514.5237	511.8171	508.1589	504.5115	501.1252	497.9141	494.8130	491.8403	488.9537
12	501.5422	502.5986	501.7473	500.3799	495.3154	494.8752	491.9480	489.0143	485.4821	483.4688	480.9094	478.1448
Q	5.18211	4.05010	0.0	0.0	0.0	0.3	0.0	0.0	3.0	0.0	0.0	0.0
PHI	176387.6	166261.0	170476.5	164932.1	159950.4	162097.0	153056.8	146619.9	139156.4	135046.1	128249.2	125139.0
TCSM	621.7	622.9	622.8	622.8	621.5	621.4	621.2	620.9	620.1	619.9	617.7	615.9
TCTR	623.0	623.0	623.0	623.0	623.0	623.0	623.0	622.8	620.4	621.5	620.3	618.7



TIME--	3.0000	3.0100	3.1000	3.1500	3.2000	3.2499	3.2999	3.3499	3.3999	3.4499	3.4999	3.5499
NODE												
1	459.4087	454.8364	453.3118	451.8313	450.3943	448.9985	447.6428	446.3257	445.0461	443.8035	442.5974	441.4272
2	449.5532	448.2014	446.8867	445.6064	444.3604	443.1477	441.9688	440.8220	439.7085	438.6274	437.5806	436.5685
3	443.2307	442.0750	440.9441	439.8401	438.7637	437.7163	436.6975	435.7070	434.7451	433.8117	432.9054	432.0267
4	437.3987	436.4121	435.4417	434.4905	433.5613	432.6573	431.7793	430.9291	430.1121	429.3247	428.5608	427.8294
5	433.8042	432.9119	432.0320	431.1702	430.3303	429.5176	428.7268	427.9628	427.2308	426.5273	425.8494	425.1932
6	432.0813	431.2273	430.3877	429.5664	428.7682	427.9985	427.2619	426.5535	425.8795	425.2452	424.6467	424.0781
7	430.1570	429.3418	428.5459	427.7705	427.0213	426.3042	425.6231	424.9730	424.3507	423.7603	423.2049	422.6797
8	428.1174	427.3350	426.5864	425.8656	425.1688	424.5018	423.8693	423.2673	422.6918	422.1487	421.6347	421.1451
9	426.2952	425.5310	424.8286	424.1492	423.5037	422.8951	422.3187	421.7693	421.2513	420.7593	420.2984	420.8735
10	424.2424	423.4819	422.8433	422.2161	421.6122	421.0336	420.4837	420.0061	419.5385	419.1115	418.6944	418.3022
11	421.8396	421.0488	420.5190	419.9514	419.5069	419.0745	418.6515	418.2437	417.8568	417.5051	417.1841	416.8910
12	419.4890	418.6130	418.2625	417.7368	417.5615	417.0394	416.5095	416.1589	415.7936	415.4935	415.2083	415.0435
Q	0.0	0.0	0.0	0.0	0.0	0.0	0.0	0.0	0.0	0.0	0.0	0.0
PHI	27338.6	29451.6	25706.9	25839.1	22990.4	23926.8	23734.2	22078.1	19921.0	17406.3	17374.0	13932.4
TCSM	472.3	470.5	468.6	467.1	465.2	463.4	461.5	459.6	458.0	456.8	455.3	454.1
TCTR	465.1	463.3	461.5	459.8	456.1	456.5	454.9	453.4	451.9	450.5	449.1	447.7

TIME--	3.5999	3.6499	3.6999	3.7499	3.7999	3.8499	3.8999	3.9499	3.9999	4.0499	4.0999	4.1499
NODE												
1	440.2937	439.1975	438.1367	437.1116	436.1204	435.1609	434.2307	433.3289	432.4541	431.6050	430.7803	429.9807
2	435.5933	434.6550	433.7510	432.8760	432.0281	431.2043	430.4024	429.6208	428.8593	428.1180	427.4017	426.7075
3	431.2449	430.4631	429.7073	428.9709	428.2515	427.5484	426.8533	426.1743	425.5127	424.8708	424.2524	423.6604
4	427.2395	426.6125	425.9910	425.3730	424.7634	424.1570	423.5584	422.9629	422.3718	421.7843	421.2020	420.6343
5	424.7881	424.2581	423.7080	423.1519	422.6018	422.0474	421.4910	420.9321	420.3730	419.8132	419.2532	418.6935
6	423.6160	423.1313	422.6064	422.0745	421.5503	421.0186	420.4800	419.9477	419.4234	418.9084	418.3928	417.8768
7	422.3315	421.8940	421.3845	420.8760	420.3801	419.8859	419.3477	418.8662	418.4197	418.0010	417.5335	417.1088
8	421.0115	420.5121	420.0952	419.6099	419.1426	418.6394	418.1387	417.6978	417.2966	416.9204	416.5143	416.1482
9	419.8691	419.4861	419.0333	418.6472	418.0354	417.5532	417.0454	416.6521	416.2975	415.9663	415.7217	415.5141
10	418.6260	418.2290	417.5952	417.1843	416.7822	416.2622	415.7037	415.4736	415.1770	414.8538	414.7590	414.6313
11	417.2471	416.7576	416.9553	416.6750	416.3132	414.7334	414.3022	414.1111	413.8543	413.6577	413.6418	413.5837
12	415.9836	415.2820	414.2297	414.2297	413.8792	413.1775	412.8267	412.5267	412.2867	412.1011	412.0758	412.0511
Q	0.0	0.0	0.0	0.0	0.0	0.0	0.0	0.0	0.0	0.0	0.0	0.0
PHI	13704.4	18388.9	22283.7	15064.0	16731.1	19242.7	17176.6	13913.2	13990.8	13396.0	10135.9	10190.0
TCSM	453.2	452.0	450.6	449.4	448.1	446.7	445.7	444.5	443.3	442.2	441.2	439.8
TCTR	446.4	445.1	443.9	442.7	441.5	440.4	439.3	438.2	437.2	436.2	435.2	434.3

TIME--	4.1999	4.2499	4.2999	4.3499	4.3999	4.4499	4.4999	4.5499	4.5999	4.6499	4.6999	4.7499
NODE												
1	429.2061	428.4570	427.7324	427.0320	426.3550	425.7000	425.0662	424.4531	423.8601	423.2859	422.7302	422.1917
2	426.0381	425.3943	424.7739	424.1748	423.5947	423.0322	422.4883	421.9612	421.4502	420.9555	420.4788	420.0208
3	423.0984	422.5576	422.0388	421.5334	421.0405	420.5525	420.0994	419.6501	419.2151	418.7927	418.3813	417.9783
4	420.3782	419.9438	419.5189	419.0947	418.6775	418.2711	417.8884	417.5300	417.1921	416.8744	416.5755	416.2941
5	418.7050	418.3374	417.9668	417.5845	417.2100	416.8504	416.5159	416.1775	415.8542	415.5465	415.2507	414.9621
6	417.8999	417.5623	417.2141	416.8462	416.4915	416.1336	415.7857	415.4524	415.1299	414.8239	414.5221	414.2311
7	417.3181	416.9119	416.5840	416.2261	415.8943	415.5979	415.1057	414.8022	414.5269	414.2858	414.0658	413.8653
8	416.1135	415.8308	415.5156	415.1582	414.8547	414.5994	414.3315	414.0405	413.7986	413.5474	413.2888	412.9736
9	415.3303	415.0554	414.7419	414.3738	414.1077	413.8985	413.6459	413.3596	413.1555	412.9187	412.6508	412.3515
10	414.4756	414.1853	413.8638	413.4702	413.2688	413.1159	412.8735	412.5813	412.3399	412.0982	411.8582	411.6436
11	413.5242	413.1599	412.8193	412.3730	412.3074	412.2363	411.9688	411.6533	411.3304	411.3748	410.9619	410.8123
12	412.6511	412.1248	411.7739	411.2476	411.4229	411.4229	411.0720	410.7209	410.3965	410.5454	410.0188	410.2185
Q	0.0	0.0	0.0	0.0	0.0	0.0	0.0	0.0	0.0	0.0	0.0	0.0
PHI	9458.8	12994.6	12508.4	13968.7	9980.7	8804.0	10895.3	11283.0	7350.7	10166.9	11991.1	9599.1
TCSM	438.7	437.9	436.8	435.8	434.9	434.2	433.5	432.8	431.7	431.2	430.5	429.3
TCTR	433.4	432.5	431.6	430.8	430.0	429.2	428.5	427.8	427.1	426.4	425.7	425.1

TIME--	4.7999	4.8499	4.8999	4.9499	4.9999	5.0499	5.0999	5.1499	5.1999	5.2499	5.2999	5.3499
NODE												
1	421.6699	421.1636	420.6719	420.1948	419.7314	419.2810	418.8442	418.4207	418.0107	417.6159	417.2329	416.8632
2	419.5594	419.1140	418.6846	418.2659	417.8584	417.4629	417.0811	416.7135	416.3605	416.0220	415.6970	415.3844
3	417.5850	417.2009	416.8262	416.4595	416.1027	415.7605	415.4344	415.1233	414.8279	414.5474	414.2778	414.0173
4	415.7455	415.4124	415.0876	414.7678	414.4575	414.1697	413.9014	413.6487	413.4131	413.1919	412.9739	412.7598
5	414.5911	414.2891	413.9946	413.7014	413.4216	413.1672	412.9497	412.7588	412.5935	412.4523	412.3170	412.1915
6	414.0215	413.7344	413.4548	413.1731	412.9099	412.6899	412.4851	412.2930	412.1223	411.9700	411.8300	411.6913
7	413.3862	413.1162	412.8535	412.5828	412.3403	412.1560	411.9733	411.8079	411.6541	411.5244	411.3869	411.3191
8	412.7141	412.4629	412.2180	411.9546	411.7402	411.6067	411.4543	411.3074	411.1973	411.0790	410.8970	410.7841
9	412.1111	411.8770	411.6475	411.3857	411.2058	411.1338	410.9976	410.8856	410.7961	410.6438	410.4915	410.4590
10	411.4288	411.2122	411.0000	410.7317	410.6094	410.6267	410.4905	410.3853	410.3628	410.2490	410.3195	410.1682
11	410.6235	410.4304	410.2373	409.9424	409.9209	410.0442	409.9033	409.8337	409.8938	409.7852	409.4304	409.4182
12	409.8433	409.8677	409.4922	409.1411	409.3157	409.6677	409.3157	409.3167	408.4422	409.3167	408.7900	408.4456
Q	0.0	0.0	0.0	0.0	0.0	0.0	0.0	0.0	0.0	0.0	0.0	0.0
PHI	9037.8	8843.6	8656.0	9855.3	4037.2	3424.9	7536.7	5591.7	3751.2	5663.5	8706.8	4331.1
TCSM	429.1	428.8	428.4	427.9	427.2	426.5	425.9	424.9	424.0	423.5	422.2	420.6
TCTR	424.5	423.9	423.3	422.8	422.2	421.7	421.2	420.7	420.2	419.7	419.3	418.1



TIME--	5.3999	5.4499	5.4999	5.5499	5.5999	5.6499	5.6999	5.7499	5.7999	5.8499	5.8999	5.9499
NODE												
1	416.5095	416.1563	415.8359	415.5166	415.2007	414.8921	414.6262	414.3503	414.0940	413.8287	413.5771	413.3352
2	416.0825	414.7953	414.5081	414.2059	413.9741	413.7222	413.4795	413.2458	413.0190	412.7971	412.5801	412.3672
3	413.7634	413.5121	413.2808	413.0537	412.8352	412.6252	412.4231	412.2271	412.0349	411.8420	411.6497	411.4572
4	412.5486	412.3440	412.1482	411.9626	411.7859	411.6185	411.4514	411.2883	411.1238	410.9550	410.7747	410.6033
5	411.7949	411.6155	411.4453	411.2886	411.1421	410.9946	410.8518	410.7065	410.5547	410.3980	410.2170	410.0574
6	411.4255	411.2583	411.1033	410.9597	410.8254	410.6897	410.5585	410.4204	410.2727	410.0991	409.9358	409.7834
7	411.0181	410.8650	410.7253	410.6008	410.4871	410.3857	410.2371	410.1950	409.9592	409.7764	409.6196	409.4761
8	410.5918	410.4551	410.3359	410.2312	410.1375	410.0576	409.9048	409.7732	409.6250	409.4224	409.2503	409.1492
9	410.2129	410.0933	409.9939	409.9092	409.8347	409.6963	409.6128	409.4749	409.3208	409.0899	408.9731	408.8542
10	409.7847	409.6887	409.6150	409.5549	409.5027	409.3391	409.2930	409.1313	408.9670	408.6941	408.6250	408.5190
11	409.2630	409.2249	409.1858	409.1557	409.1311	408.9206	408.9294	408.7102	408.5130	408.1545	408.2351	408.1248
12	408.7900	408.7900	408.7900	408.7900	408.7900	408.4430	408.6145	408.2634	408.0979	407.5810	407.9121	407.7355

Q	0.0	0.0	0.0	0.0	0.0	0.0	0.0	0.0	0.0	0.0	0.0	0.0
PHI	5924.6	4733.8	4288.0	3956.6	3689.2	6202.0	2814.6	6017.5	3404.1	8195.1	2315.3	4792.2
TCSM	422.1	421.9	421.4	423.9	420.4	420.2	419.5	419.1	419.8	418.4	417.7	417.4
TCTR	418.4	418.0	417.6	417.2	416.9	416.5	416.2	415.8	415.4	415.2	414.9	414.6

TIME--	6.0999	6.0499	6.0999	6.1499	6.1999	6.2499	6.2999	6.3499	6.3999	6.4499	6.4999	6.5499
NODE												
1	413.1901	412.8713	412.6484	412.4338	412.2268	412.0269	411.8340	411.6465	411.4635	411.2842	411.1087	410.9314
2	412.1592	411.9579	411.7627	411.5771	411.4006	411.2312	411.0654	410.9014	410.7371	410.5706	410.4031	410.2358
3	411.2751	411.0984	410.9326	410.7803	410.6377	410.4953	410.3530	410.2043	410.0476	409.8940	409.7180	409.5557
4	410.4419	410.2922	410.1619	410.0479	409.9397	409.8233	409.6999	409.5835	409.4839	409.3209	409.0455	408.8372
5	409.9141	409.7856	409.6846	409.6038	409.5164	409.4039	409.2893	409.1112	408.9360	408.7583	408.5920	408.4475
6	409.6516	409.5366	409.4541	409.3918	409.3120	409.1949	409.0542	408.8901	408.7519	408.5200	408.3569	408.2227
7	409.3606	409.2529	409.2051	409.1675	409.3908	408.9570	408.8105	408.6316	408.4690	408.2422	408.0869	407.9648
8	409.0566	408.9507	408.9604	408.9490	408.8638	408.6992	408.5805	408.3386	408.1986	407.9302	407.7202	407.6985
9	408.7898	408.7166	408.7583	408.7712	408.6606	408.4521	408.2842	408.0935	407.8355	407.5360	407.3176	407.2592
10	408.4980	408.4697	408.5554	408.5908	408.4226	408.1431	407.9778	407.6990	407.4599	407.2903	407.2056	407.1970
11	408.1799	408.1763	408.3691	408.4109	408.1106	407.7153	407.5533	407.2246	406.9295	406.6801	406.4435	406.3141
12	407.9121	407.9121	408.2632	408.2632	407.7366	407.2097	407.2097	406.6831	406.3318	406.5076	406.5076	406.6831

Q	0.0	0.0	0.0	0.0	0.0	0.0	0.0	0.0	0.0	0.0	0.0	0.0
PHI	2303.9	2857.0	-39.2	1600.7	5828.3	7203.9	4144.1	7632.9	7285.4	3433.0	3630.5	1704.2
TCSM	417.2	416.5	416.2	416.2	416.0	415.6	415.8	415.0	415.3	415.1	414.9	414.4
TCTR	414.4	414.1	413.8	413.6	413.3	413.1	412.9	412.6	412.4	412.2	412.0	411.8

TIME--	6.5999	6.5499	6.5999	6.7499	6.7999	6.8499	6.8999	6.9499	6.9999	7.0499	7.0999	7.1499
NODE												
1	410.7583	410.5881	410.4216	410.2588	410.1018	409.9502	409.8037	409.6625	409.5259	409.3936	409.2644	409.1394
2	410.0708	409.9124	409.7598	409.6155	409.4783	409.3484	409.2234	409.1021	408.9841	408.8684	408.7554	408.6455
3	409.4019	409.2590	409.1272	409.0071	408.8965	408.7908	408.6893	408.5940	408.4857	408.3782	408.2783	408.1826
4	408.7532	408.6367	408.5320	408.4436	408.3635	408.2898	408.1929	408.1023	408.0109	407.9122	407.8293	407.7493
5	408.1362	408.0446	408.1626	408.1311	408.0422	407.9692	407.8857	407.7998	407.7109	407.6229	407.5444	407.4775
6	407.5192	407.4527	407.3836	407.3300	407.2689	407.2167	407.1322	407.0484	406.9633	406.8741	406.8025	406.7438
7	407.0019	406.9450	406.8894	406.8349	406.7753	406.6487	406.5615	406.4792	406.3954	406.3064	406.2451	406.1973
8	406.6724	406.6357	406.5940	406.5591	406.5630	406.4735	406.3770	406.2976	406.2075	406.1265	406.0811	406.0476
9	406.4822	406.4590	406.4268	406.4670	406.4236	406.3047	406.2061	406.1323	406.0388	405.9622	405.9385	405.9194
10	406.2915	406.2708	406.2458	406.3406	406.2588	406.1030	406.0042	405.9426	405.8401	405.7727	405.7849	405.7825
11	406.1213	406.1630	406.1447	406.2393	406.1789	406.0301	405.9546	405.8199	405.7425	405.6476	405.6252	405.6355
12	406.0344	406.0586	406.0586	406.2100	406.0586	406.0576	406.0576	406.0576	406.0576	406.0576	406.0576	406.0576

Q	0.0	0.0	0.0	0.0	0.0	0.0	0.0	0.0	0.0	0.0	0.0	0.0
PHI	-244.4	2804.8	2010.2	-868.0	3570.1	4574.7	2672.7	2286.0	3416.7	2333.3	682.0	1383.7
TCSM	414.2	413.9	413.4	412.8	412.6	412.5	412.3	412.3	412.1	411.8	411.8	411.4
TCTR	411.6	411.5	411.3	411.1	410.9	410.8	410.6	410.4	410.3	410.1	409.9	409.8

TIME--	7.1999	7.2499	7.2999	7.3499	7.3999	7.4499	7.4999	7.5499	7.5999	7.6499	7.6999	7.7499
NODE												
1	409.3183	409.2011	409.0878	408.9780	408.8718	408.7692	408.6694	408.5725	408.4775	408.3840	408.2915	408.2092
2	408.9398	408.8377	408.7398	408.6451	408.5533	408.4644	408.3781	408.2943	408.2130	408.1341	408.0573	407.9826
3	408.6023	408.5068	408.4161	408.3293	408.2464	408.1674	408.0921	408.0203	407.9519	407.8869	407.8251	407.7663
4	408.3187	408.2309	408.1488	408.0725	407.9999	407.9309	407.8654	407.8034	407.7447	407.6893	407.6370	407.5877
5	407.9927	407.9280	407.8684	407.8139	407.7643	407.7196	407.6797	407.6444	407.6135	407.5869	407.5645	407.5461
6	407.6560	407.6037	407.5561	407.5131	407.4746	407.4405	407.4107	407.3851	407.3636	407.3461	407.3325	407.3228
7	407.3176	407.2783	407.2440	407.2146	407.1901	407.1704	407.1554	407.1450	407.1391	407.1376	407.1404	407.1475
8	406.9994	406.9728	406.9510	406.9340	406.9209	406.9117	406.9063	406.9045	406.9061	406.9109	406.9188	406.9297
9	406.7720	406.7507	406.7338	406.7212	406.7128	406.7084	406.7070	406.7084	406.7125	406.7199	406.7302	406.7434
10	406.5328	406.5239	406.5189	406.5167	406.5172	406.5202	406.5254	406.5326	406.5416	406.5522	406.5651	406.5802
11	406.3328	406.3318	406.3318	406.3318	406.3318	406.3318	406.3318	406.3318	406.3318	406.3318	406.3318	406.3318
12	406.0576	406.0576	406.0576	406.0576	406.0576	406.0576	406.0576	406.0576	406.0576	406.0576	406.0576	406.0576

Q	0.0	0.0	0.0	0.0	0.0	0.0	0.0	0.0	0.0	0.0	0.0	0.0
PHI	1355.9	2672.7	1705.1	2889.7	483.0	3901.1	2073.8	3144.2	3428.1	5005.9	2891.3	1950.9
TCSM	411.6	411.4	411.4	411.1	410.7	410.4	410.4	410.2	410.2	410.2	410.0	409.8
TCTR	409.7	409.5	409.4	409.3	409.1	409.0	408.9	408.9				



\*\*\*\*\*  
\*\*\*\*\* ENERGY BALANCE \*\*\*\*\*  
\*\*\*\*\*

FF-3010J AND TE-301MJ  
CALIBRATION RUN NO. 1.1 DATE: MAY 5 TIME: 0:32:52

CHANGE IN PIN INTERNAL ENERGY CONTENT = 7.827926 BTU/FT  
DETERMINED BY SUMMATION OF DELTA U'S OVER THE INTERVAL FROM T=0 TO TEND.  
CHANGE IN PIN INTERNAL ENERGY CONTENT = 7.823809 BTU/FT  
DETERMINED BY DIFFERENCE IN PIN END POINT ENTHALPIES.  
TOTAL HEAT INPUT = INTEGRAL OF QDOT\*DT = 0.202502 BTU/FT

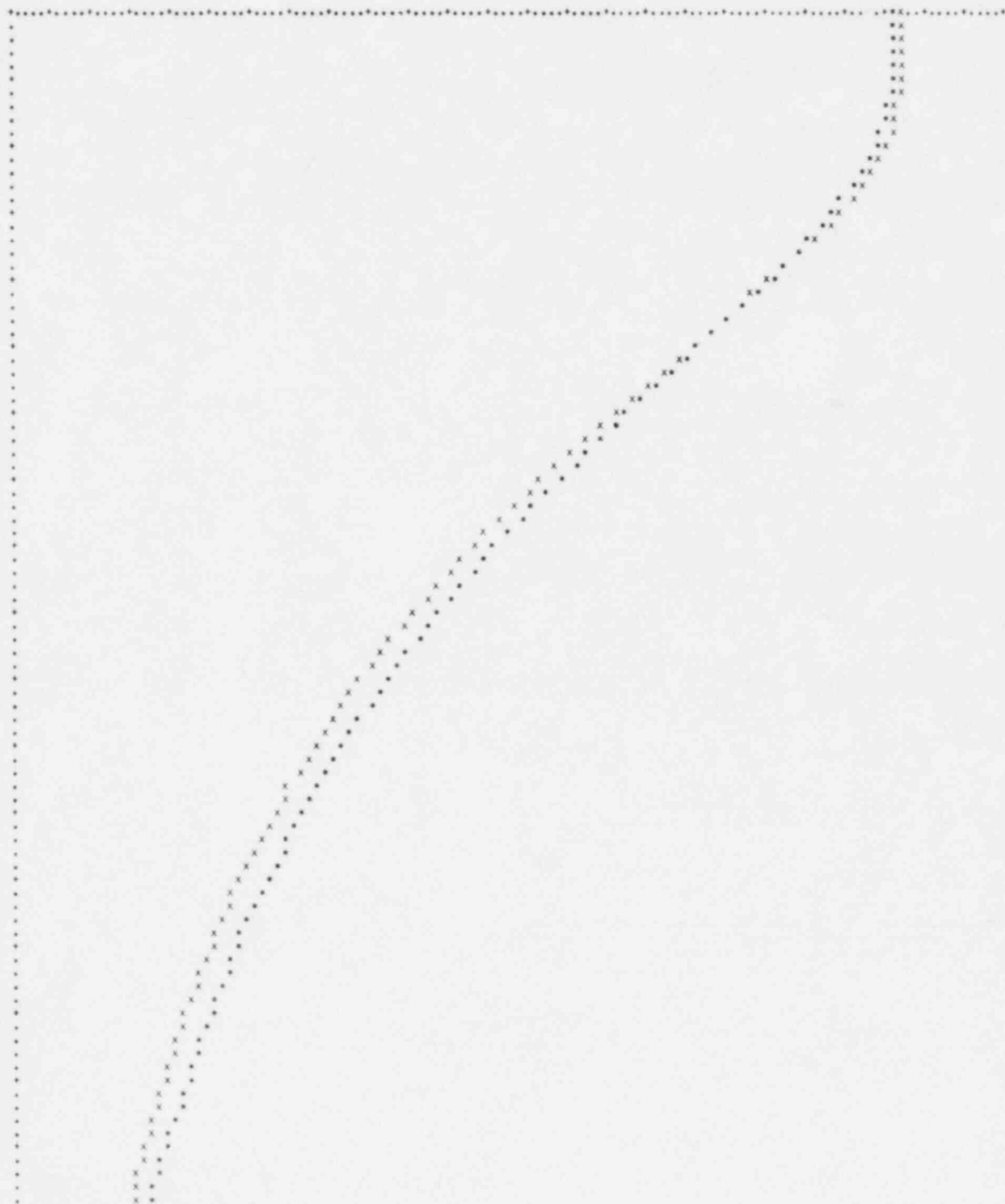
INTEGRAL OF SURFACE FLUX VERSUS TIME CURVE \*2.0\*PI\*R0= 8.025964 BTU/FT

PERCENTAGE ERROR IN OVERALL HEAT BALANCE = 0.0556 PERCENT  
ERROR IN OVERALL HEAT BALANCE (VIA METHOD 2)= 0.0043 PERCENT

VARIANCE FOR THIS RUN = 0.31557144E 04

Y FROM 4.00000000E 02 TO 5.50000000E 02 AS A FUNCTION OF X FROM 0.0 TO 1.10000000E 01  
WITH Y INTERVAL SIZE 2.00000000E 00 AND WITH X INTERVAL SIZE 4.99999970E-02

THE X AXIS HAS BEEN SHIFTED FROM 0.0 TO Y = 4.00000000E 02



\*\*\*\*\*  
 \*\*\*\*\* TRANSIENT RESULTS \*\*\*\*\*  
 \*\*\*\*\*

TE-3010J AND TE-301WJ  
 CALIBRATION RUN NO. 1.2 DATE: MAY 5 TIME: 17:32:27

TIME-TEMPERATURE-NODE TABLE

TIME HAS UNITS OF SEC  
 Q HAS UNITS OF BTU/SEC/FT (\*\*PFA\*QAVG)  
 TEMPERATURE HAS UNITS OF DEG F  
 INTERFACE FLUX (PHI) HAS UNITS OF BTU/HR/FT\*\*2  
 TCSM IS THE OBSERVED CENTER TC TEMPERATURE IN DEG F  
 TCTR IS THE CALCULATED CENTER TC TEMPERATURE

TIME--	0.0	0.0500	0.1000	0.1500	0.2000	0.2500	0.3000	0.3500	0.4000	0.4500	0.5000	0.5500
NODE												
1	819.6578	819.5837	819.0471	818.0574	816.4839	814.2903	811.4810	808.0879	804.1584	799.7471	794.9105	789.7351
2	819.6578	818.6436	816.1311	812.2417	807.2427	801.4265	795.0427	788.2847	781.2922	774.1641	766.9661	759.7419
3	819.6578	815.0928	807.2386	797.9360	788.0417	778.1240	768.4231	759.0342	749.9812	741.2532	732.8240	724.6543
4	819.6578	803.6841	786.1746	770.3428	756.3535	743.8760	732.5840	722.2224	712.6008	703.5674	695.3103	686.8506
5	819.6578	784.2195	761.0491	743.8569	729.7063	717.4404	706.4915	696.5159	687.2876	678.6292	670.4275	662.6094
6	802.8245	770.5281	748.6853	732.1502	718.4631	706.5491	695.8894	686.1570	677.1353	668.6465	660.5911	652.9031
7	762.5544	745.5388	728.8552	714.5476	702.1721	691.1812	681.2280	672.0593	663.4993	655.3828	647.6423	640.2314
8	721.0432	712.4395	701.4290	690.5679	680.4751	671.1006	662.3740	654.1563	646.3804	638.9728	631.8514	624.9565
9	688.2241	683.3926	678.0432	673.9634	669.9468	665.2125	660.5750	656.3123	652.2598	648.3674	644.5614	640.8443
10	658.3913	655.2627	652.4717	649.6790	646.5479	643.1255	639.3644	635.2126	631.6384	627.6003	623.1484	618.3229
11	628.6504	626.8379	623.8657	619.9373	615.4973	610.3335	605.2052	600.0625	594.8764	589.6188	584.2909	578.8537
12	601.8637	600.4368	598.7766	596.2708	593.2271	588.9938	584.7665	580.5247	575.1099	569.5129	564.4221	559.3257
Q	9.33682	0.38302	0.0	0.0	0.0	0.0	0.0	0.0	0.0	0.0	0.0	0.0
PHI	3178.048	3183.773	303405.4	289250.3	274253.8	266374.9	254519.9	247357.4	239982.3	238172.8	229229.6	223350.7
TCSM	822.9	824.1	824.2	824.3	823.3	823.0	822.5	821.8	820.5	819.0	816.8	814.4
TCTR	819.7	819.7	819.7	819.7	819.7	819.7	819.7	819.5	818.9	817.9	816.3	814.0
TIME--	0.6000	0.6500	0.7000	0.7500	0.8000	0.8500	0.9000	0.9500	1.0000	1.0500	1.1000	1.1500
NODE												
1	784.1814	778.3877	772.3668	766.1563	759.7900	753.2981	746.7068	740.0396	733.3186	726.5625	719.7881	713.0110
2	782.5210	745.3210	738.1553	731.0317	723.9558	716.9326	709.9600	703.0690	695.2400	689.4846	682.8074	676.2119
3	716.7488	709.5439	701.5364	694.2043	687.0325	680.0137	673.1423	666.4103	659.8259	653.3774	647.0586	640.8679
4	679.0254	671.4900	664.2053	657.1409	650.2778	643.5121	637.1375	630.8464	624.7307	618.7778	612.9797	607.3315
5	655.1190	647.8997	640.9282	634.1877	627.5135	621.2717	615.1345	609.1929	603.4331	597.8411	592.4048	587.1248
6	645.5271	638.4197	631.5508	624.8845	618.4285	612.1926	606.1675	600.3433	594.7012	589.2292	583.9125	578.7576
7	633.1038	626.2202	619.5579	613.0793	606.8152	600.7738	594.9587	589.3379	583.8955	578.6196	573.4939	568.5361
8	617.9741	611.4519	605.1213	598.9385	592.9932	587.2678	581.7805	576.4445	571.2951	566.3027	561.4458	556.7371
9	603.8479	597.0885	591.0880	585.7954	580.1641	574.7854	569.5986	564.5933	559.7305	555.0146	550.4180	545.9200
10	588.0353	582.8303	577.1702	571.5583	566.2864	561.2786	556.4329	551.7551	547.1902	542.7656	538.4365	534.3494
11	571.4551	566.0100	560.7051	555.3611	550.5354	545.9644	541.4029	537.1794	532.9331	528.8301	524.7847	521.0779
12	554.2256	549.1213	544.1816	539.0886	534.8044	530.7075	526.6967	522.6724	518.7351	514.9675	511.1970	507.9380
Q	0.0	0.0	0.0	0.0	0.0	0.0	0.0	0.0	0.0	0.0	0.0	0.0
PHI	218268.1	213841.3	208566.1	206058.3	196158.9	189744.8	185155.0	179891.2	176045.4	171318.4	167901.7	150750.2
TCSM	810.9	807.2	803.1	798.3	793.4	788.6	783.3	777.5	771.7	765.7	759.4	753.2
TCTR	811.1	807.7	803.7	799.2	794.4	789.1	783.6	777.7	771.7	765.5	759.1	752.6

\*\*\*\*\*  
 \*\*\*\*\* ENERGY BALANCE \*\*\*\*\*  
 \*\*\*\*\*

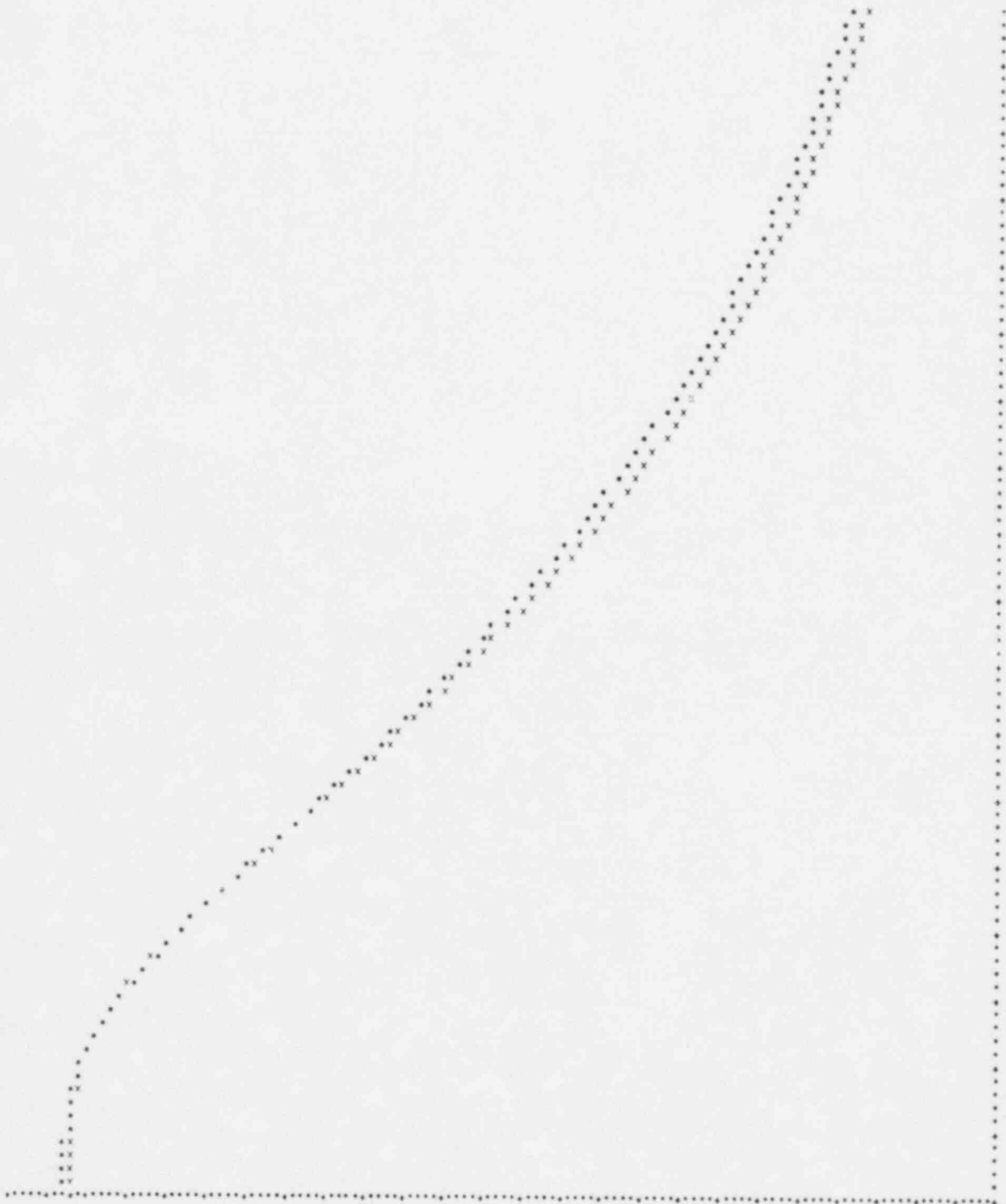
TE-3010J AND TE-301WJ  
 CALIBRATION RUN NO. 1.2 DATE: MAY 5 TIME: 17:32:27

CHANGE IN PIN INTERNAL ENERGY CONTENT = 15.663849 BTU/FT  
 DETERMINED BY SUMMATION OF DELTA U'S OVER THE INTERVAL FROM TND TO TEND.  
 CHANGE IN PIN INTERNAL ENERGY CONTENT = 15.651159 BTU/FT  
 DETERMINED BY DIFFERENCE IN PIN END POINT ENTHALPIES.  
 TOTAL HEAT INPUT = INTEGRAL OF QDOT\*DT = 0.019151 BTU/FT

INTEGRAL OF SURFACE FLUX VERSUS TIME CURVE #2.0\*PI\*PO= 15.677749 BTU/FT

PERCENTAGE ERROR IN OVERALL HEAT BALANCE = 0.0309 PERCENT  
 ERROR IN OVERALL HEAT BALANCE (VIA METHOD 2)= 0.0475 PERCENT

VARIANCE FOR THIS RUN = 0.41445703E 04

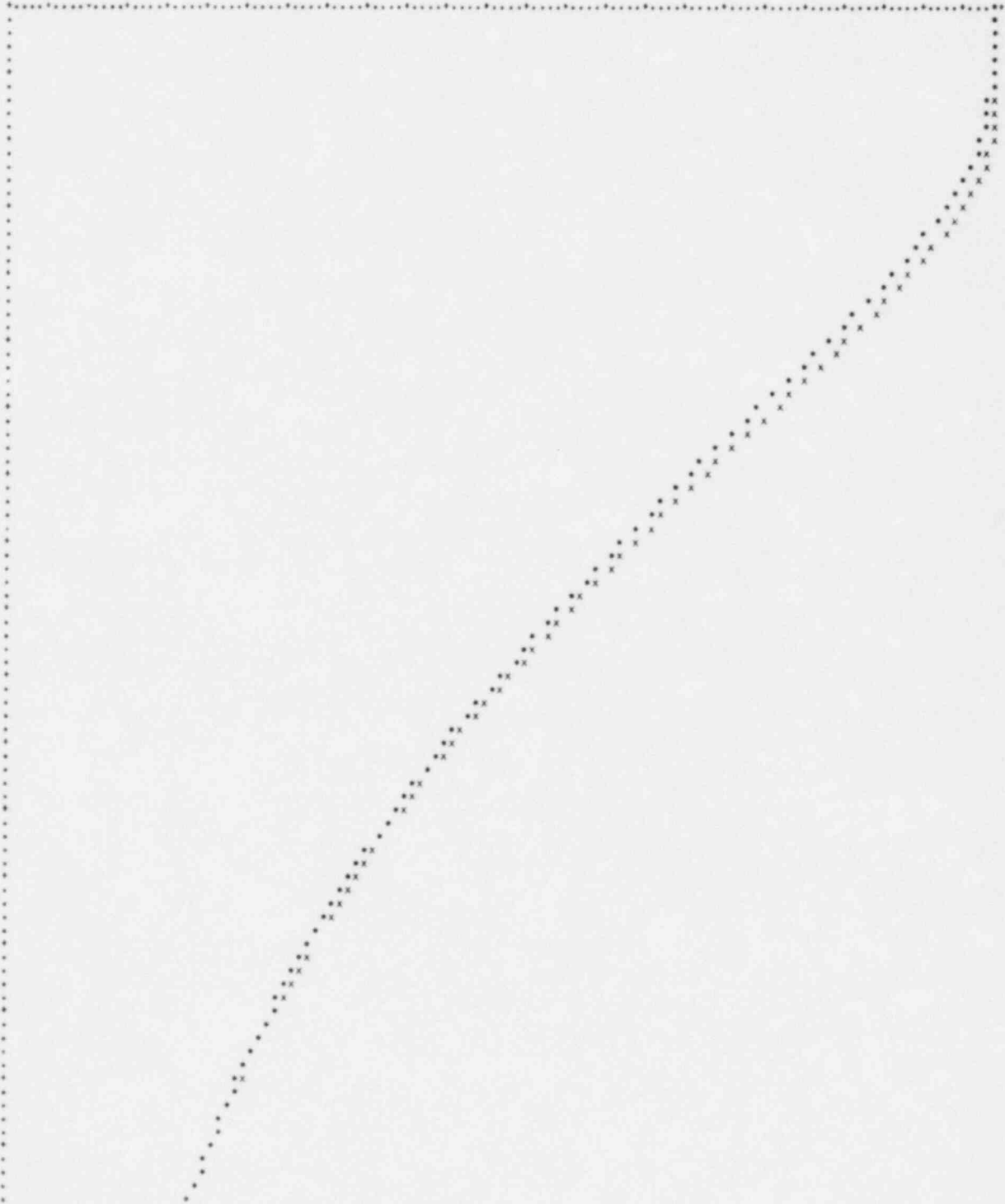


A FROM 4.0000000E 02 TO 0.5000000E 02 AS A FUNCTION OF X FROM 0.0  
 TO 1.1000000E 01  
 WITH A INTERVAL SIZE 3.5999999E 00 AND WITH X INTERVAL SIZE 4.9999970E-02  
 THE X AXIS HAS BEEN SHIFTED FROM 0.0 TO 4.0



Y FROM 4.50000000E 02 TO 1.05000000E 03 AS A FUNCTION OF X FROM 0.0 TO 1.10000000E 01  
WITH Y INTERVAL SIZE 4.79999924E 00 AND WITH X INTERVAL SIZE 4.99999970E-02

THE X AXIS HAS BEEN SHIFTED FROM 0.0 TO Y = 4.50000000E 02





\*\*\*\*\* TRANSIENT RESULT \*\*\*\*\*  
 CALIBRATION RUN NO. 1\*\* DATE: MAY 6 TIME: 14:51:14  
 TIME-TEMPERATURE-NODE TABLE:  
 TIME HAS UNITS OF SEC  
 Q HAS UNITS OF R/HR/DEGREE F=PPA\*QAVG  
 TEMPERATURE HAS UNITS OF DEG F  
 INTERFACE FLUX UNITS OF BTU/HR/FT\*\*2  
 IC5W IS THE OVERALL CENTER TC TEMPERATURE IN DEG F  
 IC1W IS THE CALCULATED CENTER TC TEMPERATURE

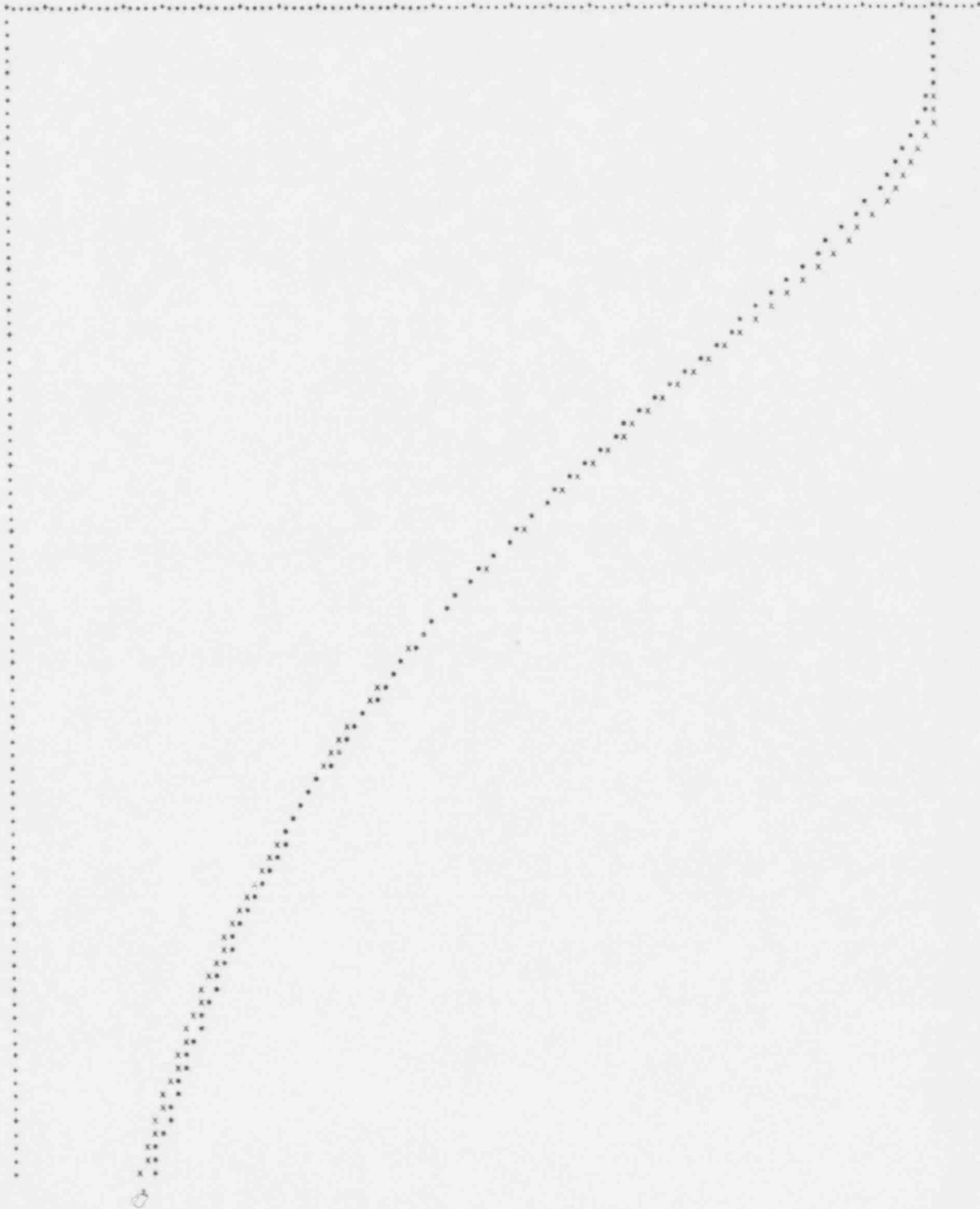
TIME--	Q	IC5W	IC1W	TIME--	Q	IC5W	IC1W
0.0	0.0	0.0	0.0	1.0	0.0	0.0	0.0
0.0	0.0	0.0	0.0	2.0	0.0	0.0	0.0
0.0	0.0	0.0	0.0	3.0	0.0	0.0	0.0
0.0	0.0	0.0	0.0	4.0	0.0	0.0	0.0
0.0	0.0	0.0	0.0	5.0	0.0	0.0	0.0
0.0	0.0	0.0	0.0	6.0	0.0	0.0	0.0
0.0	0.0	0.0	0.0	7.0	0.0	0.0	0.0
0.0	0.0	0.0	0.0	8.0	0.0	0.0	0.0
0.0	0.0	0.0	0.0	9.0	0.0	0.0	0.0
0.0	0.0	0.0	0.0	10.0	0.0	0.0	0.0
0.0	0.0	0.0	0.0	11.0	0.0	0.0	0.0
0.0	0.0	0.0	0.0	12.0	0.0	0.0	0.0
0.0	0.0	0.0	0.0	13.0	0.0	0.0	0.0
0.0	0.0	0.0	0.0	14.0	0.0	0.0	0.0
0.0	0.0	0.0	0.0	15.0	0.0	0.0	0.0
0.0	0.0	0.0	0.0	16.0	0.0	0.0	0.0
0.0	0.0	0.0	0.0	17.0	0.0	0.0	0.0
0.0	0.0	0.0	0.0	18.0	0.0	0.0	0.0
0.0	0.0	0.0	0.0	19.0	0.0	0.0	0.0
0.0	0.0	0.0	0.0	20.0	0.0	0.0	0.0
0.0	0.0	0.0	0.0	21.0	0.0	0.0	0.0
0.0	0.0	0.0	0.0	22.0	0.0	0.0	0.0
0.0	0.0	0.0	0.0	23.0	0.0	0.0	0.0
0.0	0.0	0.0	0.0	24.0	0.0	0.0	0.0
0.0	0.0	0.0	0.0	25.0	0.0	0.0	0.0
0.0	0.0	0.0	0.0	26.0	0.0	0.0	0.0
0.0	0.0	0.0	0.0	27.0	0.0	0.0	0.0
0.0	0.0	0.0	0.0	28.0	0.0	0.0	0.0
0.0	0.0	0.0	0.0	29.0	0.0	0.0	0.0
0.0	0.0	0.0	0.0	30.0	0.0	0.0	0.0
0.0	0.0	0.0	0.0	31.0	0.0	0.0	0.0
0.0	0.0	0.0	0.0	32.0	0.0	0.0	0.0
0.0	0.0	0.0	0.0	33.0	0.0	0.0	0.0
0.0	0.0	0.0	0.0	34.0	0.0	0.0	0.0
0.0	0.0	0.0	0.0	35.0	0.0	0.0	0.0
0.0	0.0	0.0	0.0	36.0	0.0	0.0	0.0
0.0	0.0	0.0	0.0	37.0	0.0	0.0	0.0
0.0	0.0	0.0	0.0	38.0	0.0	0.0	0.0
0.0	0.0	0.0	0.0	39.0	0.0	0.0	0.0
0.0	0.0	0.0	0.0	40.0	0.0	0.0	0.0
0.0	0.0	0.0	0.0	41.0	0.0	0.0	0.0
0.0	0.0	0.0	0.0	42.0	0.0	0.0	0.0
0.0	0.0	0.0	0.0	43.0	0.0	0.0	0.0
0.0	0.0	0.0	0.0	44.0	0.0	0.0	0.0
0.0	0.0	0.0	0.0	45.0	0.0	0.0	0.0
0.0	0.0	0.0	0.0	46.0	0.0	0.0	0.0
0.0	0.0	0.0	0.0	47.0	0.0	0.0	0.0
0.0	0.0	0.0	0.0	48.0	0.0	0.0	0.0
0.0	0.0	0.0	0.0	49.0	0.0	0.0	0.0
0.0	0.0	0.0	0.0	50.0	0.0	0.0	0.0
0.0	0.0	0.0	0.0	51.0	0.0	0.0	0.0
0.0	0.0	0.0	0.0	52.0	0.0	0.0	0.0
0.0	0.0	0.0	0.0	53.0	0.0	0.0	0.0
0.0	0.0	0.0	0.0	54.0	0.0	0.0	0.0
0.0	0.0	0.0	0.0	55.0	0.0	0.0	0.0
0.0	0.0	0.0	0.0	56.0	0.0	0.0	0.0
0.0	0.0	0.0	0.0	57.0	0.0	0.0	0.0
0.0	0.0	0.0	0.0	58.0	0.0	0.0	0.0
0.0	0.0	0.0	0.0	59.0	0.0	0.0	0.0
0.0	0.0	0.0	0.0	60.0	0.0	0.0	0.0
0.0	0.0	0.0	0.0	61.0	0.0	0.0	0.0
0.0	0.0	0.0	0.0	62.0	0.0	0.0	0.0
0.0	0.0	0.0	0.0	63.0	0.0	0.0	0.0
0.0	0.0	0.0	0.0	64.0	0.0	0.0	0.0
0.0	0.0	0.0	0.0	65.0	0.0	0.0	0.0
0.0	0.0	0.0	0.0	66.0	0.0	0.0	0.0
0.0	0.0	0.0	0.0	67.0	0.0	0.0	0.0
0.0	0.0	0.0	0.0	68.0	0.0	0.0	0.0
0.0	0.0	0.0	0.0	69.0	0.0	0.0	0.0
0.0	0.0	0.0	0.0	70.0	0.0	0.0	0.0
0.0	0.0	0.0	0.0	71.0	0.0	0.0	0.0
0.0	0.0	0.0	0.0	72.0	0.0	0.0	0.0
0.0	0.0	0.0	0.0	73.0	0.0	0.0	0.0
0.0	0.0	0.0	0.0	74.0	0.0	0.0	0.0
0.0	0.0	0.0	0.0	75.0	0.0	0.0	0.0
0.0	0.0	0.0	0.0	76.0	0.0	0.0	0.0
0.0	0.0	0.0	0.0	77.0	0.0	0.0	0.0
0.0	0.0	0.0	0.0	78.0	0.0	0.0	0.0
0.0	0.0	0.0	0.0	79.0	0.0	0.0	0.0
0.0	0.0	0.0	0.0	80.0	0.0	0.0	0.0
0.0	0.0	0.0	0.0	81.0	0.0	0.0	0.0
0.0	0.0	0.0	0.0	82.0	0.0	0.0	0.0
0.0	0.0	0.0	0.0	83.0	0.0	0.0	0.0
0.0	0.0	0.0	0.0	84.0	0.0	0.0	0.0
0.0	0.0	0.0	0.0	85.0	0.0	0.0	0.0
0.0	0.0	0.0	0.0	86.0	0.0	0.0	0.0
0.0	0.0	0.0	0.0	87.0	0.0	0.0	0.0
0.0	0.0	0.0	0.0	88.0	0.0	0.0	0.0
0.0	0.0	0.0	0.0	89.0	0.0	0.0	0.0
0.0	0.0	0.0	0.0	90.0	0.0	0.0	0.0
0.0	0.0	0.0	0.0	91.0	0.0	0.0	0.0
0.0	0.0	0.0	0.0	92.0	0.0	0.0	0.0
0.0	0.0	0.0	0.0	93.0	0.0	0.0	0.0
0.0	0.0	0.0	0.0	94.0	0.0	0.0	0.0
0.0	0.0	0.0	0.0	95.0	0.0	0.0	0.0
0.0	0.0	0.0	0.0	96.0	0.0	0.0	0.0
0.0	0.0	0.0	0.0	97.0	0.0	0.0	0.0
0.0	0.0	0.0	0.0	98.0	0.0	0.0	0.0
0.0	0.0	0.0	0.0	99.0	0.0	0.0	0.0
0.0	0.0	0.0	0.0	100.0	0.0	0.0	0.0

\*\*\*\*\* ENERGY BALANCE \*\*\*\*\*  
 IC5W IS THE OVERALL CENTER TC TEMPERATURE IN DEG F  
 IC1W IS THE CALCULATED CENTER TC TEMPERATURE

\*\*\*\*\* TRANSIENT RESULT \*\*\*\*\*  
 CALIBRATION RUN NO. 1\*\* DATE: MAY 6 TIME: 14:51:14  
 TIME-TEMPERATURE-NODE TABLE:  
 TIME HAS UNITS OF SEC  
 Q HAS UNITS OF R/HR/DEGREE F=PPA\*QAVG  
 TEMPERATURE HAS UNITS OF DEG F  
 INTERFACE FLUX UNITS OF BTU/HR/FT\*\*2  
 IC5W IS THE OVERALL CENTER TC TEMPERATURE IN DEG F  
 IC1W IS THE CALCULATED CENTER TC TEMPERATURE

Y FROM 3.00000000E 02 TO 7.50000000E 02 AS A FUNCTION OF X FROM 0.0 TO 1.00000000E 01  
WITH Y INTERVAL SIZE 3.59999943E 00 AND WITH X INTERVAL SIZE 4.99999970E-02

THE X AXIS HAS BEEN SHIFTED FROM 0.0 TO Y = 3.00000000E 02



TC-3010 AND TC-301M  
CALIBRATION RUN NO. 411 DATE: SEP 9 TIME: 10:22Z

TIME-TEMPERATURE-NODE TABLE  
TIME HAS UNITS OF SEC  
Q HAS UNITS OF BTU/SEC/FT (PPPA\*GA/G)  
TEMPERATURE HAS UNITS OF DEG F  
INTEGRAL FLUX HAS UNITS OF BTU/HOUR/FT\*\*2  
TC3M IS THE ORIGINATOR CENTER TC TEMPERATURE IN DEG F  
TC1M IS THE CALCULATED CENTER TC TEMPERATURE

TIME--	Q	TC1M	TC3M	TIME--	Q	TC1M	TC3M
0.0	0.5500	658.7666	658.7666	1.0000	0.5500	657.9139	657.9139
0.0500	0.5500	658.7666	658.7666	1.0500	0.5500	657.9139	657.9139
0.1000	0.5500	658.7666	658.7666	1.1000	0.5500	657.9139	657.9139
0.1500	0.5500	658.7666	658.7666	1.1500	0.5500	657.9139	657.9139
0.2000	0.5500	658.7666	658.7666	1.2000	0.5500	657.9139	657.9139
0.2500	0.5500	658.7666	658.7666	1.2500	0.5500	657.9139	657.9139
0.3000	0.5500	658.7666	658.7666	1.3000	0.5500	657.9139	657.9139
0.3500	0.5500	658.7666	658.7666	1.3500	0.5500	657.9139	657.9139
0.4000	0.5500	658.7666	658.7666	1.4000	0.5500	657.9139	657.9139
0.4500	0.5500	658.7666	658.7666	1.4500	0.5500	657.9139	657.9139
0.5000	0.5500	658.7666	658.7666	1.5000	0.5500	657.9139	657.9139
0.5500	0.5500	658.7666	658.7666	1.5500	0.5500	657.9139	657.9139
0.6000	0.5500	658.7666	658.7666	1.6000	0.5500	657.9139	657.9139
0.6500	0.5500	658.7666	658.7666	1.6500	0.5500	657.9139	657.9139
0.7000	0.5500	658.7666	658.7666	1.7000	0.5500	657.9139	657.9139
0.7500	0.5500	658.7666	658.7666	1.7500	0.5500	657.9139	657.9139
0.8000	0.5500	658.7666	658.7666	1.8000	0.5500	657.9139	657.9139
0.8500	0.5500	658.7666	658.7666	1.8500	0.5500	657.9139	657.9139
0.9000	0.5500	658.7666	658.7666	1.9000	0.5500	657.9139	657.9139
0.9500	0.5500	658.7666	658.7666	1.9500	0.5500	657.9139	657.9139
1.0000	0.5500	658.7666	658.7666	2.0000	0.5500	657.9139	657.9139
1.0500	0.5500	658.7666	658.7666	2.0500	0.5500	657.9139	657.9139
1.1000	0.5500	658.7666	658.7666	2.1000	0.5500	657.9139	657.9139
1.1500	0.5500	658.7666	658.7666	2.1500	0.5500	657.9139	657.9139
1.2000	0.5500	658.7666	658.7666	2.2000	0.5500	657.9139	657.9139
1.2500	0.5500	658.7666	658.7666	2.2500	0.5500	657.9139	657.9139
1.3000	0.5500	658.7666	658.7666	2.3000	0.5500	657.9139	657.9139
1.3500	0.5500	658.7666	658.7666	2.3500	0.5500	657.9139	657.9139
1.4000	0.5500	658.7666	658.7666	2.4000	0.5500	657.9139	657.9139
1.4500	0.5500	658.7666	658.7666	2.4500	0.5500	657.9139	657.9139
1.5000	0.5500	658.7666	658.7666	2.5000	0.5500	657.9139	657.9139
1.5500	0.5500	658.7666	658.7666	2.5500	0.5500	657.9139	657.9139
1.6000	0.5500	658.7666	658.7666	2.6000	0.5500	657.9139	657.9139
1.6500	0.5500	658.7666	658.7666	2.6500	0.5500	657.9139	657.9139
1.7000	0.5500	658.7666	658.7666	2.7000	0.5500	657.9139	657.9139
1.7500	0.5500	658.7666	658.7666	2.7500	0.5500	657.9139	657.9139
1.8000	0.5500	658.7666	658.7666	2.8000	0.5500	657.9139	657.9139
1.8500	0.5500	658.7666	658.7666	2.8500	0.5500	657.9139	657.9139
1.9000	0.5500	658.7666	658.7666	2.9000	0.5500	657.9139	657.9139
1.9500	0.5500	658.7666	658.7666	2.9500	0.5500	657.9139	657.9139
2.0000	0.5500	658.7666	658.7666	3.0000	0.5500	657.9139	657.9139

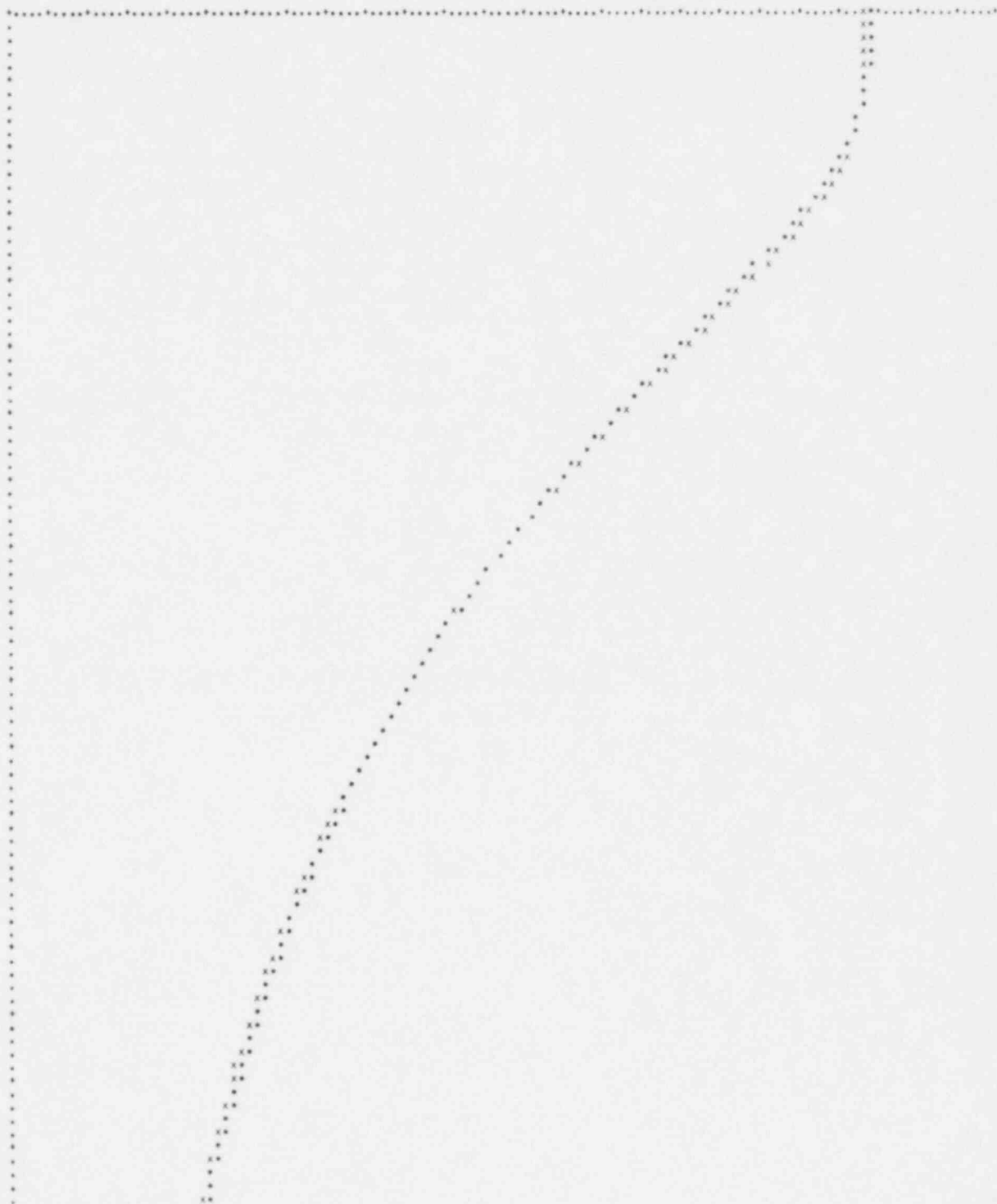
\*\*\*\*\*  
\*\*\*\*\*  
\*\*\*\*\*

TC-3010 AND TC-301M  
CALIBRATION RUN NO. 411 DATE: SEP 9 TIME: 10:22Z

CHANGE IN PIN INTERNAL ENERGY CENTER \* 4.62187 BTU/FT  
DETERMINED BY SUBTRACTION OF ORBITAL Q'S OVER THE INTERVAL FROM T4 TO TEND  
CHANGE IN PIN INTERNAL ENERGY CENTER \* 4.61755 BTU/FT  
DETERMINED BY DIFFERENCE IN PIN END POINT ENTHALPIES  
TOTAL HEAT INPUT \* INTEGRAL OF Q1\*DT \* 0.0  
BTU/FT  
INTERNAL OF SURFACE FLUX VERSUS TIME CURVE \* 2.08149 BTU/FT  
PERCENTAGE ERROR IN ORBITAL HEAT BALANCE \* 0.0030 PERCENT  
GROSS IN ORBITAL HEAT BALANCE (VIA METHOD 2) \* 0.0030 PERCENT  
VARIANCE FOR THIS RUN \* 3.02728512E 03

Y FROM 4.00000000E 02 TO 7.00000000E 02 AS A FUNCTION OF X FROM 0.0 TO 1.00000000E 01  
WITH Y INTERVAL SIZE 2.39999998E 00 AND WITH X INTERVAL SIZE 4.79999997E-02

THE X AXIS HAS BEEN SHIFTED FROM 0.0 TO Y = 4.79999998E 00



Appendix F

EXAMPLE OF ORTCAL - PART IV OUTPUT

Table F.1. ORTCAL - Part IV level regression for G level  
(at thermocouple position TE-318BG)

\*\*\*\*\*  
 \*\*\* THERMOCOUPLE NUMBER: TE-318BG \*\*\*  
 \*\*\*\*\*

## NOMENCLATURE:

Q(KW)/ROD = NOMINAL POWER INPUT PER ROD IN KW  
 DELTA R = GAP BETWEEN INNER AND OUTER S.S. SHEATHS (MILS OF INCHES)  
 TIME = WALL CLOCK TIME

## NOTE:

ASTERISK DENOTES BIAS POINT

RUN NO.	DATE TIME	Q(KW)/ROD	DELTA R (OBSERVED)	DELTA R (CALCULATED)	VARIANCE	WEIGHTING FACTOR
* 1.1	*****MAY	4*				
	23:36:56	30.3	0.04142	0.03970	0.960803E-05	1.0000
	23:44:18	40.1	0.03911	0.03891	0.217917E-05	1.0000
	23:53:20	40.5	0.03949	0.03886	0.173743E-05	1.0000
	* 0:29: 6	50.7	0.03795			
* 1.2	*****MAY	5*				
	14:31:56	40.7	0.03737	0.04566	0.987121E-04	1.0000
	14:50:53	50.7	0.03718	0.04440	0.444385E-04	1.0000
	15:39:21	50.6	0.03988	0.04387	0.289226E-04	1.0000
	15:56:45	60.9	0.03833	0.04293	0.174683E-04	1.0000
	16:18: 7	71.2	0.04007	0.04170	0.643215E-05	1.0000
	16:50:43	81.2	0.04084	0.04046	0.119112E-05	1.0000
	*17:13:10	91.6	0.03949			
* 1.3	*****MAY	5*				
	19:21:26	102.2	0.04026	0.04606	0.861626E-05	1.0000
	19:53:59	112.1	0.04045	0.04491	0.742836E-05	1.0000
	20:22:51	124.5	0.03988	0.04366	0.344360E-05	1.0000
	*21: 4:19	124.6	0.04296			
* 1.4	*****MAY	6*				
	12:35:24	91.6	0.03564	0.03755	0.136629E-04	1.0000
	12:57:41	91.5	0.03679	0.03737	0.161433E-04	1.0000
	13:35:46	91.4	0.03583	0.03732	0.324030E-05	1.0000
	*13:48:44	91.3	0.03699			
* 2.1	*****MAY	19*				
	4: 6: 2	30.6	0.04084	0.04471	0.954300E-04	1.0000
	4:28:22	41.0	0.03891	0.04382	0.688763E-04	1.0000
	5: 8:30	51.1	0.03833	0.04287	0.477013E-04	1.0000
	5:37:54	61.4	0.03679	0.04199	0.330631E-04	1.0000
	6: 0: 0	71.5	0.03467	0.04125	0.233608E-04	1.0000
	6:45:11	81.9	0.03506	0.04017	0.124695E-04	1.0000
	7: 5:50	91.8	0.03429	0.03931	0.687268E-05	1.0000
	7:35:54	102.0	0.03602	0.03798	0.128860E-05	1.0000
	* 8:37: 4	112.1	0.03679			
* 2.2	*****MAY	19*				
	22:42:55	30.7	0.04084	0.04691	0.415466E-04	1.0000
	23:10:47	40.9	0.04065	0.04594	0.338013E-04	1.0000
	23:32:51	51.1	0.03968	0.04499	0.297249E-04	1.0000
	23:57:45	61.3	0.03833	0.04408	0.276237E-04	1.0000
	0:31: 6	71.5	0.03776	0.04310	0.269016E-04	1.0000
	0:55:49	81.8	0.03622	0.04225	0.256004E-04	1.0000
	1:23: 3	91.9	0.03660	0.04116	0.292236E-04	1.0000
	2:30:44	102.2	0.03583	0.04021	0.310215E-04	1.0000
	2:55:20	112.3	0.03545	0.03928	0.334934E-04	1.0000
	3:18:32	124.3	0.03506	0.03815	0.385975E-04	1.0000
	4:35:52	124.2	0.03564	0.03806	0.148006E-04	1.0000
	7: 5:39	124.4	0.03487	0.03845	0.239017E-05	1.0000
	* 7:51:40	124.6	0.03795			
	8:15:29	112.2	0.03506	0.03975	0.375903E-05	1.0000
	8:41: 8	102.3	0.03718	0.04023	0.570144E-05	1.0000

Table F.1. (continued)

RUN NO.	DATE TIME	Q(KW)/ROD	DELTA R (OBSERVED)	DELTA R (CALCULATED)	VARIANCE	WEIGHTING FACTOR
	9:19:59	92.0	0.04045	0.04060	0.741463E-05	1.0000
	9:43:39	81.9	0.04122	0.04149	0.120243E-04	1.0000
	10: 7:36	71.5	0.04200	0.04245	0.177074E-04	1.0000
	10:31:29	61.3	0.04392	0.04331	0.234455E-04	1.0000
	10:55:49	50.5	0.04508	0.04437	0.329178E-04	1.0000
	11:19:26	40.7	0.04488	0.04548	0.467457E-04	1.0000
	11:44:10	30.3	0.04566	0.04662	0.652588E-04	1.0000
* 3.1	*****MAY	27*				
	1:14:13	30.7	0.04816	0.05432	0.499328E-04	1.0000
	1:36: 0	40.9	0.04450	0.05344	0.407959E-04	1.0000
	2: 2:32	51.1	0.04392	0.05236	0.332886E-04	1.0000
	2:23:56	61.4	0.04238	0.05139	0.294067E-04	1.0000
	2:45:31	71.6	0.04219	0.05027	0.280552E-04	1.0000
	3:11:21	81.8	0.04045	0.04935	0.257618E-04	1.0000
	3:32:41	92.0	0.03930	0.04841	0.262081E-04	1.0000
	4: 1:10	102.0	0.03911	0.04736	0.287727E-04	1.0000
	4:25:28	112.3	0.03949	0.04617	0.334042E-04	1.0000
	4:48:45	124.5	0.04026	0.04465	0.402958E-04	1.0000
	5:17: 8	124.4	0.04354	0.04396	0.217084E-04	1.0000
*	6:22:58	124.4	0.04431			
	6:49:48	111.9	0.04238	0.04605	0.359745E-05	1.0000
	7:31:58	101.9	0.04450	0.04664	0.633430E-05	1.0000
	8: 0:56	91.8	0.04585	0.04747	0.109428E-04	1.0000
	8:23:50	81.7	0.04700	0.04839	0.168949E-04	1.0000
	8:46:21	71.4	0.04951	0.04923	0.224316E-04	1.0000
	9: 9:52	61.4	0.05047	0.05031	0.309025E-04	1.0000
	9:42: 8	51.0	0.05220	0.05139	0.417148E-04	1.0000
	10: 4:17	40.8	0.05220	0.05269	0.593262E-04	1.0000
	10:26:10	30.7	0.05644	0.05370	0.763916E-04	1.0000
* 4.1	*****JUNE	17*				
	13:41: 8	30.7	0.05201	0.05375	0.457420E-04	1.0000
	14:36:24	61.3	0.05028	0.04985	0.392647E-05	1.0000
	*15: 7:57	92.0	0.04681			
* 4.2	*****JUNE	18*				
	9:12:26	30.7	0.04970	0.05022	0.436890E-04	1.0000
	9:53:33	61.4	0.04450	0.04688	0.146049E-04	1.0000
	10:27:42	92.1	0.04546	0.04326	0.847549E-05	1.0000
	11: 5:15	112.3	0.03718	0.04302	0.456798E-05	1.0000
	*11:40:33	124.3	0.04103			
* 5.1	*****JULY	8*				
	9:51:54	30.8	0.06415	0.06682	0.594177E-04	1.0000
	10:41:25	61.3	0.05875	0.06279	0.298462E-04	1.0000
	11:35:17	92.0	0.05490	0.05894	0.255009E-04	1.0000
	11:41: 1	91.9	0.05606	0.05875	0.259403E-04	1.0000
	*13:10: 5	124.3	0.05529			
* 6.1	*****AUG.	4*				
	9:59:10	30.8	0.05741	0.06645	0.639770E-04	1.0000
	11: 5: 4	62.0	0.05875	0.06176	0.333252E-04	1.0000
	11:39:36	91.9	0.05702	0.05793	0.186665E-04	1.0000
	12:13:36	124.2	0.05587	0.05439	0.179668E-06	1.0000
	*13:19: 7	124.1	0.05471			
* 7.1	*****AUG.	19*				
	16:44:27	30.6	0.06030	0.06406	0.593628E-04	1.0000
	17:55:35	51.0	0.05779	0.06114	0.363830E-04	1.0000
	19: 2:42	101.4	0.05548	0.05494	0.717888E-05	1.0000
	*20: 6:22	124.5	0.05278			
* 8.3	*****NOV.	5*				
	13:41:33	31.5	0.05509	0.06219	0.561584E-04	1.0000
	14: 9: 0	52.5	0.05143	0.05987	0.334900E-04	1.0000
	14:29:59	73.9	0.04912	0.05740	0.275390E-04	1.0000
	14:49:41	84.0	0.04797	0.05626	0.281170E-04	1.0000
	14:53:35	95.0	0.04739	0.05499	0.313488E-04	1.0000
	15: 9:45	105.4	0.04739	0.05371	0.380997E-04	1.0000

Table F.1. (continued)

RUN NO.	DATE TIME	Q(KW)/ROD	DELTA R (OBSERVED)	DELTA R (CALCULATED)	VARIANCE	WEIGHTING FACTOR
	15:44:12	104.6	0.04874	0.05388	0.945282E-05	1.0000
	16: 5: 0	109.1	0.04720	0.05370	0.776024E-05	1.0000
	16:18:35	113.8	0.04700	0.05327	0.532036E-05	1.0000
	*17: 5: 4	124.3	0.05124			
* 9.1	*****NOV. 19*					
	12:51:18	30.6	0.06338	0.06309	0.416382E-04	1.0000
	13:29:59	31.1	0.06376	0.06304	0.431213E-04	1.0000
	13:52:35	51.5	0.05895	0.06048	0.360512E-04	1.0000
	14:16:33	71.4	0.05509	0.05814	0.405910E-04	1.0000
	14:38:36	81.5	0.05394	0.05690	0.443367E-04	1.0000
	14:47:36	91.6	0.05240	0.05576	0.447510E-04	1.0000
	15: 2:29	102.0	0.05182	0.05447	0.527252E-04	1.0000
	15:21:34	101.6	0.05432	0.05406	0.216137E-04	1.0000
	15:38:27	101.4	0.05529	0.05408	0.547528E-05	1.0000
	*15:53:39	101.2	0.05452			
*10.1	*****DEC. 8*					
	11:25:18	31.3	0.06550	0.06613	0.368248E-04	1.0000
	11:47:24	41.5	0.06261	0.06478	0.297020E-04	1.0000
	12: 9:36	61.6	0.05818	0.06233	0.434830E-04	1.0000
	12:39: 8	82.1	0.05509	0.05981	0.479645E-04	1.0000
	13:27: 2	81.7	0.06049	0.05916	0.257772E-05	1.0000
	13:32:52	81.6	0.06030	0.05926	0.108497E-05	1.0000
	13:43:16	81.5	0.06030	0.05934	0.339670E-06	1.0000
	13:46: 3	81.5	0.05991	0.05941	0.130596E-06	1.0000
	*13:52:47	81.5	0.05953			
*11.1	*****JAN. 13*					
	13:49:36	30.8	0.07262	0.07053	0.390037E-04	1.0000
	14:12:27	51.3	0.06530	0.06789	0.366852E-04	1.0000
	14:34:40	81.7	0.06049	0.06385	0.489612E-04	1.0000
	14:53:30	81.5	0.06184	0.06356	0.182598E-04	1.0000
	15:17: 6	81.1	0.06319	0.06347	0.328581E-05	1.0000
	15:27:52	81.0	0.06357	0.06349	0.646596E-06	1.0000
	*15:36:42	80.9	0.06357			
*12.1	*****JAN. 27*					
	11:20:34	30.7	0.07262	0.07215	0.595116E-04	1.0000
	11:44:22	51.0	0.06839	0.06922	0.554169E-04	1.0000
	12: 8:16	81.6	0.06184	0.06520	0.739929E-04	1.0000
	12:33: 5	81.6	0.06357	0.06473	0.189223E-04	1.0000
	12:59:52	81.2	0.06473	0.06474	0.669309E-06	1.0000
	*13: 9:19	81.8	0.06473			
*13.1	*****FEB. 10*					
	10:33:25	30.8	0.06723	0.06921	0.396606E-04	1.0000
	10:54: 5	51.4	0.06107	0.06658	0.376076E-04	1.0000
	11:14: 1	61.0	0.05933	0.06533	0.363945E-04	1.0000
	11:25:44	71.3	0.05856	0.06389	0.350681E-04	1.0000
	11:40:22	81.7	0.05721	0.06257	0.341881E-04	1.0000
	12:15:12	81.3	0.05914	0.06236	0.910649E-05	1.0000
	*13:47: 8	81.6	0.06222			
*14.1	*****MAR. 9*					
	11:17:50	30.9	0.07763	0.06970	0.339477E-04	1.0000
	11:40: 0	51.2	0.06742	0.06714	0.350464E-04	1.0000
	12: 2:29	81.7	0.06049	0.06322	0.427391E-04	1.0000
	12:25: 4	81.4	0.06203	0.06298	0.223444E-04	1.0000
	12:49:10	81.1	0.06338	0.06289	0.743379E-05	1.0000
	13:18:51	81.0	0.06338	0.06319	0.554790E-07	1.0000
	*13:34:23	81.5	0.06319			
*15.1	*****MAR. 23*					
	10:32: 1	30.6	0.06742	0.06737	0.632996E-04	1.0000
	10:55:54	51.2	0.06280	0.06470	0.578178E-04	1.0000
	11:40: 2	81.5	0.06049	0.06017	0.836105E-05	1.0000
	12:21:39	101.9	0.05837	0.05790	0.193144E-06	1.0000
	*13: 8:45	101.9	0.05798			



Table F.1. (continued)

RUN NO.	DATE TIME	Q(KW)/ROD	DELTA R (OBSERVED)	DELTA R (CALCULATED)	VARIANCE	WEIGHTING FACTOR
*16.1	*****APR. 27*					
	12:28:55	30.7	0.07551	0.06634	0.496399E-04	1.0000
	12:55:12	51.2	0.06530	0.06383	0.376190E-04	1.0000
	13:21:11	87.8	0.05760	0.05932	0.389671E-04	1.0000
	14: 0:52	102.0	0.05664	0.05748	0.687718E-05	1.0000
	*14:42:59	101.8	0.05760			
*17.1	*****MAY 26*					
	11:23: 5	30.7	0.07763	0.07641	0.453552E-04	1.0000
	11:45:13	51.1	0.06742	0.07382	0.308533E-04	1.0000
	12: 9:15	89.4	0.05914	0.06896	0.226364E-04	1.0000
	12:35:46	101.8	0.05760	0.06776	0.455475E-05	1.0000
	12:52:17	101.8	0.05837	0.06790	0.254195E-05	1.0000
	13:10:40	101.7	0.06627	0.06665	0.445203E-08	1.0000
	*13:13:25	101.8	0.06646			
*18.1	*****JUNE 15*					
	16:53:51	30.6	0.07513	0.07067	0.375023E-04	1.0000
	17:17:18	51.0	0.06877	0.06760	0.857048E-05	1.0000
	17:36:32	81.7	0.06338	0.06363	0.234771E-05	1.0000
	17:54:39	81.5	0.06415	0.06371	0.824472E-08	1.0000
	*18: 7:50	81.5	0.06376			
*19.1	*****JUNE 29*					
	12: 8:50	30.6	0.07397	0.06460	0.371338E-04	1.0000
	12:31:59	51.0	0.06935	0.06144	0.135704E-04	1.0000
	13: 6:26	81.7	0.06164	0.05766	0.117737E-04	1.0000
	13:31:46	101.8	0.05664	0.05616	0.123965E-06	1.0000
	*13:40:39	101.8	0.05625			
*20.1	*****AUG. 22*					
	11:41:52	30.5	0.08438	0.07445	0.479370E-04	1.0000
	12: 5:46	51.9	0.07744	0.07104	0.169269E-04	1.0000
	12:35:35	81.6	0.06993	0.06693	0.403976E-05	1.0000
	13: 1:53	101.8	0.06530	0.06484	0.202356E-07	1.0000
	*13:21:45	101.8	0.06492			
*21.1	*****SEPT. 21*					
	11:49:40	30.9	0.08611	0.07271	0.322082E-04	1.0000
	12:10:45	51.4	0.07686	0.06955	0.125999E-04	1.0000
	12:43:59	71.9	0.07156	0.06670	0.404892E-05	1.0000
	15:20:14	91.8	0.06492	0.06493	0.283326E-09	1.0000
	*15:22: 6	91.8	0.06492			
*22.1	*****OCT. 12*					
	11:48:40	31.1	0.07860	0.06990	0.345103E-04	1.0000
	12:17:55	80.7	0.06704	0.06267	0.187099E-04	1.0000
	12:29:23	101.9	0.06203	0.06053	0.896044E-05	1.0000
	12:50:23	102.0	0.06049	0.06117	0.177920E-07	1.0000
	*13: 0:25	102.0	0.06107			
*23.1	*****NOV. 30*					
	11:22: 7	31.1	0.07648	0.07230	0.412720E-04	1.0000
	11:41:15	51.8	0.06896	0.06939	0.231342E-04	1.0000
	11:58:35	72.4	0.06550	0.06641	0.143703E-04	1.0000
	12:19:17	101.9	0.06126	0.06300	0.370245E-05	1.0000
	12:38:44	101.7	0.06222	0.06310	0.275060E-07	1.0000
	*12:44:28	101.7	0.06299			
*23.2	*****DEC. 15*					
	10: 5:18	31.0	0.07417	0.07043	0.389465E-04	1.0000
	10:27:17	61.5	0.06704	0.06595	0.142475E-04	1.0000
	10:39: 4	61.6	0.06704	0.06592	0.131172E-04	1.0000
	11: 9:20	102.1	0.06107	0.06122	0.325414E-06	1.0000
	11:16:15	102.2	0.05991	0.06154	0.817671E-07	1.0000
	*11:23:26	102.1	0.06126			
*23.3	*****JAN. 19*					
	15: 7: 0	31.0	0.07917	0.06932	0.344421E-04	1.0000
	15:28:51	51.9	0.07070	0.06637	0.175449E-04	1.0000
	15:48:34	82.4	0.06511	0.06242	0.603905E-05	1.0000
	16:13:41	101.8	0.06194	0.06049	0.587538E-07	1.0000
	*16:17:13	101.9	0.06068			

Table F.1. (continued)

RUN NO.	DATE TIME	Q(KW)/ROD	DELTA R (OBSERVED)	DELTA R (CALCULATED)	VARIANCE	WEIGHTING FACTOR
*24.1	*****FFR. 15*					
	10:42: 1	30.5	0.07128	0.06977	0.407776E-04	1.0000
	11: 8:40	51.2	0.06665	0.06671	0.178997E-04	1.0000
	11:28:20	72.1	0.06338	0.06396	0.938186E-05	1.0000
	12:29: 8	102.0	0.05933	0.06065	0.575870E-07	1.0000
	*12:50:11	102.0	0.06049			

\*\*\*\*\*  
 SHEATH GAP THERMAL EXPANSION MODEL REGRESSION PROGRAM  
 \*\*\*\*\*

( AT THERMOCOUPLE POWER LEVEL G )

BEST FIT PARAMETERS FOR THERMAL EXPANSION MODEL:

WHERE,

$$L-L_0 = L_0 * ( C(1) * (T-T_0) + C(2) * (T**2 - T_0**2) + C(3) * (T**3 - T_0**3) ) - 1.0$$

$$C(1) = -0.75735846E-01$$

$$\text{STD DEVIATION} = 0.31148357E-01$$

$$C(2) = 0.18951051E-01$$

$$\text{STD DEVIATION} = 0.43889806E-02$$

$$C(3) = -0.81113449E-05$$

$$\text{STD DEVIATION} = 0.21466240E-05$$

VARIANCE OF FIT = 0.50953846E-01

VARIANCE OF FIT DIVIDED BY THE SUM OF THE WEIGHTING FACTORS = 0.16165548E-04

TOTAL NUMBER OF DATA POINTS = 3691

Table F.2. ORTCAL - Part IV individual regression for TE-318BG

\*\*\*\*\*  
 \*\*\* THERMOCOUPLE NUMBER: TE-318BG \*\*\*  
 \*\*\*\*\*

## NOMENCLATURE:

Q(KW)/ROD = NOMINAL POWER INPUT PER ROD IN KW

DELTA R = GAP BETWEEN INNER AND OUTER S.S. SHEATHS (MILS OF INCHES)

TIME = WALL CLOCK TIME

## NOTE:

ASTERISK DENOTES BIAS POINT

RUN NO.	DATE TIME	Q(KW)/ROD	DELTA R (OBSERVED)	DELTA R (CALCULATED)	VARIANCE	WEIGHTING FACTOR
* 1.1	*****MAY	4*				
	23:36:56	30.3	0.04142	0.04044	0.802082E-04	1.0000
	23:44:18	40.1	0.03911	0.03923	0.178631E-04	1.0000
	23:53:20	40.5	0.03949	0.03910	0.144493E-04	1.0000
	* 0:29: 6	50.7	0.03795			
* 1.2	*****MAY	5*				
	14:31:56	40.7	0.03737	0.04525	0.128405E-02	1.0000
	14:50:53	50.7	0.03718	0.04432	0.517181E-03	1.0000
	15:39:21	50.6	0.03988	0.04452	0.246157E-03	1.0000
	15:56:45	60.9	0.03833	0.04346	0.146777E-03	1.0000
	16:18: 7	71.2	0.04007	0.04174	0.628921E-04	1.0000
	16:50:43	81.2	0.04084	0.04040	0.121914E-04	1.0000
	*17:13:10	91.6	0.03949			
* 1.3	*****MAY	5*				
	19:21:26	102.2	0.04026	0.04496	0.683349E-04	1.0000
	19:53:59	112.1	0.04045	0.04374	0.614502E-04	1.0000
	20:22:51	124.5	0.03988	0.04284	0.284077E-04	1.0000
	*21: 4:19	124.7	0.04296			
* 1.4	*****MAY	6*				
	12:35:24	91.6	0.03564	0.03683	0.188314E-03	1.0000
	12:57:41	91.5	0.03679	0.03652	0.217104E-03	1.0000
	13:35:46	91.4	0.03583	0.03698	0.449411E-04	1.0000
	*13:48:44	91.3	0.03699			
* 2.1	*****MAY	19*				
	4: 6: 2	30.6	0.04084	0.04607	0.782336E-03	1.0000
	4:28:22	41.0	0.03891	0.04476	0.574933E-03	1.0000
	5: 8:30	51.1	0.03833	0.04346	0.407281E-03	1.0000
	5:37:54	61.4	0.03679	0.04239	0.282239E-03	1.0000
	6: 0: 0	71.5	0.03467	0.04156	0.196454E-03	1.0000
	6:45:11	81.9	0.03506	0.04031	0.105048E-03	1.0000
	7: 5:50	91.8	0.03429	0.03946	0.557499E-04	1.0000
	7:35:54	102.0	0.03602	0.03797	0.105011E-04	1.0000
	* 8:37: 4	112.1	0.03679			
* 2.2	*****MAY	19*				
	22:42:55	30.7	0.04084	0.04554	0.291211E-03	1.0000
	23:10:47	40.9	0.04065	0.04406	0.233203E-03	1.0000
	23:32:51	51.1	0.03968	0.04277	0.208484E-03	1.0000
	23:57:45	61.3	0.03833	0.04165	0.200134E-03	1.0000
	0:31: 6	71.5	0.03776	0.04050	0.204620E-03	1.0000
	0:55:49	81.8	0.03622	0.03959	0.207294E-03	1.0000
	1:23: 3	91.9	0.03660	0.03840	0.250818E-03	1.0000
	2:30:44	102.2	0.03583	0.03748	0.281653E-03	1.0000
	2:55:20	112.3	0.03545	0.03663	0.316406E-03	1.0000
	3:18:32	124.3	0.03506	0.03558	0.368756E-03	1.0000
	4:35:52	124.2	0.03564	0.03660	0.184107E-03	1.0000
	7: 5:39	124.4	0.03487	0.03798	0.453838E-04	1.0000
	* 7:51:40	124.6	0.03795			
	8:15:29	112.2	0.03506	0.03984	0.437794E-04	1.0000
	8:41: 8	102.3	0.03718	0.04019	0.791015E-04	1.0000

Table F.2. (continued)

RUN NO.	DATE TIME	Q(KW)/ROD	DELTA R (OBSERVED)	DELTA R (CALCULATED)	VARIANCE	WEIGHTING FACTOR
	9:19:59	92.0	0.04045	0.04043	0.115594E-03	1.0000
	9:43:39	81.9	0.04122	0.04124	0.181622E-03	1.0000
	10: 7:36	71.5	0.04200	0.04215	0.252631E-03	1.0000
	10:31:29	61.3	0.04392	0.04299	0.313568E-03	1.0000
	10:55:49	50.5	0.04508	0.04411	0.398950E-03	1.0000
	11:19:26	40.7	0.04488	0.04537	0.515259E-03	1.0000
	11:44:10	30.3	0.04566	0.04671	0.667382E-03	1.0000
* 3.1	*****MAY	27*				
	1:14:13	30.7	0.04816	0.05277	0.353027E-03	1.0000
	1:36: 0	40.9	0.04450	0.05145	0.281836E-03	1.0000
	2: 2:32	51.1	0.04392	0.05004	0.231445E-03	1.0000
	2:23:56	61.4	0.04238	0.04883	0.212988E-03	1.0000
	2:45:31	71.6	0.04219	0.04752	0.218536E-03	1.0000
	3:11:21	81.8	0.04045	0.04558	0.221924E-03	1.0000
	3:32:41	92.0	0.03930	0.04564	0.247467E-03	1.0000
	4: 1:10	102.0	0.03911	0.04459	0.289929E-03	1.0000
	4:25:28	112.3	0.03949	0.04344	0.347113E-03	1.0000
	4:48:45	124.5	0.04026	0.04203	0.416290E-03	1.0000
	5:17: 8	124.4	0.04354	0.04230	0.258202E-03	1.0000
* 6:22:58		124.4	0.04431			
	6:49:48	111.9	0.04238	0.04611	0.448688E-04	1.0000
	7:31:58	101.9	0.04450	0.04657	0.948120E-04	1.0000
	8: 0:56	91.8	0.04595	0.04729	0.168384E-03	1.0000
	8:23:50	81.7	0.04700	0.04815	0.256750E-03	1.0000
	8:46:21	71.4	0.04951	0.04890	0.332355E-03	1.0000
	9: 9:52	61.4	0.05047	0.04995	0.425995E-03	1.0000
	9:42: 8	51.0	0.05220	0.05110	0.526923E-03	1.0000
	10: 4:17	40.8	0.05220	0.05255	0.678808E-03	1.0000
	10:26:10	30.7	0.05644	0.05371	0.817382E-03	1.0000
* 4.1	*****JUNE	17*				
	13:41: 8	30.7	0.05201	0.05247	0.418396E-03	1.0000
	14:36:24	61.3	0.05028	0.04928	0.336731E-04	1.0000
	*15: 7:57	92.0	0.04681			
* 4.2	*****JUNE	18*				
	9:12:26	30.7	0.04970	0.04850	0.302637E-03	1.0000
	9:53:33	61.4	0.04450	0.04518	0.168420E-03	1.0000
	10:27:42	92.1	0.04546	0.04217	0.170636E-03	1.0000
	11: 5:15	112.3	0.03718	0.04306	0.580364E-04	1.0000
	*11:40:33	124.3	0.04103			
* 5.1	*****JULY	8*				
	9:51:54	30.8	0.06415	0.06477	0.447656E-03	1.0000
	10:41:25	61.3	0.05875	0.05990	0.308789E-03	1.0000
	11:35:17	92.0	0.05490	0.05672	0.459228E-03	1.0000
	11:41: 1	91.9	0.05606	0.05653	0.461855E-03	1.0000
	*13:10: 5	124.3	0.05529			
* 6.1	*****AUG.	4*				
	9:59:10	30.8	0.05741	0.06457	0.475781E-03	1.0000
	11: 5: 4	62.0	0.05875	0.06046	0.561328E-03	1.0000
	11:39:36	91.9	0.05702	0.05663	0.391681E-03	1.0000
	12:13:36	124.2	0.05587	0.05432	0.145354E-05	1.0000
	*13:19: 7	124.1	0.05471			
* 7.1	*****AUG.	19*				
	16:44:27	30.6	0.06030	0.06211	0.426855E-03	1.0000
	17:55:35	51.0	0.05779	0.05977	0.487793E-03	1.0000
	19: 2:42	101.4	0.05548	0.05462	0.136780E-03	1.0000
	*20: 6:22	124.5	0.05278			
* 8.3	*****NOV.	5*				
	13:41:33	31.5	0.05509	0.06060	0.443554E-03	1.0000
	14: 9: 0	52.5	0.05143	0.05731	0.259277E-03	1.0000
	14:29:59	73.9	0.04912	0.05451	0.271582E-03	1.0000
	14:49:41	84.0	0.04797	0.05334	0.311352E-03	1.0000
	14:53:35	95.0	0.04739	0.05207	0.372015E-03	1.0000
	15: 9:45	105.4	0.04739	0.05075	0.446100E-03	1.0000

Table F.2. (continued)

RUN NO.	DATE TIME	Q(KW)/ROD	DELTA R (OBSERVED)	DELTA R (CALCULATED)	VARIANCE	WEIGHTING FACTOR
	15:44:12	104.6	0.04874	0.05357	0.170746E-03	1.0000
	16: 5: 0	109.1	0.04720	0.05361	0.120959E-03	1.0000
	16:18:35	113.8	0.04700	0.05322	0.812439E-04	1.0000
	*17: 5: 4	124.3	0.05124			
* 9.1	*****NOV. 18*					
	12:51:18	30.6	0.06338	0.06131	0.293555E-03	1.0000
	13:29:59	31.1	0.06376	0.06113	0.309668E-03	1.0000
	13:52:35	51.5	0.05895	0.05778	0.273614E-03	1.0000
	14:16:33	71.4	0.05509	0.05507	0.327447E-03	1.0000
	14:38:36	81.5	0.05394	0.05381	0.369049E-03	1.0000
	14:47:36	91.6	0.05240	0.05279	0.386517E-03	1.0000
	15: 2:29	102.0	0.05182	0.05155	0.461792E-03	1.0000
	15:21:34	101.6	0.05432	0.05233	0.221013E-03	1.0000
	15:38:27	101.4	0.05529	0.05333	0.629185E-04	1.0000
	*15:53:39	101.2	0.05452			
*10.1	*****DEC. 9*					
	11:25:18	31.3	0.06550	0.06424	0.301208E-03	1.0000
	11:47:24	41.5	0.06261	0.06261	0.238824E-03	1.0000
	12: 9:36	61.6	0.05818	0.05950	0.367694E-03	1.0000
	12:39: 8	82.1	0.05509	0.05703	0.402667E-03	1.0000
	13:27: 2	81.7	0.05049	0.05862	0.265767E-04	1.0000
	13:32:52	81.6	0.06030	0.05894	0.113682E-04	1.0000
	13:43:16	81.5	0.06020	0.05917	0.349899E-05	1.0000
	13:46: 3	81.5	0.05991	0.05931	0.132078E-05	1.0000
	*13:52:47	81.5	0.05953			
*11.1	*****JAN. 13*					
	13:49:36	30.8	0.07262	0.06918	0.327338E-03	1.0000
	14:12:27	51.3	0.06530	0.06564	0.334845E-03	1.0000
	14:34:40	81.7	0.06049	0.06118	0.422040E-03	1.0000
	14:53:30	81.5	0.06184	0.06188	0.153775E-03	1.0000
	15:17: 6	81.1	0.06319	0.06276	0.300522E-04	1.0000
	15:27:52	81.0	0.06357	0.06319	0.628595E-05	1.0000
	*15:36:42	80.9	0.06357			
*12.1	*****JAN. 27*					
	11:20:34	30.7	0.07262	0.07037	0.564368E-03	1.0000
	11:44:22	51.0	0.06839	0.06655	0.532947E-03	1.0000
	12: 8:16	81.6	0.06184	0.06201	0.655462E-03	1.0000
	12:33: 5	81.6	0.06357	0.06300	0.159597E-03	1.0000
	12:59:52	81.2	0.06472	0.06440	0.692754E-05	1.0000
	*13: 9:19	81.8	0.06473			
*13.1	*****FEB. 10*					
	10:33:25	30.8	0.06723	0.06718	0.318530E-03	1.0000
	10:54: 5	51.4	0.06107	0.06390	0.308972E-03	1.0000
	11:14: 1	61.0	0.05933	0.06259	0.297473E-03	1.0000
	11:25:44	71.3	0.05856	0.06123	0.291705E-03	1.0000
	11:40:22	81.7	0.05721	0.06012	0.294818E-03	1.0000
	12:15:12	81.3	0.05914	0.06115	0.100449E-03	1.0000
	*13:47: 8	81.6	0.06222			
*14.1	*****MAR. 9*					
	11:17:50	30.9	0.07763	0.06771	0.267004E-03	1.0000
	11:40: 0	51.2	0.06742	0.06451	0.287384E-03	1.0000
	12: 2:29	81.7	0.06049	0.06060	0.361560E-03	1.0000
	12:25: 4	81.4	0.06203	0.06111	0.201593E-03	1.0000
	12:49:10	81.1	0.06338	0.06189	0.766445E-04	1.0000
	13:18:51	81.0	0.06338	0.06311	0.781734E-06	1.0000
	*13:34:23	81.5	0.06319			
*15.1	*****MAR. 23*					
	10:32: 1	30.6	0.06742	0.06567	0.501562E-03	1.0000
	10:55:54	51.2	0.06280	0.06193	0.500354E-03	1.0000
	11:40: 2	81.5	0.06049	0.05862	0.923950E-04	1.0000
	12:21:39	101.9	0.05837	0.05775	0.209945E-05	1.0000
	*13: 8:45	101.9	0.05798			

Table F.2. (continued)

RUN NO.	DATE TIME	Q(KW)/ROD	DELTA R (OBSERVED)	DELTA R (CALCULATED)	VARIANCE	WEIGHTING FACTOR
*16.1	*****APR. 27*					
	12:28:55	37.7	0.07551	0.06468	0.373535E-03	1.0000
	12:55:12	51.2	0.06530	0.06139	0.295129E-03	1.0000
	13:21:11	87.8	0.05760	0.05653	0.323968E-03	1.0000
	14: 0:52	102.0	0.05664	0.05647	0.722832E-04	1.0000
	*14:42:58	101.8	0.05760			
*17.1	*****MAY 26*					
	11:23: 5	30.7	0.07763	0.07437	0.321093E-03	1.0000
	11:45:13	51.1	0.06742	0.07108	0.235547E-03	1.0000
	12: 9:15	89.4	0.05914	0.06668	0.312597E-03	1.0000
	12:35:46	101.8	0.05760	0.06722	0.960571E-04	1.0000
	12:52:17	101.8	0.05837	0.06797	0.308796E-04	1.0000
	13:10:40	101.7	0.06627	0.06665	0.432931E-07	1.0000
	*13:13:25	101.8	0.06646			
*18.1	*****JUNE 15*					
	16:53:51	30.6	0.07513	0.06908	0.308057E-03	1.0000
	17:17:18	51.0	0.06877	0.06622	0.624206E-04	1.0000
	17:36:32	81.7	0.06338	0.06304	0.234145E-04	1.0000
	17:54:39	81.5	0.06415	0.06370	0.695318E-07	1.0000
	*18: 7:50	81.5	0.06376			
*19.1	*****JUNE 29*					
	12: 8:50	30.6	0.07397	0.06254	0.256347E-03	1.0000
	12:31:59	51.0	0.06935	0.05953	0.149579E-03	1.0000
	13: 6:26	81.7	0.06164	0.05616	0.178693E-03	1.0000
	13:31:46	101.8	0.05664	0.05606	0.152226E-05	1.0000
	*13:40:39	101.8	0.05625			
*20.1	*****AUG. 22*					
	11:41:52	30.5	0.08438	0.07316	0.338672E-03	1.0000
	12: 5:46	51.9	0.07744	0.06920	0.131470E-03	1.0000
	12:35:35	81.6	0.06993	0.06608	0.773254E-04	1.0000
	13: 1:53	101.8	0.06530	0.06481	0.169650E-06	1.0000
	*13:21:45	101.8	0.06492			
*21.1	*****SEP. 21*					
	11:49:40	30.9	0.08611	0.07086	0.223242E-03	1.0000
	12:10:45	51.4	0.07686	0.06766	0.115301E-03	1.0000
	12:43:59	71.9	0.07166	0.06591	0.805847E-04	1.0000
	15:20:14	91.8	0.06492	0.06494	0.525210E-08	1.0000
	*15:22: 6	91.8	0.06492			
*22.1	*****OCT. 12*					
	11:48:40	31.1	0.07860	0.06801	0.251074E-03	1.0000
	12:17:55	80.7	0.06704	0.06075	0.261713E-03	1.0000
	12:29:23	101.9	0.06203	0.05960	0.109566E-03	1.0000
	12:50:23	102.0	0.06049	0.06115	0.345898E-06	1.0000
	*13: 0:25	102.0	0.06107			
*23.1	*****NOV. 30*					
	11:22: 7	31.1	0.07648	0.07029	0.286230E-03	1.0000
	11:41:15	51.8	0.06896	0.06692	0.192059E-03	1.0000
	11:58:35	72.4	0.06550	0.06451	0.227325E-03	1.0000
	12:19:17	101.9	0.06126	0.06240	0.559753E-04	1.0000
	12:38:44	101.7	0.06222	0.06311	0.285530E-06	1.0000
	*12:44:28	101.7	0.06299			
*23.2	*****DEC. 15*					
	10: 5:18	31.0	0.07417	0.06856	0.273926E-03	1.0000
	10:27:17	51.5	0.06704	0.06396	0.196527E-03	1.0000
	10:39: 4	61.6	0.06704	0.06417	0.207092E-03	1.0000
	11: 9:20	102.1	0.06107	0.06106	0.485437E-05	1.0000
	11:16:15	102.2	0.05991	0.06154	0.739574E-06	1.0000
	*11:23:26	102.1	0.06126			
*23.3	*****JAN. 19*					
	15: 7: 0	31.0	0.07917	0.06806	0.312597E-03	1.0000
	15:28:51	51.9	0.07070	0.06522	0.269000E-03	1.0000
	15:48:34	82.4	0.06511	0.06168	0.126416E-03	1.0000
	16:13:41	101.8	0.06184	0.06045	0.488448E-06	1.0000
	*16:17:13	101.9	0.06048			

Table F.2. (continued)

RUN NO.	DATE TIME	Q(KW)/ROD	DELTA P (OBSERVED)	DELTA R (CALCULATED)	VARIANCE	WEIGHTING FACTOR
*24.1	*****FEB. 15*					
	10:42: 1	30.5	0.07128	0.06833	0.299707E-03	1.0000
	11: 8:40	51.2	0.06665	0.06549	0.230164E-03	1.0000
	11:28:20	72.1	0.06338	0.06300	0.181000E-03	1.0000
	12:29: 8	102.0	0.05933	0.06066	0.595021E-06	1.0000
	*12:50:11	102.0	0.06049			

BEST FIT PARAMETERS FOR THERMAL EXPANSION MODEL:

WHERE,

$$L-L_0 = L_0 * (C(1) * (T-T_0) + C(2) * (T**2 - T_0**2) + C(3) * (T**3 - T_0**3)) - 1.0$$

$$C(1) = 0.62502546E-01$$

$$\text{STD DEVIATION} = 0.12002551E-02$$

$$C(2) = 0.60506764E-02$$

$$\text{STD DEVIATION} = 0.17433237E-01$$

$$C(3) = -0.43716855E-05$$

$$\text{STD DEVIATION} = 0.87200751E-05$$

VARIANCE OF FIT = 0.14908461E-01

VARIANCE OF FIT DIVIDED BY THE SUM OF THE WEIGHTING FACTORS = 0.81365113E-04

TOTAL NUMBER OF DATA POINTS = 213

Table F.3. Summary of ORTCAL - Part IV regression  
for TE position 318BG

```
*****  
*** THERMOCOUPLE NUMBER: TE-318BG ***  
*****
```

SUMMARY:

```
LEVEL REGRESSION---NO ERRORS  
INDIVIDUAL T/C REGRESSION---NO ERRORS  
THE FIRST DERIVATIVES OF BOTH SOLUTIONS ARE POSITIVE AT ALL BIAS POINTS.  
SUMMATION OF VARIANCES FOR BOTH SOLUTIONS:  
  BY LEVEL SOLUTION= 0.36986982E-02  
  BY INDIVIDUAL T/C SOLUTION= 0.31808661E-02
```



Table F.4. Summary of ORTCAL -- Part IV regressions  
for THTF bundle 1 through Run 24.1

\*\*\*\*\*  
\*\*\*LEVEL A \*\*\*  
\*\*\*\*\*

(THTF BUNDLE NUMBER 1 DOES NOT HAVE ROD THERMOCOUPLES ON THIS LEVEL)

\*\*\*\*\*  
\*\*\*LEVEL B \*\*\*  
\*\*\*\*\*

(THTF BUNDLE NUMBER 1 DOES NOT HAVE ROD THERMOCOUPLES ON THIS LEVEL)

\*\*\*\*\*  
\*\*\*LEVEL C \*\*\*  
\*\*\*\*\*

(THTF BUNDLE NUMBER 1 DOES NOT HAVE ROD THERMOCOUPLES ON THIS LEVEL)

\*\*\*\*\*  
\*\*\*LEVEL D \*\*\*  
\*\*\*\*\*

INDIVIDUAL THERMOCOUPLE LISTING:

T/C NO.	TYPE OF REGRESSION	C(1)	C(2)	C(3)	TMAX
301AD	FAILED				
304AD	FAILED				
309AD	FAILED				
310AD	INDIVIDUAL	-40.145	0.10251	-0.554344E-04	753.8
312AD	FAILED				
313AD	INDIVIDUAL	-78.915	0.15663	-0.834799E-04	733.8
317AD	INDIVIDUAL	-46.153	0.09332	-0.481768E-04	702.8
318AD	FAILED				
320AD	FAILED				
322AD	INDIVIDUAL	-22.445	0.04177	-0.839944E-05	680.1
323AD	INDIVIDUAL	22.742	-0.01605	0.102341E-04	706.8
325AD	INDIVIDUAL	-73.235	0.14489	-0.751986E-04	697.7
326AD	FAILED				
331AD	FAILED				
338AD	FAILED				
339AD	FAILED				
341AD	INDIVIDUAL	-42.871	0.08579	-0.454424E-04	700.5
349AD	FAILED				
324AD	DEAD				
333AD	DEAD				
330AD	METRASCOPE				
332AD	METRASCOPE				
334AD	METRASCOPE				
319AD	METRASCOPE				

TOTAL NUMBER OF INDIVIDUAL T/C REGRESSIONS= 7  
MEAN REGRESSION COEFFICIENTS: -40.145 0.08698 -0.436996E-04

\*\*THERE WERE NO LEVEL T/C REGRESSIONS AVAILABLE IN THE COT ARRAYS.

Table F.4. (continued)

\*\*\*\*\*  
 \*\*\*LEVEL E \*\*\*  
 \*\*\*\*\*

## INDIVIDUAL THERMOCOUPLE LISTING:

T/C NO.	TYPE OF REGRESSION	C(1)	C(2)	C(3)	TMAX
301AE	LEVEL				
304AE	INDIVIDUAL	-12.477	0.02524	-0.117173E-04	732.9
309AE	INDIVIDUAL	-15.172	0.03732	-0.188683E-04	750.0
312AE	INDIVIDUAL	1.700	0.01745	-0.118790E-04	805.3
313AE	INDIVIDUAL	-23.179	0.06178	-0.326217E-04	767.2
317AE	INDIVIDUAL	-3.335	0.03144	-0.181708E-04	760.8
318AE	INDIVIDUAL	-24.553	0.04865	-0.243825E-04	747.1
320AE	INDIVIDUAL	9.150	0.01445	-0.102358E-04	783.6
322AE	INDIVIDUAL	-33.075	0.06626	-0.283788E-04	730.3
323AE	INDIVIDUAL	44.742	-0.04066	0.223233E-04	738.1
324AE	INDIVIDUAL	-53.540	0.09497	-0.471450E-04	737.4
325AE	INDIVIDUAL	-38.113	0.08856	-0.456615E-04	738.9
326AE	INDIVIDUAL	-49.722	0.09929	-0.560044E-04	750.7
331AE	INDIVIDUAL	-27.586	0.05592	-0.265679E-04	750.6
333AE	INDIVIDUAL	-24.444	0.04972	-0.259172E-04	729.8
338AE	INDIVIDUAL	-48.352	0.08909	-0.480215E-04	723.5
339AE	LEVEL				
341AE	INDIVIDUAL	26.910	-0.01910	0.809371E-05	765.2
349AE	LEVEL				
310AE	DEAD				
330AE	METRASCOPE				
332AE	METRASCOPE				
334AE	METRASCOPE				
319AE	METRASCOPE				

TOTAL NUMBER OF INDIVIDUAL T/C REGRESSIONS= 16  
 MEAN REGRESSION COEFFICIENTS: -16.940 0.04502 -0.234471E-04

LEVEL REGRESSION COEFFICIENTS: -34.541 0.07141 -0.380442E-04

\*\*\*\*\*  
 \*\*\*LEVEL F \*\*\*  
 \*\*\*\*\*

## INDIVIDUAL THERMOCOUPLE LISTING:

T/C NO.	TYPE OF REGRESSION	C(1)	C(2)	C(3)	TMAX
301BF	INDIVIDUAL	27.830	-0.04133	0.234332E-04	839.6
304BF	INDIVIDUAL	47.101	-0.07012	0.396057E-04	789.2
309BF	INDIVIDUAL	40.691	-0.05123	0.278024E-04	815.6
310BF	INDIVIDUAL	29.594	-0.02492	0.149031E-04	867.8
312BF	INDIVIDUAL	38.644	-0.03982	0.235163E-04	844.9
313BF	INDIVIDUAL	15.654	-0.00410	0.488843E-05	832.6
317BF	INDIVIDUAL	66.609	-0.08061	0.419395E-04	829.0
320BF	INDIVIDUAL	20.451	-0.01351	0.760119E-05	848.7
322BF	INDIVIDUAL	-5.305	0.01975	-0.634452E-05	834.7
323BF	INDIVIDUAL	30.344	-0.02199	0.118078E-04	840.1
324BF	INDIVIDUAL	-26.506	0.04789	-0.174963E-04	798.1
325BF	INDIVIDUAL	4.604	0.01245	-0.932566E-06	823.7
326BF	INDIVIDUAL	24.905	-0.02847	0.139857E-04	813.3

Table F.4. (continued)

T/C NO.	TYPE OF REGRESSION	C(1)	C(2)	C(3)	TMAX
331BF	LEVEL				
333BF	INDIVIDUAL	13.323	-0.01177	0.755858E-05	799.8
338BF	INDIVIDUAL	38.478	-0.04941	0.253618E-04	814.7
341BF	INDIVIDUAL	44.908	-0.04935	0.241982E-04	865.2
349BF	LEVEL				
318BF	DEAD				
339BF	DEAD				
330BF	METRASCOPE				
332BF	METRASCOPE				
334BF	METRASCOPE				
319BF	METRASCOPE				

TOTAL NUMBER OF INDIVIDUAL T/C REGRESSIONS= 16  
 MEAN REGRESSION COEFFICIENTS: 25.708 -0.02541 0.151143E-04

LEVEL REGRESSION COEFFICIENTS: 13.754 -0.01112 0.937150E-05

\*\*\*\*\*  
 \*\*\*LEVEL G \*\*\*  
 \*\*\*\*\*

## INDIVIDUAL THERMOCOUPLE LISTING:

T/C NO.	TYPE OF REGRESSION	C(1)	C(2)	C(3)	TMAX
301BG	LEVEL				
304BG	INDIVIDUAL	32.639	-0.04861	0.267623E-04	802.5
309BG	INDIVIDUAL	13.724	-0.01608	0.832567E-05	842.5
310BG	INDIVIDUAL	-7.174	0.02513	-0.127434E-04	915.3
312BG	INDIVIDUAL	-16.731	0.05432	-0.272220E-04	879.9
313BG	INDIVIDUAL	-18.048	0.03750	-0.165786E-04	376.3
317BG	INDIVIDUAL	10.245	0.00694	-0.518925E-05	884.7
318BG	INDIVIDUAL	6.250	0.00606	-0.437169E-05	817.2
320BG	INDIVIDUAL	-9.195	0.04095	-0.206186E-04	907.0
322BG	INDIVIDUAL	8.295	0.00275	0.186155E-05	804.4
323BG	LEVEL				
325BG	INDIVIDUAL	23.491	-0.01084	0.386484E-05	842.1
326BG	LEVEL				
331BG	INDIVIDUAL	3.865	0.01003	-0.551025E-05	847.8
333BG	INDIVIDUAL	-8.755	0.02086	-0.102926E-04	826.6
338BG	INDIVIDUAL	-8.384	0.02445	-0.142865E-04	790.1
339BG	INDIVIDUAL	101.792	-0.14269	0.676555E-04	802.9
341BG	INDIVIDUAL	9.414	0.00128	-0.457405E-05	853.4
349BG	LEVEL				
324BG	DEAD				
330BG	METRASCOPE				
332BG	METRASCOPE				
334BG	METRASCOPE				
319BG	METRASCOPE				

TOTAL NUMBER OF INDIVIDUAL T/C REGRESSIONS= 15  
 MEAN REGRESSION COEFFICIENTS: 9.429 0.00080 -0.861132E-06

LEVEL REGRESSION COEFFICIENTS: -7.574 0.01895 -0.811134E-05

Table F.4. (continued)

\*\*\*\*\*  
 \*\*\*LEVEL H \*\*\*  
 \*\*\*\*\*

## INDIVIDUAL THERMOCOUPLE LISTING:

T/C NO.	TYPE OF REGRESSION	C(1)	C(2)	C(3)	TMA
301CH	FAILED				
302AH	FAILED				
303AH	FAILED				
304CH	FAILED				
305AH	FAILED				
306AH	FAILED				
307AH	FAILED				
308AH	FAILED				
309CH	FAILED				
310CH	FAILED				
311AH	FAILED				
312CH	FAILED				
313CH	FAILED				
314AH	FAILED				
315AH	FAILED				
316AH	FAILED				
317CH	FAILED				
318CH	FAILED				
320CH	FAILED				
321AH	FAILED				
322CH	FAILED				
323CH	FAILED				
324CH	FAILED				
325CH	FAILED				
326CH	FAILED				
327AH	FAILED				
328AH	FAILED				
331CH	FAILED				
333CH	FAILED				
336AH	FAILED				
337AH	FAILED				
338CH	FAILED				
339CH	FAILED				
340AH	FAILED				
341CH	FAILED				
342AH	FAILED				
343AH	FAILED				
344AH	FAILED				
345AH	FAILED				
346AH	FAILED				
348AH	FAILED				
349CH	FAILED				
329AH	METRASCOPE				
330CH	METRASCOPE				
332CH	METRASCOPE				
334CH	METRASCOPE				
335AH	METRASCOPE				
319CH	METRASCOPE				
347AH	METRASCOPE				

\*\*THERE WERE NO INDIVIDUAL T/C REGRESSIONS FOR THIS LEVEL (IN THE CDT ARRAYS);  
 THEREFORE, MEAN REGRESSION COEFFICIENTS COULD NOT BE DETERMINED.

\*\*THERE WERE NO LEVEL T/C REGRESSIONS AVAILABLE IN THE CDT ARRAYS.

Table F.4. (continued)

\*\*\*\*\*  
 \*\*\*LEVEL I \*\*\*  
 \*\*\*\*\*

## INDIVIDUAL THERMOCOUPLE LISTING:

T/C NO.	TYPE OF REGRESSION	C(1)	C(2)	C(3)	TMAX
301CI	FAILED				
302AI	INDIVIDUAL	101.633	-0.10599	0.542323E-04	787.1
303AI	INDIVIDUAL	35.907	-0.04657	0.281355E-04	792.9
304CI	INDIVIDUAL	84.407	-0.13872	0.763129E-04	786.7
305AI	FAILED				
306AI	INDIVIDUAL	36.449	-0.04454	0.229843E-04	782.9
307AI	INDIVIDUAL	44.855	-0.06283	0.351923E-04	780.3
308AI	INDIVIDUAL	101.157	-0.14772	0.795754E-04	786.3
309CI	INDIVIDUAL	74.945	-0.11030	0.594786E-04	769.4
310CI	INDIVIDUAL	68.017	-0.09146	0.486445E-04	866.5
311AI	INDIVIDUAL	83.262	-0.11893	0.614463E-04	817.6
312CI	INDIVIDUAL	50.068	-0.05423	0.279295E-04	867.2
313CI	INDIVIDUAL	56.041	-0.07554	0.406202E-04	830.0
314AI	INDIVIDUAL	24.036	-0.03954	0.231110E-04	779.7
315AI	INDIVIDUAL	55.597	-0.06413	0.336418E-04	857.9
316AI	INDIVIDUAL	158.330	-0.20181	0.100393E-03	830.0
317CI	INDIVIDUAL	71.019	-0.08404	0.404205E-04	825.3
318CI	INDIVIDUAL	-60.349	0.10318	-0.513518E-04	761.5
320CI	INDIVIDUAL	87.506	-0.12072	0.607520E-04	820.1
321AI	INDIVIDUAL	.688	-0.03887	0.208915E-04	792.9
322CI	INDIVIDUAL	.059	-0.09992	0.554906E-04	791.8
323CI	INDIVIDUAL	61.557	-0.07802	0.411323E-04	800.9
324CI	INDIVIDUAL	134.927	-0.20256	0.105696E-03	795.0
325CI	INDIVIDUAL	28.018	-0.02401	0.138970E-04	890.5
326CI	INDIVIDUAL	72.655	-0.09801	0.487478E-04	781.2
327AI	FAILED				
328AI	FAILED				
331CI	INDIVIDUAL	49.934	-0.07167	0.364730E-04	800.8
333CI	INDIVIDUAL	20.810	-0.03336	0.197699E-04	775.8
336AI	INDIVIDUAL	123.997	-0.18210	0.974085E-04	789.2
337AI	INDIVIDUAL	52.692	-0.07007	0.364213E-04	829.0
338CI	INDIVIDUAL	84.093	-0.13427	0.744063E-04	752.0
339CI	INDIVIDUAL	199.274	-0.31182	0.162764E-03	746.6
340AI	INDIVIDUAL	122.479	-0.17397	0.883182E-04	781.5
341CI	INDIVIDUAL	43.098	-0.05395	0.252785E-04	823.8
342AI	INDIVIDUAL	75.392	-0.10435	0.543323E-04	805.7
343AI	INDIVIDUAL	78.240	-0.10785	0.547511E-04	840.8
344AI	INDIVIDUAL	135.132	-0.20422	0.112431E-03	782.2
345AI	INDIVIDUAL	96.196	-0.10319	0.549271E-04	801.2
346AI	FAILED				
348AI	INDIVIDUAL	-38.580	0.08541	-0.478837E-04	781.0
349CI	FAILED				
329AI	METRASCOPE				
330CI	METRASCOPE				
332CI	METRASCOPE				
334CI	METRASCOPE				
335AI	METRASCOPE				
319CI	METRASCOPE				
347AI	METRASCOPE				

TOTAL NUMBER OF INDIVIDUAL T/C REGRESSIONS= 36  
 MEAN REGRESSION COEFFICIENTS: 69.582 -0.09485 0.499102E-04

\*\*THERE WERE NO LEVEL T/C REGRESSIONS AVAILABLE IN THE CDT ARRAYS.

Table F.4. (continued)

\*\*\*\*\*  
 \*\*\*LEVEL J \*\*\*  
 \*\*\*\*\*

## INDIVIDUAL THERMOCOUPLE LISTING:

T/C NO.	TYPE OF REGRESSION	C(1)	C(2)	C(3)	TMAX
301DJ	FAILED				
302CJ	FAILED				
303CJ	FAILED				
304DJ	FAILED				
305CJ	INDIVIDUAL	32.613	-0.04492	0.244870E-04	790.2
306CJ	FAILED				
307CJ	FAILED				
308CJ	FAILED				
309DJ	FAILED				
310DJ	FAILED				
311CJ	INDIVIDUAL	516.864	-0.69963	0.322674E-03	800.9
312DJ	INDIVIDUAL	34.520	-0.04147	0.214911E-04	854.5
313DJ	FAILED				
314CJ	FAILED				
316CJ	FAILED				
317DJ	INDIVIDUAL	-5.229	0.00825	0.113172E-05	831.9
318DJ	FAILED				
320DJ	FAILED				
321CJ	INDIVIDUAL	28.377	-0.03674	0.176082E-04	796.8
322DJ	FAILED				
323DJ	FAILED				
324DJ	FAILED				
325DJ	FAILED				
326DJ	FAILED				
327CJ	INDIVIDUAL	-20.504	0.05405	-0.267689E-04	816.4
328CJ	INDIVIDUAL	12.777	-0.00929	0.601217E-05	796.7
331DJ	FAILED				
333DJ	FAILED				
336CJ	FAILED				
337CJ	INDIVIDUAL	9.621	-0.00318	0.232490E-05	800.6
338DJ	FAILED				
339DJ	FAILED				
340CJ	FAILED				
341DJ	FAILED				
342CJ	INDIVIDUAL	59.095	-0.08291	0.412412E-04	805.1
343CJ	FAILED				
344CJ	INDIVIDUAL	36.696	-0.06126	0.345548E-04	792.8
346CJ	FAILED				
347CJ	FAILED				
349DJ	FAILED				
315CJ	FAILED				
348CJ	DEAD				
329CJ	METRASCOPE				
330DJ	METRASCOPE				
332DJ	METRASCOPE				
334DJ	METRASCOPE				
335CJ	METRASCOPE				
319DJ	METRASCOPE				

TOTAL NUMBER OF INDIVIDUAL T/C REGRESSIONS= 10  
 MEAN REGRESSION COEFFICIENTS: 70.483 -0.09171 0.444755E-04

\*\*THERE WERE NO LEVEL T/C REGRESSIONS AVAILABLE IN THE COT ARRAYS.

Table F.4. (continued)

\*\*\*\*\*  
 \*\*\*LEVEL K \*\*\*  
 \*\*\*\*\*

## INDIVIDUAL THERMOCOUPLE LISTING:

T/C NO.	TYPE OF REGRESSION	C(1)	C(2)	C(3)	TMAX
345CK	LEVEL				
301DK	LEVEL				
304DK	LEVEL				
309DK	LEVEL				
310DK	INDIVIDUAL	91.646	-0.14155	0.795902E-04	810.6
312DK	INDIVIDUAL	77.787	-0.09674	0.487595E-04	830.8
313DK	INDIVIDUAL	136.906	-0.19427	0.997185E-04	816.9
317DK	INDIVIDUAL	103.397	-0.14459	0.797189E-04	797.4
318DK	INDIVIDUAL	101.476	-0.15675	0.849126E-04	757.9
320DK	INDIVIDUAL	108.178	-0.14533	0.756317E-04	794.8
322DK	LEVEL				
323DK	INDIVIDUAL	146.132	-0.21907	0.118053E-03	767.8
324DK	INDIVIDUAL	154.367	-0.24060	0.131740E-03	737.9
325DK	INDIVIDUAL	16.369	-0.00441	0.968150E-05	851.6
326DK	INDIVIDUAL	44.778	-0.06551	0.336453E-04	763.8
331DK	LEVEL				
333DK	INDIVIDUAL	103.184	-0.16032	0.846731E-04	755.8
338DK	LEVEL				
339DK	LEVEL				
341DK	INDIVIDUAL	72.986	-0.09905	0.480061E-04	803.9
349DK	LEVEL				
330DK	METRASCOPE				
332DK	METRASCOPE				
334DK	METRASCOPE				
319DK	METRASCOPE				

TOTAL NUMBER OF INDIVIDUAL T/C REGRESSIONS= 12  
 MEAN REGRESSION COEFFICIENTS: 96.434 -0.13901 0.745108E-04

LEVEL REGRESSION COEFFICIENTS: 81.768 -0.12620 0.703059E-04

\*\*\*\*\*  
 \*\*\*LEVEL L \*\*\*  
 \*\*\*\*\*

## INDIVIDUAL THERMOCOUPLE LISTING:

T/C NO.	TYPE OF REGRESSION	C(1)	C(2)	C(3)	TMAX
301EL	LEVEL				
302CL	LEVEL				
303CL	INDIVIDUAL	32.361	-0.04441	0.228885E-04	752.6
304EL	LEVEL				
305CL	INDIVIDUAL	53.659	-0.09059	0.537827E-04	739.1
306CL	INDIVIDUAL	0.593	0.00747	-0.274301E-05	757.9
307CL	INDIVIDUAL	128.385	-0.19780	0.103781E-03	752.6
308CL	INDIVIDUAL	103.061	-0.15800	0.832313E-04	769.2
309EL	LEVEL				
310EL	INDIVIDUAL	54.601	-0.07572	0.431188E-04	827.2
311CL	LEVEL				

Table F.4. (continued)

T/C NO.	TYPE OF REGRESSION	C(1)	C(2)	C(3)	TMAX
312EL	INDIVIDUAL	63.907	-0.08272	0.438729E-04	806.6
313EL	INDIVIDUAL	91.992	-0.13357	0.753222E-04	772.8
315CL	LEVEL				
316CL	INDIVIDUAL	48.008	-0.07060	0.352876E-04	758.6
317EL	INDIVIDUAL	68.804	-0.09035	0.477697E-04	774.1
318EL	LEVEL				
320EL	INDIVIDUAL	80.302	-0.10514	0.525661E-04	799.4
321CL	LEVEL				
322EL	LEVEL				
323EL	INDIVIDUAL	69.632	-0.08945	0.467995E-04	771.5
324EL	LEVEL				
325EL	LEVEL				
326EL	LEVEL				
327CL	INDIVIDUAL	63.355	-0.07504	0.373441E-04	797.9
328CL	INDIVIDUAL	-10.119	0.01435	-0.391968E-05	786.7
331EL	INDIVIDUAL	60.665	-0.08451	0.401095E-04	752.4
333EL	LEVEL				
336CL	INDIVIDUAL	39.215	-0.04245	0.211927E-04	764.9
337CL	INDIVIDUAL	75.069	-0.10655	0.570739E-04	773.0
338EL	INDIVIDUAL	111.697	-0.16530	0.873686E-04	767.5
339EL	LEVEL				
340CL	LEVEL				
341EL	LEVEL				
342CL	INDIVIDUAL	144.561	-0.22279	0.115207E-03	757.0
343CL	INDIVIDUAL	76.913	-0.08896	0.475425E-04	778.3
344CL	INDIVIDUAL	41.751	-0.05930	0.323666E-04	766.8
345CL	LEVEL				
346CL	LEVEL				
347CL	LEVEL				
348CL	LEVEL				
349EL	LEVEL				
314CL	DEAD				
329CL	METRASCOPE				
330EL	METRASCOPE				
332EL	METRASCOPE				
334EL	METRASCOPE				
335CL	METRASCOPE				
319EL	METRASCOPE				

TOTAL NUMBER OF INDIVIDUAL T/C REGRESSIONS= 21  
 MEAN REGRESSION COEFFICIENTS: 66.591 -0.09340 0.495219E-04

LEVEL REGRESSION COEFFICIENTS: 56.016 -0.09044 0.500993E-04



Table F.4. (continued)

\*\*\*\*\*  
 \*\*\*LEVEL M \*\*\*  
 \*\*\*\*\*

## INDIVIDUAL THERMOCOUPLE LISTING:

T/C NO.	TYPE OF REGRESSION	C(1)	C(2)	C(3)	TMAX
301EM	FAILED				
304EM	FAILED				
309EM	FAILED				
325EM	FAILED				

\*\*THERE WERE NO INDIVIDUAL T/C REGRESSIONS FOR THIS LEVEL (IN THE CDT ARRAYS);  
 THEREFORE, MEAN REGRESSION COEFFICIENTS COULD NOT BE DETERMINED.

\*\*THERE WERE NO LEVEL T/C REGRESSIONS AVAILABLE IN THE CDT ARRAYS.

\*\*\*\*\*  
 \*\*\*LEVEL N \*\*\*  
 \*\*\*\*\*

## INDIVIDUAL THERMOCOUPLE LISTING:

T/C NO.	TYPE OF REGRESSION	C(1)	C(2)	C(3)	TMAX
301FN	LEVEL				
304FN	LEVEL				
325FN	INDIVIDUAL	169.070	-0.27175	0.160929E-03	732.6
309FN	DEAD				

TOTAL NUMBER OF INDIVIDUAL T/C REGRESSIONS= 1  
 MEAN REGRESSION COEFFICIENTS: 169.070 -0.27175 0.160929E-03

LEVEL REGRESSION COEFFICIENTS: 64.366 -0.12514 0.863555E-04

Appendix G

DEVELOPMENT OF THE MODIFIED RUSSELL EQUATION

G.1 Introduction

The thermal conductivities of porous media (solid + gas) are best correlated with Russell's<sup>42</sup> equation,

$$\frac{k_{\text{comp}}}{k_{\text{cont}}} = \frac{\nu p^{2/3} + 1 + p^{2/3}}{\nu(p^{2/3} - p) + 1 - p^{2/3} + p}, \quad (\text{G.1})$$

where the subscripts comp and cont denote values for the composite mixture and the continuous phase;  $p$  is the porosity (i.e., volume fraction of voids) given for a solid-gas mixture by

$$p = \frac{\rho_{\text{sol}} - \rho_{\text{comp}}}{\rho_{\text{sol}} - \rho_{\text{gas}}}. \quad (\text{G.2})$$

The term  $\nu$  is the ratio of the thermal conductivity of the gas to that of the continuous phase; that is,

$$\nu = \frac{k_{\text{gas}}}{k_{\text{cont}}}. \quad (\text{G.3})$$

Note, for  $p = 0$  (i.e., solid with no gas voids), Eq. (G.1) reduces to

$$\frac{k_{\text{comp}}}{k_{\text{cont}}} = 1. \quad (\text{G.4})$$

For  $p = 1$  (all gas), Eq. (G.1) reduces to

$$\frac{k_{\text{comp}}}{k_{\text{cont}}} = \nu = \frac{k_{\text{gas}}}{k_{\text{cont}}}, \quad (\text{G.5})$$

or

$$k_{\text{comp}} = k_{\text{gas}}. \quad (\text{G.6})$$

So, Eq. (G.1) is applicable for  $0 < p < 1$ .

When gas is the continuous phase of a solid-gas mixture (e.g., powders), Laubitz<sup>43</sup> noted that Eq. (G.1) does not give good agreement with

experimental data. However, by doubling the right-hand side of Eq. (G.1) and adding a radiative heat transfer mechanism, the accuracy of Eq. (G.1) is restored; that is,

$$k_{\text{comp}} = 2k_{\text{cont}} [\text{Eq. (G.1)}] + 4\sigma T^3 \epsilon \frac{a}{p} (1 - p^{2/3} + p^{4/3}), \quad (\text{G.7})$$

where

$\epsilon$  = emissivity,

$a$  = linear dimension of the particles,

$\sigma$  = Stefan-Boltzman constant,

$T$  = absolute temperature.

Laubitz studied powders ( $\text{MgO}$ ,  $\text{Al}_2\text{O}_3$ , and  $\text{ZrO}_2$ ) with porosities ranging from 0.55 to 0.75.

#### G.2 Application to BDHT Heater MgO

The initial attempt to apply the Russell equation to the MgO cores of the BDHT fuel pin simulators involved a slight modification of Eq. (G.7) (this gives the best fit for Laubitz's experimental powder data). The approach taken is that the multiplier in Eq. (G.7) is an adjustable parameter; also, the emissivity and particle linear dimension product ( $\epsilon \cdot a$ ) in the second part of Eq. (G.7) is an adjustable parameter; therefore, the modified equation appears as

$$k_{\text{comp}} = C_1 k_{\text{cont}} \left[ \frac{\sqrt{p^{2/3} + 1 - p^{2/3}}}{\sqrt{(p^{2/3} - p) + 1 - p^{2/3} + p}} \right] + 4\sigma T^3 \frac{C_2}{p} (1 - p^{2/3} + p^{4/3}), \quad (\text{G.8})$$

where  $C_1$  and  $C_2$  are adjustable parameters.

If the solid MgO is treated as the continuous phase and the porous material is air, literature data<sup>6</sup> is available for the thermal conductivity of MgO with porosities of 0.0, 0.050-0.100, and 0.220 (Fig. G.1).

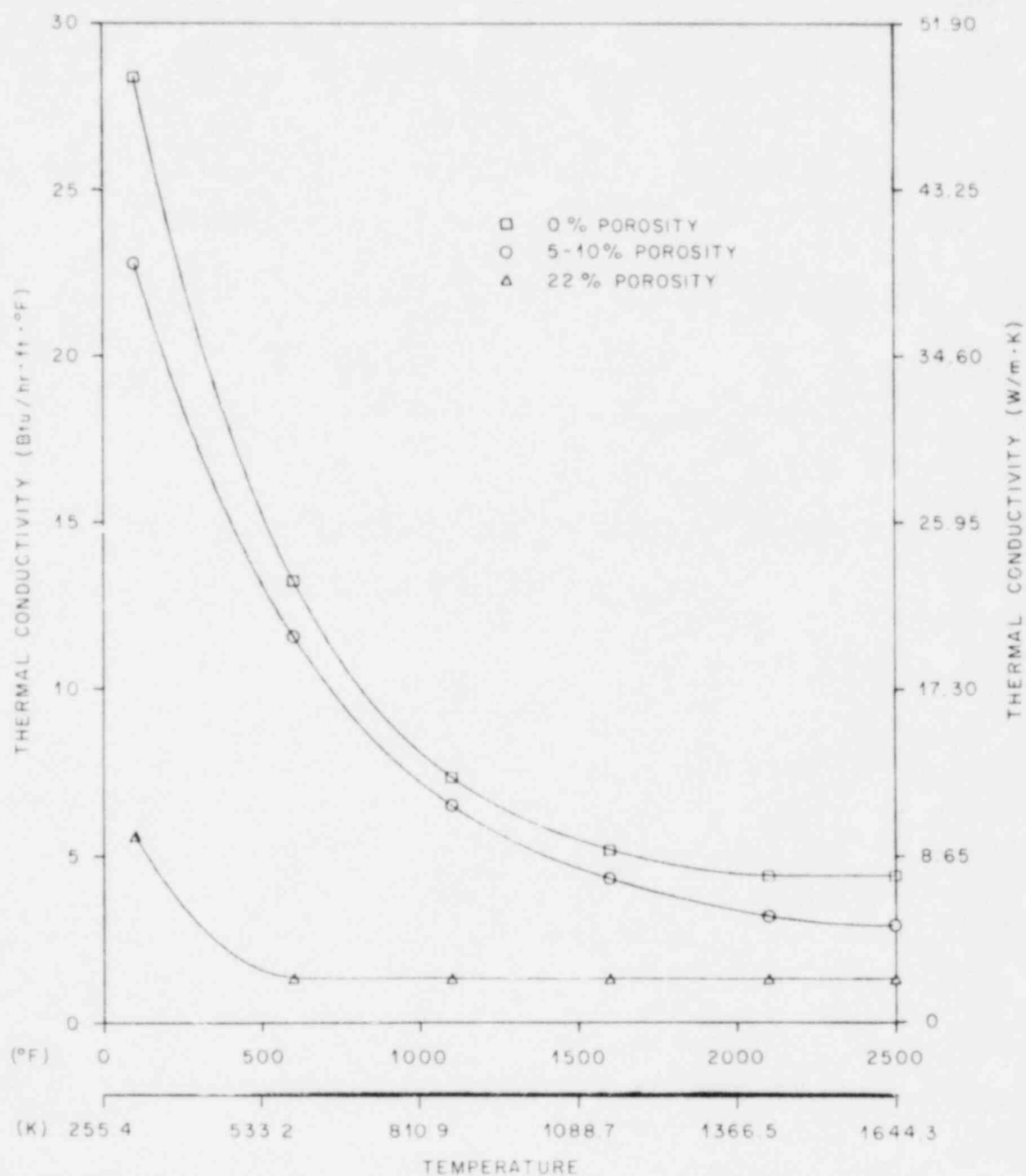


Fig. G.1. MgO thermal conductivity as a function of temperature and porosity (literature data).

Therefore, the following function could be formulated

$$F(C_1, C_2) = \sum_{j=1,2} \sum_{i=1,80} (k_{\text{comp}_i} - k_{\text{lit}_i})^2, \quad (\text{G.9})$$

where

$k_{\text{comp}}$  = MgO thermal conductivity calculated by Eq. (G.8),

$k_{\text{lit}}$  = literature value of MgO thermal conductivity,

$\sum_{i=1,80}$  represents the discretized temperature domain (200–1800°F),

$\sum_{j=1,2}$  represents the 0.050 and 0.220 porosity curves, and

$C_1$  and  $C_2$  are the adjustable parameters of Eq. (G.8).

Equation (G.9) is minimized with respect to the  $C_1$  and  $C_2$  parameters and essentially represents a least-squares fit of Eq. (G.8) to the literature data.

Unfortunately, the "best" fit of Eq. (G.8) to the literature data is very poor at best. The  $k_{\text{comp}}(x)$  values are overlaid with  $k_{\text{lit}}$  values in Fig. G.2 and G.3 for 0.05 and 0.22 porous MgO, respectively. No further attempt to fit Eq. (G.8) to the literature data has been made.

A modified form of Eq. (G.1) was used in lieu of intermediate trial equations. First, the Russell equation [Eq. (G.1)] was rearranged in the following form:

$$\frac{k_{\text{comp}}}{k_{\text{cont}}} = \frac{1 + p^{2/3} (v - 1)}{1 + p^{2/3} (v - 1) - p (v - 1)}. \quad (\text{G.10})$$

The form of the equation which was fitted to the literature data,

$$\frac{k_{\text{comp}}}{k_{\text{cont}}} = \frac{1 + (C_1 p)^{C_2} (v - 1)}{1 + (C_1 p)^{C_2} (v - 1) - (C_1 p) (v - 1)}, \quad (\text{G.11})$$

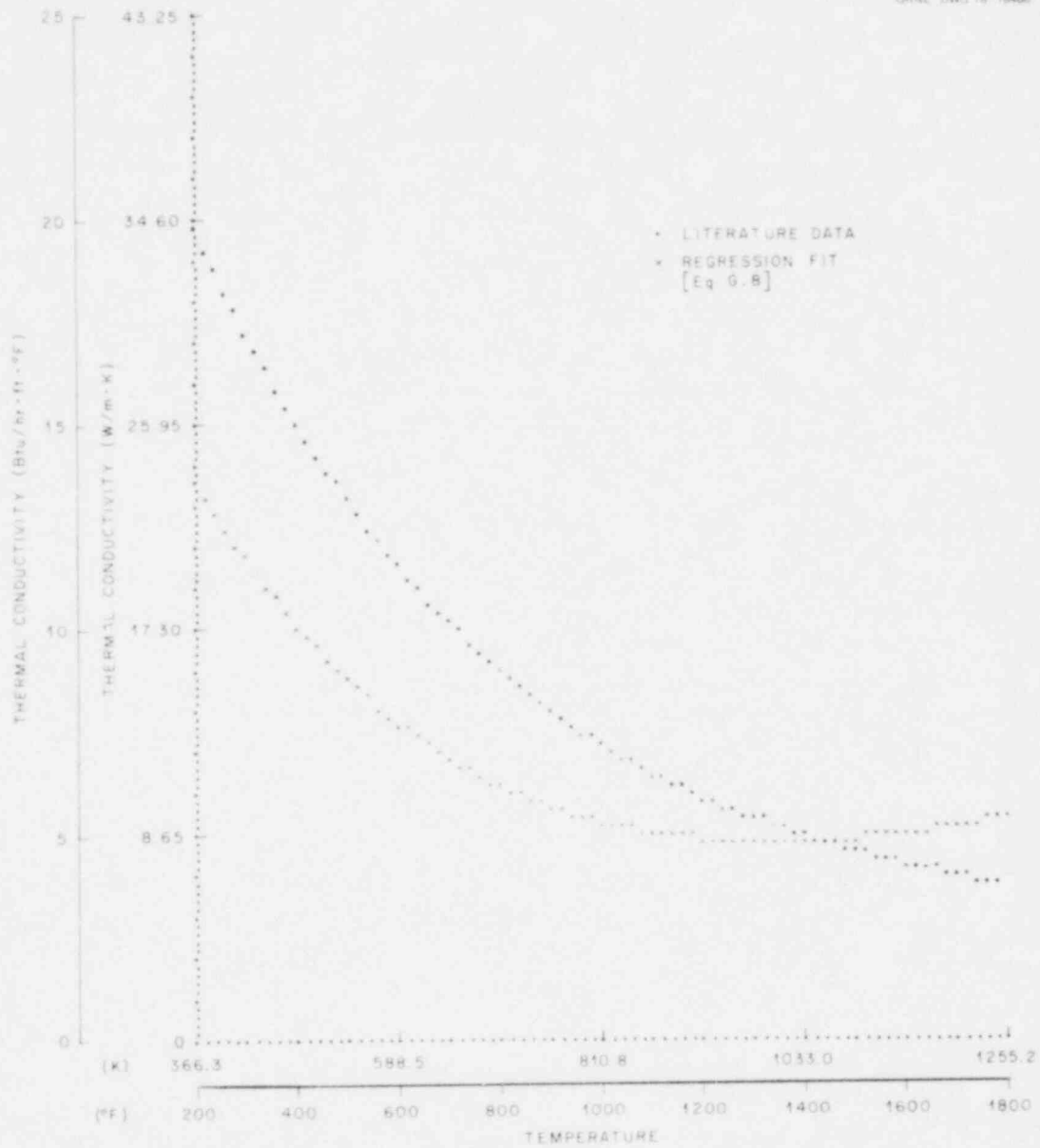


Fig. G.2.  $k_{MgO}$  vs temperature for 5% porous MgO [literature data and regression fit of Eq. (G.8)].

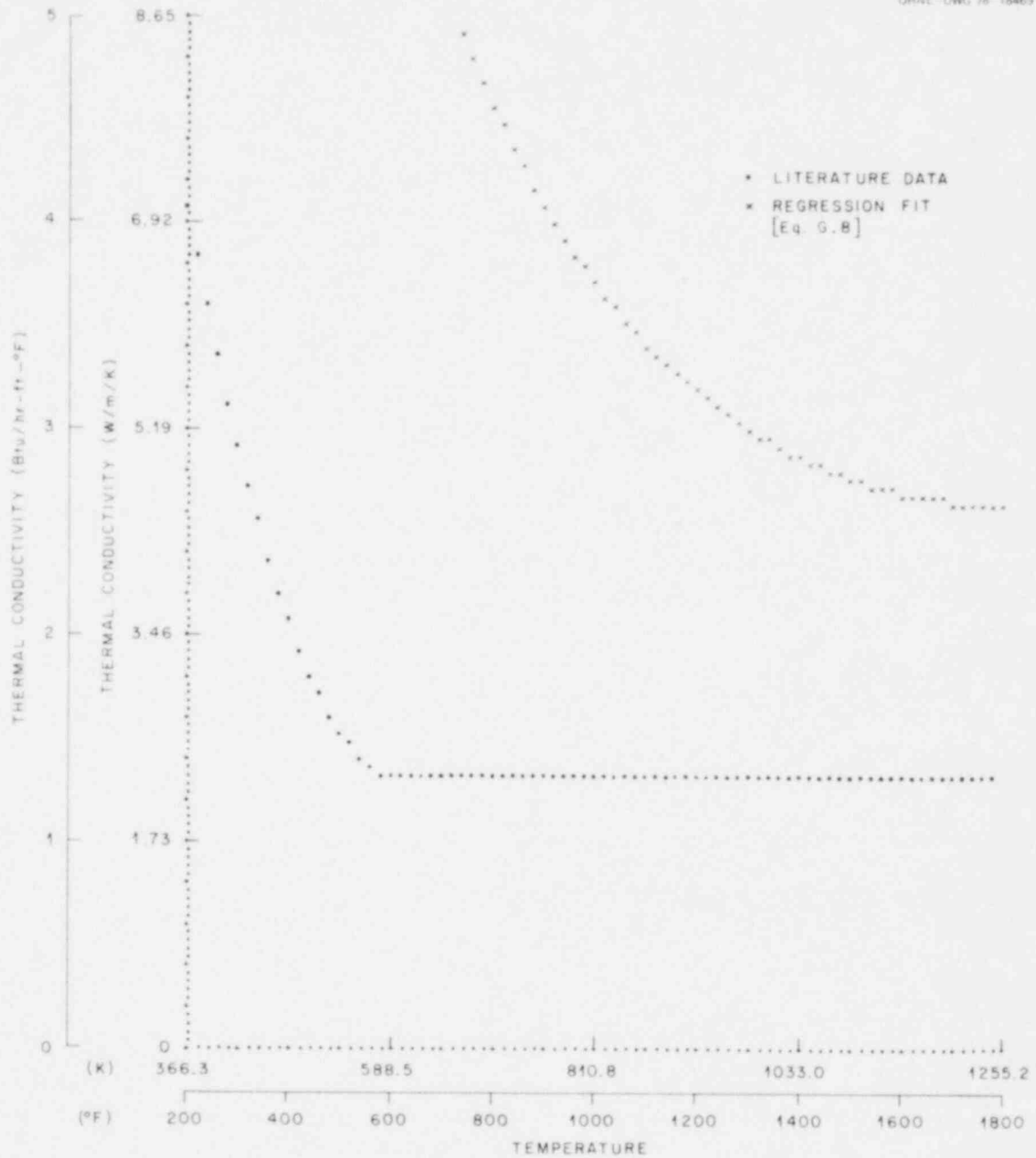


Fig. G.3.  $k_{\text{MgO}}$  vs temperature for 22% porous MgO [literature data and regression fit of Eq. (G.8)].



shows  $C_1$  and  $C_2$  as the parameters. Again, Eq. (G.9) was minimized with respect to  $C_1$  and  $C_2$ . The least-squares fit resulted in  $C_1 = 3.891$  and  $C_2 = 0.856$ . Overlays of  $k_{\text{comp}}$  vs  $k_{\text{lit}}$  are presented in Figs. G.4 and G.5 for this regression fit.

The modified form of the Russell equation which will be used to determine the MgO thermal conductivity given the temperature and porosity is

$$\frac{k_{\text{MgO}}(T)}{k_{\text{MgO}}(T) \text{ at } 0\% \text{ p}} = \frac{1 + (3.891p)^{0.856} (\nu - 1)}{1 + (3.891p)^{0.856} (\nu - 1) - (3.891p)(\nu - 1)}, \quad (\text{G.12})$$

where  $p$  = porosity,  $\nu = k_{\text{air}}(T)/k_{\text{MgO}}(T)$  at 0%  $p$ , and  $T$  = temperature. A plot [using Eq. (G.12)] similar to Fig. G.1 and illustrating the family of curves for  $k_{\text{MgO}}$  (with the parameter being porosity) is presented in Fig. G.6.

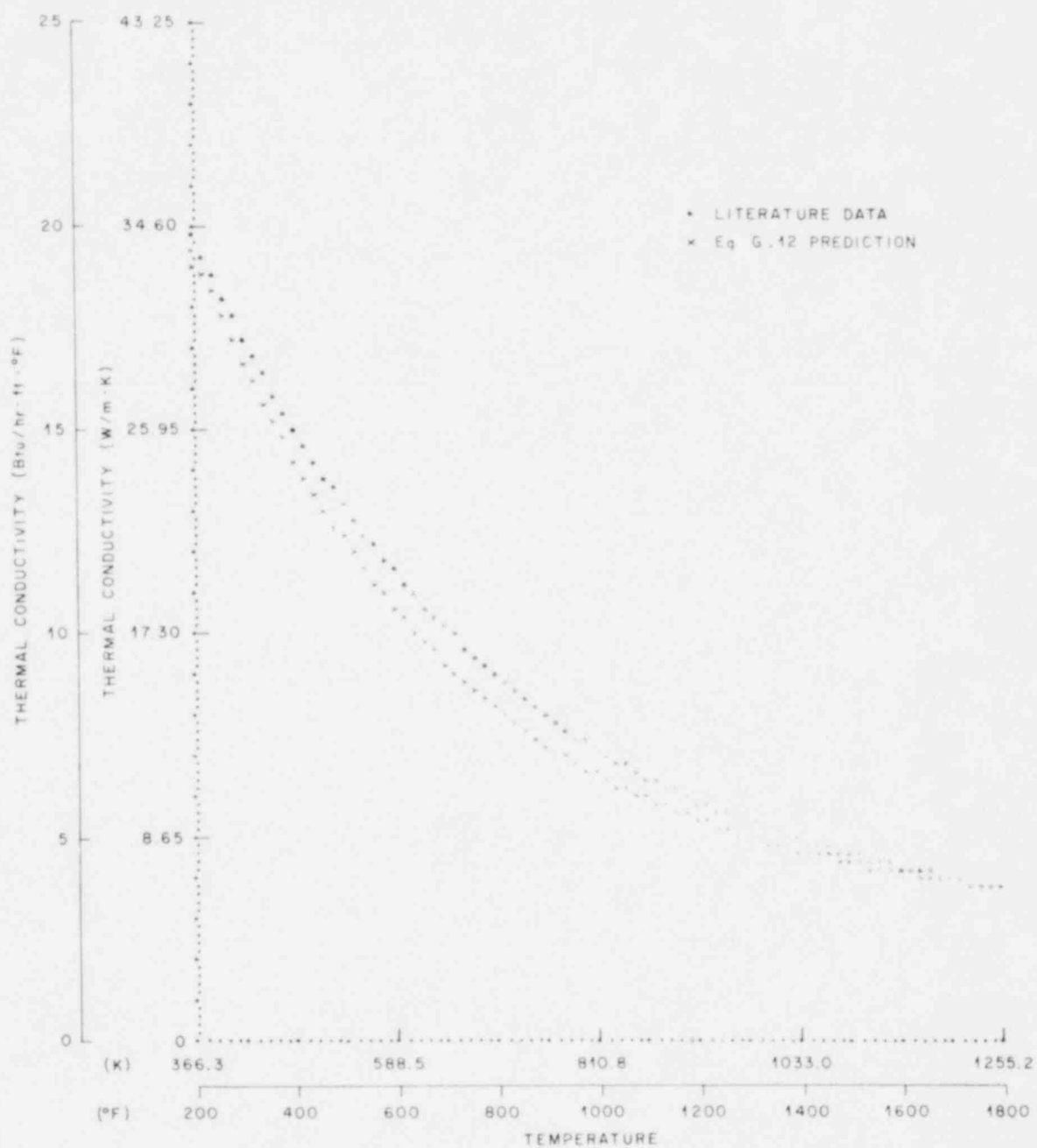


Fig. G.4.  $k_{MgO}$  vs temperature for 5% porous MgO [literature data and regression fit of Eq. (G.12)].

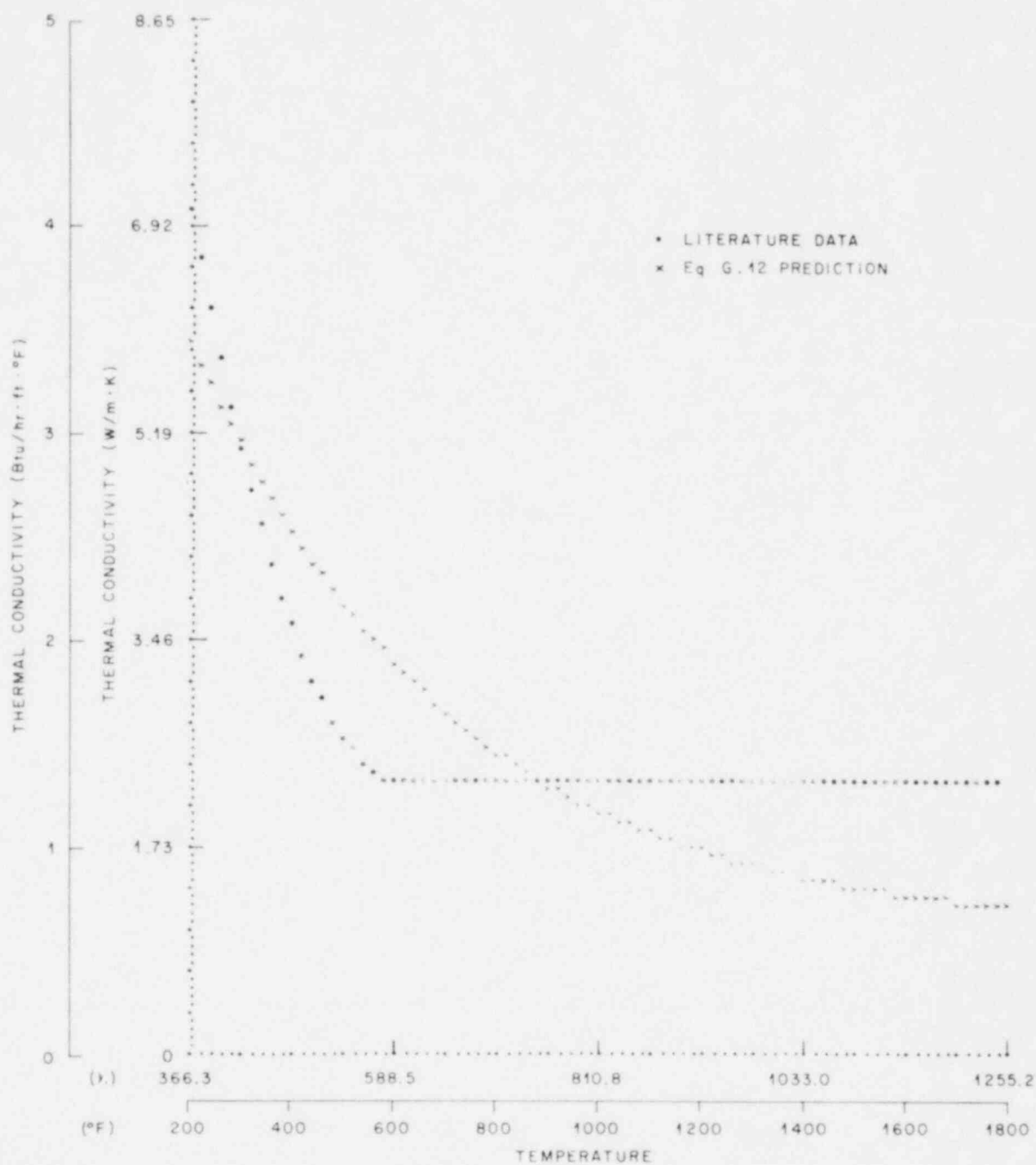


Fig. G.5.  $k_{MgO}$  vs temperature for 22% porous MgO [literature data and regression fit of Eq. (G.12)].

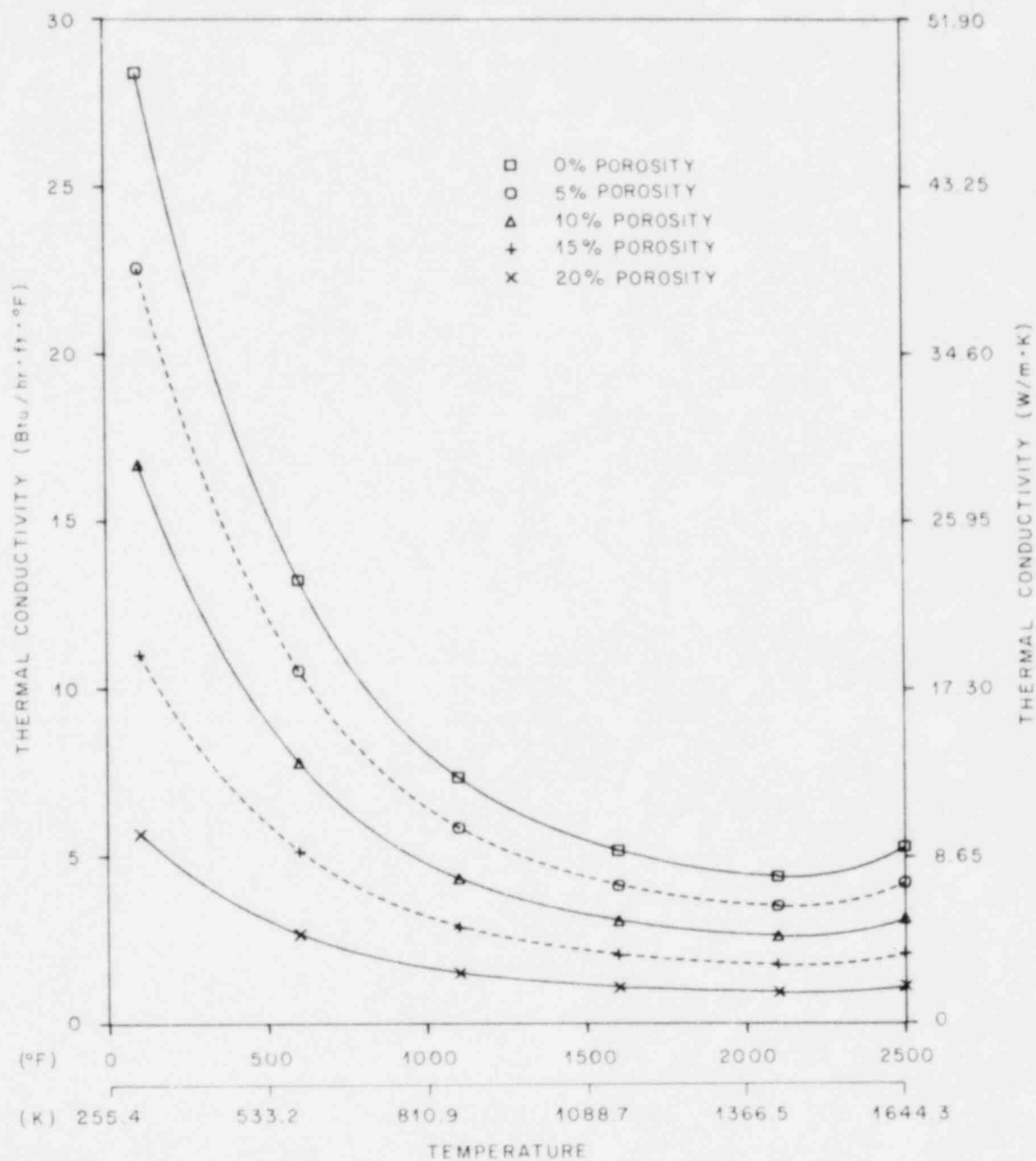


Fig. G.6. MgO thermal conductivity as a function of temperature and porosity [modified Russel equation - Eq. (G.12)].

NUREG/CR-0342  
ORNL/NUREG-51  
Dist. Category R2

Internal Distribution

- |                      |                                      |
|----------------------|--------------------------------------|
| 1. M. Bender         | 16. F. R. Mynatt                     |
| 2. R. E. Bohanan     | 17-26. L. J. Ott                     |
| 3. K. W. Childs      | 27. H. Postma                        |
| 4. S. B. Cliff       | 28. Myrtlelen Sheldon                |
| 5. W. G. Craddick    | 29. J. A. Smolen                     |
| 6. R. D. Dabbs       | 30. R. E. Textor                     |
| 7. H. L. Falkenberry | 31. H. E. Trammell                   |
| 8. R. M. Flanders    | 32. D. B Trauger                     |
| 9. M. H. Fontana     | 33. J. D. White                      |
| 10. R. C. Hagar      | 34. Patent Office                    |
| 11. R. F. Hibbs      | 35-36. Central Research Library      |
| 12. H. W. Hoffman    | 37. Document Reference Section       |
| 13. A. F. Johnson    | 38-40. Laboratory Records Department |
| 14. B. F. Maskewitz  | 41. Laboratory Records (RC)          |
| 15. R. W. McCulloch  |                                      |

External Distribution

- 42-43. Director, Division of Reactor Safety Research, Nuclear Regulatory Commission, Washington, D.C. 20555
44. Office of Assistant Manager, Energy Research and Development, DOE, ORO
- 45-360. Given distribution as shown in category R2 (TIC-2, NTIS-25)